

# Functional consequences of biased signalling at neuronal G protein-coupled receptors

Groom, Sam

*Award date:*
2021

*Awarding institution:*
University of Bath

**PHD**

# Functional consequences of biased signalling at neuronal G protein-coupled receptors

Groom, Sam

*Award date:*
2021

*Awarding institution:*
University of Bath

# Functional consequences of biased signalling at neuronal G protein-coupled receptors

Sam Groom

A thesis submitted for the degree of Doctor of Philosophy

University of Bath

Department of Pharmacy and Pharmacology

December 2020

## Declaration of any previous submission of the work

The material presented here for examination for the award of a higher degree by research has not been incorporated into submission for another degree.

*Candidate Signature:* 

## Declaration of authorship

I am the author of this thesis, and the work described therein was carried out by myself personally, with the exception of Chapter 4 and Chapter 5 where 10% of the work in each chapter was carried out in collaboration with other researchers. Specifically, this refers to experimental work described within Chapter 4.2.4, which was conducted with the assistance of Dr Rob Hill, and within Chapter 5.2.10, which was conducted in collaboration with Miss Nina Kathleen Blum, Dr Andrea Kliewer and Professor Stefan Schulz at Friedrich-Schiller-University, Jena, Germany.

*Candidate Signature:* 

## Publications

**Groom, S**., Blum, N. K., Conibear, A. E., Disney, A., Hill, R., Husbands, S. M., Li, Y., Toll, L., Kliewer, A., Schulz, S., Henderson, G., Kelly, E., & Bailey, C. P. (2020). A novel G protein-biased agonist at the μ opioid receptor induces substantial receptor desensitization through G protein-coupled receptor kinase. *British Journal of Pharmacology*. https://doi.org/10.1111/bph.15334

## Select Conference Abstracts

**Groom S**., Blum, N., Conibear A., Disney A., Husbands S., Yangmei L., Toll L., Henderson G., Kliewer, A., Schulz, S., Kelly E., Bailey C. A novel G protein-biased agonist at the μ opioid receptor induces substantial receptor desensitization through G protein-coupled receptor kinase. **British Pharmacological Society Annual Meeting (Virtual), 2020** – *Oral Presentation.*

**Groom S**., Conibear A., Disney A., Husbands S., Yangmei L., Toll L., Henderson G., Kelly E., Bailey C. 'Compound 1': An apparent G protein biased μ opioid receptor agonist that induces receptor desensitization through GRK. **British Pharmacological Society Annual Meeting, Edinburgh 2019** – *Oral Presentation.*

**Groom S**., Conibear A., Disney A., Husbands S., Yangmei L., Toll L., Henderson G., Kelly E., Bailey C. 'Compound 1': A G-protein-biased MOPr agonist that induces MOPr desensitization apparently through GRK. **International Narcotics Research Conference, New York 2019** – *Poster Presentation*.

**Groom S**., Conibear A., Disney A., Husbands S., Yangmei L., Toll L., Henderson G., Kelly E., Bailey C. Exploring rapid desensitization of μ opioid receptors induced by G-protein biased agonists. **British Pharmacological Society Annual Meeting, London 2018** – *Poster Presentation*.

**Groom S**., Conibear A., Disney A., Husbands S., Yangmei L., Toll L., Henderson G., Kelly E., Bailey C. Exploring rapid desensitization of μ opioid receptors induced by G-protein biased agonists. **International Narcotics Research Conference, San Diego 2018** – *Poster Presentation*.

**Groom S**., Conibear A., Disney A., Husbands S., Yangmei L., Toll L., Henderson G., Kelly E., Bailey C. Exploring rapid desensitization of μ opioid receptors induced by G-protein biased agonists. **7th Focused Meeting on Cell Signalling, Nottingham 2018** – *Oral Communication*.

# Table of Contents


***Chapter 1: Introduction ..... 1***

**1.1 G protein-coupled receptors ..... 1**

1.1.1 Classification, biology and structural characteristics ..... 1

1.1.2 GPCRs as therapeutic targets ..... 4

1.1.3 G protein coupling and signal transduction ..... 5

1.1.4 Regulation of GPCR function ..... 7

1.1.5 G protein-independent signalling ..... 9

1.1.6 Biased agonism at GPCRs ..... 11

**1.2 The μ opioid receptor (MOPr) system ..... 15**

1.2.1 Opioids and the opioid system ..... 15

1.2.2 The opioid receptor family ..... 16

1.2.3 G protein-dependent signalling of MOPr ..... 17

1.2.4 Opioid-induced analgesia ..... 19

1.2.5 Regulation of MOPr signalling ..... 20

1.2.6 G protein-independent signalling of MOPr ..... 24

**1.3 Biased signalling at MOPr ..... 26**

1.3.1 Rationale for the development of G protein-biased MOPr agonists ..... 26

1.3.2 The pharmacology of reportedly biased agonists at MOPr ..... 28

1.3.3 MOPr regulation and tolerance induced by G protein-biased agonists ..... 31

**1.4 Scope and aims of this thesis ..... 33**

***Chapter 2: Materials & Methods ..... 34***

**2.1 In vitro cell signalling studies ..... 34**

2.1.1 General cell culture methods and transfection ..... 34

2.1.2 Bioluminescence Resonance Energy Transfer (BRET) assays ..... 34

2.1.3 Quantification of biased signalling ..... 39

2.1.4 Surface MOPr enzyme-linked immunosorbent assay (ELISA) ..... 41

2.1.5 Phosphosite-specific immunoblotting of MOPr ..... 42

**2.2 Animal housing & welfare ..... 44**

**2.3 Rat vas deferens assay ..... 45**

2.3.1 Tissue preparation ..... 45

2.3.2 Experimental procedures ..... 45

2.3.3 Data processing and Schild analysis ..... 46

**2.4 Brain slice electrophysiology ..... 49**

2.4.1 Brain slice preparation ..... 49

2.4.2 Whole cell voltage-clamped experiments ..... 49

2.4.3 Data analysis ..... 50

**2.5 Warm water tail immersion test of nociception ..... 51**

2.5.1 Experimental procedure ..... 51

2.5.2 Data analysis ..... 51

**2.6 Materials ..... 53**

***Chapter 3: Characterisation of putatively G protein-biased MOPr agonists 54***

**3.1 Introduction ..... 54**

**3.2 Results ..... 57**

3.2.1 Compound 1 is a G protein-biased agonist at MOPr ..... 57

3.2.1.1 Characterising opioid-induced $G\alpha_i$ activation and arrestin-3 recruitment ..... 57

3.2.1.2 Quantifying the G protein-biased signalling of Compound 1 at MOPr ..... 61

3.2.1.3 Inhibition of DAMGO-induced arrestin-3 recruitment by partial MOPr agonists ..... 67

3.2.2 Compound 1 is a partial agonist at MOPr and DOPr, but lacks agonist activity at KOPr ..... 71

3.2.3 Investigating the affinity of partial MOPr agonists in isolated rat vas deferens 74

**3.3 Discussion ..... 82**

3.3.1 Summary of findings ..... 82

3.3.2 Compound 1 is a G protein-biased agonist ..... 83

3.3.3 Limitations in methods of bias calculations in the case of partial agonists 84

3.3.4 Reflection on the use of BRET methods to study receptor signalling ..... 85

3.3.5 Notes on inactivity of SR-17018 ..... 87

3.3.6 Potential limitations of the RVD Schild experiment ..... 88

3.3.7 Studying the long-term effects of G protein-biased agonists at MOPr ..... 88

***Chapter 4: Investigating receptor desensitization induced by G protein-biased MOPr agonists ..... 90***

**4.1 Introduction ..... 90**

**4.2 Results ..... 93**

4.2.1 Assessing the function and desensitization of opioid-induced GIRK currents in rat locus coeruleus neurons ..... 93

4.2.2 Apparent Compound 1-induced MOPr desensitization is not due to peptide degradation or indirect GIRK inhibition ..... 101

4.2.3 PZM21 is a low efficacy partial MOPr agonist in LC neurons ..... 104

4.2.4 Compound 1 induces small but measurable antinociception in mice ..... 106

**4.3 Discussion ..... 113**

4.3.1 The intrinsic efficacy of Compound 1 and PZM21 in LC neurones ..... 113

4.3.2 PZM21 induced minimal rapid MOPr desensitization ..... 114

4.3.3 Compound 1 induced substantial MOPr desensitization ..... 114

4.3.4 Compound 1 induced antinociception ..... 115

***Chapter 5: Investigating the potential mechanisms of Compound 1-induced MOPr desensitization ..... 118***

**5.1 Introduction ..... 118**

**5.2 Results ..... 120**

5.2.1 Investigating the mechanisms of Compound 1-induced MOPr desensitization in rat LC neurones .....120

5.2.2 Compound 1-induced MOPr desensitization in rat LC neurones is not dependent on PKC.....122

5.2.3 Compound 1-induced MOPr desensitization in rat LC neurones is GRK-dependent 128

5.2.4 Compound 1-induced MOPr desensitization in rat LC neurones is independent of JNK .....135

5.2.5 Controls for kinase inhibition work in rat LC neurones and summary of current findings.....138

5.2.6 A summary of the mechanisms regulating Compound 1-induced MOPr desensitization in rat LC neurones .....143

5.2.7 Investigating the dependence of agonist-induced arrestin-3 recruitment on GRK2 expression in recombinant cells.....145

5.2.8 Investigating opioid-induced arrestin-2 recruitment in recombinant cells 149

5.2.9 Characterising opioid-induced MOPr internalization in recombinant cells 151

5.2.10 Defining the patterns of agonist-induced MOPr phosphorylation .....153

**5.3 Discussion .....157**

5.3.1 A summary of findings regarding the mechanisms of Compound 1-induced MOPr regulation in rat LC neurones and recombinant cells .....157

5.3.2 On positive controls for the study of the potential roles of JNK .....160

5.3.3 The potential role of off-target kinases inhibited by Compound 101 in Compound 1-induced desensitization .....160

5.3.4 On the partial inhibition of MOPr desensitization by GRK inhibitors in LC neurones 161

***Chapter 6: Discussion.....163***

**6.1 Research Summary and Introduction to Discussion .....163**

**6.2 PKC is not involved in Compound 1-induced desensitization in LC neurones 166**

**6.3 Thoughts on our approach to characterise the mechanisms involved in Compound 1-induced desensitization in LC neurones.....169**

6.3.1 Non-selective kinase inhibition .....169

6.3.2 Modulation of kinase activity through genetic approaches .....169

6.3.3 The viability of recombinant systems in the study of MOPr desensitization 170

**6.4 Relating observations of Compound 1-induced MOPr desensitization between studies in recombinant systems and LC neurones .....172**

6.4.1 Considering the influence of systems bias in the case of Compound 1 ..172

6.4.2 Potential methods to address remaining questions surrounding the mechanism of Compound 1-induced MOPr desensitization .....173

**6.5 Potential non-canonical roles of GRK in Compound 1-induced MOPr desensitization .....177**

6.5.1 GRK-dependent phosphorylation of non-C-terminal MOPr residues.....177

6.5.2 Exploring a potential non-phosphorylation-dependent mechanism of GRK in Compound 1-induced MOPr desensitization.....178

**6.6 The potential structural determinants underlying the biased signalling of Compound 1.....180**

**6.7 Investigating Compound 1-induced tolerance .....182**

**6.8 Assessing the therapeutic potential of current and future biased agonists at MOPr.....185**

**6.9 The potential of harnessing biased signalling to aid the development of effective therapeutics at other GPCR targets .....189**

**6.10 Final Conclusion .....193**

***Chapter 7: References.....194***

## Table of Figures

Figure 1.1 – A representative structure of a Class A GPCR ..... 3

Figure 1.2 – A schematic of the mechanisms and timescales of GPCR regulation ..... 8

Figure 1.3 – A schematic description of biased agonism at GPCRs ..... 12

Figure 1.4 – MOPr-dependent G protein signalling in the context of synaptic transmission ..... 18

Figure 1.5 – Agonist-selective mechanisms of MOPr desensitization dependent on agonist efficacy ..... 22

Figure 1.6 – Functional effects of MOPr-mediated G protein and arrestin signalling ..... 25

Figure 1.7 – The potential pharmacological profile of G protein-biased agonists at MOPr ..... 27

Figure 1.8 – The chemical structures of both non-biased and reportedly biased agonists at MOPr ..... 30

Figure 2.1 – The methodological principles of the G protein activation BRET assay in the case of MOPr ..... 36

Figure 2.2 – The methodological principles of the arrestin recruitment BRET assay in the case of arrestin-3 ..... 37

Figure 3.1 – Opioid-induced $G_i$ G protein activation and arrestin-3 recruitment in HEK293 cells transiently expressing recombinant MOPrs. ..... 59

Figure 3.2 – Calculation of biased agonism at MOPr through $\Delta$ normalised $E_{Max}$. ..... 64

Figure 3.3 – Calculation of biased agonism at MOPr through $\Delta\Delta\log(\tau/K_A)$ ..... 65

Figure 3.4 – Calculation of biased agonism at MOPr through $\Delta\Delta\log(\tau)$ ..... 66

Figure 3.5 – Partial antagonism of DAMGO-induced arrestin-3 recruitment by MOPr partial agonists. ..... 69

Figure 3.6 – Assessing the selectivity agonist activity of Compound 1 across the opioid receptors. ..... 72

Figure 3.7 – DAMGO inhibits electrically-evoked contractions of the RVD. ..... 75

Figure 3.8 – Single representative experiments showing competitive inhibition of DAMGO activity in the RVD by partial MOPr agonists. ..... 76

Figure 3.9 – Schild plots for inhibition of DAMGO responses in the RVD by partial MOPr agonists. ..... 77

Figure 3.10 – Combined graphs showing inhibition of DAMGO activity in the RVD by partial MOPr agonists. ..... 78

Figure 3.11 – Modulation of electrically-evoked contractions of the RVD by partial MOPr agonists. ..... 80

Figure 3.12 – SR17018 does not inhibit DAMGO-induced inhibition of electrically-evoked contractions of the RVD. ..... 81

Figure 4.1 – Example traces of opioid-evoked GIRK currents in rat LC neurones ..... 94

Figure 4.2 – Example traces showing GIRK currents evoked through MOPr and $\alpha_2$ adrenoceptor activation in rat LC neurones ..... 96

Figure 4.3 – The amplitude of peak opioid-evoked GIRK currents in rat LC neurones. 97

Figure 4.4 – Rapid desensitization of opioid-evoked GIRK currents in rat LC neurones ..... 98

Figure 4.5 – Opioid-induced desensitization in rat LC neurones ..... 99

Figure 4.6 – Noradrenaline-evoked GIRK currents in opioid-treated LC neurones ..... 100

Figure 4.7 – Decay in Compound 1 currents is not a product of peptide degradation 102

Figure 4.8 – Decay in Compound 1 currents is not a product of indirect GIRK inhibition ..... 103

Figure 4.9 – PZM21 partially antagonises morphine-evoked GIRK currents ..... 105

Figure 4.10 – Antinociception induced by Compound 1 and morphine in CD1 mice .. 108

Figure 4.11 – Compound 1-induced antinociception in C57/BL6 MOPr KO and WT mice ..... 111

Figure 5.1 – The effect of DMSO on desensitization of Compound 1-evoked GIRK currents ..... 121

Figure 5.2 – Inhibition of PKC has no effect on Compound 1-induced desensitization .....123

Figure 5.3 – Activation of PKC has no impact on Compound 1-induced desensitization .....125

Figure 5.4 –The role of PKC in morphine-induced MOPr desensitization in rat LC neurones .....127

Figure 5.5 – The GRK inhibitor Compound 101 inhibits DAMGO-induced desensitization .....129

Figure 5.6 – The GRK inhibitor Compound 101 attenuates Compound 1-induced desensitization .....130

Figure 5.7 – Inhibitors of off-target kinases inhibited by Compound 101 have no effect on Compound 1-induced desensitization .....131

Figure 5.8 – The GRK inhibitor 14as inhibits DAMGO-induced MOPr desensitization .....133

Figure 5.9 – 14as inhibits Compound 1-induced MOPr desensitization.....134

Figure 5.10 – Inhibition of JNK has no impact on acute DAMGO-induced desensitization .....136

Figure 5.11 – JNK inhibition has no effect on Compound 1-induced desensitization .137

Figure 5.12 – Examined kinase inhibitors had no effect on the magnitude of DAMGO-evoked GIRK currents.....139

Figure 5.13 – Examined kinase inhibitors had no effect on the magnitude of Compound 1-evoked GIRK currents .....140

Figure 5.14 – Kinase inhibitors and DAMGO have no heterologous effect on noradrenaline-evoked GIRK currents.....141

Figure 5.15 – Kinase inhibitors and Compound 1 have no heterologous effect on noradrenaline-evoked GIRK currents.....142

Figure 5.16 – Summarising current findings around the mechanisms of Compound 1-induced MOPr regulation .....144

Figure 5.17 – The impact of GRK2 expression on opioid-induced arrestin-3 recruitment in recombinant HEK 293 cells transiently expressing MOPr.....147

Figure 5.18 – Assessing opioid-induced arrestin-2 recruitment in recombinant HEK 293 cells expressing MOPr.....150

Figure 5.19 – Characterising opioid-induced loss of surface MOPr in recombinant HEK 293 cells through ELISA. .....152

Figure 5.20 – Determining the patterns of opioid-induced MOPr phosphorylation in recombinant HEK 293 cells through phosphospecific immunoblotting. .....156

Figure 5.21 – A schematic summary of our findings on the mechanisms of Compound 1-induced MOPr regulation in rat LC neurones and in recombinant HEK 293 cells.....158

Figure 6.1 – A schematic depicting the relative contribution of PKC and GRK to MOPr desensitization, dependent on agonist efficacy.....168

## List of Tables

Table 3.1 – The $pEC_{50}$ and $E_{Max}$ values for opioids in the $G_i$ protein activation and arrestin-3 recruitment assays. .....60

Table 3.2 – $pIC_{50}$ and maximum inhibition values for inhibition of DAMGO-induced arrestin-3 recruitment.....70

Table 3.3 – $pEC_{50}$ and $E_{Max}$ values for Compound 1 and respective tool agonists for $G_i$ G protein activation at MOPr, DOPr and KOPr .....73

Table 3.4 – Fitted $pA_2$ and slope values for partial MOPr agonists from two methods of Schild analysis. .....79

Table 5.1 – Revisiting quantification of biased agonism at MOPr in presence of overexpressed GRK2.....148

## Acknowledgements

This work was performed under the supervision of Dr Chris Bailey, Professor Eamonn Kelly and Professor Sue Wonnacott. Financial support was provided from the British Pharmacological Society through the award of the AJ Clark studentship, for which I am honoured and incredibly grateful.

I would like to extend my thanks to my supervisors for their excellent guidance throughout my PhD. Chris, I am incredibly grateful for your endless support. In particular, I am thankful for the time and patience it must have required to teach me electrophysiology in the early days. I really appreciate the great working relationship we have enjoyed over the past 3 years and I am excited for it continue. Thank you to Eamonn for all of the support and enthusiasm which helped make my time in Bristol so productive and rewarding. Thank you also to Sue for her guidance throughout my PhD, as well as the kind financial support provided during my write up. Additionally, I would like to thank Graeme Henderson for his guidance throughout my PhD. My thanks also go to the 4S annexe staff at Bath, in particular Jane and Martin, for the time they dedicated to my training, as well as their incredible patience.

I would like to thank all the members of the Bailey lab who have shaped my PhD experience so positively. In particular, thanks to Giulia for being a great friend and ephys lab mate, and also for passively teaching me a rich vocabulary of Italian expletives! Thanks also to all my fellow PhD students, past and present, from the 5W PhD office for their friendship.

My warm thanks to the excellent members of the Kelly-Henderson lab in Bristol. Special thanks to Yahia for giving me a crash course in BRET and ELISA and to Rob for his help on the tail flick experiments. Thanks also to Alex and Nokomis, my go-to-people in Bristol, for putting up with my endless stream of questions!

I would also like to thank all my friends in Bath, especially my long-time friend and housemate Will. Thanks also to my ‘Butter the Pavement’ bandmates Michael, Owen and Brandon for all the memories and for all the great gigs, which provided an excellent outlet for PhD-related frustration.

I am forever grateful to my wonderful Mum and Dad, Julie and Paul. I owe it all to the endless love, inspiration and support you have provided me throughout my life. And finally, to Char, my partner and best friend, thank you for being by my side through it all and thank you for believing in me. Thanks also for letting me live with you in your tiny Manchester flat while I wrote my thesis in lockdown!

## Abstract

Opioids remain unsurpassed as our most effective treatment for severe pain despite their propensity to induce serious on-target adverse effects. Both the therapeutic and adverse effects of opioids are mediated through their activation of the μ opioid receptor (MOPr), a G protein-coupled receptor (GPCR). The disclosure of biased signalling at GPCRs has heralded the development of a new generation of refined GPCR-targeting drugs. G protein-biased agonists at MOPr have been developed in the anticipation that they will be effective analgesics, devoid of the adverse-effects of traditional, balanced opioids. Additionally, G protein-biased MOPr agonists also have the potential to induce less receptor desensitization than balanced opioids due to their low coupling to traditional pathways of receptor regulation (arrestin and GRK). This implies that tolerance to their effects may develop slower and to a lesser extent than in the case of traditional opioids, making them clinically beneficial. As such, we sought to characterise the receptor desensitization and regulation induced by G protein-biased MOPr agonists. Firstly, we characterised the biased signalling profiles of a series of putatively G protein-biased agonists at MOPr in recombinant systems using BRET assays of G protein coupling and arrestin recruitment. These assays demonstrated that the cyclic endomorphin analogue Tyr-c[D-Lys-Phe-Tyr-Gly] (Compound 1) is a G protein-biased agonist at MOPr with a similar intrinsic activity for G protein signalling as morphine. In contrast, we demonstrate that the reportedly G protein-biased agonist PZM21 is in fact a non-biased lower efficacy agonist. We then investigated the receptor desensitization induced by previously characterised MOPr agonists in rat locus coeruleus (LC) neurones using patch clamp electrophysiology. It was hypothesised that G protein-biased agonists would induce less rapid MOPr desensitization due to their weak coupling to arrestin and GRK pathways. Intriguingly, the G protein-biased agonist Compound 1 conversely induced substantial receptor desensitization in LC neurones, to a greater degree than the balanced opioid morphine. Using pharmacological tools, it was determined that Compound 1-induced desensitization in LC neurones was in fact GRK-dependent, but PKC-independent. MOPr phosphorylation and internalization was studied in recombinant systems to outline the potential mechanisms underlying the implied GRK-dependent, arrestin-independent mechanism of Compound 1-induced desensitization. In these assays, Compound 1 induced minimal MOPr phosphorylation and internalization, in line with its G protein-biased profile. Together, the work within this thesis characterised Compound 1 as a novel G protein-biased agonist at MOPr, which intriguingly induces substantial receptor desensitization through GRK. Our findings refute the assumption that G protein-biased agonists will evade receptor desensitization and the subsequent development of tolerance.

## Abbreviations

| | |
|---|---|
| 7 transmembrane domain | 7TM |
| AC | Adenyl cyclase |
| aCSF | Artificial cerebrospinal fluid |
| ADP | Adenosine diphosphate |
| ANOVA | Analysis of variance |
| AT1R | Angiotensin II type I receptor |
| ATP | Adenosine triphosphate |
| AUC | Area under the curve |
| BBB | Blood brain barrier |
| BRET | Bioluminescence resonance energy transfer |
| BSA | Bovine serum albumin |
| cAMP | Cyclic adenosine monophosphate |
| CaSR | Calcium sensing receptor |
| CGRP | Calcitonin gene-related peptide |
| CNS | Central nervous system |
| COVID-19 | Coronavirus disease 2019 |
| CPD101 | Takeda Compound 101 |
| DAG | Diacylglycerol |
| DAMGO | [D-Ala2,N-Me-Phe4,Gly5-ol]-enkephalin |
| DMEM | Dulbecco’s modified Eagle’s medium |
| DMSO | Dimethyl sulfoxide |
| DOPr | δ opioid receptor |
| DR | Dose ratio |
| DRG | Dorsal root ganglion |
| ECL | Extracellular loop |
| ELISA | Enzyme-linked immunosorbent assay |

| | |
|---|---|
| ERK | Extracellular-signal related kinase |
| FBS | Foetal bovine serum |
| FDA | US Food and Drug Administration |
| FFA1 | Free fatty acid 1 receptor |
| GDP | Guanosine diphosphate |
| GFP | Green fluorescent protein |
| GIRK | G protein-coupled inwardly-rectifying potassium channel |
| GLP-1 | Glucagon-like peptide-1 |
| GLP-1R | Glucagon-like peptide-1 receptor |
| GPCR | G protein-coupled receptor |
| GRK | G protein-coupled receptor kinase |
| GSK3 | Glycogen synthase kinase-3 |
| GTP | Guanosine triphosphate |
| HEK 293 cells | Human embryonic kidney 293 cells |
| ICL | Intracellular loop |
| IP3 | Inositol 1,4,5-triphosphate |
| JNK | c-Jun N-terminal kinase |
| JNK2 | c-Jun N-terminal kinase 2 |
| JNK3 | c-Jun N-terminal kinase 3 |
| KO | Knockout |
| KOPr | κ opioid receptor |
| LC | Locus coeruleus |
| MAPK | Mitogen-activated protein kinase |
| mGluR | Metabotropic glutamate receptor |
| MOPr | μ opioid receptor |
| MPE | Maximum possible effect |
| MSK1 | Mitogen- and stress-activated kinase 1 |

| | |
|---|---|
| NA | Noradrenaline |
| NK-1R | Neurokinin 1 receptor |
| NLX | Naloxone |
| NOPr | nociceptin/orphanin FQ receptor |
| OX1 | Orexin receptor 1 |
| OX2 | Orexin receptor 2 |
| PAG | Periaqueductal gray |
| PFA | Paraformaldehyde |
| PH | Pleckstrin homology |
| PI3K | Phosphatidylinositol 3-kinase |
| PIP2 | Phosphatidylinositol 4,5-biphosphate |
| PKA | Protein kinase A |
| PKC | Protein kinase C |
| PLC | Phospholipase C |
| PMA | Phorbol 12-myristate 13-acetate |
| PRK2 | Protein kinase C-related protein kinase |
| RET | Resonance energy transfer |
| RGS | Regulators of G protein signalling |
| RH | Regulator of G protein signalling homology |
| Rluc | Renilla luciferase |
| ROCK2 | Rho-associated protein kinase 2 |
| RVD | Rat vas deferens |
| RVM | Rostral ventromedial medulla |
| SBDD | Structure-based drug design |
| SDS | Sodium dodecyl sulfate |
| SEM | Standard error of the mean |
| SGK1 | Serum and glucocorticoid-regulated kinase |

| | |
|---|---|
| TBS | Tris-buffered saline |
| TM | Transmembrane domain |
| VGCCs | Voltage-gated calcium channels |

# Chapter 1: Introduction

## 1.1 G protein-coupled receptors

### *1.1.1 Classification, biology and structural characteristics*

G protein-coupled receptors (GPCRs) constitute a large family of evolutionary-related membrane signalling proteins. GPCRs function as cell surface receptors, to transmit signals from the extracellular space, through the plasma membrane, to the intracellular space; enabling cells to respond to external stimuli. Canonically, GPCRs transduce signals through conformational rearrangement and subsequent functional coupling to intracellular heterotrimeric guanine nucleotide binding proteins known as G proteins (Chapter 1.1.3). There is a diverse array of stimuli to which different GPCRs can respond, including protons, photons, mechanical force, lipids, neurotransmitters and hormones. In a reflection of such diverse stimuli, GPCRs are expressed in all tissue types, with their function implicated in the regulation of many physiological and pathophysiological processes.

GPCRs represent the largest superfamily of membrane receptors, comprising over 800 different receptors, around 400 of which are olfactory (Hauser et al., 2017). The superfamily of GPCRs is sub-divided into 6 classes based on evolutionary sequence homology. 4 of these classes are found in humans: Class A (rhodopsin-like), Class B1 (secretin receptor-like), Class B2 (adhesion receptors), Class C (metabotropic glutamate receptor-like) and Class F (frizzled-like) (Schiöth et al., 2005). Class A rhodopsin-like receptors are by far the largest sub-family of GPCRs, containing approximately 670 human receptors, accounting for around 80% of the total population (Gloriam et al., 2007). The Class A family of GPCRs can be further subdivided by the type of endogenous stimuli they are activated by. These subfamilies include aminergic receptors (e.g. muscarinic acetylcholine receptors, adrenoceptors and dopamine receptors), peptide receptors (e.g. opioid receptors and orexin receptors), protein receptors (e.g. chemokine receptors), lipid receptors (e.g. cannabinoid receptors and prostanoid receptors) and nucleotide receptors (e.g. adenosine receptors and P2Y receptors) (Hauser et al., 2017). Despite belonging to a given class due to their structural homology, approximately 30% of the ~400 non-olfactory human GPCRs have not been definitively paired with their endogenous ligands, designating them as “orphan” receptors (Laschet et al., 2018; Hauser et al., 2020). Orphan GPCRs, of which a great proportion are class A receptors, represent a huge untapped source of therapeutically unexplored biology.

The GPCR family share a conserved architecture, consisting of an extracellular amino-terminus (N-terminus), 7 hydrophobic $\alpha$-helical transmembrane domains (TM1-7) connected by three extracellular and intracellular loops (ECLs and ICLs respectively), and an intracellular carboxyl-terminal (C-terminal) tail (Figure 1.1). This shared structure has led to alternative nomenclature referring to the family as 7 transmembrane domain (7TM) receptors. The ICLs serve as interaction sites for intracellular signalling proteins, including G proteins (Chapter 1.1.3.), with the individual conformation and structure of these regions defining the selectivity of G protein interactions for a specific receptor. The intracellular C-terminal tail, and in some cases the ICLs, of the receptor is involved in the regulation of receptor function as an interaction site for intracellular kinases (Chapter 1.1.4.). For non-sensory GPCRs, the hydrophobic core formed by the 7 TM domains constitutes the orthosteric binding pocket for both endogenous and exogenous ligands. The TM domain residues which form the ligand binding pocket define the binding and functional interactions of the receptor with ligands, giving the receptor stimulus specificity. While the composition of the binding pocket is quite distinct between families of GPCRs, the orthosteric binding pocket is highly conserved for GPCRs within the same sub-family (Manglik et al., 2012; Thal et al., 2016). Receptor function can also be regulated at sites outside of the orthosteric binding pocket, termed allosteric sites (Conn et al., 2009). Allosteric modulation of GPCR function can be induced by some specific exogenous ligands (Keov et al., 2011), but also modulation in the physiological functioning of the receptor such as by sodium ions at the sodium ion binding site, a well-described regulatory mechanism conserved across Class A GPCRs (Liu et al., 2012).

Over the past 20 years, recent technological breakthroughs in X-ray crystallography have facilitated a structural revolution in the field of GPCRs (Congreve et al., 2020). The developed techniques have overcome traditional problems concerning GPCR crystallography through the stabilization of receptors in a detergent solution during purification. This has been achieved through the use of thermostabilising receptor mutagenesis (Magnani et al., 2016), antibody fragments (Steyaert et al., 2011), fusion proteins (Chun et al., 2012) and high-affinity ligands (Zhang et al., 2015). To date, the structures of 70 unique GPCRs have been determined through such methods, a figure which is rising year-on-year (Congreve et al., 2020). Recently, an increasing number of GPCR structures have been solved through an alternate method: electron cryo-microscopy (cryo-EM) (Garcia-Nafria et al., 2020). For example, pioneering work illustrated the structure of agonist-bound $\mu$ opioid receptor in complex with $G_i$ G protein through cryo-EM methods (Koehl et al., 2018).

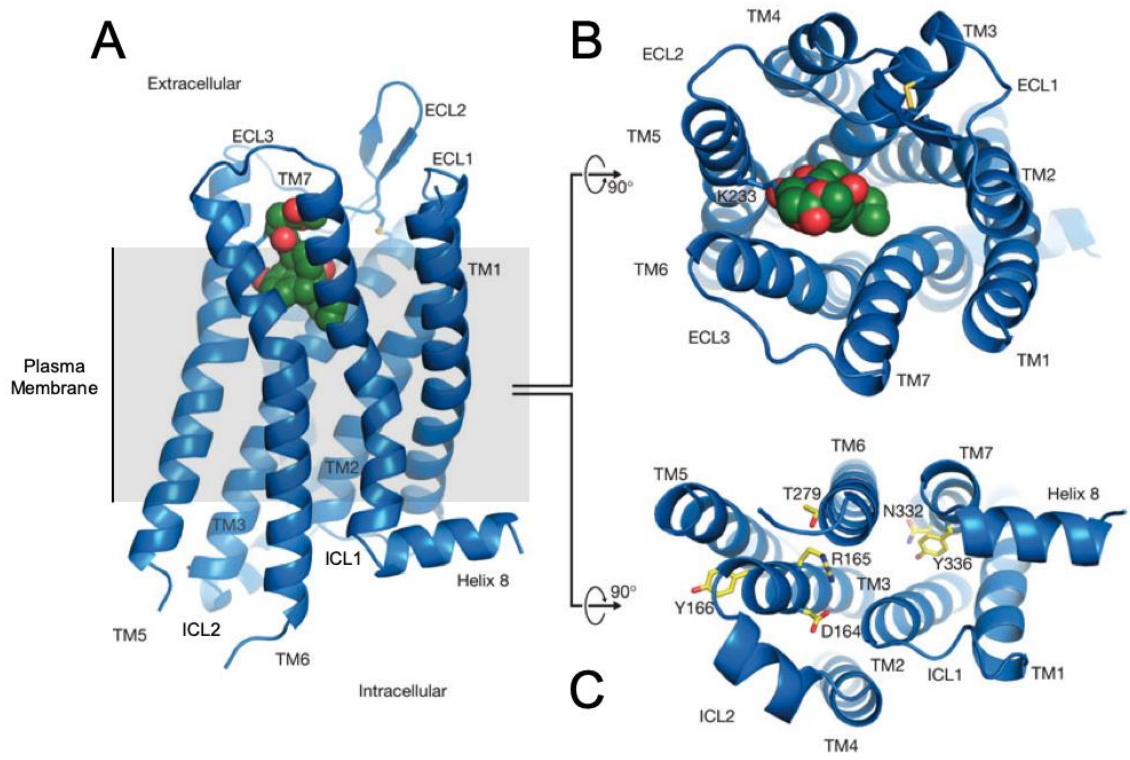


**Figure 1.1 – A representative structure of a Class A GPCR**

*A schematic representation of the inactive structure of the μ opioid receptor (blue) bound to the antagonist β-FNA (green and red spheres) showing views of the receptor from the membrane plane (A), the extracellular side (B) and the intracellular side (C). Figure is adapted from Manglik et al. (2012). TM = transmembrane helix, ECL = extracellular loop, ICL = intracellular loop.*

Detailed crystal structures of GPCRs have provided the field with remarkable insight into the relationship between receptor structure and function. For instance, comparisons of active and inactive receptor crystal structures can provide an understanding of the conformational basis of GPCR activation (Weis et al., 2018). Additionally, a crystal structure reveals the molecular shape of the orthosteric binding pocket of a receptor and the residues which constitute it, enabling refined structure-based drug design (SBDD) (Congreve et al., 2020). SBDD at GPCRs have been of particular interest to drug discovery, particularly in the refinement of ligand-specificity between largely homologous receptor subtypes. In particular, examples of crystallography-driven SBDD include the development of the adenosine 2A receptor antagonist AZD4635, which is selective for the adenosine 2A receptor over the adenosine A1 receptor (Congreve et al., 2012). This drug is now in Phase II clinical trials after showing preclinical efficacy in cancer studies as an immune modulator (Borodovsky et al., 2018). Similarly, SBDD has been utilised to

develop agonists of the M1 muscarinic receptor, a pro-cognitive therapeutic target for neurodegenerative diseases (Shirey et al., 2009). These agonists have selectivity for M1 over the other highly homologous muscarinic receptor subtypes (M2, M3 and M5 in particular) (Thal et al., 2016). While there are no current examples of licensed drugs developed with the aid of crystallography-aided SBDD, this approach will likely bear fruit in the near future with many agents in clinical trials.

### *1.1.2 GPCRs as therapeutic targets*

GPCRs are widely considered to be exemplary drug targets from many perspectives. As a family of membrane receptors, they are implicated in a large array of pathophysiological processes. Additionally, the structure of the orthosteric site of non-sensory GPCRs, which is evolutionarily designed for the binding of signalling molecules, is exceptionally well-suited to the design of compatible small synthetic molecules (Shoichet et al., 2012), giving them good druggability. The shared fundamentals of GPCR signalling and behaviour across the receptor family also give GPCRs the tendency to be relatively tractable drug targets.

As a reflection of this, recent analysis from Hauser et al. (2017) indicates that over a third of all drugs currently approved by the US Food and Drug Administration (FDA) exert their therapeutic effects through GPCRs. This equates to 475 drugs acting at 108 unique GPCR targets, highlighting the importance of GPCR-targeting agents in our current therapeutic arsenal, with the aminergic and opioid GPCR families accounting for the majority (77%) of the 108 established GPCR drug targets.

Recent trends in GPCR drug discovery have demonstrated the expansion of our pool of druggable GPCRs. There are a number of recently approved agents targeting novel GPCRs previously untargeted by established therapeutics, with many more novel GPCRs targeted by agents in clinical trials (Hauser et al., 2017). This includes the orexin receptors (Sakurai et al., 1998) and the calcitonin gene-related peptide (CGRP) receptor (Edvinsson et al., 2018), which are now targeted by clinically approved drugs for insomnia and migraine respectively (Yang, 2014; Edvinsson et al., 2018). With 66 further novel GPCR targets highlighted in clinical trials, it is hoped that the pool of druggable GPCRs will be expanded in coming years (Hauser et al., 2017). Moreover, there is an enormous untapped therapeutic potential held in the 30% of non-olfactory GPCRs that are orphan receptors (Chapter 1.1.1). Given growing evidence implicating orphan receptors in disease (Dershem et al., 2019), one would hypothesise that a number of current orphan GPCRs will come to be valuable therapeutic targets in the near future.

A number of contemporary developments in GPCR biology and pharmacology have rallied momentum in GPCR drug discovery in recent years. Firstly, while crystallography-based SBDD (Chapter 1.1.1.) has yet to be fully utilised to develop an approved therapeutic agent, it has undoubtedly transformed GPCR drug discovery (Congreve et al., 2020). The wealth of structural information now provided for GPCRs allows for the development of more selective, refined GPCR-targeting agents.

Another mechanism employed within drug discovery to refine agonist selectivity is the development of allosteric, rather than orthosteric, GPCR-targeting agents (Conn et al., 2009). By developing drugs at characterised allosteric sites, selectivity issues arising from high homology in the orthosteric sites in related receptors are effectively circumvented. A small number of allosteric modulators at GPCRs are clinically approved thus far, including cinacalcet, a positive allosteric modulator at the calcium sensing receptor (CaSR) approved for the treatment of hyperparathyroidism (de Francisco, 2005). Allosteric modulators act to increase or decrease the affinity or efficacy of endogenous signalling molecules, therefore maintaining temporal control of endogenous signalling, but in an amplified or reduced manner. This is particularly appealing for the treatment of neurological conditions such as schizophrenia, where maintaining the temporal manner of endogenous signalling may alleviate potentially serious adverse effects following pharmacological intervention (Foster et al., 2017).

Finally, the phenomenon of biased signalling, alternatively termed functional selectivity, has more recently energised GPCR drug discovery (Kenakin, 2011; Michel et al., 2018). Drug discovery groups targeting an array of GPCRs have attempted to harness biased signalling to develop more selective GPCR drugs, which may evade the traditional adverse effects of activating a GPCR by preferentially activating selected pathways downstream of receptor activation. This thesis focuses on the phenomenon of biased signalling (Chapter 1.1.6) in the context of the μ opioid receptor (MOPr) (Chapter 1.3).

### *1.1.3 G protein coupling and signal transduction*

Upon activation by an agonist, GPCRs undergo a conformational change which favours the physical interaction (coupling) of the receptor with intracellular heterotrimeric G proteins. Relatively small agonist-induced changes in conformation at the binding pocket are transduced to produce larger conformational changes in the TM helices toward the intracellular portion of the GPCR. Structural insights suggest a conserved, archetypal mechanism of activation for Class A, with activation inducing “outswing” movement of TM6 (Figure 1.1) which results in an “open” receptor confirmation which allows for the coupling of G proteins through revealing previously occluded relevant residues (Huang et al., 2015; Wang et al., 2020; Wingler et al., 2020).

The heterotrimeric G protein complex is composed of Gα, Gβ and Gγ subunits, with Gβ and Gγ forming a stable heterodimer termed Gβγ. The function of G protein complexes is dependent on guanosine nucleotide exchange at the Gα subunit, as well as the function of GTPases. In an inactive state, guanosine diphosphate (GDP) is bound to the Gα subunit of the heterotrimeric G protein complex. Upon coupling of the G protein with the activated receptor, the GPCR acts as an exchange factor to enhance the release of GDP from the G protein, leading to the subsequent binding of guanosine triphosphate (GTP). GTP binding to Gα promotes a destabilising conformational change in the G protein complex resulting in dissociation of the Gα and Gβγ subunits, which are subsequently able to interact with downstream enzymes or channels through which they modulate cellular responses. G protein signalling is terminated upon hydrolysis of GTP to GDP, a process which can be catalysed by GTPase activating proteins, also termed regulators of G protein signalling (RGS) (Oldham et al., 2008).

The G protein family consists of numerous individual subunit isoforms, with 20 different Gα isoforms, 5 different Gβ isoforms and 12 different Gγ isoforms. The coupling profile of G protein signalling downstream of a GPCR is primarily dictated by the isoform of the Gα subunit to which the receptor couples (Hepler et al., 1992). The isoforms of the Gα subunits are grouped into the following 4 subfamilies: $G\alpha_s$, $G\alpha_{i/o}$, $G\alpha_{q/11}$ and $G\alpha_{12/13}$ (Wettschureck et al., 2005). Activated $G\alpha_s$ G proteins directly bind and stimulate adenyl cyclase (AC), increasing the latter's catalytic production of the second messenger cyclic adenosine monophosphate (cAMP) from adenosine triphosphate (ATP). An increase in cAMP activates cAMP-dependent pathways including protein kinase A (PKA). Activated $G\alpha_I$ family G proteins conversely inhibit the activity of AC through direct binding, thereby inhibiting AC-dependent cAMP production from ATP. All $G\alpha_{i/o}$ family members are sensitive to pertussis toxin, which inhibits G protein function through ADP-ribose modification of a unique cysteine residue within the C-terminus of $G\alpha_{i/o}$ G proteins. Activated $G\alpha_{q/11}$ G proteins directly activate phospholipase C (PLC), which in turn hydrolyses the membrane lipid phosphatidylinositol 4,5-biphosphate ($PIP_2$) to produce the second messengers inositol 1,4,5-triphosphate ($IP_3$) and diacylglycerol (DAG). $IP_3$ initiates an increase in cytosolic calcium levels through interaction with $IP_3$ sensitive calcium ($Ca^{2+}$) channels on the endoplasmic reticulum. DAG and increased intracellular $Ca^{2+}$ both directly activate protein kinase C (PKC). $G\alpha_{12/13}$ G proteins pathways are the major pathway through which GPCRs are able to activate the Rho family of GTPases (Hart et al., 1998).

While Gα subunits were traditionally thought to be the sole transducers of G protein signalling, it is now well established that Gβγ subunits also function as signal transducers

(Campbell et al., 2018). Notably, Gβγ subunits signal through interactions with a variety of selection of ion channels, with the specificity of such interactions dependent on the associated Gα protein (Khan et al., 2013). More specifically, $G\alpha_{i/o}$-associated Gβγ subunits signal through interactions with N-type and P/Q-type calcium ($Ca^{2+}$) channels and inwardly rectifying potassium ($K^{+}$) channels (Khan et al., 2013).

### *1.1.4 Regulation of GPCR function*

The signalling of GPCRs is negatively regulated through a conserved two-step mechanism: receptor phosphorylation and the subsequent binding of arrestin proteins (Gurevich et al., 2019) (Figure 1.2).

The primary mechanism of GPCR desensitization occurs upon receptor activation, whereby serine and threonine residues of the intracellular C-terminal tail and intracellular loops of the receptor are rapidly phosphorylated by GPCR kinases (GRKs). There are seven human GRK isoforms, which can be subdivided by their structure, expression and function: GRK1-like (GRK1 and GRK7), GRK2-like (GRK2 and GRK3) and GRK4-like (GRK4, GRK5 and GRK6). The expression of the GRK1-like family proteins is restricted to the visual system, whereas GRK2-like and GRK4-like proteins are ubiquitously expressed (Pitcher et al., 1998). As soluble proteins, GRKs require specific mechanisms to control their recruitment to membrane-localised GPCRs and subsequent phosphorylation. Regarding the non-visual GRKs, GRK2/3 bind Gβγ subunits through their pleckstrin homology (PH) domains (Koch et al., 1993; Lodowski et al., 2003). The recruitment of GRK2/3 to the membrane subsequent to Gβγ dissociation thus presents a negative feedback loop of regulation for G protein signalling. GRK4/5/6 lack a PH domain and instead associate with the plasma membrane via palmitoylation (Stoffel et al., 1994). Intriguingly, GRK4/5/6 are also associated with constitutive phosphorylation of non-activated GPCRs (Li et al., 2015), whereas GRK2/3 are associated with agonist-induced phosphorylation of GPCRs (Gurevich et al., 2019). The patterns of GRK-dependent GPCR phosphorylation and its functional implications are further explored in the case of MOPr (Chapter 1.2.5).

Desensitization and receptor phosphorylation can also occur through heterologous, non-GRK dependent mechanisms. For example, both activated or non-activated GPCRs can be desensitized through second messenger-dependent kinases (such as PKA or PKC) which could themselves be activated through the activation of other receptors (Kelly et al., 2008). The mechanisms and implications of heterologous desensitization in GPCR signalling are further explored in the case of MOPr (Chapter 1.2.5).

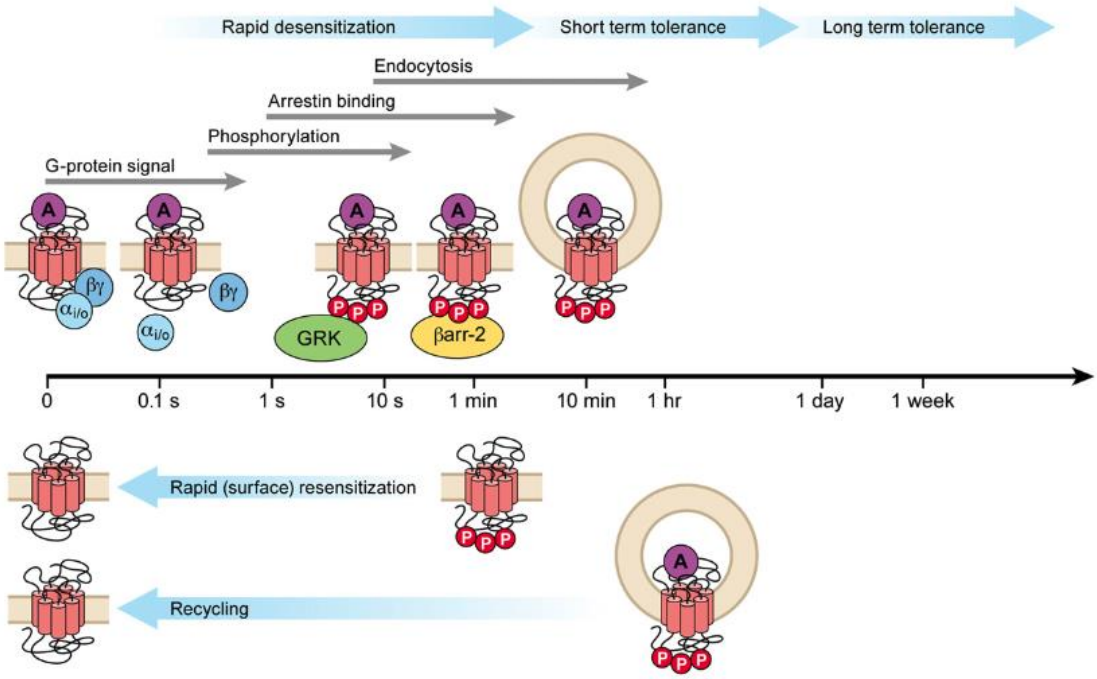


**Figure 1.2 – A schematic of the mechanisms and timescales of GPCR regulation**

*Upon agonist binding to a GPCR by an agonist (denoted A) the heterotrimeric G protein is activated and separates. Rapid receptor phosphorylation by G protein receptor kinase (GRK) family proteins occurs on the intracellular portions of the GPCR, causing desensitization of GPCR responses. The phosphorylated GPCR now has high affinity for arrestin proteins (in this case β-arrestin 2, or arrestin-3), which bind the receptor and act as adaptors for endocytotic machinery to promote GPCR internalization. The internalization of receptors can lead to the development of tolerance to the effects of an agonist. GPCR function is restored upon either dephosphorylation or, following endocytosis, reinsertion to the plasma membrane through recycling endosomes. Figure is reproduced from Williams et al. (2013).*

Phosphorylation of GPCRs by GRKs is generally insufficient to provide full desensitization of G protein signalling. Instead, the recruitment of arrestin proteins to GPCRs is essential for the extensive uncoupling of G proteins from the receptor (Figure 1.2). There are 4 isoforms of arrestin (arrestin 1-4). The expression of arrestin-1 and arrestin 4 is exclusive to the visual system, where arrestin-2 (β-arrestin-1) and arrestin-3 (β-arrestin-2) are expressed ubiquitously. The phosphorylation of GPCRs by GRKs increases the affinity of the intracellular portions of the receptor for arrestin proteins. The arrestin-bound receptor is sterically inhibited from G protein coupling, effectively desensitizing the G protein signalling of a receptor. Aside from steric hinderance, arrestin proteins function as adaptor proteins to facilitate GPCR internalization (Figure 1.2). As such, non-visual arrestins specifically bind clathrin (Goodman et al., 1996) and the clathrin adaptor AP2 (Laporte et al., 1999) to promote the formation of clathrin coated pits through which GPCRs under endocytosis (Magalhaes et al., 2012).

Following endocytosis, the vesicles containing the receptor shed their clathrin coating to become early endosomes (Hanyaloglu et al., 2008). The acidified environment of the early endosome promotes dissociation of ligand and arrestin from the receptor, as well as receptor dephosphorylation by phosphatase enzymes. The fate of the endocytosed GPCR is then dictated by endocytic sorting. GPCRs may undergo rapid recycling and membrane insertion if sorted through recycling endosomes, leading to resensitization of the receptor and restored function at the cell surface (Figure 1.2). Alternatively, GPCRs may undergo degradation through lysosomal pathways, leading to a downregulation of receptor function which is only restored following transcription and translation of new receptor protein. Emerging findings around GPCR signalling within endosomal pathways, termed compartmentalised signalling, are serving to redefine our current understanding of GPCR signalling (Irannejad et al., 2014; Pavlos et al., 2017). The pharmacological significance of compartmentalised signalling to the functionality of numerous GPCRs remains to be fully realised.

### *1.1.5 G protein-independent signalling*

Beyond their traditional function in GPCR receptor desensitization and internalization, studies over the past two decades have demonstrated that GRKs and arrestin proteins additionally serve as effective signal transducers in their own right (Gurevich et al., 2006; Gurevich et al., 2019). This implicates both GRKs and arrestins as key mediators of G protein-independent signalling downstream of GPCRs.

GRKs have been demonstrated to phosphorylate and thus regulate numerous non-GPCR proteins, including toll-like receptors, receptor tyrosine kinases as well as other

receptor serine/threonine kinases among others (Gurevich et al., 2019). While in many cases, the functional relevance of GRK-mediated regulation of these pathways is poorly defined, the numerous interactions of GRK outside of GPCR signalling suggest they hold physiologically important non-canonical roles. Phosphorylation-independent roles have also been demonstrated for GRK subtypes, illustrating another non-canonical pathway of GPCR regulation and signalling by GRK. For example, negative regulation of $G\alpha_{q/11}$ proteins by GRK2/3 has been demonstrated via a sequestration mechanism dependent on binding through its regulator of G protein signalling (RGS) homology (RH) domain (Dhami et al., 2002; Ribeiro et al., 2009). Similarly, as previously mentioned (Chapter 1.1.4.), GRK2/3 bind $G\beta\gamma$ subunits through their pleckstrin homology (PH) domain (Koch et al., 1993; Lodowski et al., 2003). In addition to mediating GRK recruitment to the membrane upon GPCR activation, this process also negatively regulates $G\beta\gamma$ function through sequestration. This has been outlined as a heterologous mechanism of desensitization for the $G\beta\gamma$-dependent function of G protein-coupled inwardly rectifying potassium channels (GIRKs) downstream of adenosine A1 and MOPr in recombinant systems (Raveh et al., 2010) and at $\kappa$ opioid receptor (Abraham et al., 2018). However, the functional relevance of this process to rapid MOPr desensitization in mature adult mammalian neurones is disputed (Llorente et al., 2012).

The first accounts of arrestin-dependent signalling illustrated that GPCR-bound arrestins promote activation of the mitogen-activated protein kinases (MAPKs) extracellular signal-regulated kinase 1 (ERK1) and ERK2 (ERK1/2), through both Src-dependent and cRaf1-dependent activation pathways (Luttrell et al., 1999; Luttrell et al., 2001). Subsequently, the number of binding partners demonstrated for arrestin has increased greatly (Xiao et al., 2007), firmly demonstrating them as genuine mediators of G protein-independent signalling. Other signalling pathways activated through visual arrestins include c-Jun N-terminal kinase 3 (JNK-3) (McDonald et al., 2000), glycogen synthase kinase-3 (GSK3) (Beaulieu et al., 2007) and phosphatidylinositol 3-kinase (PI3K) (Wang et al., 2006).

However, recent findings suggest that arrestin-dependent activation of ERK1/2 signalling does not occur in cells genetically devoid of G protein signalling (Alvarez-Curto et al., 2016; Grundmann et al., 2018). Additionally, GPCR-dependent ERK1/2 signalling is relatively unaltered in cells lacking visual arrestins, with arrestin-dependent ERK1/2 itself dependent on prior activation of G protein (O'Hayre et al., 2017; Grundmann et al., 2018). Together, these findings do not refute the existence of arrestin-dependent ERK1/2 signalling, but they do imply that this process is instead mainly dependent on G protein signalling (Gurevich et al., 2019).

### *1.1.6 Biased agonism at GPCRs*

Historically, GPCRs had been conceptualised as simple switches, residing in either an active or inactive state. In this regard, GPCRs were envisaged to couple to one G protein and its respective signalling pathway. This simple perception of GPCR signalling has been eroded by observations that (i) GPCRs are able to couple to more than one individual family of G protein isoforms (Crawford et al., 1992; Schmidt et al., 1995) and moreover that (ii) GPCRs can signal through G protein-independent pathways, such as via arrestins (Chapter 1.1.5.) (Gurevich et al., 2006; Gurevich et al., 2019). As such, GPCRs are now considered allosteric microprocessors, which can signal through multiple transducers (Smith et al., 2018). This concept is based on the notion that GPCRs can occupy a range of conformational states, which have different affinities for the coupling of intracellular signalling partners (Smith et al., 2018).

The term biased agonism (Jarpe et al., 1998) refers to the ability of an agonist to stabilise different receptor conformations which preferentially couple to individual intracellular signalling partners at the expense of others (Kenakin, 2011; Kenakin, 2018) (Figure 1.3). For example, a GPCR agonist preferentially signalling through specific G protein subtypes over others, (e.g. $G\alpha_q$ over $G\alpha_i$), or an agonist favouring the activation of G protein over arrestin signalling pathways, or vice versa (Figure 1.3).

Biased signalling has been harnessed by drug discovery groups to innovate the development of GPCR-targeting drugs, with the potential that biased agonists may represent new improved therapeutics. The rationale for harnessing biased agonism to yield improved therapeutics broadly follows one of two scenarios (Kenakin, 2017). Firstly, biased agonism could be used to emphasize favourable GPCR-dependent signalling. For example, at glucagon-like peptide-1 (GLP-1) receptor (GLP-1R), GLP-1 dependent insulin release is arrestin-2 dependent (Sonoda et al., 2008), suggesting arrestin-biased GLP-1R ligands may be superior to non-biased (or “balanced”) agonists. Secondly, biased agonism could be utilised to de-emphasize the signalling of pathways which mediate clinically adverse effects of GPCR activation. This rationale is best explored at MOPr, where G protein-biased agonists have been developed with the intention of evading opioid-induced respiratory depression, constipation and tolerance which has been suggested to be arrestin-dependent (Raehal et al., 2005), but, in case of respiratory depression and constipation, see (Kliewer et al., 2019; Kliewer et al., 2020) (Chapter 1.3.1.).

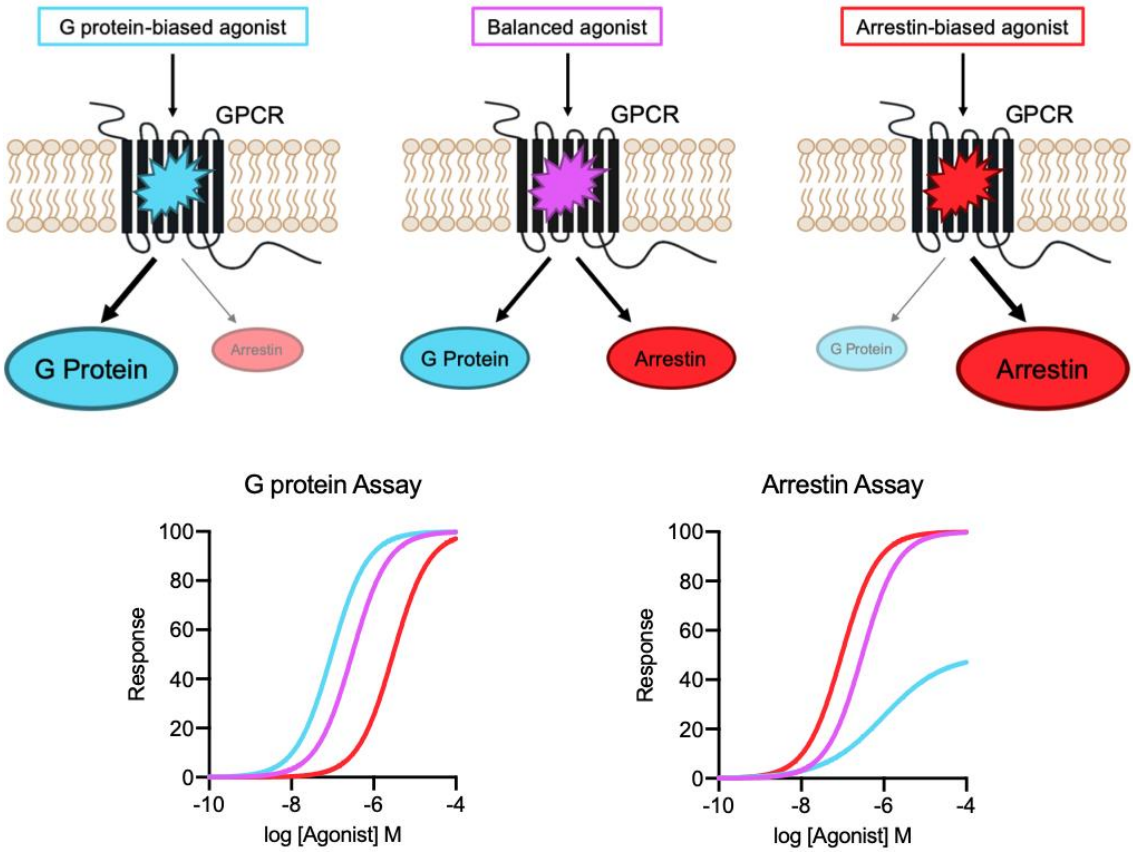


**Figure 1.3 – A schematic description of biased agonism at GPCRs**

*A balanced, or non-biased, agonist (pink) stabilises an active receptor conformation which couples equally to G protein and arrestin signalling pathways. A G protein-biased agonist (light blue) stabilises a distinct receptor conformation which favours coupling to G protein, with minimal coupling to arrestin pathways. The arrestin-biased agonist (red) stabilises another distinct receptor conformation, which preferentially couples to arrestin, with minimal G protein coupling. Expected concentration-response curves for G protein signalling and arrestin signalling in cell-based assays are presented for each agonist (pink = balanced agonist, light blue = G protein-biased agonist, red = arrestin-biased agonist). When compared to the balanced reference agonist, responses of the G protein-biased agonist for G protein signalling are leftward shifted, but responses are reduced and rightward shifted for arrestin signalling. G protein responses induced by the arrestin-biased are rightward shift compared to the balanced agonist, but arrestin responses evoked by this arrestin-biased agonist are leftward shifted.*

Another example where biased agonism could allow for the effective evasion of particular clinical effects of GPCR activation is the development of G protein-biased agonists at the δ opioid receptor (Conibear et al., 2020), for which the development of agonists as analgesics has previously been hampered by proconvulsive effects of balanced δ opioid receptor agonists (Broom et al., 2002).

Some approved GPCR-targeting ligands have retroactively been characterised as biased, including carvedilol, an arrestin-biased agonist at β adrenoceptors (Wisler et al., 2007) and nalfurafine, a G protein-biased κ opioid receptor agonist (Schattauer et al., 2017). However, as the rational development of biased ligands at GPCRs is still in its infancy, we are yet to observe the widespread clinical approval of ligands specifically designed to be bias. The exception to this is the recent clinical approval of TRV130 (oliceridine, Trevena Inc.) (Lambert et al., 2020), a reportedly G protein-biased agonist at MOPr (DeWire et al., 2013); but see (Yudin et al., 2019; Gillis et al., 2020a; Singleton et al., 2021), approved for the treatment of severe pain. MOPr (Chapter 1.2.) is arguably the most advanced target for the development of biased ligands at GPCRs (Chapter 1.3.).

Aside from MOPr, one of the first drugs to harness biased agonism and so enter clinical trials was the angiotensin II type I receptor (AT1R) agonist TRV120027 (TRV027), developed by Trevena Inc. TRV027 was specifically developed as an arrestin-biased agonist, effectively acting as an antagonist for G protein-mediated AT1R signalling induced by endogenous angiotensin (Violin et al., 2010). TRV027 demonstrated efficacy in preclinical models of congestive heart failure with reduced blood pressure and, unlike conventional clinically used AT1R antagonists, increased cardiac performance (Boerrigter et al., 2011). However, TRV027 failed to meet its primary endpoint in a Phase II clinical trial (Pang et al., 2017). Interestingly, arrestin-biased AT1R agonists have recently been suggested as treatments for coagulopathy associated with coronavirus disease 2019 (COVID-19) (Manglik et al., 2020), with TRV027 currently under repurposing clinical trials for this indication.

Ligand bias is typically assessed through the definition of pharmacological parameters (efficacy, potency) in separate cell signalling assays performed in recombinant systems, yielding graphs of the type presented in Figure 1.3. The quantification of biased agonism has developed over the past decade, with common analyses often founded on utilisation of the operational model (Black et al., 1983; Kenakin, 2017). The optimisation of biased signalling within drug discovery is limited by the often-unappreciated technical complexity of such experiments and analysis. For one, kinetic context at both ligand-receptor level, and in the comparison of ligand effects between assays run under

different time-frames, complicates interpretation of biased agonism (Lane et al., 2017). In addition, in recombinant systems, the differential levels of signal amplification between G protein and arrestin signalling assays often result in confounding results whereby partial agonists appear as biased agonists, due to the contributing effect of receptor reserve (Kelly, 2013; Gillis et al., 2020c).

Additionally, translating of defined signalling bias from *in vitro* observations to *in vivo* therapeutic effects is a particular challenge (Kenakin, 2018; Michel et al., 2018). Cellular context, in particular the stoichiometry ratios and levels of receptor and signalling proteins expressed in a specific cell, can impact the relative function of biased agonists (Kenakin, 2020). As such, cellular context at therapeutically interesting cell populations could lead to unanticipated effects of biased agonists *in vivo*. More broadly, one could argue that only with the advent of recent technological advances are we really coming to understand the specific signalling pathways responsible for the specific GPCR-dependent physiological responses. Accordingly, it may be too soon to select a desirable bias profile for GPCR ligands under development (Michel et al., 2018) (Chapter 6.8).

## 1.2 The μ opioid receptor (MOPr) system

### *1.2.1 Opioids and the opioid system*

Substances derived from the opium poppy plant *Papaver somniferum*, termed opiates, have been used for millennia, both therapeutically for their analgesic properties and recreationally for their ability to induce euphoria for millennia (Brownstein, 1993). In the modern day, opioids as a drug class remain unsurpassed as our most effective analgesics for the treatment of significant pain. However, their clinical utility has been limited by an assortment of common, on-target adverse effects. These include the risk of developing addiction (due to their euphoric, rewarding nature), constipation, respiratory depression, and the loss of therapeutic effect over repeat administration (termed tolerance).

In the early 19$^{th}$ century, morphine was isolated as an active opiate from the opium poppy, allowing for its use in surgery and for post-operative pain (Brownstein, 1993). However, the characteristic adverse effects of morphine fostered a century-spanning drive to develop safer opioids, without the typical addictive properties. Heroin was synthesised in the late 19$^{th}$ century as one of the first opioids developed as a potent morphine alternative, purportedly devoid of abuse liability. While in hindsight this appears rather ironic, in reality this presents merely the first of several similar claims for novel opioids, spanning up to the modern day. Regardless, the unrelinquishing efforts of medicinal chemistry to develop the 'holy grail', an opioid devoid of adverse effects (Corbett et al., 2006), have yielded thousands of opioids, providing the area with a rich pharmacology.

In the 1970s, endogenous opioid peptides were first identified with the discovery of the enkephalins by John Hughes and Hans Kosterlitz (Hughes et al., 1975). Subsequent studies have characterised a number of other endogenous opioid peptides including the endorphins and the dynorphins (Corbett et al., 2006). These peptides are generated by the proteolytic cleavage of the precursor proteins pro-enkephalin (the enkephalins), pro-opiomelanocortin (the endorphins) and prodynorphin (the dynorphins). The synthetic tool peptide DAMGO ([D-Ala$_2$,N-Me-Phe$_4$,Gly$_5$-ol]-enkephalin) is a highly MOPr-selective agonist derived from the enkephalins (Figure 1.8). Despite their isolation from bovine brain tissue (Zadina et al., 1997), the selective MOPr-targeting endomorphin peptides (endomorphin-1 and endomorphin-2) are not currently definitively classified as endogenous opioids as their respective precursor protein or encoding gene have not been identified (Terskiy et al., 2007).

### *1.2.2 The opioid receptor family*

All opioid analgesics, including morphine, exert their therapeutic and adverse effects through agonist activity at the μ opioid receptor (MOPr) (Matthes et al., 1996). The MOPr is one subtype among the opioid receptor family, which includes the δ opioid receptor (DOPr) and κ opioid receptor (KOPr). These classical opioid receptors share a high level of sequence homology (around 70%) and to a degree share an overlapping pharmacology (Mollereau et al., 1994). Later, a previously orphan receptor, the nociceptin/orphanin FQ receptor (NOPr), was identified and which has relatively high sequence homology with the classical opioid receptors (Henderson et al., 1997). However, the pharmacology of NOPr is markedly different to that of the classical opioid receptors, owing to low homology in its orthosteric binding site (Thompson et al., 2012). All opioid receptors are G protein-coupled receptors (GPCRs) of the Class A family. In recent years, high-resolution crystal structures (Chapter 1.1.1.) of MOPr (Manglik et al., 2012; Huang et al., 2015; Koehl et al., 2018), DOPr (Granier et al., 2012; Fenalti et al., 2015), KOPr (Che et al., 2018), and NOPr (Thompson et al., 2012) have all been solved.

There are currently 41 clinically approved therapeutics targeting opioid receptors (Hauser et al., 2017), all of which primarily target MOPr. While DOPr and KOPr present promising therapeutic targets for the development of analgesics, as well as in other indications, particularly emotional disorders, drug discovery programmes targeting these receptors have been hindered by the proconvulsive effects of DOPr activation (Pradhan et al., 2011) and the dysphoric and hallucinogenic effects of KOPr activation (Crowley et al., 2015).

The opioid system, consisting of the opioid receptors and the endogenous opioid peptides (Chapter 1.2.1.) broadly functions as a central regulator of pain control and is a key mediator of hedonic homeostasis. The opioid receptors are widely expressed in the central and peripheral nervous system (Mansour et al., 1994; Calo et al., 2000), as well as in non-neuronal cells (Hutchinson et al., 2011). Specifically, regions particularly high in MOPr expression include the periaqueductal grey (PAG), the locus coeruleus (LC), the thalamus, dorsal root ganglion (DRG) and the dorsal horn of the spinal cord (Pasternak et al., 2013), regions widely implicated in pain perception and analgesia (Chapter 1.2.4.).

### *1.2.3 G protein-dependent signalling of MOPr*

In neurones, activation of MOPr broadly acts as an inhibitor of neuronal signalling. Upon activation, MOPr couples to inhibitory G proteins of the $G\alpha_{i/o}$ family, a shared characteristic of all opioid family GPCRs. Upon MOPr-dependent activation and separation of heterotrimeric G proteins, the dissociated $G\alpha_{i/o}$ proteins inhibit adenyl cyclase preventing generation of cAMP (Minneman et al., 1976) (Figure 1.4). This reduction in cAMP levels reduces the downstream activity of the cAMP-dependent kinase PKA.

However, the modulation of ion channels through the dissociated $G\beta\gamma$ subunit presents the principle mechanism through which MOPr modulates neuronal function. Presynaptically, MOPr activation induces $G\beta\gamma$-dependent inhibition of voltage-gated calcium channels (Schroeder et al., 1991; Seward et al., 1991). This process inhibits the calcium-dependent fusion of synaptic vesicles with the presynaptic membrane, reducing subsequent neurotransmitter release. Postsynaptically, $G\beta\gamma$ activates G protein-coupled inwardly-rectifying potassium (GIRK) channels (Williams et al., 1982; North et al., 1985). The MOPr-dependent activation of GIRK channels causes an increase in potassium conductance within affected neurones, efflux of $K^+$ ions, and hyperpolarisation of the cell membrane, preventing depolarisation and neuronal firing.

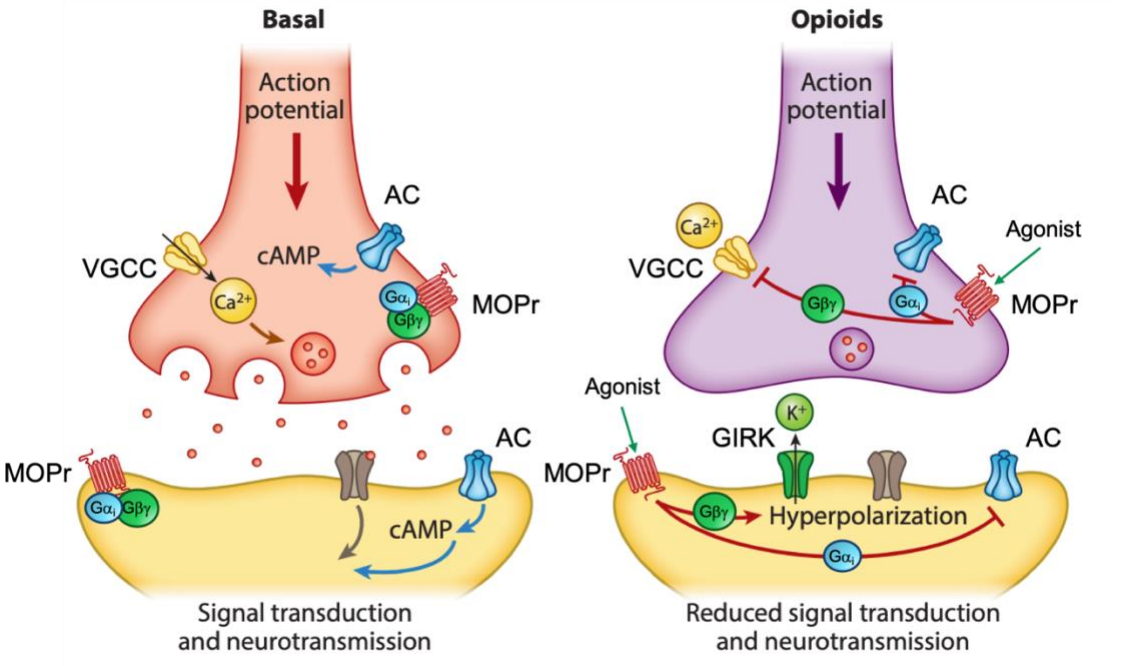


**Figure 1.4 – MOPr-dependent G protein signalling in the context of synaptic transmission**

*The presynaptic and postsynaptic effects of agonist-evoked MOPr-dependent G protein signalling on transmission of nociceptive signals. Under basal conditions (left) a noxious stimulus triggers the firing of an action potential. Upon reaching the synaptic terminal, the depolarising action potential triggers the opening of presynaptic voltage-gated calcium channels (VGCCs), propagating the fusion of synaptic vesicles with the membrane and subsequent neurotransmitter release. These neurotransmitters (e.g. glutamate) then activate postsynaptic AMPA and NMDA receptors, to transduce nociceptive signals along pain circuits. Agonist-induced activation of MOPr (right) promotes activation and dissociation of heterotrimeric $G_i$ G proteins, with activated $G\alpha_i$ subunits downstream of both pre- and postsynaptic MOPr inhibiting adenyl cyclase (AC) to reduce cAMP production. Presynaptically, activated $G\beta\gamma$ subunits inhibit VGCC opening, resulting in reduced neurotransmitter release. Postsynaptically, activated $G\beta\gamma$ subunits activation G protein gated inwardly rectifying potassium channels (GIRKs), causing membrane hyperpolarisation. Through these mechanisms, the MOPr-mediated effects of opioids reduce transduction of nociceptive stimuli. Figure adapted from Corder et al. (2018).*

### *1.2.4 Opioid-induced analgesia*

Opioids have been used for millennia to provide analgesia, and their clinical value in the treatment of severe pain remains unsurpassed today. The action of opioids on pain is selective, with opioids modulating the perception of pain without interfering with the basic sensations such as light touch, where local anaesthetics such as lidocaine completely block sensory transmission (Pasternak et al., 2013). Opioid-induced, MOPr-dependent analgesia occurs at numerous sites within both peripheral and central neuronal circuits which shape the pain experience, as summarised below.

Pain is vital to survival as a natural physiological response to noxious stimuli. As such, pain prevents injury through evoking reflexive reactions away from harmful stimuli and promoting a tendency to protect an injured, pained body part allowing it to heal. Noxious stimuli are first perceived by sensory neurones of dorsal root ganglia (DRG) and trigeminal ganglia which innervate peripheral tissue, relaying this information to the spinal cord and medulla. The somatosensory neurones of the DRG transduce pain signals through the dorsal horn to second-order neurones in the spinal cord through release of pronociceptive neurotransmitters, including glutamate, substance P and calcitonin gene-related peptide (CGRP). Opioid receptors, including MOPr, are widely expressed at a number of sites which converge in the dorsal horn, including presynaptically on peripheral somatosensory neurones of the DRG, postsynaptically on second-order projection neurones and on excitatory interneurons (Arvidsson et al., 1995; Aicher et al., 2000; Corder et al., 2018). Activation of opioid receptors in this region, and ensuing regions mentioned, produces antinociception, through limiting the release of pro-nociceptive neurotransmitters (presynaptic) and restricting the excitability of postsynaptic neurones through the ion channel-dependent mechanisms outlined above (Chapter 1.2.3, Figure 1.4). The peripheral MOPrs of the DRG can be selectively targeted by drugs with low blood-brain-barrier permeability, with some results suggesting they can produce analgesia without CNS-related adverse effects (Vadivelu et al., 2011). However, recent work has highlighted that DRG MOPrs are not required for the antinociception induced by system morphine administration (Corder et al., 2017). This highlights the reliance of opioid analgesia on the function of MOPr in central pain pathways, outlined below.

The second-order neurones of the dorsal horn propagate noxious stimuli to the thalamus, forming the ascending anterolateral tract. Here these neurones synapse with third-order neurones which project this signal to the somatosensory cortex resulting in the perception of pain (Corder et al., 2018). Aside from the somatosensory cortex, numerous thalamic projections, including those to the anterior cingulate cortex and amygdala, form

the affective component of pain, which coalesce to construct the perception of pain as a complex, subjective and emotional process (Corder et al., 2018). This is of particular interest in opioid analgesia, where patient reports typically suggest that under morphine, the sensation of pain is still present but that aversive qualities are reduced (Price et al., 1985). In a similar vein, release of endogenous opioid release in the anterior cingulate cortex is a well-documented mechanism through which placebo-induced analgesia can occur (Bingel et al., 2006).

Of particular interest to the action of opioids is the descending pain modulatory pathway, which modulates nociceptive signalling at the level of the dorsal horn. The periaqueductal grey (PAG), locus coeruleus (LC) and principally the rostral ventromedial medulla (RVM) form the key nodes involved in the descending pain modulatory system. Indeed, microinjection of the selective MOPr agonist DAMGO into the PAG or RVM is sufficient to produce opioid-induced analgesia (Rossi et al., 1994), with rich MOPr expression present in the PAG, LC and RVM (Mansour et al., 1994).

### *1.2.5 Regulation of MOPr signalling*

As outlined in Chapter 1.1.4, the regulation of MOPr is broadly underpinned by a two-step process. MOPr regulation is initiated by the largely GRK-dependent phosphorylation of the intracellular loops and C-terminal tail of MOPr, with subsequent arrestin recruitment leading to receptor desensitization and internalization. (Chapter 1.1.4, Figure 1.2).

The two primary sites of agonist-induced phosphorylation at MOPr are the $^{354}$TSST$^{357}$ and $^{370}$TREHPSTANT$^{379}$ cassettes, located in the C-terminal tail (Lemel et al., 2020). As AGC family protein kinases, GRKs phosphorylate serine and threonine residues within these cassettes. The study of opioid-induced receptor phosphorylation has been progressed by the development of phosphorylation state-specific antibodies (Doll et al., 2011) and more recently phosphorylation-site deficient MOPr mutants (Kliewer et al., 2019). Agonist-induced MOPr phosphorylation within the $^{370}$TREHPSTANT$^{379}$ cassette is hierarchical, where all opioids appear to phosphorylate Ser$^{375}$, but sequential phosphorylation of flanking S/T residues within this cassette (Thr$^{370}$, Ser$^{376}$ and Ser$^{379}$) is observed for high efficacy agonists such as DAMGO, but less so for partial agonists such as morphine (Just et al., 2013). The phosphorylation of these MOPr residues in HEK 293 cells induced by DAMGO has been demonstrated to be dependent on GRK2 and GRK3, where morphine-induced Ser$^{375}$ appeared to be dependent on GRK5 (Doll et al., 2012). GRK-dependent phosphorylation of the $^{370}$TREHPSTANT$^{379}$ motif is necessary for sustained MOPr interaction with arrestin-3, and the consequent internalization and downregulation of MOPr signalling (Miess et al., 2018) (Chapter 1.1.4, Figure 1.2).

Studies in CRISPR/Cas9-edited HEK 293 cells have demonstrated that MOPr internalization and arrestin recruitment induced by high efficacy MOPr agonists is primarily dependent on GRK2 rather than GRK3 (Møller et al., 2020)

The role of agonist-induced GRK-dependent phosphorylation in rapid MOPr desensitization has been extensively studied in the more physiological setting of the locus coeruleus (LC) through electrophysiological experiments in brain slices (Birdsong et al., 2020). Potassium currents evoked through the opening of GIRK channels downstream of MOPr activation provide a real-time measure of MOPr function, and its rapid desensitization. Pharmacological inhibition of GRK by Compound 101 (a reportedly GRK2/3 selective inhibitor (Thal et al., 2011)) inhibits the rapid MOPr desensitization induced by DAMGO, morphine, Met-enkephalin and endomorphin-2 in rat LC neurones (Lowe et al., 2015). The importance of these S/T sites in MOPr desensitization in LC neurones has also been highlighted genetically, with Met-enkephalin-induced rapid MOPr phosphorylation diminished in both mice and rats expressing the phosphorylation-site deficient MOPr mutant constructs (Arttamangkul et al., 2019a; Kliewer et al., 2019).

Other intracellular kinases have been described to regulate rapid desensitization of MOPr, the most prominent of which is Protein Kinase C (PKC) (Kelly et al., 2008). In recombinant systems, inhibition of PKC reduces MOPr desensitization induced by morphine, but not DAMGO (Johnson et al., 2006). Similarly, in rat LC neurones, activation of PKC through either phorbol 12-myristate 13-acetate (PMA) or activation of $G_q$-coupled $M_3$ muscarinic receptors specifically increases rapid MOPr desensitization evoked by morphine and Met-enkephalin, but not DAMGO (Bailey et al., 2004). Evidence for the role of PKC in desensitization induced by morphine, but not DAMGO, is strengthened by findings in LC neurones from PKC$\alpha$ knockout mice (Bailey et al., 2009b). Intriguingly, the overexpression of a dominant negative GRK2 mutant in rat LC neurones inhibited DAMGO-induced MOPr desensitization but had no effect on morphine-induced MOPr desensitization (Bailey et al., 2009b). Together, the relative contribution of GRK and PKC to MOPr-desensitization is hypothesised to be agonist-selective, dependent on the intrinsic efficacy of the agonist (Kelly et al., 2008). As such, low efficacy partial agonists such as morphine primarily induce MOPr desensitization through PKC, with little GRK involvement. Conversely, high efficacy full agonists such as DAMGO evoke MOPr desensitization solely through GRK, with no PKC involvement (Figure 1.5). The precise mechanisms underpinning the agonist-induced regulation of MOPr by PKC are poorly understood. There is however some evidence that $Ser^{363}$ and $Thr^{370}$ undergo PKC-dependent phosphorylation induced by PMA and morphine in recombinant systems (Doll et al., 2011; Feng et al., 2011).

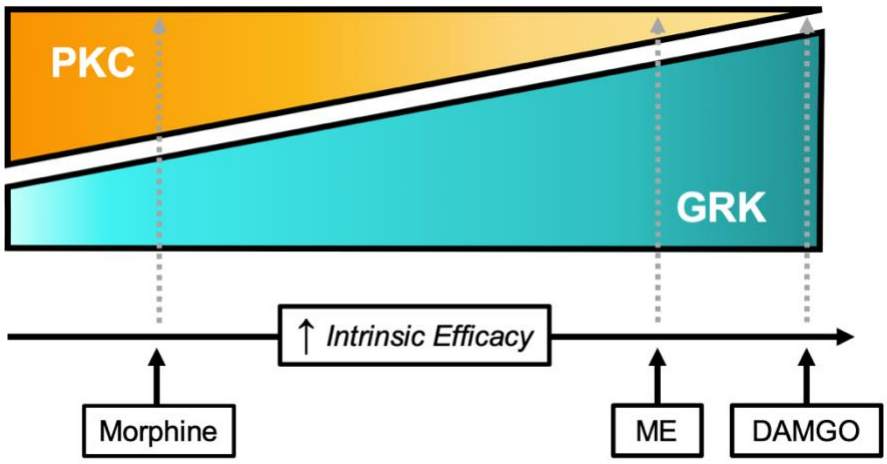


**Figure 1.5 – Agonist-selective mechanisms of MOPr desensitization dependent on agonist efficacy**

*An illustration of the current hypothesis around agonist-selective mechanisms of MOPr desensitization with relation to the relative contribution of PKC and GRK. MOPr desensitization induced by the partial agonist morphine is primarily mediated by PKC, with a smaller contribution by GRK. MOPr desensitization induced by the full agonist DAMGO is regulated solely by GRK with no contribution from PKC. Met-Enkephalin, an agonist of slightly lower efficacy than DAMGO, induces MOPr desensitization primarily through GRK, however PKC also has been demonstrated to play a partial role. Together this suggests the relative contribution of PKC to agonist-induced MOPr desensitization scales dependent on agonist efficacy. The presentation of this diagram was adapted from Kelly et al. (2008).*

There are a wide range of additional protein kinases which have reported roles in MOPr regulation (Williams et al., 2013). One such kinase is c-Jun-N-terminal kinase 2 (JNK2). JNK2 has been implicated as a mediator of analgesic tolerance to morphine in mice (Melief et al., 2010). Additionally, JNK2 has been shown to regulate cellular tolerance to morphine in dorsal root ganglion neurons (Mittal et al., 2012). Other implicated kinases include extracellular signal regulated 1/2 (ERK1/2) (Macey et al., 2006; Dang et al., 2009) phospholipase D2 (Koch et al., 2004) and c-Src (Walwyn et al., 2007).

Drug tolerance is defined as a loss of responsiveness to an agonist upon repeated exposure (Williams et al., 2013). The phenomenon of opioid tolerance is evident in clinical practice and also in whole-animal studies (McQuay, 1999; Morgan et al., 2011). In both cases, the precise cellular and molecular mechanisms underlying these

processes are difficult to resolve. However, there is a good body of evidence that agonist-induced MOPr desensitization, through phosphorylation and internalization, is an important molecular mechanism as a progenitor of tolerance (Bailey et al., 2009a; Arttamangkul et al., 2019a). The role of GRK and arrestin proteins in the development of tolerance to opioids has been demonstrated through the use of genetically modified mice.

Pivotal early studies in arrestin-3 knockout mice demonstrated that analgesia induced by morphine was enhanced and prolonged relative to wild type mice, with the degree of tolerance developed to the antinociceptive effects of morphine diminished (Bohn et al., 1999; Bohn et al., 2000; Bohn et al., 2002). Genetic studies into the role of GRK, in particular GRK2, as the key modulator of MOPr phosphorylation and tolerance, have been limited given that homozygous deletion of GRK2 is embryonically lethal (Lemel et al., 2020). Conditional or inducible GRK2 knockout animals may present a future strategy to address this, alongside the recent development of systemically active pharmacological GRK inhibitors (Waldschmidt et al., 2017). However, more recent approaches have studied the role of GRK phosphorylation in opioid-induced tolerance using phosphosite-deficient MOPr mutant mice. This was first examined in MOPr mutants in MOPr mutants in which the principal GRK phosphorylation site $Ser^{375}$ was substituted for alanine (S375A), and consequently analgesic tolerance to DAMGO and fentanyl, but not morphine, were diminished (Grecksch et al., 2011). More recently, knock-in mice expressing a 'total phosphosite-deficient' MOPr have been generated, with alanine substitutions for all 11 serine/threonine residues within the C-terminal tail (11S/T-A) (Kliewer et al., 2019). In the 11S/T-A mice, antinociceptive tolerance to fentanyl and morphine is significantly reduced, highlighting that phosphorylation of these residues is necessary for the development of tolerance to both high and low efficacy agonists (Kliewer et al., 2019). Intriguingly, these studies replicated previous findings for S375A mice, with tolerance to fentanyl but not morphine diminished, suggesting that phosphorylation of C-terminal S/T residue(s) outside of $Ser^{375}$ regulates morphine tolerance (Grecksch et al., 2011; Kliewer et al., 2019).

In parallel with findings for morphine-induced MOPr desensitization, PKC has also been demonstrated to be a key mediator of antinociceptive tolerance to morphine through use of pharmacological PKC inhibitors (Bohn et al., 2002; Hull et al., 2010). Additionally, the agonist-selective mechanisms of MOPr desensitization previously highlighted (Figure 1.5) are mirrored for opioid-induced tolerance, with the high efficacy agonist DAMGO inducing tolerance through GRK with no PKC involvement and morphine, a lower efficacy agonist, inducing tolerance through PKC with little GRK involvement (Hull et al., 2010).

### *1.2.6 G protein-independent signalling of MOPr*

As previously described in broad terms, aside from their function in GPCR regulation, arrestins and GRKs activated downstream of GPCRs are able to function as platforms for G protein-independent GPCR signalling (Chapter 1.1.5). The principal signalling pathway through which arrestin-dependent signalling occurs appears to involve the activation of ERK1/2 MAPKs (Luttrell et al., 1999; Luttrell et al., 2001).

Particular interest in the physiological relevance of this signalling originated from pivotal work in arrestin-3 knockout mice (Bohn et al., 1999; Bohn et al., 2000; Raehal et al., 2005). As expected, initial findings in this model demonstrated the importance of arrestin proteins in the development of opioid tolerance (Bohn et al., 1999). Subsequent work within these models intriguingly showed that morphine-induced constipation and respiratory depression were reduced in the arrestin-3 knockout mice (Raehal et al., 2005), implying that these common opioid-induced on-target adverse effects were mediated by G protein-independent, arrestin-3-dependent mechanisms. These findings fostered a dominant hypothesis within the opioid field, that the analgesic effects of MOPr activation are G protein-dependent, but the clinically limiting adverse effects of MOPr activation are arrestin-3-dependent (Figure 1.6). As a direct consequence of this, drug discovery groups have sought to harness biased agonism at MOPr in anticipation of developing safer opioid analgesics (Chapter 1.3) (Conibear et al., 2019).

However, recent evidence has directly contradicted previous findings in arrestin-3 knockout mice (Gillis et al., 2020b). Firstly, in mice expressing phosphosite-deficient MOPr the observed degree of opioid-induced respiratory depression and constipation was similar to that in wild type animals (Kliewer et al., 2019). Additionally, recent studies in arrestin-3 knockout mice failed to reproduce the original findings of Raehal et al. (2005), with morphine- and fentanyl-induced respiratory depression persisting in arrestin-3 knockout mice (Kliewer et al., 2020). In addition, recent mechanistic evidence in brain regions regulating respiratory function have similarly demonstrated that opioid-induced respiratory depression occurs in the main through activation of GIRK channels and inhibition of VGCCs downstream of MOPr activation, not through arrestin-mediated signalling (Levitt et al., 2015; Montandon et al., 2016; Wei et al., 2019). Together, these data imply that GRK/arrestin-dependent MOPr signalling does not regulate specific adverse effects of opioids as previously hypothesised (Figure 1.6). However, within this new evidence, it is clear that in mice expressing phosphosite-deficient MOPr, morphine and fentanyl-induced receptor desensitization and antinociceptive tolerance is reduced (Kliewer et al., 2019). In line with findings in arrestin-3 knockout mice (Bohn et al., 2000), this reaffirms the role of GRK/arrestin pathways in MOPr regulation (Figure 1.6).

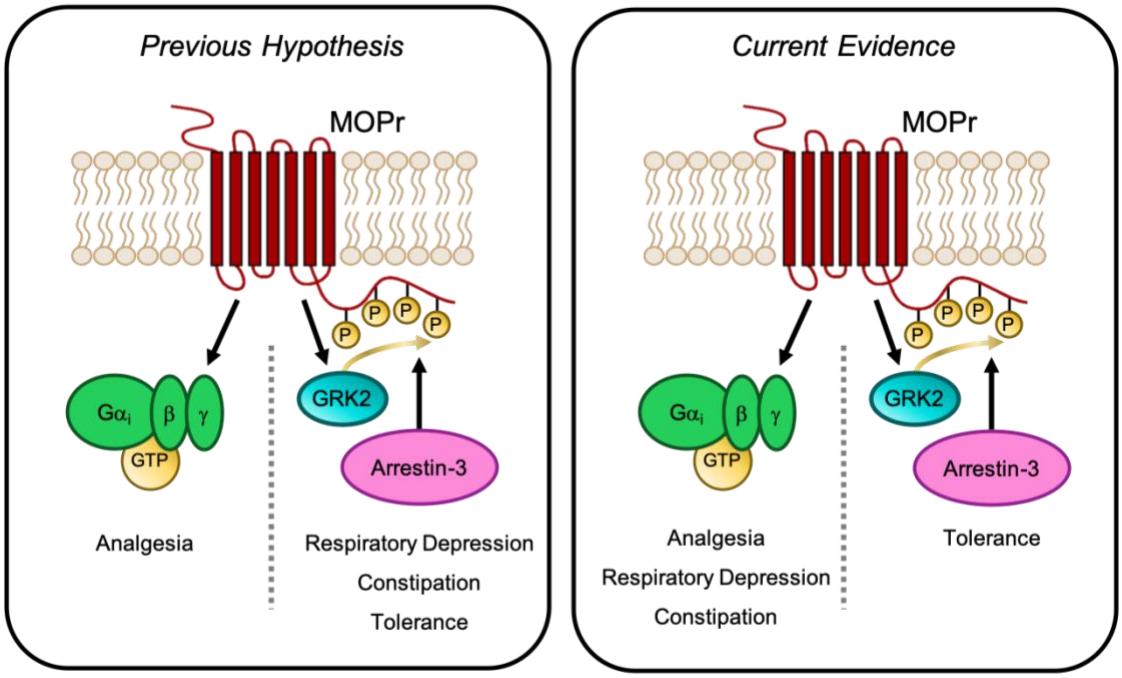


**Figure 1.6 – Functional effects of MOPr-mediated G protein and arrestin signalling**

*A schematic depiction showing the signalling pathways responsible for MOPr-dependent, opioid-induced physiological effects under (left) previous hypothesis (Raehal et al., 2005) and (right) in light of current evidence (Kliewer et al., 2019; Kliewer et al., 2020).*

## 1.3 Biased signalling at MOPr

### *1.3.1 Rationale for the development of G protein-biased MOPr agonists*

In light of recent developments, it is evident that ligands at GPCRs have the potential to preferentially couple to specific signalling downstream of receptor activation, through the phenomenon of biased signalling (Chapter 1.1.6). Previous hypotheses regarding arrestin-mediated signalling at MOPr (Chapter 1.2.6, Figure 1.6) (Raehal et al., 2005) actively drove drug discovery to seek and develop G protein biased agonists at MOPr (Conibear et al., 2019). By preferentially coupling to G protein signalling and evading arrestin-3 signalling, it was postulated that G protein-biased MOPr agonists would retain the analgesic properties of typical opioids with fewer of the adverse effects which are archetypal of opioids (Figure 1.7). The therapeutic potential of G protein-biased agonists under this hypothesis is evidently of particular interest, as it may provide a means to the 'holy grail' – an opioid analgesic without adverse effects. As such, following significant focus and intent from drug discovery groups, a number of reportedly G protein-biased agonists at MOPr have been developed (Chapter 1.3.2).

However, in light of recent evidence regarding arrestin-mediated MOPr signalling (Chapter 1.2.6, Figure 1.6), the rationale underlying the anticipated therapeutic potential of G protein-biased agonists at MOPr has recently come under significant scrutiny (Gillis et al., 2020b). Nevertheless, the reaffirmed role of GRK/arrestin pathways in MOPr desensitization and the development of tolerance to opioids (Chapter 1.2.6) suggests that G protein-biased MOPr agonists would induce less MOPr desensitization and tolerance than typical, non-biased opioids (Figure 1.7). If G protein-biased MOPr agonists are indeed less susceptible to the develop of analgesic tolerance, they would present substantial clinical benefit in the treatment of chronic pain compared to typical opioids.

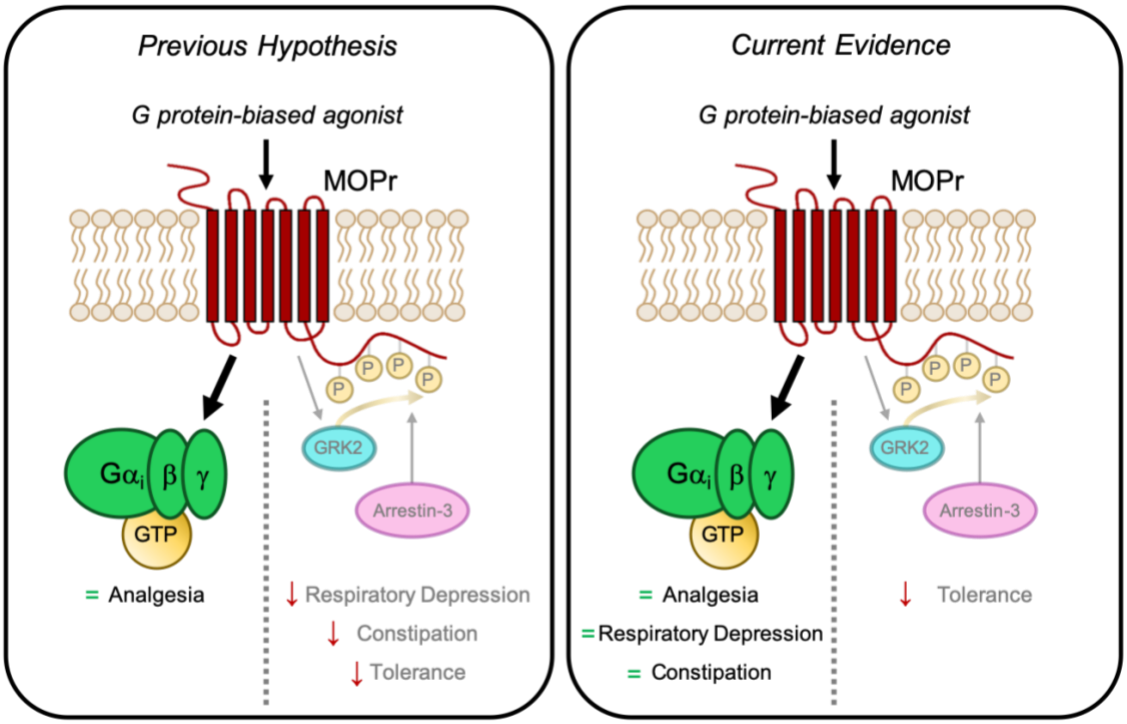


**Figure 1.7 – The potential pharmacological profile of G protein-biased agonists at MOPr**

*A schematic depiction of the potential pharmacological profile of G protein-biased agonists at MOPr effects under (left) previous hypothesis of arrestin-dependent signalling at MOPr (Raehal et al., 2005) and (right) in light of current evidence (Kliewer et al., 2019; Kliewer et al., 2020) (Figure 1.6).*

### *1.3.2 The pharmacology of reportedly biased agonists at MOPr*

Opioid ligands which possess bias for either G protein or arrestin signalling have been reported over the past decade (Conibear et al., 2019). Indeed, many programmes specifically seeking to develop biased ligands at MOPr have yielded novel MOPr agonists. Additionally, a number of established opioids have retrospectively been redefined as biased ligands based on new data on their signalling profiles (Rivero et al., 2012).

The first noteworthy small molecule specifically developed as a G protein-biased agonist at MOPr was TRV130, also known as oliceridine. TRV130 was reported to be G protein-biased relative to morphine in comparisons of its activity between cAMP accumulation assays and assays of arrestin-3 recruitment (DeWire et al., 2013). In preclinical studies, TRV130 was demonstrated to be an effective analgesic in comparison to morphine, but possessed a somewhat favourable adverse effect profile, inducing less respiratory depression and constipation than morphine at equi-effective doses for analgesia (DeWire et al., 2013). Despite displaying minimal benefit relative to morphine in clinical trials, with little to no evidence of a favourable adverse effect profile (Singla et al., 2019), TRV130 was recently clinically approved for the treatment of severe pain (Markham, 2020). Additionally, the reported G protein-biased profile of TRV130 has been called in to question (Dekan et al., 2019; Gillis et al., 2020a), with suggestions that its pharmacological profile is instead due to its low intrinsic efficacy relative to morphine (Yudin et al., 2019; Gillis et al., 2020a).

The novel ligand PZM21 was also specifically designed and developed as G protein-biased agonist at MOPr. PZM21 demonstrated substantial activity in assays of cAMP accumulation with minimal levels of arrestin-3 recruitment, however no formal calculations of biased agonism were conducted (Manglik et al., 2016). In preclinical mouse studies by Manglik et al. (2016), PZM21 produced analgesia comparable to morphine in mouse hot plate assays, but was less liable to induce respiratory depression, constipation and reward. This is in line with the previously anticipated profile of G protein-biased agonists at MOPr (Figure 1.7). Intriguingly, PZM21 did not produce analgesia in mouse tail flick assays, presenting a potential discrepancy between its effects on affective (hot plate) and reflective (tail flick) nociception (Manglik et al., 2016). However, PZM21 was found to induce respiratory depression to comparable levels as morphine by a separate subsequent study (Hill et al., 2018b). Additionally, in a similar manner to TRV130, the reportedly biased signalling profile of PZM21 has been subject to opposing reports (Hill et al., 2018b; Gillis et al., 2020a), with again its low efficacy being proposed

as the signalling parameter which is responsible for its pharmacological profile (Yudin et al., 2019; Gillis et al., 2020a).

The synthesis of the SR-series of small molecules by Schmid et al. (2017) yielded a range of MOPr agonists with reported varied biased profiles. SR17018 displayed the highest degree of G protein-bias within this series, displaying relative bias for activity in GTPγS assays over arrestin-3 recruitment compared to DAMGO. SR17018 produced effective analgesia *in vivo* yet was reported to induce minimal respiratory depression (Schmid et al., 2017). Attempts to repeat the *in vivo* experiments of MOPr pharmacology for SR17018 have been limited by its very poor solubility (Gillis et al., 2020a). Additionally, the reportedly biased signalling profile of SR17018 is disputed by other reports, again suggesting it is instead a low efficacy partial agonist (Gillis et al., 2020a).

The development of the novel opioid peptide bilorphin came from a rather “left field” source of an Australian estuarine fungus (Dekan et al., 2019). Dekan et al. (2019) demonstrated that bilorphin exhibited a greater degree of G protein-bias than TRV130 in recombinant systems. Importantly, the G protein efficacy of bilorphin was similar to morphine both in a system of physiological receptor expression (LC electrophysiology) and in cells expressing recombinant MOPr pharmacologically depleted of receptor reserve. This suggests the perceived bias profile of bilorphin is not in fact due to weak partial agonism. Unfortunately, the study of bilorphin pharmacology *in vivo* was limited by a lack of systemic activity due to poor blood-brain barrier penetration.

The endomorphin peptides, endomorphin-1 and endomorphin-2, were among the first ligands formally demonstrated to possess bias at MOPr. In contrast to the preceding discussion, the endomorphin peptides were demonstrated to be biased for arrestin-signalling over G protein-signalling (McPherson et al., 2010; Rivero et al., 2012; Burgueño et al., 2017; Dekan et al., 2019). The functional significance of this observation is yet to be defined in physiological terms. Interestingly, a number of cyclic endomorphin analogues, originally developed to improve the metabolic stability of these peptides (Czapla et al., 2000; Wilson et al., 2000), possess attractive *in vivo* pharmacology akin to the hypothesised pharmacological of G protein-biased agonists (Zadina et al., 2016; Webster et al., 2020). In the absence of formal assessment for the signalling properties of this agonists, it could be speculated that these cyclic endomorphins are indeed G protein-biased agonists at MOPr. This could indicate that the endomorphin scaffold could be disposed to yielding biased agonists. The recent development of a series of cyclic endomorphin analogues with by high MOPr affinity by Li et al. (2016) has yielded Try-c[D-Lys-Phe-Try-Gly] (termed Compound 1) (Figure 1.8), which is of significant interest to this project as a potentially G protein-biased MOPr agonist (Chapter 3.1).

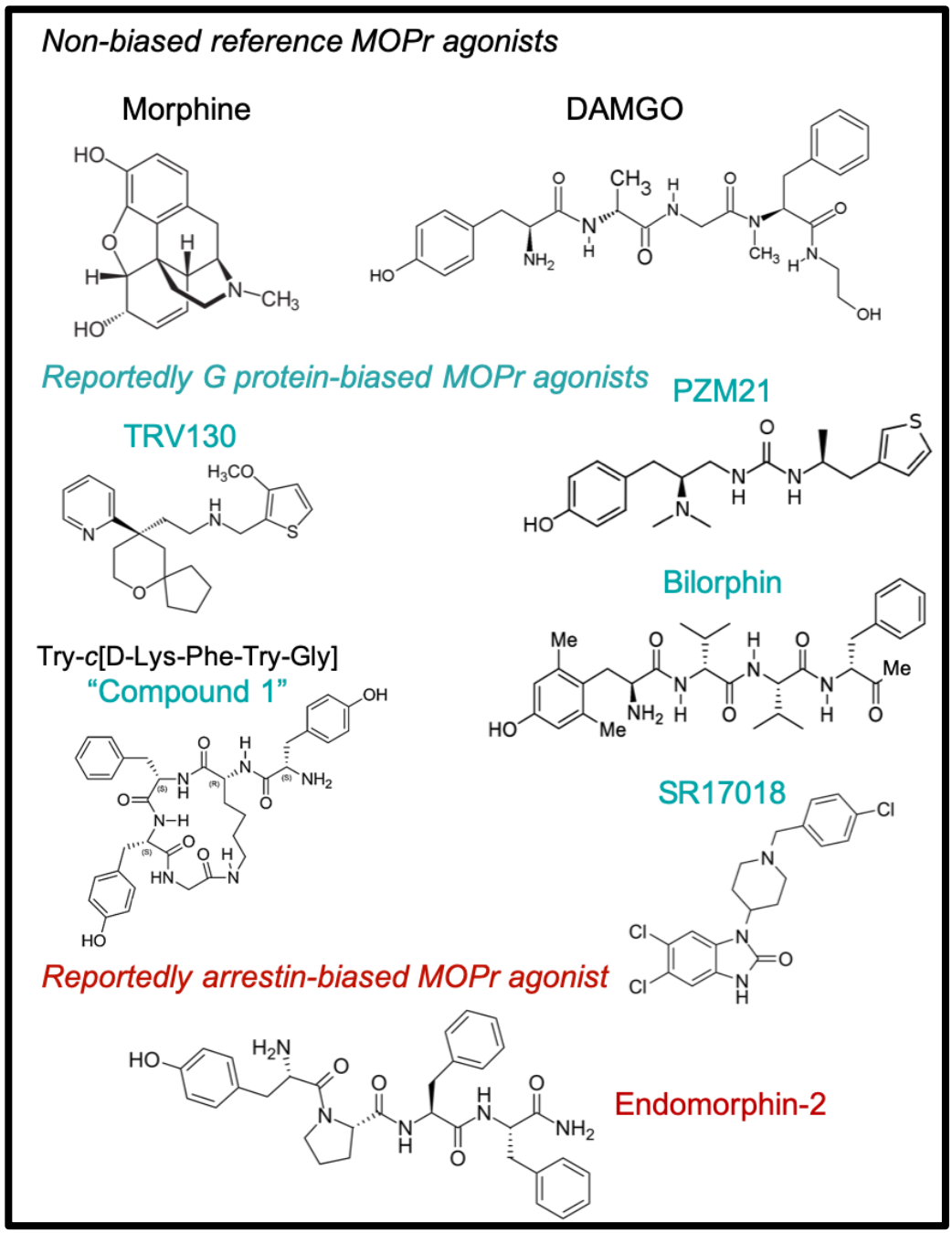


**Figure 1.8 – The chemical structures of both non-biased and reportedly biased agonists at MOPr**

*The chemical structures of non-biased (or 'balanced') reference MOPr agonists (black), as well as reportedly G protein-biased (blue) and arrestin-biased (red) at MOPr. Morphine and DAMGO are non-biased reference agonists at MOPr. Reported G protein-biased MOPr agonists include TRV130, PZM21, Try-c[D-Lys-Phe-Try-Gly] (Compound 1), SR17018 and bilorphin. Endomorphin-2 is reported to be an arrestin-biased agonists at MOPr. The reported data for reportedly biased MOPr ligands is summarised in Chapter 1.3.2.*

### *1.3.3 MOPr regulation and tolerance induced by G protein-biased agonists*

Current evidence around arrestin-mediated MOPr signalling suggests that GRK/arrestin pathways are responsible for the rapid desensitization of MOPr and the subsequent development of tolerance *in vivo* (Chapter 1.2.6, Figure 1.6) (Bohn et al., 2000; Arttamangkul et al., 2019a; Kliewer et al., 2019). In turn, this suggests that G protein-biased agonists at MOPr may induce less receptor desensitization and may subsequently be less liable to develop tolerance to their effects *in vivo* (Figure 1.7). However, agonist-selective non-GRK dependent mechanisms of receptor desensitization and tolerance are well described at MOPr, particularly concerning PKC (Kelly et al., 2008). It is possible that G protein-biased agonists may instead induce MOPr desensitization and tolerance through such non-GRK mechanisms. Studies of G protein-biased agonist pharmacology have largely focussed on analgesia and respiratory depression, with limited evidence available on their ability to induce receptor desensitization and tolerance (Conibear et al., 2019).

Although the arrestin/GRK coupling induced by G protein-biased MOPr agonists is relatively well studied in recombinant systems, MOPr desensitization induced by these ligands in a physiological setting has not been examined. One would hypothesise however that G protein-biased agonists would induce lower levels of MOPr desensitization than balanced agonists, due to their low coupling to related GRK/arrestin pathways (Figure 1.7). As anticipated, the arrestin-biased MOPr agonist endomorphin-2 produces substantially more receptor desensitization in rat LC neurones than the balanced agonist morphine, with which it shares a similar G protein efficacy (Rivero et al., 2012).

Current evidence around tolerance induced by reportedly G protein-biased MOPr agonists is variable. In mice, TRV130 has been demonstrated to induce less antinociceptive tolerance than morphine after 3-4 days repeated administration (Altarifi et al., 2017; Liang et al., 2019). A separate study by Singleton et al. (2021) also demonstrated that TRV130 produces potent antinociception in mice, without evidence of tolerance. However, tolerance to the antinociceptive effects of TRV130 was observed upon reduction of MOPr availability through use of heterozygous MOPr knockout mice (Singleton et al., 2021). Similarly tolerance was not observed to the antinociceptive effects of SR17018 after 6 days of repeated oral dosing (Grim et al., 2020) However, PZM21 produced robust antinociceptive tolerance in mice over 4 days of repeated administration (Hill et al., 2018b). Together this limited, variable evidence potentially implies that G protein-biased agonists at MOPr may induce less tolerance, which would make them clinically beneficial compared to typical opioids. However, the validity of the

proposed biased profile of the aforementioned agonists is keenly debated (Chapter 1.3.2), and the long-term functional consequences of biased signalling at MOPr therefore requires further evaluation.

## 1.4 Scope and aims of this thesis

Opioid agonists at MOPr remain unsurpassed as our most effective therapeutic option for the treatment of moderate to severe pain. This is despite their clinical utility being severely limited by the propensity of opioids to induce serious on-target adverse effects such as respiratory depression, and the rapid development of tolerance to their analgesic effects. Historically, drug discovery has relentlessly pursued the development of novel, safer opioid drugs through a series of means. The characterisation of biased signalling at GPCRs could potentially bring about a new generation GPCR-targeting therapeutics, selective and refined in their pharmacological profile. Biased signalling has been widely harnessed at MOPr with the development of a panel of reportedly G protein-biased MOPr agonists developed, in the anticipation that they will be effective analgesics devoid of typical opioids adverse effects.

The long-term functional effects of G protein-biased MOPr agonists remain understudied. There is potential that G protein-biased agonists at MOPr may induce less receptor desensitization due to their low coupling to common receptor regulatory pathways (GRK and arrestin). It is therefore hypothesised that subsequent tolerance to the effects of G protein-biased opioids may develop more slowly and to a lesser extent than traditional opioids, making them clinically appealing. However, agonist-selective non GRK-dependent mechanisms of agonist-induced receptor desensitization and tolerance are well described at MOPr in the case of morphine. This implies that non-GRK/arrestin pathways could also regulate MOPr function upon activation by G protein-biased agonists and drive the development of tolerance to these novel opioids.

The work within this thesis seeks to characterise the receptor desensitization and regulation induced by biased agonists at MOPr to further our understanding of their long-term functional effects. Accordingly, the specific aims of this thesis are as follows:

1. To characterise the signalling properties and biased signalling profiles of putatively G protein biased MOPr agonists using recombinant BRET assays and isolated tissue experiments (Chapter 3).

2. To investigate receptor desensitization induced by previously characterised G protein-biased MOPr agonists in rat locus coeruleus neurones in brain slices using patch clamp electrophysiology (Chapter 4).

3. To characterise using pharmacological tools the mechanisms involved in the potential MOPr desensitization induced by G protein-biased agonists in locus coeruleus neurones (Chapter 5).

# Chapter 2: Materials & Methods

## 2.1 In vitro cell signalling studies

### *2.1.1 General cell culture methods and transfection*

Human embryonic kidney (HEK) 293 cells were cultured in Dulbecco's modified Eagle's medium (DMEM) containing L-Glutamine (ThermoFisher), supplemented with 10 % (v/v) foetal bovine serum (FBS) (Life Technologies), 100 U/ml penicillin and 100 μg/ml streptomycin (Invitrogen). Cells were maintained at 37°C in a humidified atmosphere of 95 % air and 5 % $CO_2$. Cells were seeded onto 10 cm dishes and grown to approximately 80 % confluency before transient transfection.

HEK 293 cells were transiently transfected with required plasmids using lipofectamine 2000 (Invitrogen) transfection. Transient transfections were conducted approximately 48 hours prior to the desired assay time. DMEM growth media was removed and cultured cells were washed with phosphate-buffered saline before replacement of growth media with reduced serum OptiMEM media (ThermoFisher). The desired plasmid DNA for the individual experiment was diluted in OptiMEM media to a total volume of 500μl to the experiment-specific desired concentrations outlined below. Separately, the lipofectamine reagent was diluted in OptiMEM at a ratio of 1 : 2.7 DNA (μg) to lipofectamine (μl). DNA and lipofectamine solutions were incubated at room temperature for 5 min before they were combined. After 20 min incubation at room temperature, the DNA-lipofectamine solution was then added gently, dropwise to the HEK 293 cells. Cells were incubated with DNA-lipofectamine in OptiMEM media overnight before the replacement of the media with DMEM growth media the following day. Cells were allowed to grow in DMEM growth media for a further 24-32 hours before assay.

### *2.1.2 Bioluminescence Resonance Energy Transfer (BRET) assays*

A number of bioluminescence resonance energy transfer (BRET) assays were utilised in our studies to determine the ability of opioid agonists to induce activation of $G\alpha_i$ G proteins downstream of opioid receptors, and recruitment of both arrestin-3 and arrestin-2 at MOPr. The optimisation of these BRET assay platforms was conducted previously by Dr Gerta Gasiuniate, demonstrating the optimal ratio of donor : acceptor DNA and the absence of BRET signal in cells transfected with pcDNA alone (Gasiunaite, 2017).

Assays of BRET are dependent on energy transfer between a bioluminescent donor and a fluorescent acceptor, such as Renilla luciferase (Rluc) and green fluorescent protein (GFP) respectively. Rluc catalyses the oxidation of the introduced substrate

coelenterazine to coelenteramide, a process which emits light with a peak at a 410 nm wavelength (for coelenterazine 400a). Light of this wavelength is then able to excite GFP, which then emits light at a longer wavelength of 515 nm. However, due to the efficacy of this energy transfer being heavily dependent on distance, BRET will only occur when the distance between the BRET donor and acceptor is very low (less than approximately 100 Å). The magnitude of this energy transfer can be quantified through calculation of the ratio between the acceptor and donor emissions peaks: the BRET ratio. An increase in the BRET ratio indicates that the distance between the donor and acceptor has decreased, while a decrease in the BRET ratio reflects the distance between the donor and acceptor increasing.

The use of BRET donor and acceptor tags provides an effective method to study protein-protein interactions in a whole cell environment. The configurations for our BRET assays for $G\alpha_i$ activation and arrestin translocation are schematically depicted in Figures 2.1 and 2.2.

In our assays of opioid-induced $G\alpha_i$ activation, HEK 293 cells were transiently transfected with 3 μg of $G\alpha_i$-RlucII and 3 μg $GFP_{10}$-$G\gamma_2$ as well as 3 μg of rat HA-MOPr, human HA-DOPr or human HA-KOPr per 10 cm dish (Figure 2.1). Under no receptor activation, the labelled G protein subunits remain associated and in close proximity, producing a BRET signal (Figure 2.1A). Upon receptor activation by an agonist, the labelled G protein subunits dissociate, or rearrange, resulting in a reduction in the BRET ratio (Figure 2.1B).

In assays of opioid-induced arrestin-3 translocation, HEK 293 cells were transiently transfected with 5 μg of human MOPr-RlucII and 5 μg of either arrestin-3-$GFP_{10}$ or arrestin-2-$GFP_{10}$ per 10 cm dish (Figure 2.2). In assay of arrestin-3 recruitment in which GRK2 was overexpressed, cells were in addition transfected with 5 μg of wild type GRK2 or pcDNA3.1. In this instance, under basal conditions the labelled MOPr and arrestin proteins are not in close proximity, meaning the BRET ratio is low (Figure 2.2A). Upon MOPr activation by an agonist, the labelled arrestin protein is recruited to the receptor bringing the BRET donor and acceptor in close proximity thereby increasing the BRET ratio (Figure 2.2B).

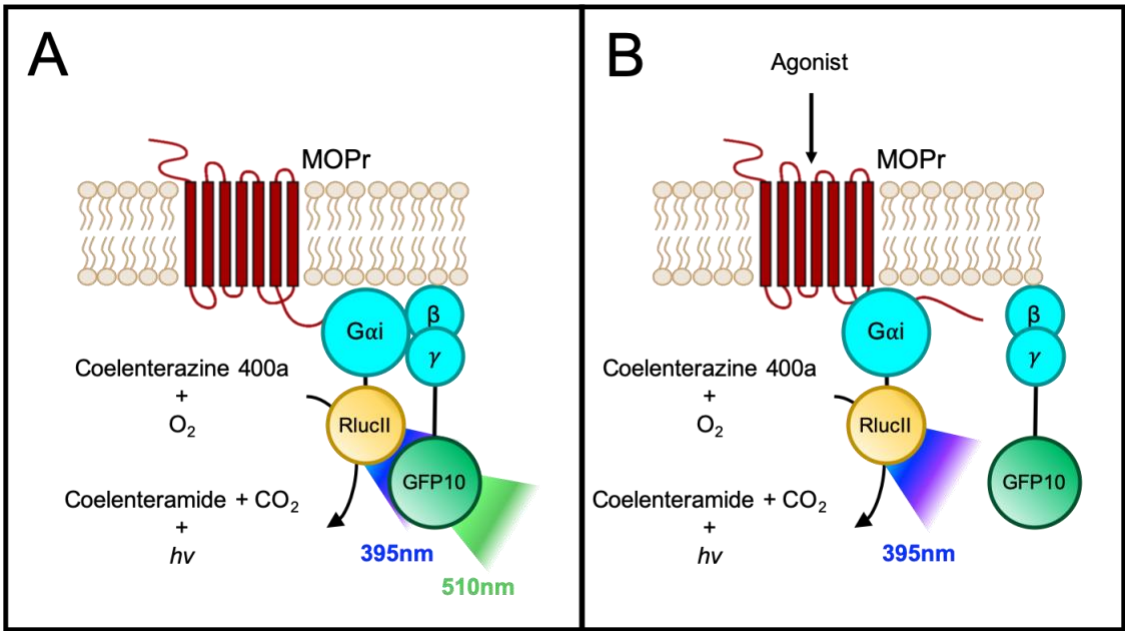


**Figure 2.1 – The methodological principles of the G protein activation BRET assay in the case of MOPr**

*In both scenarios, renillia luciferase II (RlucII), which is conjugated to the G$\alpha_i$ subunit, catalyses the oxidation of added Coelenterazine 400a to coelenteramide, a process which releases light (hv) of 395 nm wavelength. (A) Under basal conditions (no agonist), the BRET donor/acceptor tagged G protein subunits are in close proximity. Hereby, the 395 nm light emitted from the RlucII excites the GFP10 which is tagged to the associated G$\gamma$ subunit, in turn releasing light of a longer wavelength (510 nm). (B) Upon addition of an agonist and subsequent activation of MOPr, the G protein subunits dissociate or rearrange relative to one another. As such, the BRET donor (RlucII) and acceptor (GFP10) are no longer in close proximity and a reduction in BRET occurs.*

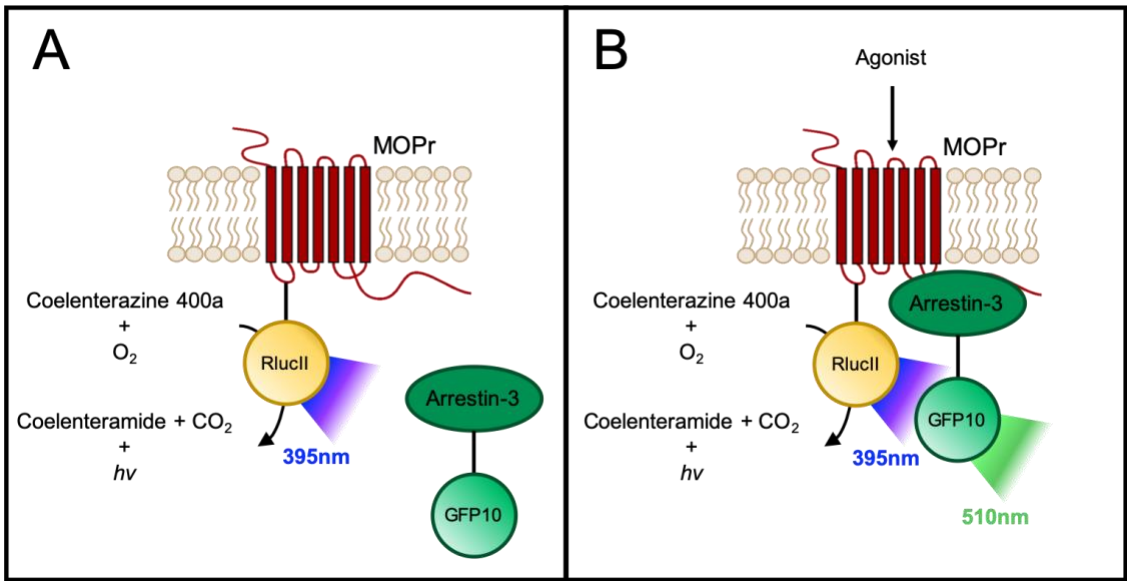


**Figure 2.2 – The methodological principles of the arrestin recruitment BRET assay in the case of arrestin-3**

*In both scenarios, renillia luciferase II (RlucII), which is conjugated to MOPr, catalyses the oxidation of added Coelenterazine 400a to coelenteramide, a process which releases light (hv) of 395 nm wavelength. (A) Under basal conditions (no agonist), the BRET donor/acceptor tagged receptor and arrestin-3 are not in close proximity. Therefore, no increase in BRET is observed. (B) However, upon activation of MOPr by an agonist, the GFP10-tagged arrestin-3 is recruited to MOPr-RlucII, bringing them in to close proximity. Now the 395 nm light emitted from the RlucII excites the GFP10 which is tagged onto arrestin-3, in turn releasing light of a longer wavelength (510 nm). As such, an increase in BRET is indicative of an increase in agonist-induced arrestin-3 recruitment.*

In all BRET assay configurations, transfected HEK 293 cells were resuspended in clear, serum-free DMEM (ThermoFisher) and then transferred to flat-bottomed 96 well Corning plates at 90 μl per well 1 hour prior to assaying. Drug solutions, dissolved in water or DMSO, were diluted to the required concentration in clear, serum free DMEM, with the final assay concentration of DMSO never exceeding 0.1% v/v. 10 μl of the drug dilutions was added to the plated cell suspension prior to measurements of BRET activity. Drugs were incubated with cell suspensions at 37°C within the FLUOstar Omega microplate reader (BMG Labtech) for 2 min or 10 min for the G protein and arrestin assays respectively. These incubation times were based on previous optimisations conducted within the University of Bristol laboratory by Dr Katy Sutcliffe (Sutcliffe, 2019). Coelenterazine 400a (5 μM final concentration, dissolved in methanol) was injected into the wells of the cell plate by the FLUOstar Omega microplate reader prior to the taking of BRET measurements. Measurements of BRET were recorded using the following filters: acceptor (GFP), 410 ± 80 nm; and donor (RlucII), 515 ± 30 nm. BRET signals were recorded at both 5- and 8-seconds post coelenterazine 400a injection and results were averaged to form the final result for each well.

All conditions were performed in duplicate and the average response was taken. For the $G\alpha_i$ activation assays, the percentage decrease in the BRET ratio was calculated to express opioid-induced responses, with the BRET ratio from transfected cells treated with media + DMSO used as the baseline control. In the case of the arrestin recruitment assays, measurements of BRET are presented as BRET ratio minus the background BRET ratio obtained from transfected cells treated with media + DMSO.

Concentration-response data from 5 independent experiments was combined and fitted using non-linear curve models in GraphPad Prism version 8, in order to obtain $pEC_{50}$ and $E_{Max}$ values. The equation for the 3-parameter logistic equation is given below (Equation 1).

$$(1) \quad Y = Bottom + \frac{(Top - Bottom)}{1 + 10^{(logEC_{50} - \log[A])}}$$

where Top and Bottom represent the maximal and minimal asymptotes of the concentration response curve, $EC_{50}$ is the molar concentration of agonist required to induce a response halfway between the Top and Bottom values and [A] is the molar concentration of the agonist, and Y is response. Given that the BRET ratio output of the assays had baseline values subtracted, the minimal asymptote of concentration-response curves was constrained to 0.

A 3-parameter logistic fit was utilized in our studies as opposed to a 4-parameter logistic fit in order to reduce uncertainty around parameter fitting within our models. As such, the Hill Slope value of our concentration response curves was effectively constrained to 1 (effect on fitted parameters described in Chapter 3.2.1.1).

Concentration-response data to our test agonists were compared to those determined for the well-characterised MOPr control ligands DAMGO and morphine, which were run in the same experiments. Fitted parameters for test agonists were statistically compared to control agonists through one-way ANOVA with post-hoc Tukey tests.

### *2.1.3 Quantification of biased signalling*

A number of analytical methods were employed in Chapter 3 in attempts to quantify potential biased agonism at MOPr in our BRET assays of opioid induced G protein and arrestin signalling (Chapter 3.2.1.2).

The prevailing method used for the analysis of biased agonism at GPCRs is through the generation of a pathway-specific metric of agonist activity, the transduction coefficient ($\tau/K_A$), calculated using a form of the Black-Leff operational model. The operational model describes the response of an experimental system to an agonist (Equation 2).

$$(2)\ Y = basal + \frac{(E_M - basal)\,\tau^n[A]^n}{\tau^n[A]^n + ([A] + K_A)^n}$$

Where basal is the response in absence of agonist, $E_M$ is the theoretical maximal possible response of the system, $\tau$ is the operational efficacy (a composite factor of an agonist's intrinsic efficacy, effector coupling and receptor density), n is the slope of the transducer function, [A] is the concentration of agonist and $K_A$ is the functional equilibrium dissociation constant, and Y is response. The fitted $\tau$ values from this analysis were utilised for analyses of signalling bias through the $\Delta\Delta\log(\tau)$ methodology (Chapter 3.2.1.2, Figure 3.4) (Burgueño et al., 2017).

In order to allow for curve fitting, the transduction coefficient ($\tau/K_A$) was expressed as a single parameter, R. To obtain this coefficient, concentration response data were fitted to a modified version of the operational model (Equation 3), which was derived from Equation 2 (Sutcliffe, 2019).

$$(3)\ Y = basal + \frac{(E_M - basal)}{1 + \left(\frac{\left(\frac{[A]}{10^{log K_A}} + 1\right)^n}{\frac{}{10^{log R}[A]}}\right)}$$

In use of both equations 2 and 3 for fitting concentration response data, the basal value was constrained to 0 and the n value was constrained to be shared across all agonist concentration-response curves.

The following calculation was made to remove influence of systems bias, through normalisation of the pathway specific metric of agonist activity ($\tau/K_A$) to that of the reference agonist morphine in each assay (Equations 4).

$$(4)\quad \Delta\log\left(\frac{\tau}{K_A}\right) = \log\left(\frac{\tau}{K_A}\right)_{Test\ Agonist} - \log\left(\frac{\tau}{K_A}\right)_{Morphine}$$

The $\Delta\log(\tau/K_A)$ thereby provides an index of an agonist's activity at a specific pathway, relative to a reference agonist. In order to calculate potential biased signalling between assays of G protein activity and arrestin-3 recruitment for a specific agonist, the following calculation was made (Equation 5), resulting in a final $\Delta\Delta\log(\tau/K_A)$ value. The antilog value of an agonist's $\Delta\Delta\log(\tau/K_A)$ value was then reported as its "bias factor".

$$(5)\quad \Delta\Delta\log\left(\frac{\tau}{K_A}\right) = \Delta\log\left(\frac{\tau}{K_A}\right)_{G\ Protein} - \Delta\log\left(\frac{\tau}{K_A}\right)_{Arrestin-3}$$

The standard error values for each agonist's $\Delta\log(\tau/K_A)$ values was calculated through Equation 6. The error associated with an agonist's $\Delta\log(\tau/K_A)$ value was then propagated through Equation 7.

$$(6)\quad S.E._{\Delta\log\left(\frac{\tau}{K_A}\right)} = \sqrt{\left(S.E.M._{\log\left(\frac{\tau}{K_A}\right)_{Test\ Agonist}}\right)^2 + \left(S.E.M._{\log\left(\frac{\tau}{K_A}\right)_{Morphine}}\right)^2}$$

$$(7)\quad S.E._{\Delta\Delta\log\left(\frac{\tau}{K_A}\right)} = \sqrt{\left(S.E._{\Delta\log\left(\frac{\tau}{K_A}\right)_{G\ protein}}\right)^2 + \left(S.E._{\Delta\log\left(\frac{\tau}{K_A}\right)_{Arrestin-3}}\right)^2}$$

An identical approach was used to calculate mean and error values within the methodologically similar $\Delta\Delta\log(\tau)$ analysis (Burgueño et al., 2017), with $\log(\tau/K_A)$ in Equations 4-7 substituted by the metric $\log(\tau)$.

For partial agonists, in systems of low receptor reserve, the fitted maximal asymptote of an agonist's concentration-response curves ($E_{Max}$) from basic logistic fitting (Equation 1) can be used as a robust affinity-independent estimate of that agonist's intrinsic efficacy or $\tau$ (Stephenson, 1956; Dekan et al., 2019). A comparison of an agonist's normalised $E_{Max}$ values, or $\Delta$ normalised $E_{Max}$ between different pathways (for instance between G protein activation and arrestin-3 recruitment) can be used as an efficacy-dependent

measure of agonist bias (Dekan et al., 2019). To calculate the Δ normalised $E_{Max}$ values for our agonists, the $E_{Max}$ values of our test agonists were normalised to that of morphine and subtracted between the pathways (Equation 8). The standard error of Δ normalised $E_{Max}$ values was propagated through Equation 9.

(8) $$\Delta Normalised\ E_{Max} = Normalised\ E_{Max\ G\ protein} - Normalised\ E_{Max\ Arrestin-3}$$

(9) $$S.E._{\Delta Normalised\ E_{Max}} = \sqrt{\left(S.E._{Normalised\ E_{Max\ G\ protein}}\right)^2 + \left(S.E._{Normalised\ E_{Max\ Arrestin-3}}\right)^2}$$

The resulting agonist-specific bias factors, either ΔΔlog($\tau/K_A$), ΔΔlog(τ) or Δ Normalised $E_{Max}$, were each compared through one-way ANOVA with Tukey's post-hoc test to define statistical significance.

### *2.1.4 Surface MOPr enzyme-linked immunosorbent assay (ELISA)*

In order to study opioid-induced internalization of MOPr, we assessed surface expression of rat HA-MOPr in HEK 293 cells using an enzyme-linked immunosorbent assay (ELISA), based on previously used methods (Rivero et al., 2012).

HEK 293 cells at approximately 80% confluency were transiently transfected with HA-MOPr pcDNA (5 μg per 10 cm dish) using the lipofectamine 2000 transfection method (Chapter 2.1.1). Transfected cells were then plated in a 24 well plate coated with 0.1 mg/ml poly-L-lysine (Sigma-Aldrich) 24 hours prior to assay. Wild type, non-transfected HEK 293 cells were also plated in the same 24 well plate to be used as background controls.

The following morning, cell media was replaced with serum-free clear DMEM. Drug dilutions, made in serum-free clear DMEM, were then incubated with the cells for 15 to 60 min at 37°C before the media was aspirated and the reaction was fixed with 3.7 % (v/v) paraformaldehyde (PFA) (VWR) for exactly 5 minutes. The PFA solution was then aspirated and fixed cells were washed 3 times with tris-buffered saline (TBS) to remove remaining PFA. Fixed cells were then incubated with 1% (w/v) bovine serum albumin (BSA) (Sigma-Aldrich), in TBS, for 45 min to reduce non-specific antibody binding. Subsequently, the BSA solution was aspirated and cells were incubated with the primary mouse anti-HA monoclonal antibody (1:1000, in TBS containing 1% BSA) (#MMS-101R, BioLegend) for 1 hour. The primary antibody containing TBS was then aspirated and cells were again washed 3 times with TBS before they were blocked with 1% BSA, incubated for 15 min. The blocking media was then aspirated, and cells were incubated

with the secondary goat anti-mouse IgG alkaline phosphatase conjugate antibody (1:1000, in TBS containing 1% BSA) (#A5153, Sigma Aldrich). The secondary antibody solution was then aspirated, and cells were washed with TBS 3 times before they were incubated with alkaline phosphatase substrate (Bio-Rad Laboratories) for 1 h at 37°C to detect the signal from the secondary antibody conjugate. The alkaline phosphatase substrate was transferred from the 24 well cell plate to a 96 well reading plate and the alkaline phosphatase reaction was terminated by the addition of 0.4 M NaOH, at a 1:1 ratio. Absorbance (405 nm) of the samples was then assayed on a Tecan Infinite plate reader (Tecan).

Absorbance values were normalised to values in wells containing untreated HEK 293 cells expressing MOPr (100%) and untreated, non-transfected WT HEK 293 cells (0%). All ELISA experiments were performed in triplicate and an average taken to constitute each repeat. Total agonist-induced loss of surface MOPr over time was assessed by determining the total area under the curve (AUC) for each agonist over the 60-minute time course using in built analysis in GraphPad Prism (version 8). A one sample t test was used to determine whether the generated AUC for induced surface loss of MOPr by an agonist was significantly different from 0. If the AUC of agonist-induced loss of surface MOPr over time was significantly higher than 0, it was inferred it induced significant loss of surface receptor.

### *2.1.5 Phosphosite-specific immunoblotting of MOPr*

In order to study agonist-induced phosphorylation of C-terminal MOPr residues, we sought to utilise immunoblotting through phosphospecific antibodies. This work was kindly performed and analysed for us by Nina Kathleen Blum, supervised by Dr Andrea Kliewer and Prof Stefan Schulz at the University of Jena, Germany.

Agonist-induced MOPr phosphorylation was assessed using Western blotting with phosphospecific antibodies as previously described (Gillis et al., 2020a). Briefly, HEK 293 cells stably expressing mouse HA-MOPr were seeded on to 6 cm dishes, maintained in DMEM High Glucose (ThermoFisher) supplemented with 5% (v/v) FBS and 1% glutamine and streptomycin/penicillin. At approximately 90% confluency, cells were incubated with opioid agonists (10 μM DAMGO, 30 μM morphine and 30 μM PZM21, 1 nM – 30 μM Compound 1) for 30 min before lysis in an immunoprecipitation buffer (50mM tris-HCl (pH 7.4), 150 mM NaCl, 5 mM EDTA, 1% NP-40, 0.5% sodium deoxycholate, 0.1% sodium dodecyl sulfate (SDS)). The protease and phosphatase inhibitors complete Mini and PhosSTOP (Roche Diagnostics) were included in the immunoprecipitation buffer to conserve protein levels and induced phosphorylation. HA-tagged MOPr was

enriched using Pierce HA epitope tag antibody agarose beads (ThermoFisher). SDS sample buffer was then incubated with the samples for 25 min at 43°C to elute proteins from the beads. Samples were then separated and resolved on 8% SDS-polyacrylamide gels and after electroblotting, PVDF membranes were incubated either anti-pT370, anti-pS375, anti-T376, or anti-T379 antibodies (Just et al., 2013). Detection was performed using a chemiluminescence-detection system. Blots were subsequently stripped and incubated again with an anti-HA antibody (phosphorylation independent) to confirm equal well loading of receptor protein.

Raw blot images were used to visually assess multi-site phosphorylation induced by our panel of opioids. Levels of agonist-induced pSer375 phosphorylation from 5 individual experiments were quantified using image processing software Fiji and signals were expressed relative to that of the HA loading control. Levels of agonist-induced pSer375 phosphorylation were statistically compared to control values using one-way ANOVA with post-hoc Dunnett's tests.

## 2.2 Animal housing & welfare

Wildtype male Wistar rats were used for all electrophysiology experiments (Chapter 2.4) and all vas deferens experiments (Chapter 2.3). These rats were bred and maintained at the University of Bath. Rats were weaned at approximately P21 and subsequently housed in single sex cage groups of 5-6 rats. Cages were housed within ventilated, temperature controlled (21 ± 1°C) cabinets under a 12 h light/dark cycle (lights on at 6am). Food and water were available to the animals *ad libitum* and cages were cleaned weekly.

In warm water tail withdrawal tests of nociception conducted at the University of Bristol (Chapter 2.5), mice of CD-1 and C57BL/J strains were used. Male CD-1 mice weighing approximately 30 g were obtained from Charles River. Breeding pairs of MOPr knockout mice (*Oprm1*$^{tm1Kff}$, RRID:IMSR_JAX:007559) were initially obtained from the Jackson Laboratory for a distinct study (Hill et al., 2020), and bred in house at the University of Bristol. Both male and female MOPr knockout offspring of these mice, weighing approximately 30 g, were used in this study. Male and female C57BL/J mice weighing approximately 30 g were obtained from Charles River, for use as background strain controls for studies with the MOPr knockout mice. During their holding at the University of Bristol, all mice were maintained at 22°C on a reversed dark-light cycle, with food and water available *ad libitum*. All experiments were conducted during the animals' dark (active) phase. Mice were randomly ascribed to their treatment groups with the experimenter blind to the drug treatment. Additionally, cages of wildtype or MOPr knockout were also blinded to the experimenter. Blinding was maintained until completion of data analysis.

All animal care and experimental procedures were performed in accordance with the UK Animals (Scientific Procedures) Act 1986, the European Communities Council Directive (2010/63/EU) and the ethical review documents of the University of Bath and the University of Bristol. Animal studies are designed and reported in compliance with the ARRIVE guidelines (Kilkenny et al., 2010).

## 2.3 Rat vas deferens assay

### *2.3.1 Tissue preparation*

Male Wistar rats (6-7 weeks old) were euthanized through exposure to rising $CO_2$ concentrations in a close-contained environment. The vasa deferentia were then dissected out by making incisions at the connecting points of the prostate gland and the testis. The connecting tissue, adhering fat, and blood vessels were carefully separated from the vasa deferentia and each vas deferens was then divided into two equal sized pieces for assaying. Dissected vasa deferentia were placed in warm Krebs solution of the following composition (in mM): NaCl 118, KCl 4.74, $CaCl_2$ 2.50, $KH_2PO_4$ 1.19, $MgSO_4$ 1.20, $NaHCO_3$ 25, glucose 11.

### *2.3.2 Experimental procedures*

Sections of vas deferens tissue were maintained in organ baths (approximately 30 ml) containing Krebs solution at 37°C and aerated with 95% $O_2$ and 5% $CO_2$. One end of the vas deferens was mounted to an isometric force transducer (AD Instruments). The tissue section was then set up to sit between two stainless steel ring electrodes (submerged in the organ bath) with the opposing end of the tissue tied and mounted to a fixed hook on the electrode holder. Rat vas deferens was mounted under 1.0g initial basal tension.

After approximately 30 min equilibration, the tissue was continuously stimulated through a Grass SD9 stimulator (Grass Medical Instruments) through the two ring electrodes with square pulses of supramaximal voltage, 1 ms duration and 0.1 Hz frequency. Electrically-evoked contractions were measured isometrically and recorded through the data acquisition hardware Powerlab 4/26 (AD Instruments). The preparation was allowed to equilibrate under continuous stimulation for 1 hr prior to beginning the experiment.

Drug solutions were serially diluted in Krebs solution. The ability of DAMGO ($10^{-8}$–$10^{-4.5}$ M) to inhibit the electrically-evoked twitches of the rat vas deferens was assessed upon cumulative addition, from lowest to highest concentration. Each concentration of interest incubated with the tissue for at least 3 min before the addition of a higher concentration.

Given the insensitivity of the rat vas deferens to MOPr agonists of lower efficacy (Lemaire et al., 1978), we sought to define the affinity of our panel of partial MOPr agonists through competitive antagonist experiments against DAMGO, using classical Schild experiments (Schild, 1947). In order to assess the ability of our panel of partial agonists to inhibit DAMGO function, select concentrations were preincubated with the rat vas deferens preparation for 20 min prior to, and during, the cumulative addition of DAMGO. For each

individual preparation, only a single partial agonist was studied, with the impact of different concentrations of the partial agonist examined sequentially working from the lowest to the highest test partial agonist concentration.

### *2.3.3 Data processing and Schild analysis*

Data from the rat vas deferens preparation were processed and analysed within the LabChart software (AD Instruments) which was linked to the PowerLab recording hardware. The magnitude of electrically-evoked twitches in each condition (drug concentration) was measured by obtaining the maximum – minimum value of twitches at the end of the condition's incubation period using the inbuilt processes within LabChart. This value was obtained and averaged across the last three twitches within each condition to reduce variability, and then the average baseline response (no twitch) in the tissue at this time was subtracted from this value to give a final metric of response. The '% inhibition' of electrically-evoked contractions of the rat vas deferens was then calculated through Equation 10.

$$(10) \quad \%\, Inhibtion = 100 \times \left( \frac{1 - (Sample\ Twitch\ Height)}{Basal\ Twitch\ Height} \right)$$

Where 'basal twitch height' refers the magnitude of evoked twitches in the absence of drug, at the time point immediately prior to the addition of drug.

The DAMGO concentration response curves from each preparation, in the presence of various concentrations of partial agonist, were all fitted to the 4-parameter logistic fit outlined below (Equation 11).

$$(11) \quad Y = Bottom + \frac{(Top - Bottom)}{1 + 10^{((logEC_{50} - log[A]) \times Hill\ Slope)}}$$

Where Top and Bottom represent the maximal and minimal asymptotes of the concentration response curve, $EC_{50}$ is the molar concentration of agonist required to induce a response half way between the Top and Bottom values and [A] is the molar concentration of the agonist. In this equation, the Hill Slope is a fitted parameter which describes the steepness of the fitted concentration response curve, where in the three-parameter logistic equation described in Equation 1 it is a constant of value 1. The plotted Y values (% inhibition of evoked-twitch) were normalised to 0% (the basal magnitude of evoked-twitch) and 100% (maximum possible inhibition of twitch). Therefore, the Bottom value was given the constant value of 0. However, given that the maximum extent of inhibition of twitches achieved by opioids could be less than 100%, and naturally cannot be greater than 100% (negative twitch), the Top value was constrained to be a value

less than or equal to 100. The Hill Slope was constrained to be shared across DAMGO concentration response curves from the same tissue preparation. Differences in coupling efficacies or tissue viability could impact the Hill Slope of agonist responses, meaning constraining the Hill Slope to 1 would lead to poor curve fitting in the case of n ≠ 1. However, this should not vary within individual preparations, therefore the Hill Slope was shared to reduce error associated with parameter fitting.

The $EC_{50}$ values fitted from this regression analysis were used to calculate the dose ratios (DR) required for Schild analysis. The series of DRs were reported as log(DR - 1), where the log(DR - 1) metric was calculated as follows (Equation 12).

$$(12) \quad \log\left(\left(\frac{EC_{50_{\mathbf{B}}}}{EC_{50}}\right) - 1\right)$$

Where $EC_{50\ \mathbf{B}}$ represents the $EC_{50}$ of DAMGO in the examined concentration of an antagonist, and $EC_{50}$ is the potency of DAMGO in control conditions.

In order to construct Schild plots for each partial agonist (which in this case act as antagonists , and are henceforth referred to as such), averaged log(DR - 1) values across multiple experiments were plotted against log [B], the antagonist concentration. The Schild plot data for each agonist was then subjected to a simple linear regression fit, with both the slope unconstrained and with the slope constrained to 1. Fitted slope values from unconstrained linear regressions were statistically compared to the hypothetical value of 1 through an extra sum-of-squares F test (Kenakin, 2009).

The Schild equation (Equation 13) was used to determine the affinity of the antagonist for MOPr within the rat vas deferens preparation.

$$(13) \quad pA_2 = \log(DR - 1) - \log[B]$$

Where the $pA_2$ is the negative logarithm of the concentration of antagonist required to shift the agonist concentration response curve by a factor of 2. The $pA_2$ is equal to the equilibrium constant ($pK_B$) of antagonist binding to the receptor when the Schild slope is 1 (Schild, 1947). [B] represents the concentration of antagonist. When log(DR-1) is 0 (the x-axis intercept), this indicates a shift in the concentration response curve by a factor of 2. Therefore, according to the Schild equation (equation 13), the negative logarithm of the antagonist concentration at the x-axis intercept of the linear regression is equal to the $pA_2$. The best fit values of the x-axis intercept from linear regression performed on Schild plots containing pooled data, and the corresponding 95% confidence intervals, were then reported as the $pA_2$ of the agonist. The $pA_2$ values of select agonists were compared statistically using a one-way ANOVA with post-hoc Tukey test.

Data from competitive antagonist experiments was also alternatively fitted through an in-built 'Gaddum/Schild EC50 Shift' equation in GraphPad Prism (version 8). The benefit of this approach was primarily convenience; however, the data were also fitted as a combined set from multiple experiments, rather than in individual repeats which the former model describes. A downside to this approach is that it does not output a traditional Schild Plot, only a $pA_2$ value. The potential impact of using these two methodologies on the values of antagonist $pA_2$ and associated variance on these parameter was briefly explored using data from these experiments (Table 3.4).

## 2.4 Brain slice electrophysiology

### *2.4.1 Brain slice preparation*

Male Wistar rats (4 weeks old) were anaesthetised via intraperitoneal injection of 160 mg/kg ketamine and 20 mg/kg xylazine and then decapitated. The brains were rapidly removed and immediately submerged into ice-cold solution containing (in mM): 20 NaCl, 2.5 KCl, 1.6 $NaH_2PO_4$, 7 $MgCl_2$, 85 sucrose, 25 D-glucose, 60 $NaHCO_3$, and 0.5 $CaCl_2$, and saturated with 95% $O_2$ / 5% $CO_2$. While in this solution, coronal cuts were made with a razor blade to remove the anterior frontal cortex, the hippocampi and a portion of the cerebellum, leaving a smaller section of brain mainly composed of the midbrain and pons, containing the locus coeruleus (LC). Horizontal brain slices (230 μm in thickness) containing the LC were then prepared using a vibratome (DTK-1000, DSK). During slicing, under the guide of the naked eye, the presence of an 'open' fourth ventricle (a diamond, or heart, shape) was used as an indication of the presence of LC within a horizontal slice. LC-containing slices were then cut using a razor blade to separate the two hemispheres of each slice. Slices were then transferred to a slice holder containing an artificial cerebrospinal fluid (aCSF) containing (in mM): 125 NaCl, 2.5 KCl, 1.2 $NaH_2PO_4$, 1.2 $MgCl_2$, 11.1 D-glucose, 21.4 $NaHCO_3$, 2.4 $CaCl_2$, and 0.1 ascorbic acid, saturated with 95% $O_2$ / 5% $CO_2$ which was maintained at 32°C.

### *2.4.2 Whole cell voltage-clamped experiments*

Brain slices were submerged in a slice chamber and superfused with a continuous flow (2-3 ml/min) of aCSF saturated with 95% $O_2$ / 5% $CO_2$ at 32°C. Slices were visualised through oblique optics on an BX51WI upright microscope (Olympus). The surfaces of individual neuron somatas were cleared of debris through the application of a gentle flow of aCSF from a pipette prior to patching attempts. Whole-cell voltage-clamped recordings were made from LC neurones using recording electrodes (of 3-5 MΩ resistance) filled with intracellular recording solution containing (in mM): 115 potassium gluconate, 10 HEPES, 11 EGTA, 2 $MgCl_2$, 10 NaCl, 2 MgATP, and 0.25 $Na_2GTP$, giving an osmolarity of 270 mOsm/L. The pH of this intracellular solution was adjusted to 7.3 with KOH. Recordings of whole cell currents were amplified and filtered at 2 kHz using an Axopatch 200B amplifier (Axon Instruments) and digitised with a sampling rate of 10 kHz using a Digidata 1440a (Axon Instruments).

Activation of MOPrs on LC neurones evoked GIRK currents, providing a measurement of MOPr activation which could be monitored continuously and in real-time using whole-cell patch-clamp recordings. LC neurones were voltage clamped at -60 mV, with a

correction made for a previously calculated liquid junction potential of -12 mV for our intracellular solution. All drugs were applied to the brain slice through the superfusing solution at known concentrations. In LC neurones, it has been demonstrated that MOPrs and $\alpha_2$ adrenoceptors couple to the same population of GIRK channels (North et al., 1985). Utilising this phenomenon, we controlled for inter-cell variations in opioid-evoked current amplitude by normalising to the amplitude of the maximal $\alpha_2$ adrenoceptor-mediated GIRK current in the same cell, evoked by a supramaximal concentration of noradrenaline (NA, 100 μM). All $\alpha_2$-adrenoceptor mediated currents were examined in the presence of 1 μM prazosin and 3 μM cocaine. Naloxone (NLX) was applied after each opioid application in order to fully reverse evoked GIRK currents to a baseline level. While a concentration of 1 μM was initially used (Figure 4.1), the slow reversal of Compound 1-evoked GIRK currents with this naloxone concentration (Figure 4.1D) prompted us to increase this working concentration to 10 μM in subsequent experiments.

### *2.4.3 Data analysis*

All data from whole cell voltage clamped electrophysiological experiments were acquired using WinEDR recording software (University of Strathclyde) and analysed off-line. Where traces are presented, the best effort was taken to select individual traces from which data were representative of the entire dataset. Data points from traces were exported from WinEDR and graphically plotted using GraphPad Prism (Version 8). The decline in opioid-evoked GIRK currents was quantified through expression of the magnitude of evoked current over time as a percentage of the initial peak current. The overall of opioid-induced desensitization, '% desensitization', was representative of the magnitude of the opioid-evoked current at a set time post-peak response, either 8 min (Figure 4.5) or 10 min (all relevant figures within Chapter 5). Statistical comparisons of opioid-induced desensitization or the magnitude of opioid-evoked currents were made using one-way ANOVA with post hoc Tukey or Dunnett tests, or through unpaired, two-tailed t tests where appropriate. The utilised statistical analyses for each experiment are outlined in the respective figure legend.

## 2.5 Warm water tail immersion test of nociception

### *2.5.1 Experimental procedure*

The warm water tail immersion test of nociception was used in order to characterise the antinociceptive properties of morphine and Compound 1 (Janssen et al., 1963). Studies were conducted independently in both CD1 wildtype mice and in both C57BL/J wildtype and MOPr knockout animals (Chapter 2.2). Studies in CD1 were kindly conducted by Dr Rob Hill alongside the author, while studies in C57BL/J wildtype and MOPr knockout animals were conducted by the author alone. The methodology outlined below was used in both studies.

A water bath was maintained at 52.5°C. In order to test nociception in this assay, mice were restrained in a scruff and the tip of their tail was immersed into the 52.5°C water bath. The portion of the tail exposed to the water was standardised to approximately half of the overall tail length. The latency of the response to the nociceptive stimulus (the removal of the tail from the water) was measured using a stopwatch. Once this response was observed, or the 15 second cut-off time was reached, the tail of the mouse was immediately removed from the water bath, the tail was dried, and the mouse was returned to its home cage.

Control latency response times were obtained in all subjects at 30 min and 15 min prior to the time of injection, in order to provide a baseline value for tail flick latency in each mouse. For our studies of Compound 1-induced antinociception in CD1 mice, mice were injected with either morphine (10 mg/kg), Compound 1 (50 mg/kg and 100 mg/kg) or vehicle (saline) intraperitoneally. In our studies in C57BL/J mice, in both wild type and MOPr knockout animals, all mice were injected with Compound 1 (50 mg/kg, i.p.). The tail flick latency responses of treated animals were subsequently examined at 15, 30, 45- and 60-min post-injection.

### *2.5.2 Data analysis*

Raw values of tail flick latency (in seconds) were converted to % maximum possible effect values (% MPE) (Harris et al., 1964) through Equation 14.

$$(14) \quad \left(\frac{T_1 - T_0}{T_2 - T_0}\right) \times 100$$

Where $T_1$ is the observed tail flick latency (in seconds), $T_0$ is the baseline tail flick latency (in seconds) and $T_2$ is the cut-off time (15 seconds).

The area under the curve (AUC) was also calculated for % MPE data from baseline – 60 min post injection (Meymandi et al., 2006), using an in built equation in GraphPad (version 8). Non-parametric statistical analyses were used for the analysis of tail flick data, with the applied cut off time providing a non-normal distribution of data. A Kruskal-Wallis test with post-hoc Dunn's multiple comparisons test was used to compare AUC values between the various treatment groups in CD1 mice. A Mann-Whitney test was used to compare AUC values in wild-type and MOPr knockout C57BL/J mice.

## 2.6 Materials

DAMGO [[D-Ala$^2$, N-MePhe$^4$, Gly-ol$^5$]-enkephalin] was purchased from Bachem. Morphine sulphate was purchased from MacFarlan Smith. Naloxone hydrochloride and Takeda Compound 101 (CPD101) [3-[[[4-methyl-5-(4-pyridyl)-4H-1,2,4-triazole-3-yl] methyl] amine]-N-[2-(trifluoromethyl benzyl]benzamide hydrochloride] were purchased from HelloBio. Prazosin hydrochloride, GF102903X [2-[1-(3-dimethylaminopropyl)indol-3-yl]-3-(indol-3-yl) maleimide], PMA [phorbol 12-myrtistrate 13-acetate], GSK650394 [2-cyclopentyl-4-(5-phenyl-1H-pyrrolo[2,3-b]pyridin-3-yl-benzoic acid], Y-27632 [*trans*-4-[(1R)-1-aminoethyl]-N-4-pyridinylcyclohexanecarboxamide dihydrochloride] and SNC80 were purchased from Tocris. U-69,593 was purchased from Abcam. PZM21 [1-[(2S)-2-(dimethylamino)-3-(4-hydroxyphenyl)propyl]-3-[(2S)-1-(thiophen-3-yl)propan-2-yl]urea] hydrochloride was kindly provided by Dr Alexander Disney (University of Bath). Compound 1 [Tyr-*c*[D-Lys-Phe-Tyr-Gly]] was kindly provided by Dr Yangmei Li (University of South Carolina) and also synthesised by Biomatik Corporation. Data from both sources of Compound 1 are presented together in this thesis. SR17018 [5,6-dichloro-1-[1-[(4-chlorophenyl)methyl]-4-piperidinyl]-1,3-dihdro-2H-benzimidazol-2-one] was purchased from MedChemExpress and kindly modified to the mesylate salt by Dr Alexander Disney (University of Bath). All other reagents and drugs were purchased from Sigma Aldrich.

# Chapter 3: Characterisation of putatively G protein-biased MOPr agonists

## 3.1 Introduction

In recent years, a major drug discovery effort has been dedicated to the discovery and development of MOPr agonists which display signalling bias towards G protein signalling. This drive is founded on studies of morphine's effects in arrestin-3 knockout mice, which suggested that a number of opioid-induced adverse effects may be regulated by arrestin-dependent signalling downstream of MOPr (Bohn et al., 1999; Bohn et al., 2000; Raehal et al., 2005) (Chapter 1.3.1). However, this dogma has been weakened with the reproducibility of these original findings recently being brought into question (Kliewer et al., 2020) and studies in phosphorylation-deficient MOPr knock-in mice reporting no change in opioid-induced respiratory depression or constipation (Kliewer et al., 2019) (Chapter 1.3.1). Despite this, the development of G protein biased agonists at MOPr could provide valuable tool compounds to dissect the physiological relevance of independent signalling pathways downstream of MOPr. Additionally, attenuation of morphine tolerance in both arrestin-3 knockout (Bohn et al., 2000) and phosphorylation-deficient MOPr knock-in mice (Kliewer et al., 2019) suggests that by evading arrestin-3 recruitment, G protein-biased MOPr agonists may be less liable to the development of tolerance compared with balanced agonists.

The small molecule PZM21 was one of the first MOPr agonists defined to be G protein-biased (Manglik et al., 2016). PZM21 activated $G_i$ G protein signalling but produced minimal arrestin-3 recruitment in recombinant cell systems, suggesting that it is putatively G protein-biased in the absence of formal calculations of bias. The authors originally described PZM21 as possessing analgesic properties but being devoid of the ability to produce respiratory depression, unlike the balanced agonist morphine. However, as with the arrestin-3 knockout data, the reproducibility of findings with PZM21 regarding induced respiratory depression have also recently been brought into question (Hill et al., 2018b) (Chapter 1.3.2).

The SR-series of small molecules developed by Schmid et al. (2017) also yielded a number of MOPr agonists which reportedly displayed bias toward G protein signalling in recombinant cell systems. These included SR17018, which promoted analgesia in mice with minimal induction of respiratory depression, similarly to the profile originally described for PZM21 (Manglik et al., 2016).

A number of cyclized analogues of the endomorphins, developed to improve the metabolic stability of these therapeutically promising opioid peptides (Czapla et al., 2000; Wilson et al., 2000), have also displayed attractive *in vivo* pharmacology akin to that produced by G protein biased agonists. One such peptide, Tyr-c[D-Lys-Trp-Phe-Glu]-Gly-$NH_2$ (ZH853) was shown to have similar analgesic properties to morphine in mice but reduced propensity to induced respiratory depression and tolerance (Zadina et al., 2016). Similarly Tyr-c[D-Lys-Trp-Phe] (CYT-1010) demonstrated analgesia both preclinically and in phase I clinical trials, with a large therapeutic window for respiratory depression in rats preclinically (Webster et al., 2020). While the signalling properties of ZH853 and CYT-1010 have not been closely investigated, or published, it is evident that the attractive pharmacological profile of these peptides is akin to that previously associated with preclinical G protein-biased agonists at MOPr (Manglik et al., 2016; Schmid et al., 2017). Given that the endomorphins have been shown to display bias for arrestin signalling at MOPr (Rivero et al., 2012) (Chapter 1.3.2), it is possible that the nature of the endomorphin scaffold could be used to yield MOPr ligands with biased signalling properties. Considering this, we were interested to see whether Try-c[D-Lys-Phe-Try-Gly] (Compound 1), a recently developed novel cyclic endomorphin analogue with high affinity for MOPr (Li et al., 2016) displayed signalling bias at MOPr.

The work presented within this thesis chapter aimed to characterise the signalling profiles of the potentially G protein-biased agonists PZM21 and Compound 1 at the MOPr. This was performed in order to identify tool compounds which could be utilized to study the long-term functional consequences of biased agonism at the MOPr. In order to achieve this aim, we utilised a number of approaches: BRET-based assays in recombinant cell systems enabled refined measurements of the interactions of distinct signalling proteins, providing detailed quantification of agonist-induced MOPr signalling and bias measurements in a heterologous expression system. The electrically-evoked rat vas deferens (RVD) was also utilised as a classical bioassay of opioid activity, providing evidence of agonist- receptor interaction in a system of physiological MOPr expression.

In this chapter, I demonstrate that Compound 1 is a potent partial agonist at the MOPr, which displays G protein bias relative to the partial agonist morphine. The putatively G protein-biased MOPr agonist PZM21 however did not display G protein bias as previously described, but in fact in my studies appears to be simply a lower efficacy partial agonist at MOPr than morphine. Using the rat vas deferens, it was determined that both PZM21 and Compound 1 are high affinity, lower efficacy agonists. The work in this chapter therefore details a new G protein-biased agonist, Compound 1, which could

be a useful tool compound for determining the long-term functional consequences of biased signalling at MOPr, as well as a potentially promising therapeutic lead.

## 3.2 Results

### *3.2.1 Compound 1 is a G protein-biased agonist at MOPr*

#### *3.2.1.1 Characterising opioid-induced $G\alpha_i$ activation and arrestin-3 recruitment*

In order to characterise the signalling properties of ligands at MOPr, two separate BRET based assays were utilised in recombinant HEK293 cells. Firstly, opioid-induced $G_i$ G protein activation was assessed in HEK293 cells transiently expressing HA-MOPr as well as $G\alpha_{i1}$-*Renillia* luciferase II (RlucII) and $GFP_{10}$-$G\gamma_2$. Agonist-induced dissociation of these two labelled G protein subunits, determined by loss of BRET signal, was representative of $G_i$ G protein activation (Figure 3.1A; see Chapter 2.1.2). Opioid-induced arrestin-3 recruitment to MOPr was determined in HEK293 cells transiently transfected with MOPr-RlucII and arrestin-3-GFP. Agonist-induced association of the labelled proteins, determined by an increase in BRET signal, was representative of arrestin-3 recruitment to MOPr (Figure 3.1B; see Chapter 2.1.2).

Both DAMGO and morphine, well-documented agonists of MOPr, produced concentration-dependent increases in both $G_i$ G protein activation (Figure 3.1C) and arrestin-3 recruitment (Figure 3.1D). The putatively G protein-biased MOPr agonist PZM21 (Manglik et al., 2016) also produced concentration-dependent increases in both $G_i$ G protein activation (Figure 3.1C) and arrestin-3 recruitment (Figure 3.1D). The cyclic endomorphin analogue Compound 1 (Li et al., 2016) also produced concentration-dependent activation of $G_i$ G proteins (Figure 3.1C) and low but detectable concentration-dependent arrestin-3 recruitment (Figure 3.1D).

Hill slopes for concentration-response curves for G protein and arrestin-3 recruitment were constrained to 1 in order to improve curve fitting and reduce error in the calculation of agonist potency and efficacy (Kenakin, 2009). When the Hill slopes were unconstrainted in curve fitting, the best-fit values ($\pm$ S.E.M.) of agonist Hill slopes for $G_i$ activation and arrestin-3 recruitment were as follows: $G_i$ activation: DAMGO = 0.7 $\pm$ 0.1, morphine = 1.0 $\pm$ 0.2, PZM21 = 0.8 $\pm$ 0.2, Compound 1 = 0.8 $\pm$ 2. Arrestin-3 recruitment: DAMGO = 1.3 $\pm$ 0.3, morphine = 1.1 $\pm$ 0.4, PZM21 = 0.6 $\pm$ 0.3. The Hill slope for Compound 1-induced arrestin-3 recruitment could not be determined when its value was unconstrained due to ambiguous curve fitting. When best-fit values of the Hill slopes for all agonists in both assays were compared statistically to a hypothetical value of 1 using an extra sum-of-squares F test, only the Hill slope for DAMGO-induced $G_i$ activation was significantly different from 1 ($P < 0.05$). However, the R squared value for the curve fitting for DAMGO-induced $G_i$ activation when the Hill slope was constrained to 1 was similar

to that when the Hill slope was unconstrained (0.94 and 0.93 respectively), indicating that either model could effectively describe this response.

PZM21 and Compound 1 had significantly higher potencies for $G_i$ G protein activation than morphine (Table 3.1). No significant differences in agonist potencies were observed in the arrestin-3 assay, in part ascribed to sizable error with this parameter due to the large fitting error associated with derived parameters due to limitations in curve fit quality in the case of weak partial agonists PZM21 and Compound 1 (Table 3.1).

In systems of low receptor reserve, the maximal response ($E_{Max}$) of a partial agonist (their intrinsic activity) can be used as robust measure of their intrinsic efficacy (Stephenson, 1956; Kelly, 2013). This is particularly important when utilisation of the operational model is limited by ambiguous curve fitting in the case of low efficacy partial agonists (see Compound 1 responses in Figure 3.1D). The $E_{Max}$ values for $G_i$ G protein activation induced by morphine, PZM21 and Compound 1 were significantly lower than the full agonist DAMGO (Table 3.1), indicating they are partial agonists at MOPr for G protein activation in this system (Table 3.1). Similarly, the $E_{Max}$ values of morphine, PZM21 and Compound 1 for arrestin-3 recruitment were significantly lower than that of DAMGO (Table 3.1).

The maximum responses of morphine and Compound 1 were statistically similar for $G_i$ G protein activation, however the efficacy of Compound 1 for arrestin-3 recruitment was significantly lower than that of morphine (Table 3.1). The fact that Compound 1 had the same efficacy for $G_i$ G protein activation as morphine but induced comparatively lower levels of arrestin-3 recruitment strongly suggest that it is a G protein-biased agonist relative to morphine at the MOPr. Considering that the rank order of agonist potency was conserved between assays of G protein activation and arrestin-3 recruitment, it could be postulated that the functional selectivity of Compound 1 is driven by differences in its efficacy rather than affinity.

Similar comparisons of intrinsic efficacy examining PZM21 demonstrate that it is a low efficacy MOPr agonist, with a significantly lower efficacy for G protein activation than morphine (Table 3.1). Interestingly, the efficacy of PZM21 for arrestin-3 recruitment was statistically similar to that of morphine (Table 3.1). These data suggest that in our hands PZM21 is not a G protein-biased agonist at MOPr, contrary to the original findings for this agonist (Manglik et al., 2016). However, our finding that PZM21 has a lower efficacy for G protein activation than morphine is in agreement with other studies (Hill et al., 2018b; Yudin et al., 2019; Gillis et al., 2020a).

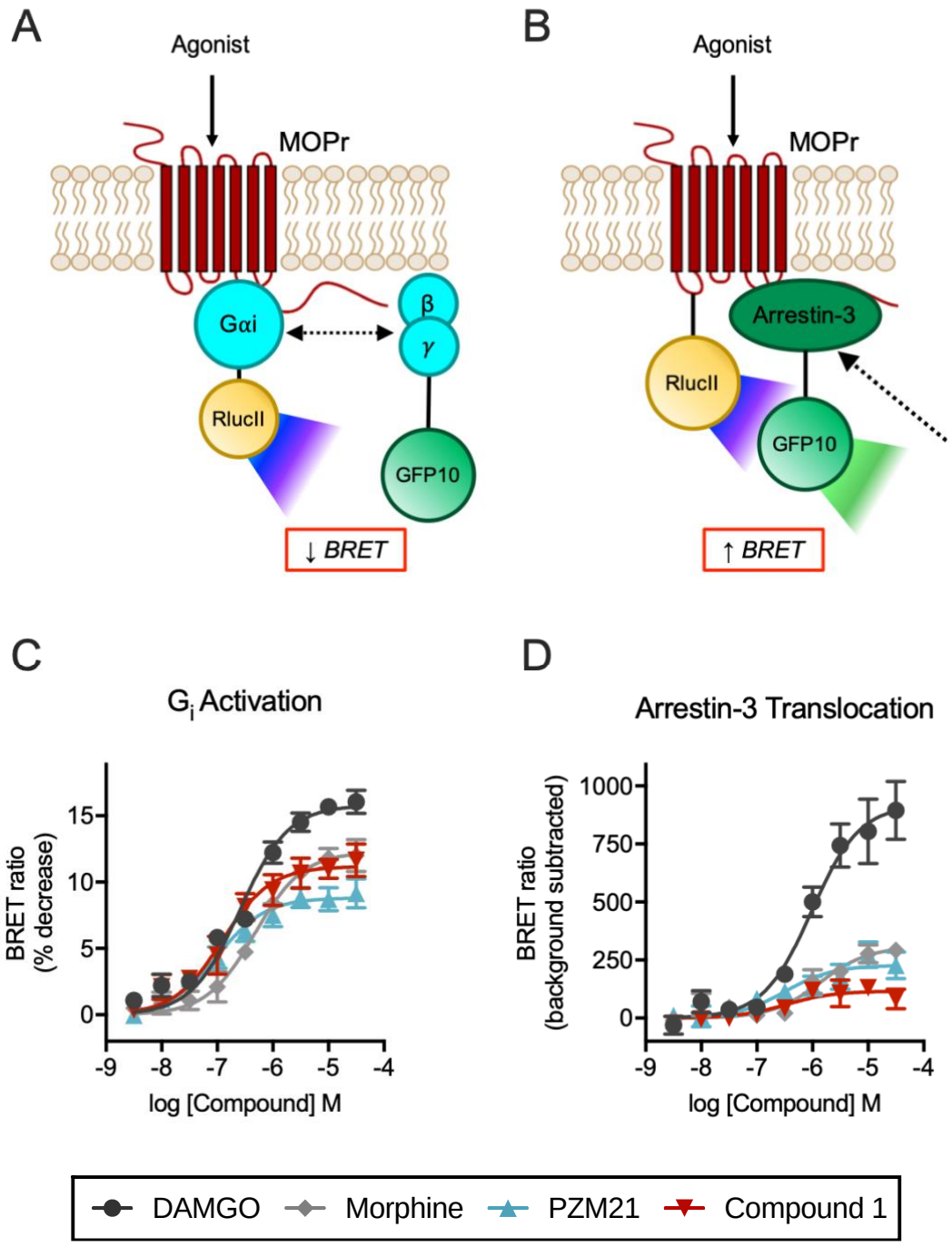


**Figure 3.1 – Opioid-induced $G_i$ G protein activation and arrestin-3 recruitment in HEK293 cells transiently expressing recombinant MOPrs.**

*(A) A schematic illustrating the principle of the $G_i$ G protein activation assay. Opioid-induced activation of MOPr results in a separation of labelled G protein subunits, resulting in a reduction in BRET signal. (B) A schematic illustrating the principle of the arrestin-3 assay. Opioid-induced MOPr activation results in translocation of arrestin-3 to the receptor. The association of the labelled MOPr and labelled arrestin-3 results in an increase in BRET signal. (C) DAMGO, morphine, PZM21 and Compound 1 produced concentration-dependent activation of $G_i$ G protein as measured as a decrease in BRET*

*signal occurring between labelled Gα & Gγ proteins. (D) DAMGO, morphine, PZM21 and Compound 1 produced concentration-dependent recruitment of labelled arrestin-3 translocation as measured by an increase in BRET signal from association of labelled MOR and arrestin-3. Fitted values for agonist $pEC_{50}$ and $E_{Max}$ were generated from combined concentration-response curves and are presented in Table 3.1. Data are representative of mean ± SEM where n=5.*

| | *$G_i$ Coupling* | | | *Arrestin-3 Recruitment* | | |
|---|---|---|---|---|---|---|
| | $pEC_{50}$ | $E_{Max}$ | | $pEC_{50}$ | $E_{Max}$ | |
| *Agonist* | (M) | BRET Ratio | % DAMGO | (M) | BRET Ratio | % DAMGO |
| DAMGO | 6.6 ± 0.1 | 15.8 ± 0.5 † | 100 | 6.0 ± 0.1 | 920 ± 56 † | 100 |
| Morphine | 6.3 ± 0.1 | 12.3 ± 0.5 | 78 ± 3 | 5.9 ± 0.2 | 307 ± 33 | 33 ± 4 |
| PZM21 | 7.0 ± 0.1 * | 8.8 ± 0.4 * | 56 ± 2 | 6.5 ± 0.2 | 227 ± 26 | 25 ± 3 |
| Compound 1 | 6.9 ± 0.1 * | 11.2 ± 0.5 | 71 ± 3 | 6.5 ± 0.4 | 116 ± 22 * | 13 ± 2 |

**Table 3.1 – The $pEC_{50}$ and $E_{Max}$ values for opioids in the $G_i$ protein activation and arrestin-3 recruitment assays.**

*Values were determined from data presented in Figure 3.1. Data are expressed as mean ± SEM, where n=5. * p < 0.05, significantly different from the respective morphine value, † p < 0.05, significantly different from all other respective values, one-way ANOVA with Tukey's post-hoc test.*

*3.2.1.2 Quantifying the G protein-biased signalling of Compound 1 at MOPr*

The *de facto* method of quantifying biased signalling at GPCRs *in vitro* is the $\Delta\Delta\log(\tau/K_A)$ method. In this method, agonism for separate signalling pathways is quantified through a transduction coefficient ($\tau/K_A$) computed using a form of the Black-Leff operational model (Black et al., 1983) (Chapter 2.1.3). However, the power of this approach is severely limited in the case of weak partial agonists, due to the large fitting error associated commonly with derived parameters due to variable curve fit quality when using the operational model (Kelly, 2013; Gillis et al., 2020c). Additionally, agonist efficacy and affinity (broadly $\tau$ and $K_A$ respectively in this case) cannot be determined separately in this analysis, as agonism is considered as a composite of these factors in the single transduction coefficient ($\tau/K_A$). Under this analysis, in a case where functional selectivity is driven by differences in efficacy alone, readouts of bias would in effect be diminished by the incorporation of affinity in modelling.

In situations where partial agonism is present, an alternate method of quantifying biased signalling has been developed which is driven by efficacy and not affinity (Burgueño et al., 2017). This analysis solely focuses on differences in agonist $\tau$ values, which are calculated by fitting agonist concentration-response curves to the operational model (Black et al., 1983). A similar process is used in that the transduction coefficient model described above to generate a normalised $\Delta\Delta\log(\tau)$ values for each agonist (Chapter 2.1.3). While this methodology recognises the limitations of the $\Delta\Delta\log(\tau/K_A)$ methods when it comes to the analysis of partial agonists, its utilisation of the operational model means its power is similarly limited where agonist response curves have variable fitting to the operational model, resulting in large values of error surrounding fitted parameters.

In systems of low receptor reserve, the intrinsic activity ($E_{Max}$) of partial agonists can be used as a robust, assumption free and affinity independent estimate of efficacy (Stephenson, 1956; Dekan et al., 2019). By normalising fitted $E_{Max}$ values of test ligands to a reference partial agonist and subtracting this normalised $E_{Max}$ value across comparison pathways, a singular $\Delta$ normalised $E_{Max}$ value can be generated for each test ligand, which can be used as an entirely efficacy-dependent measure of bias (Dekan et al., 2019) (Chapter 2.1.3). This model is less liable to be limited in cases of poor curve fitting for weak partial agonists as the asymptote of the fitted logistic function ($E_{Max}$) can be fitted more confidently than the parameter $\tau$ in the operational model, which is subject to more assumptions. While application of this model is not possible in scenarios where lower efficacy agonists appear as full agonists, such as in systems of high signal amplification or receptor reserve, this is not the case in our assays where there is relatively low receptor reserve (possibly owing to transient rather than stable MOPr

expression) and low signal amplification (through measuring separation of G protein subunits rather than second messenger systems such as cAMP).

In light of these considerations, signalling bias within our test agonists was assessed using the $\Delta$ normalised $E_{Max}$ method, with the prototypical partial agonist morphine selected as a reference agonist, as importantly morphine was a partial agonist in both signalling assays. Similarly, to the unnormalized data in Table 3.1, the normalised $E_{Max}$ value of Compound 1 for $G_i$ G protein activation was statistically similar to that of morphine, but the normalised $E_{Max}$ value of Compound 1 for arrestin-3 recruitment was significantly lower than that of morphine (Figure 3.2A). The normalised $E_{Max}$ values of PZM21 for both $G_i$ G protein coupling and arrestin-3 recruitment were significantly lower than morphine (Figure 3.2A). The $\Delta$ normalised $E_{Max}$ value for Compound 1 was significantly different from morphine, demonstrating that it is a G protein biased agonist at MOPr (Figure 3.2B). PZM21 displayed no such significant difference in $\Delta$ normalised $E_{Max}$ analysis, indicating that it is not G protein biased, in our hands, but is in fact a lower efficacy partial agonist than morphine.

When analysed through the $\Delta\Delta\log(\tau/K_A)$ method, Compound 1 does not appear G protein biased in comparison to morphine (Figure 3.3B). The transduction coefficient ($\log(\tau/K_A)$) for Compound 1-induced arrestin-3 recruitment has a large error value (Figure 3.3A), which reflects poor fitting of the operational model due to the very low efficacy coupling of Compound 1 for this pathway (Figure 3.1D). With affinity ($K_A$) accounted for within the transduction coefficient, it is clear that the high potency of Compound 1 relative to morphine opposes the impact of its lower efficacy (Figure 3.2A) in this assessment of bias (Figure 3.3A). These factors mean that the implementation of this method is limited when assessing bias in our systems.

Similarly, no significant bias is observed between our test ligands when utilising the $\Delta\Delta\log(\tau)$ method described above (Figure 3.4B) (Burgueño et al., 2017). However, Compound 1 did display statistically similar efficacy to morphine for $G_i$ G protein activation while showing significantly lower efficacy for arrestin-3 recruitment (Figure 3.4A), supporting our findings from the $\Delta$ normalised $E_{Max}$ analysis (Figure 3.2). While there was no significant difference between the $\tau$ values of Compound 1 and morphine for G protein activation, the fitted value for Compound 1 ($0.4 \pm 0.1$) is considerably lower than that of morphine ($0.6 \pm 0.1$) (Figure 3.4A). This is in spite of there being no significant differences in fitted $E_{Max}$ values of these two agonists (Table 3.1) or little discernible difference in the magnitude of the responses displayed in their concentration-response curves (Figure 3.1C). Evidently, this difference reduces the degree of bias recorded for Compound 1 in this method (Figure 3.4B). The margin of uncertainty around the fitted $\tau$

parameters for our test agonists reflects previously discussed issues around generated uncertainty in a model such as the operational one where many interdependent unknowns must be fitted from limited data for weak partial agonists (Chapter 3.3.3). For this reason, the assumption-free $\Delta$ normalised $E_{Max}$ matrix has been utilised to assess bias in our assays.

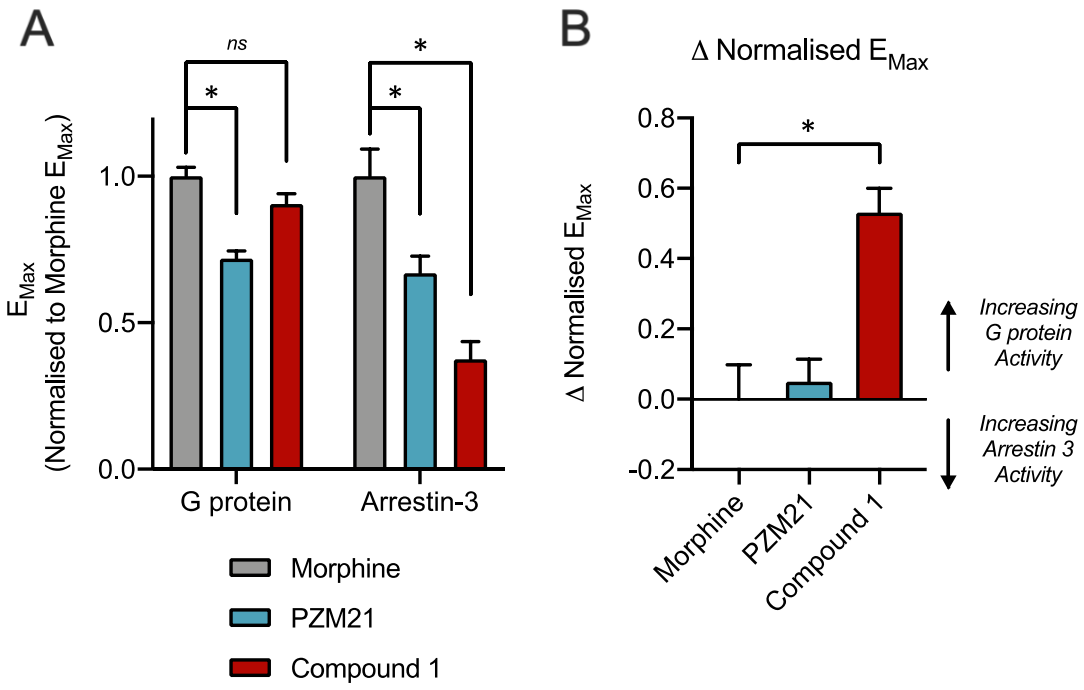


**Figure 3.2 – Calculation of biased agonism at MOPr through Δ normalised $E_{Max}$.**

*(A) $E_{Max}$ values generated from data presented in Figure 3.1 and Table 3.1 normalised to values for morphine for both $G_i$ G protein activation and arrestin-3 recruitment. (B) Calculated differences in agonist normalised $E_{Max}$ values presented in A for G protein activation versus arrestin-3 recruitment. Data are presented as mean ± SEM, where n=5. * p < 0.05, one-way ANOVA with Tukey's post-hoc test.*

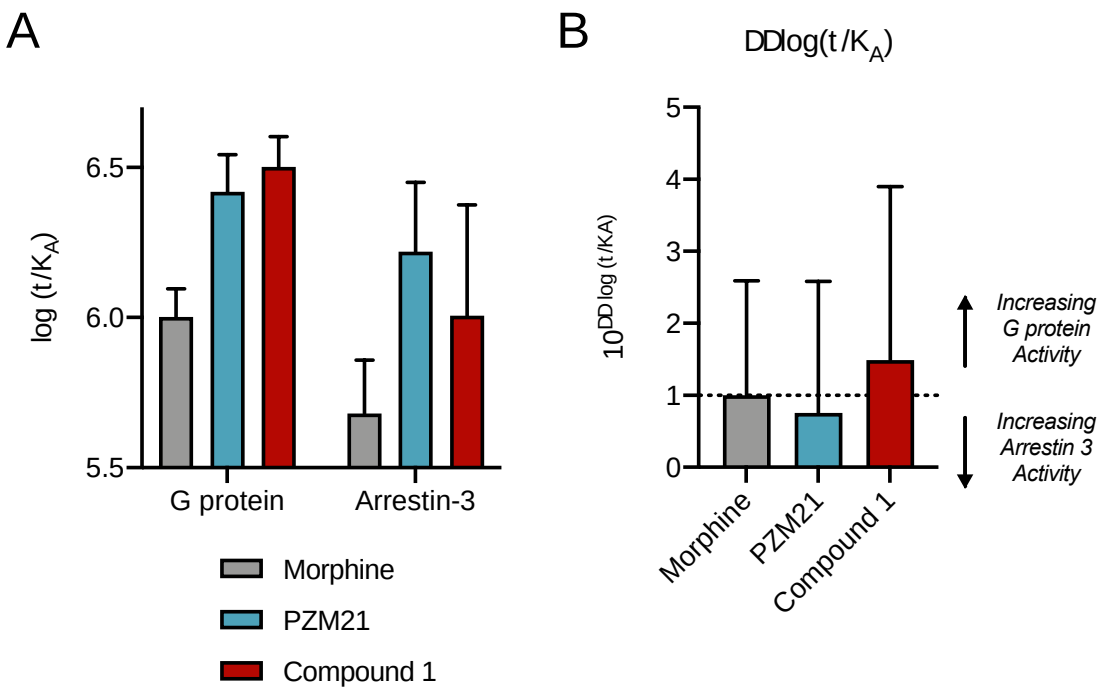


**Figure 3.3 – Calculation of biased agonism at MOPr through ΔΔlog(τ/K$_A$)**

*(A) log(τ/K$_A$) values for opioids in both the G$_i$ G protein activation and arrestin-3 recruitment assays, generated through fitting data presented in Figure 3.1C and Figure 3.1D to the operational model. (B) Differences in agonist activity, represented in the parameter log(τ/K$_A$) presented in A, across G$_i$ G protein activation and arrestin-3 recruitment when normalised to the activity of morphine. Data are presented as mean ± SEM, where n=5.*

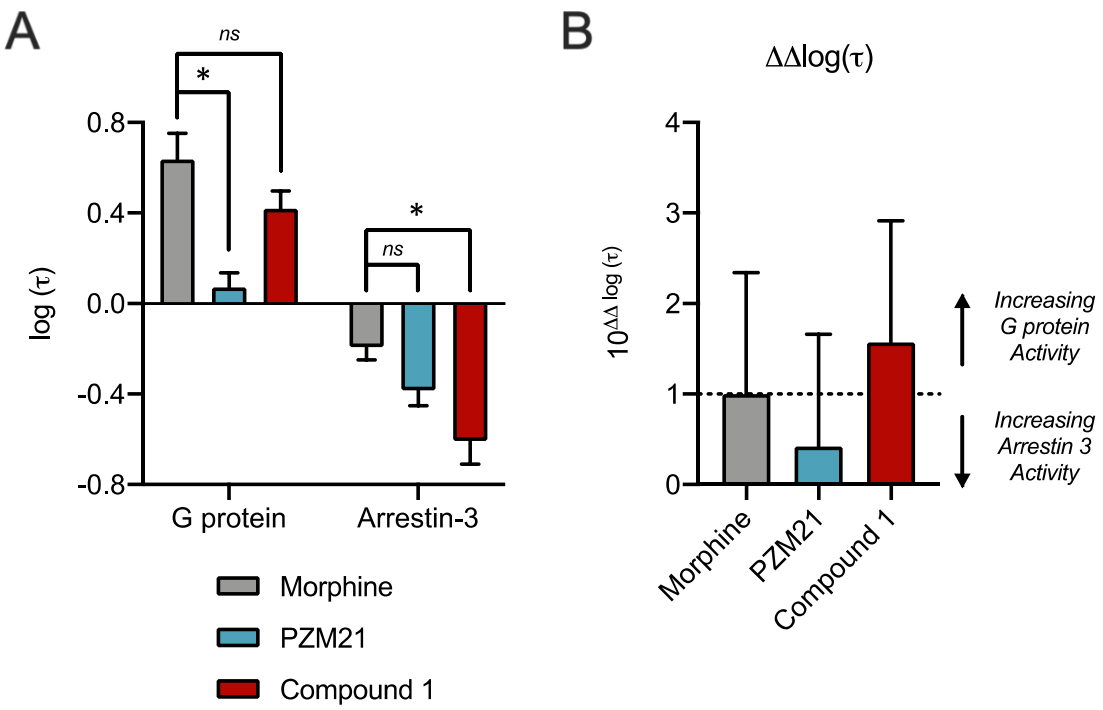


**Figure 3.4 – Calculation of biased agonism at MOPr through ΔΔlog(τ).**

*(A) The efficacy (log(τ)) of opioids for both $G_i$ G protein activation and arrestin-3 recruitment determined through fitting data presented in Figure 3.1C and Figure 3.1D to the operational model. (B) Differences in agonist efficacy, log(τ), in $G_i$ G protein activation and arrestin-3 recruitment assays when efficacy was normalised to morphine. Data are presented as mean ± SEM, where n=5. * p < 0.05, ns p > 0.05, one-way ANOVA with post-hoc Tukey test.*

*3.2.1.3 Inhibition of DAMGO-induced arrestin-3 recruitment by partial MOPr agonists*

In attempts to handle the utilisation of the operational model, and classical $\Delta\Delta\log(\tau/K_A)$ analysis, in the assessment of bias for partial agonists, some groups have attempted to separately generate affinity ($K_A$) values for weak partial agonists through competition assays in order to apply informed constraints to the operational model, leading to refined analysis (Stahl et al., 2015). This methodology was utilised in the determination of the G protein biased signalling profile of SR17018 at MOPr (Schmid et al., 2017). In order to determine functional $K_A$ values, the group tested the ability of SR17018 and related compounds to inhibit arrestin-3 recruitment induced by a submaximal (approximately $EC_{50}$) concentration of DAMGO. Curiously, in this previous study SR17018 and related compounds did not inhibit DAMGO-induced arrestin-3 recruitment in examined concentrations (up to 30μM). This is in spite of SR17018 and related ligands displaying high affinity for MOPr in radioligand binding assays and promoting MOPr-dependent G protein activation at the same concentrations. Accounting for these data, the group applied constraints to the operational model fitted to arrestin-3 recruitment induced by these ligands, inevitably affecting the final bias scores ascribed to these novel agonists.

However, the finding that the partial MOPr agonist SR17018 does not inhibit DAMGO-induced arrestin-3 recruitment at concentrations at which it promoted G protein coupling is in disagreement with the fundamental principles of receptor pharmacology. In this case, a partial agonist (such as SR17018) at high concentrations should competitively displace the full agonist (such as DAMGO) at the receptor and display its own minimal effect for the pathway, effectively behaving as an antagonist (Figure 3.5A) (Stahl et al., 2015).

We sought to investigate whether our test agonists (all of which are partial agonists in this system (Table 3.1)), as well as SR17018, would inhibit DAMGO-induced arrestin-3 recruitment in our BRET assay. HEK293 cells expressing MOPr-RlucII and arrestin-3 GFP were incubated with our test partial agonists for 30 minutes at 37°C before addition of $10^{-6}$M DAMGO and BRET readings taken (Figure 3.1B). $10^{-6}$M DAMGO was used as a submaximal concentration based on data in Table 3.1 suggesting this is approximately the $EC_{50}$ value in our arrestin-3 recruitment assay.

As anticipated, morphine (Figure 3.5B), PZM21 (Figure 3.5C) and Compound 1 (Figure 3.5D) each produced concentration-dependent inhibition of arrestin-3 recruitment induced by a submaximal concentration of DAMGO. The fitted plateau values observed with these agonists generally reflected their intrinsic activity for arrestin-3 recruitment (Table 3.1), with Compound 1 displaying a lower plateau value than morphine and PZM21 (Table 3.2). Compound 1 and PZM21 inhibited DAMGO-induced arrestin-3

recruitment with a higher potency ($pIC_{50}$) than morphine (Table 3.2), suggesting they have higher affinity for MOPr than morphine.

Intriguingly, SR171018 did not inhibit DAMGO-induced arrestin-3 recruitment at the concentrations tested (Figure 3.5E). While these data are in agreement with the original finding from Schmid et al. (2017), in other studies from our lab group we have been unable to reproduce robust G protein activation in response to SR17018 (up to $3x10^{-5}M$) in our assay systems (Ramos-Gonzalez, unpublished data). The structure of the purchased SR17018 used in this study was validated by N.M.R. (Disney, unpublished data).

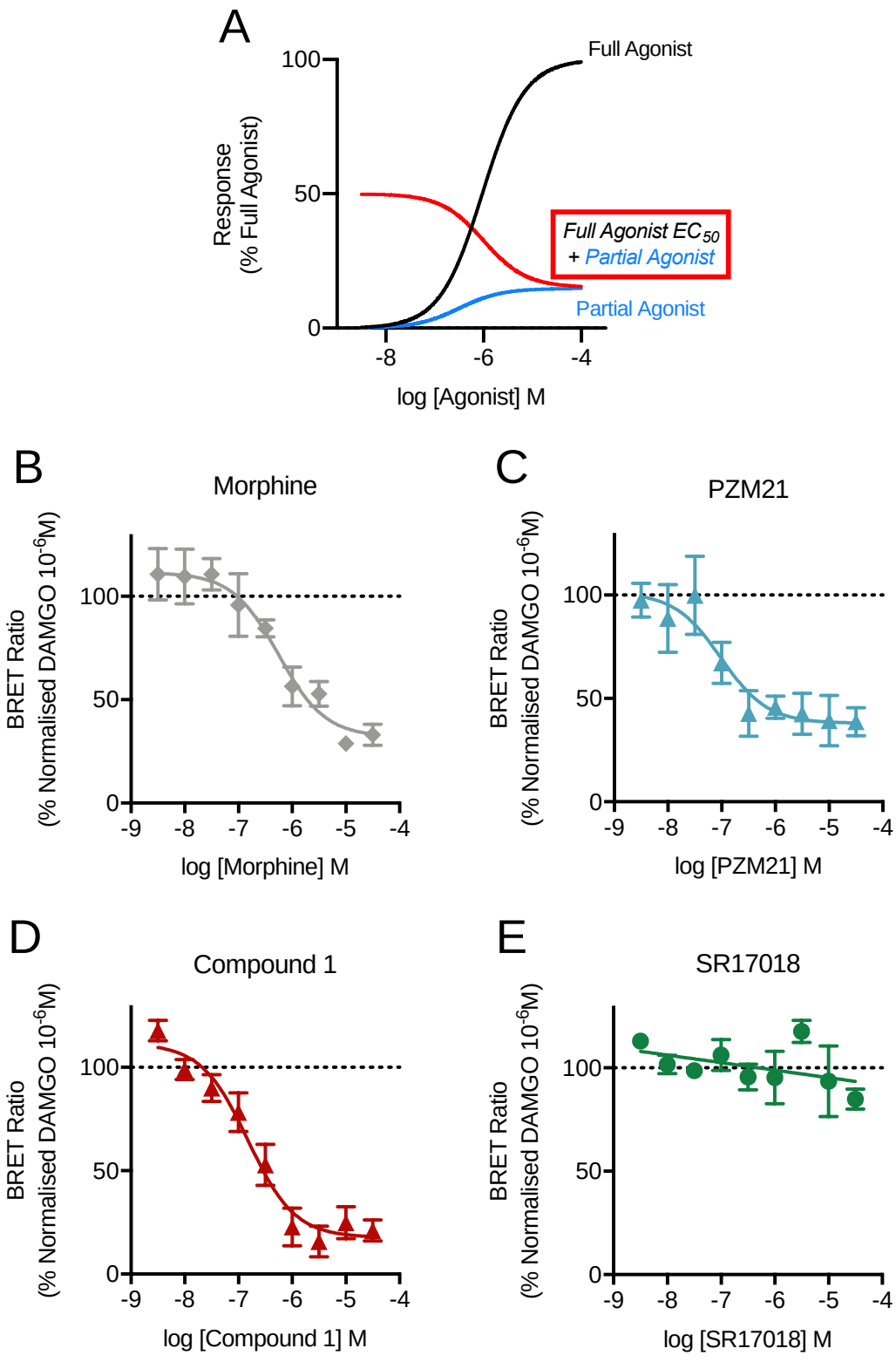


**Figure 3.5 – Partial antagonism of DAMGO-induced arrestin-3 recruitment by MOPr partial agonists.**

*(A) A schematic depicting the theoretically expected interaction between a full agonist and a partial agonist at the same receptor. Where an agonist of full efficacy (black line) produces a concentration-response with an $E_{Max}$ of 100%, the hypothetical partial agonist*

*here produces a concentration-response curve with an $E_{Max}$ of 15% (blue line). In this scenario, increasing concentrations of the partial agonist should be able to compete with a submaximal concentration (an $EC_{50}$ in this case) of the full agonist for the receptor, antagonising the function of the full agonist but producing an incomplete inhibition due their own minimal efficacy for the receptor. Increasing concentrations of morphine (B), PZM21 (C), Compound 1 (D) and SR17018 (E) were preincubated for 30 minutes at 37℃ with HEK293 cells transiently expressing MOPr-RlucII and arrestin-3-GFP before the addition of DAMGO ($10^{-6}$M) and BRET measurements subsequently taken (Figure 3.1B). Responses were normalised to those induced by DAMGO ($10^{-6}$M) alone and baseline readings of BRET were subtracted. Data are presented as mean ± SEM, where n=3-4.*

| | Morphine | PZM21 | Compound 1 | SR17018 |
|---|---|---|---|---|
| $pIC_{50}$ | 6.3 ± 0.2 | 7.0 ± 0.3 | 6.8 ± 0.1 | - |
| Bottom | 32 ± 7 | 38 ± 6 | 18 ± 4 | - |

**Table 3.2 – $pIC_{50}$ and maximum inhibition values for inhibition of DAMGO-induced arrestin-3 recruitment**

*Values were determined from data presented in Figure 3.5. Data are presented as mean ± SEM where n=3-4.*

### *3.2.2 Compound 1 is a partial agonist at MOPr and DOPr, but lacks agonist activity at KOPr*

Given the high level of homology of the orthosteric ligand binding pocket of opioid receptors and the promiscuous nature of classical MOPr receptor agonists such as morphine, we sought to determine if Compound 1 possessed agonist activity at DOPr and KOPr. Compound 1 has previously been demonstrated to have a 40-fold higher affinity for MOPr over DOPr, with very low affinity at KOPr (Li et al., 2016), however its functional activity at DOPr and KOPr had not been assessed.

A similar $G_i$ G protein activation BRET methodology was used here to that depicted in Figure 3.1A for the MOPr (Chapter 2.1.2). The ability of Compound 1 and a reference agonist (SNC80 and U69,593 for DOPr and KOPr respectively) to produce concentration-dependent activation and separation of transiently transfected labelled G proteins was assessed in HEK293 cells either expressing HA-DOPr (Figure 3.6C) or HA-KOPr (Figure 3.6E).

Both SNC80 and Compound 1 produced concentration-dependent activation of $G_i$ G proteins in HEK293 cells expressing HA-DOPr (Figure 3.6D). The intrinsic activity of Compound 1-induced $G_i$ G protein signalling in HA-DOPr expressing cells was significantly lower than that of SNC80 (Table 3.3), indicating that it is a weak partial agonist at DOPr. The potency of Compound 1 for $G_i$ G protein signalling at DOPr is slightly lower (~6 fold) than its potency at MOPr (Table 3.3), suggesting a lower degree of MOPr selectivity than found in radioligand binding assays (Li et al., 2016).

While U69,593 produced concentration-dependent activation of $G_i$ G protein signalling in HA-KOPr expressing HEK293 cells, no activation was observed with increasing concentrations of Compound 1 (Figure 3.6F). This finding is in line with the very low affinity of Compound 1 for KOPr in radioligand binding assays (Li et al., 2016). Additionally, the lack of Compound 1-induced $G_i$ G protein signalling serves as a control that Compound 1-induced G protein activation in cells expressing HA-MOPr and HA-DOPr were not due to effects on receptors endogenously expressed in HEK293 cells.

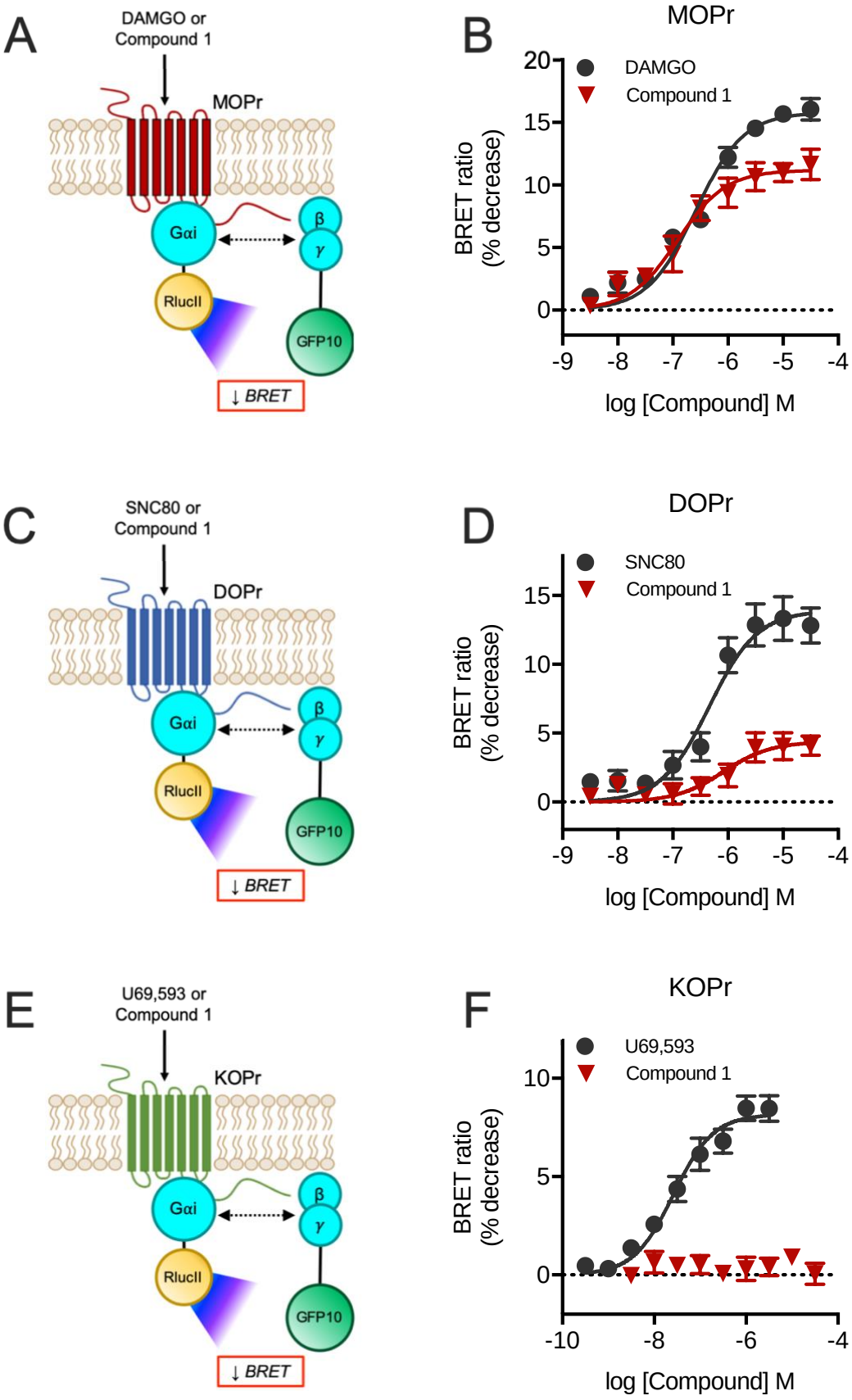


**Figure 3.6 – Assessing the selectivity agonist activity of Compound 1 across the opioid receptors.**

*Schematics describing the principle of the MOPr (A), DOPr (C) and KOPr (E) $G_i$ G protein activation assays Agonist-induced activation of opioid receptors in these assays results in a separation of labelled G protein subunits, resulting in a reduction in BRET signal. (B) Data from Figure 3.1 showing DAMGO and Compound 1 promoted separation of $G_i$ G protein subunits in HEK293 cells expressing MOPr. (D) SNC80 and Compound 1 promoted separation of labelled $G_i$ G proteins in HEK293 cells expressing DOPr. (F) U69,593, but not Compound 1, promoted separation of labelled $G_i$ G protein subunits in HEK293 cells expressing KOPr. Data are expressed as mean ± SEM, where n=5.*

| | MOPr | | DOPr | | KOPr | |
|---|---|---|---|---|---|---|
| | DAMGO | Compound 1 | SNC80 | Compound 1 | U69,593 | Compound 1 |
| $pEC_{50}$ | 6.6 ± 0.1 | 6.9 ± 0.1 | 6.3 ± 0.1 | 6.1 ± 0.3 | 7.6 ± 0.1 | - |
| $E_{Max}$ BRET Ratio | 15.8 ± 0.5 | 10.8 ± 0.5 | 13.9 ± 0.8 | 4.4 ± 0.6 | 8.2 ± 0.3 | - |
| $E_{Max}$ % Normalised | 100 | 70.8 ± 3.4 | 100 | 31.6 ± 4.0 | 100 | - |

**Table 3.3 – $pEC_{50}$ and $E_{Max}$ values for Compound 1 and respective tool agonists for $G_i$ G protein activation at MOPr, DOPr and KOPr**

*Values calculated from data presented in Figure 3.6. Data are presented as mean ± SEM where n=5.*

### *3.2.3 Investigating the affinity of partial MOPr agonists in isolated rat vas deferens*

The electrically-stimulated isolated vas deferens preparation provides an effective bioassay of opioid receptor-activity. MOPr agonists are able to inhibit the electrically-evoked release of noradrenaline through an action at presynaptic receptors (Henderson et al., 1976; Lemaire et al., 1978). While partial agonists such as morphine are able to inhibit such contractions in vas deferens preparations from mouse (Henderson et al., 1976), the electrically evoked contractions of the rat vas deferens (RVD) are sensitive to high efficacy MOPr agonists such as β-endorphin and DAMGO, but not lower efficacy agonists such as morphine (Lemaire et al., 1978). The lack of agonist activity for lower efficacy MOPr agonists in the RVD is due to the very low receptor reserve present in this system. Low efficacy agonists competitively bind MOPr, but in this system they do not possess intrinsic efficacy high enough to inhibit electrically-evoked contractions of the RVD, as done by high efficacy agonists. Therefore, when added in combination, low efficacy agonists effectively antagonise the inhibitory responses of a full agonist in the RVD (Ishii et al., 1981). Here we utilized this phenomenon for lower efficacy MOPr agonists in the RVD, to characterise the affinity of our test agonists in a system with physiological receptor expression, using traditional methods of quantifying competitive antagonism (Schild, 1947) (Chapter 2.3.3).

Cumulative addition of the full MOPr agonist DAMGO ($10^{-8}$M - $10^{-5}$M) caused concentration-dependent inhibition of electrically-evoked contractions of the isolated RVD (Figure 3.7). Generally, maximal concentrations of DAMGO reduced the electrically-evoked contractions of the RVD to non-detectable levels (Figure 3.7).

DAMGO responses in RVD were assessed in the presence of several concentrations of test partial agonists in each individual RVD preparation (Figure 3.8). After 20 minutes of preincubation, increasing concentrations of morphine (Figure 3.8A), PZM21 (Figure 3.8B) and Compound 1 (Figure 3.8C) resulted in a reduction of DAMGO potency in the RVD, resulting in a parallel rightward shift of its concentration-response curve. Concentration-response curves were fitted in order to generate dose-ratio (DR) values for each individual RVD preparation for each test partial agonist. DR values from each individual experiment were then pooled to give average DR ratio values for each test agonist concentration.

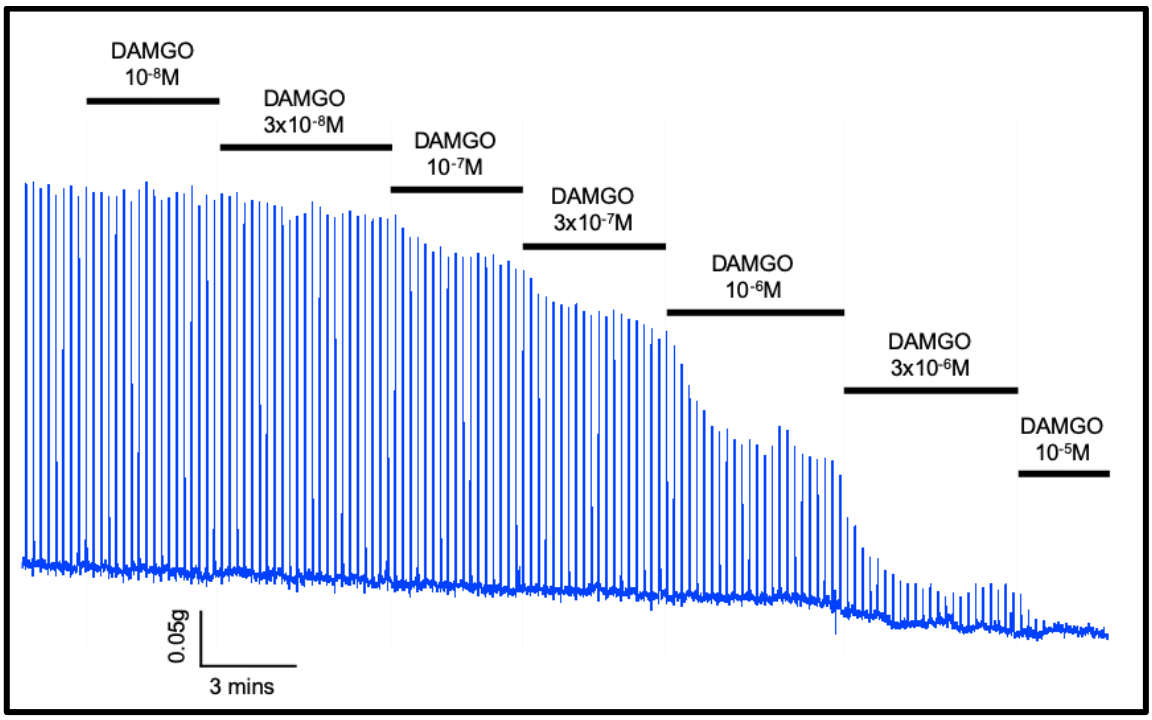


**Figure 3.7 – DAMGO inhibits electrically-evoked contractions of the RVD.**

*A representative trace from a single preparation demonstrating that cumulative addition of increasing concentrations of DAMGO inhibited the electrically evoked contractions of RVD smooth muscle.*

These averaged DR values were used to construct Schild plots for each test agonist (Figure 3.9). The slope of the constructed Schild plots was subjected to an extra sum-of-squares F test to determine whether the slope was significantly different from the hypothetical value of 1. The alternative unconstrained Schild plot slope values (value, 95% CI) for morphine (1.2, 0.6 – 1.7), PZM21 (1.3, 0.4 – 2.1) and Compound 1 (0.8, 0.1 – 1.5) were not significantly different from 1 and therefore all data was fitted to Schild plots with a constrained slope of 1.

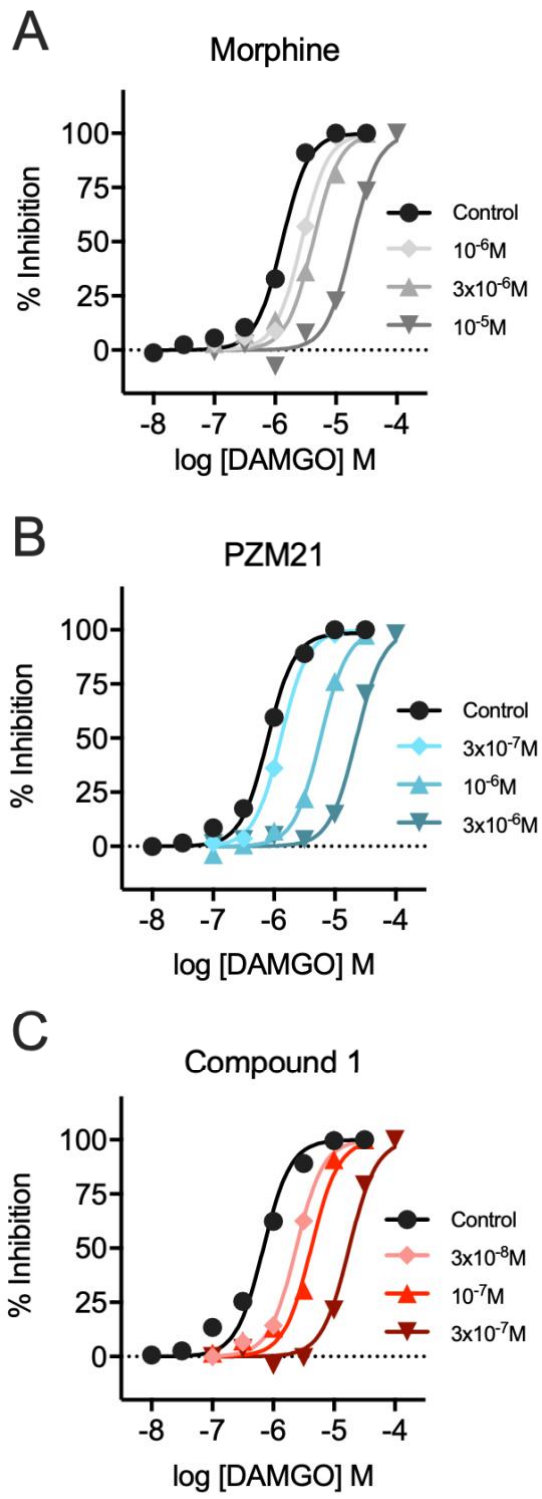


**Figure 3.8 – Single representative experiments showing competitive inhibition of DAMGO activity in the RVD by partial MOPr agonists.**

*Concentration-response curves for DAMGO-induced inhibition of electrically-evoked contractions in the RVD after 20 minutes of preincubation with increasing concentrations of morphine (A), PZM21 (B) and Compound 1 (C). Data presented are from individual preparations.*

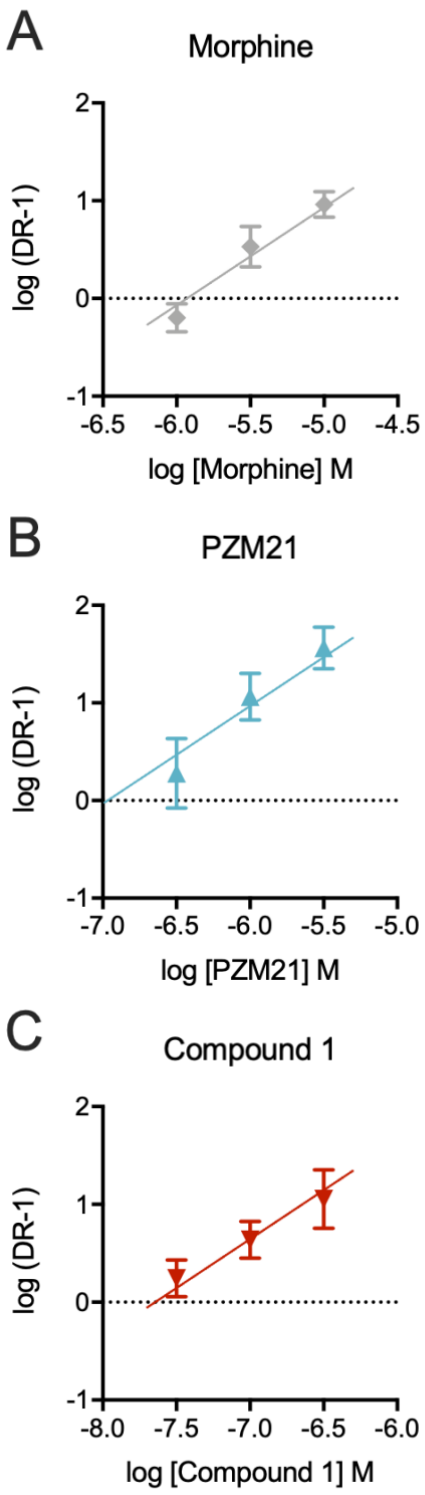


**Figure 3.9 – Schild plots for inhibition of DAMGO responses in the RVD by partial MOPr agonists.**

*Schild plots for morphine (A), PZM21 (B) and Compound 1 (C) inhibition of DAMGO-induced responses in RVD. Dose ratio (DR) values were calculated from individual experiments of the type presented in Figure 3.8 and then pooled to form Schild plots. Data presented as mean ± SEM, where n=3-6.*

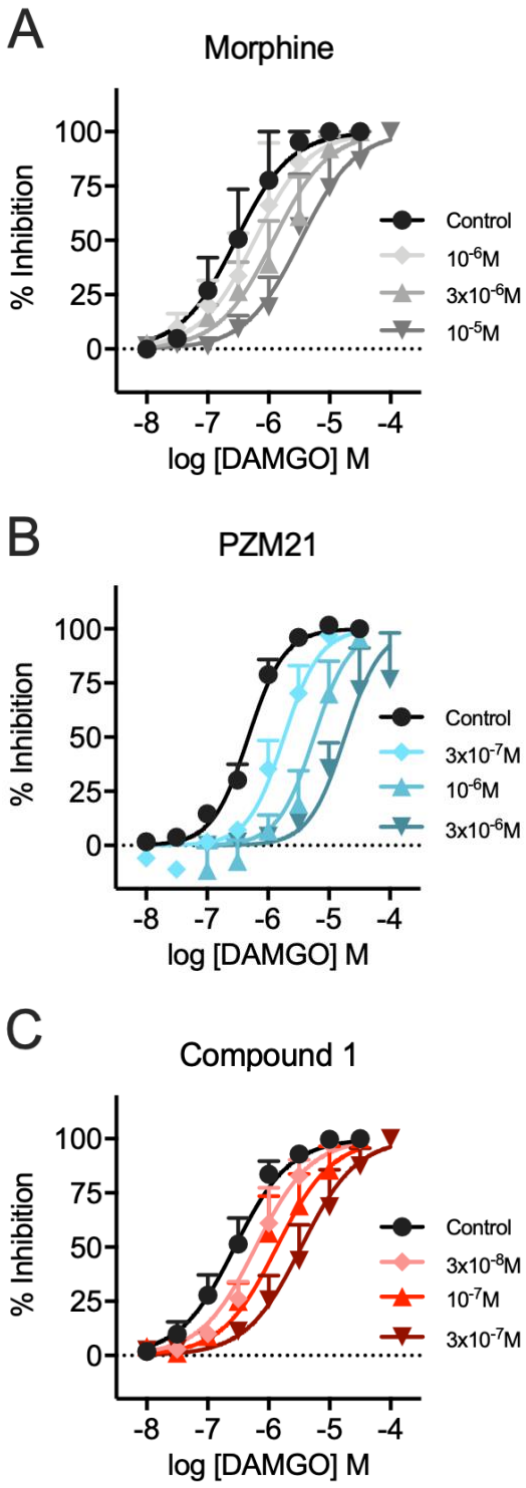


**Figure 3.10 – Combined graphs showing inhibition of DAMGO activity in the RVD by partial MOPr agonists.**

*Pooled data from multiple experiments of the type presented in Figure 3.8. Concentration-response curves for DAMGO-induced inhibition of electrically-evoked contractions in the RVD after 20 minutes preincubation of increasing concentrations of morphine (A), PZM21 (B) and Compound 1 (C). Data are presented as mean ± SEM, where n=3-6.*

Calculating DR values within each individual experiment as above reduced error resulting from variations in DAMGO potency between preparations. This is highlighted in Figure 3.10, where concentration-response curves were fitted to pooled data from all preparations. Despite the sizable error on these concentration response curves, when these combined data are fitted to a Gaddum-Schild $EC_{50}$ shift model in GraphPad Prism (Chapter 2.3.3) the fitted parameters are similar to those computed through the evaluation of individual DR and traditional construction of Schild plots, albeit with more error (Table 3.4). For this reason, statistical analyses were solely performed on $pA_2$ values generated through the individual DR calculation method (Table 3.4).

Compound 1 and PZM21 have a significantly higher $pA_2$ than morphine, demonstrating they have a higher affinity for MOPr than morphine (Figure 3.9, Table 3.4). The higher potency of PZM21 and Compound 1 in the $G_i$ G protein activation BRET (Table 3.1) and their $pIC_{50}$ values for PZM21 and Compound 1 for inhibition of DAMGO-induced arrestin-3 recruitment relative to morphine (Table 3.2) both support the above finding that they are higher affinity ligands (Table 3.4). Compound 1 also displayed a significantly higher affinity than PZM21 in the RVD (Table 3.4), which had not previously been demonstrated in other assays. (Table 3.1 and Table 3.2).

| | *Individual DR Calculation* | | *Cumulative Schild Fit* | | | |
|---|---|---|---|---|---|---|
| | $pA_2$ | 95% C.I. | $pA_2$ | 95% C.I. | Slope | 95% C.I. |
| Morphine | 5.9 | 5.7 - 6.1 | 6.0 | 5.4 - 7.0 | 1.0 | 0.4 - 1.9 |
| PZM21 | 7.0 * | 6.6 - 7.3 | 6.9 | 6.7 - 7.3 | 1.1 | 0.9 - 1.4 |
| Compound 1 | 7.6 *† | 7.4 - 7.9 | 7.6 | 7.1 - 8.3 | 1.0 | 0.6 - 1.6 |

**Table 3.4 – Fitted $pA_2$ and slope values for partial MOPr agonists from two methods of Schild analysis.**

*Values were obtained from data presented and analysed in Figure 3.9 ('Individual DR calculation') and Figure 3.10 ('Cumulative Schild Fit'). n=3-6. * $p < 0.05$, significantly different from the respective morphine value, † $p < 0.05$, significantly different from respective PZM21 value, one-way ANOVA with Tukey's post-hoc test.*

As discussed above, low efficacy MOPr agonists do not typically possess the intrinsic efficacy required to produce the functional responses associated with full MOPr agonists in the RVD, due to its very low receptor reserve. Test low efficacy agonists were preincubated with the RVD for 20 minutes before responses to DAMGO were assessed. Electrical stimulation was ongoing during this period, and so it was possible to determine whether the assessed concentrations of our test partial agonists did have any sizable effect on these electrical-evoked contractions. The magnitude of RVD electrically evoked contractions was unaffected by preincubation with morphine (Figure 3.11A) and PZM21 (Figure 3.11B) at all concentrations examined. The highest concentration of Compound 1 examined ($3x10^{-7}$M) produced slight but significant attenuation (89 ± 3% of baseline) of electrically-evoked contractions after 20 minutes of preincubation (Figure 3.11C). Given that this reduction in response is similar to that elicited at $10^{-7}$M and the examined concentration is 10-fold higher than the $pA_2$ (Table 3.4), it is presumed that this small response is near the maximal possible effect for Compound 1.

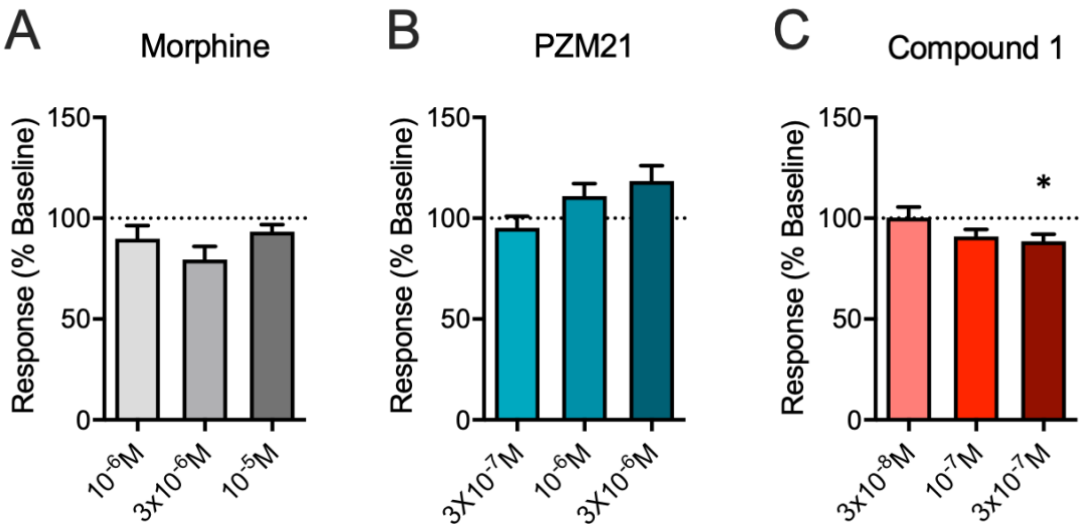


**Figure 3.11 – Modulation of electrically-evoked contractions of the RVD by partial MOPr agonists.**

*The ability of outlined concentrations of morphine (A), PZM21 (B) and Compound 1 (C) to exert their own inhibitory activity on the electrically-evoked contractions of the RVD was assessed over the 20-minute preincubation period. Data are presented as mean ± SEM, where n=3-6. * p < 0.05, significantly different from the hypothetical value of 100 (one sample t test).*

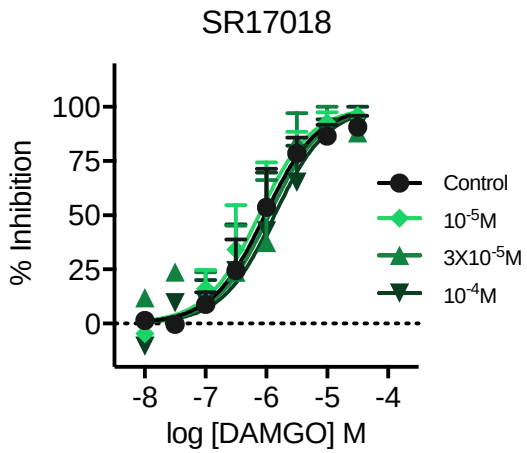


**Figure 3.12 – SR17018 does not inhibit DAMGO-induced inhibition of electrically-evoked contractions of the RVD.**

*Preincubation of the RVD with indicated concentrations of SR17018 for 20 minutes had no effect on DAMGO concentration-response curves for inhibition of electrically-evoked contraction. Data are presented as mean ± SEM, where n=3.*

The impact of high SR17018 concentrations on DAMGO responses in the RVD was also assessed (Figure 3.12). No significant differences in the potency ($pEC_{50}$) of DAMGO were observed in the presence of $10^{-5}$M (6.1 ± 0.1), $3x10^{-5}$M (6.0 ± 0.2) or $10^{-4}$M SR17018 (5.9 ± 0.2) and control (6.0 ± 0.1). This finding is in line with the inability of SR17018 to inhibit DAMGO-induced arrestin-3 recruitment (Figure 3.5). Together these data suggest that, in our hands, SR-17018 does not bind MOPr under the assay conditions tested.

## 3.3 Discussion

### *3.3.1 Summary of findings*

The aim of this chapter was to characterise the signalling of the potentially G protein-biased MOPr agonists PZM21 and Compound 1. In order to achieve this, I first investigated the ability of PZM21 and Compound 1 to induce MOPr-dependent $G_i$ G protein activation and arrestin-3 recruitment in recombinant cell systems using BRET technology (Figure 3.1). The signalling bias of PZM21 and Compound 1 was then quantified relative to the prototypical MOPr partial agonist morphine through a number of published methods (Figures 3.2 – 3.4). Through these assays, we have demonstrated in this Chapter that Compound 1 is a G protein biased agonist at MOPr, while PZM21 displayed no significant degree of biased signalling, in contrast to previous reports.

The function of Compound 1 at other opioid receptors (DOPr and KOPr) was also assessed in similar recombinant systems, in order to determine the selectivity of Compound 1 for MOPr. These assays demonstrated that Compound 1 is a weak partial agonist for DOPr, with no activity at KOPr (Figure 3.6). This selectivity data was broadly in agreement with previously published affinity data for Compound 1 conducted in radioligand binding assays (Li et al., 2016).

Additionally, we aimed to define the affinity of our agonists in a system of physiological receptor expression using the RVD as a functional bioassay. We hypothesised this would be a viable approach as lower efficacy agonists lack agonist activity in the RVD, due to very low receptor coupling levels in this tissue. This phenomenon allowed us to conduct competitive antagonist experiments, testing the ability of our test partial agonists (acting as antagonists in this circumstance) to inhibit DAMGO-induced inhibition of electrically-evoked contractions of the RVD. Schild analysis demonstrated that both PZM21 and Compound 1 are high affinity ligands for the rat MOPr, with higher affinity than morphine.

### *3.3.2 Compound 1 is a G protein-biased agonist*

In Compound 1, we have described a partial agonist at MOPr which is highly G protein-biased (Figure 3.1 and Figure 3.2). We have demonstrated that Compound 1 displayed a significantly higher degree of bias than the reportedly G protein-biased agonist PZM21, which in fact did not display significant bias in our assays (Figure 3.1 and Figure 3.2). Our finding for PZM21 was contrary to previous reports (Manglik et al., 2016), but in agreement with more recent work from other groups (Hill et al., 2018b; Yudin et al., 2019; Gillis et al., 2020a). It is difficult to contextualise the degree of biased signalling exhibited by Compound 1 through comparisons to different studies due to system-based factors and the differing methodologies used to characterise bias across reports. However, it could be possible to roughly compare the bias profile of Compound 1 to that of bilorphin, given this study used the same method of bias calculation ($\Delta$ Normalised $E_{Max}$) and the same reference ligand was used (morphine), and given that the amplification of the G protein assay appears similar (morphine is a partial agonist; Chapter 3.3.3) (Dekan et al., 2019). When compared to the $\Delta$ Normalised $E_{Max}$ values of bilorphin, Compound 1 appears to display a higher degree, or at least similar degree, of G protein-bias, although direct numerical comparisons of this parameter value for Compound 1 and bilorphin cannot be conducted as the reference ligand used for normalisation in our two studies is different (Dekan et al., 2019). Given that TRV130 (oliceridine) was also used in the bilorphin study, displaying no significant G protein-bias, it could be inferred that Compound 1 likely displays a higher degree of G protein-bias than TRV130. As such, it is likely that Compound 1 displays a greater degree of G protein-bias than ligands previously reported as biased at MOPr (Figure 1.8). However, comparative studies examining the signalling of these agonists in the same system would be required to confirm this.

In this Chapter, I have demonstrated that Compound 1 has a similar efficacy for G protein signalling as morphine (Figure 3.1, Table 3.1, Figure 3.2, Figure 3.4). This is of critical importance given the influence of efficacy on the perception of biased signalling in the case of partial agonists (Kelly, 2013; Gillis et al., 2020c). As such, agonists of lower efficacy than morphine are often declared G protein-biased, when their perceived effects are actually a function of differing amplification and receptor reserve between investigated systems (Chapter 3.3.3 and Chapter 4.3.1). An illustration of the distorting effect of efficacy on observed biased signalling comes from PZM21 (Manglik et al., 2016). While original reports suggested PZM21 was G protein-biased, in this report we demonstrate no degree of bias for PZM21, but in fact it has a lower efficacy than morphine for G protein signalling (Figure 3.1, Table 3.1, Figure 3.2 and Figure 3.4, also see Chapter 4). This is in agreement with recent findings from other groups (Yudin et al.,

2019; Gillis et al., 2020a). In fact, it has been demonstrated that low efficacy could account for the perceived biased signalling and differential therapeutic profile of most high-profile purported G protein-biased agonists at MOPr (Gillis et al., 2020a); including PZM21, TRV130 and SR-17018. In support of this, TRV130 has been demonstrated to be a low efficacy agonist relative to morphine by a number of other studies (Manglik et al., 2016; Dekan et al., 2019; Yudin et al., 2019; Vasudevan et al., 2020). This highlights the relative novelty of Compound 1, characterised here as a G protein-biased agonist with equivalent G protein efficacy to morphine, with the only other agonist clearly demonstrated to share this profile being bilorphin (Dekan et al., 2019). As such, it is important that we move to confirm the efficacy of Compound 1 in a system of physiological receptor expression. In order to do this, we characterised the function of Compound 1 in rat locus coeruleus (LC) neurones using electrophysiological methods (Chapter 4).

Having characterised a novel G protein-biased agonist at MOPr, we sought to use this as a tool compound to study the long-term functional effects of biased signalling at MOPr in neurones (scope outlined in Chapter 3.3.7). Before addressing this, I have sought to address a number of issues and discussion points specifically around data presented in this chapter in this discussion, below.

### *3.3.3 Limitations in methods of bias calculations in the case of partial agonists*

While the $\Delta\Delta\log(\tau/KA)$ approach is the standard method of quantifying biased agonism, its utilisation of the operational model limits its power when assessing the responses of weak partial agonists. This is due to the large fitting error associated with derived parameters resulting from variable curve fit quality, meaning comparisons between such parameters for specific agonists are weakened (Kelly, 2013; Dekan et al., 2019) (Chapter 3.2.2). As weak arrestin-recruitment responses for partial agonists are often responsible for such poor curve fitting quality, such parameters are often examined in amplified arrestin assays, with signal level increased through overexpression of GRK2 (Chapter 5.2.7, Table 5.1).

In light of these limitations, the $\Delta\Delta\log(\tau/KA)$ approach therefore seems inappropriate for data presented in this chapter, with Compound 1 and PZM21 being partial agonists at MOPr relative to the full agonist DAMGO (Figure 3.1 and Table 3.1). Instead we have assessed biased agonism using the 'Normalised $\Delta E_{Max}$' approach (Dekan et al., 2019), which allows for the quantification of biased signalling for partial agonists using efficacy alone.

A crisis has arisen in the misappropriation of signalling bias for MOPr ligands. One could argue this is partially due to the commonplace use of the $\Delta\Delta\log(\tau/KA)$ approach in inappropriate circumstances. The inappropriate designation of biased signalling has significantly hampered the development of the biased agonism field in the case of MOPr, and consequently at other GPCR targets.

One particular limitation of the $\Delta\Delta\log(\tau/KA)$ approach is an incorrect assumption that its normalisation accounts for all forms of systems bias (Gillis et al., 2020c). Biased signalling of MOPr ligands is often assessed through comparisons of activity between amplified assays of G protein activity (such as cAMP assays) and linear assays of arrestin recruitment. Commonly, a ceiling of effect is present in such highly amplified assays of G protein activity, particularly in cases of high levels of recombinant receptor expression (Gillis et al., 2020c). This often distorts the assessment of efficacy, with partial agonists such as morphine displaying equivalent maximum responses for G protein activation to full agonists such as DAMGO in some assays (Hothersall et al., 2017; Schmid et al., 2017; Gillis et al., 2020a; Pedersen et al., 2020). Given the linear nature of arrestin-recruitment assays, such partial agonists (which have appeared as full agonists in G protein assays) now appear as weak agonists for arrestin recruitment. As such, it is commonplace that low efficacy agonists are falsely ascribed as G-protein biased through the disregard of efficacy as a critical factor in assessment of bias (DeWire et al., 2013; Manglik et al., 2016; Schmid et al., 2017).

Such high amplification is not present in the G protein activation assay presented in this chapter (Figure 3.1B), likely due to lower signal amplification than for instance assays of cAMP accumulation and a lower level of MOPr expression arising from the transient, rather than stable, nature of expression. As such, there is good separation present between the maximum responses of partial and full agonists for G protein activation in this assay. This allows for the use of $E_{Max}$ as a robust, assumption-free approximation of efficacy. This is as an alternative to calculations of $\tau$ through the operational model, for which calculation again suffer from large error values arising from variable curve fit quality in the case of weak partial agonists (Figure 3.4).

### *3.3.4 Reflection on the use of BRET methods to study receptor signalling*

The rapid development of resonance energy transfer (RET) technologies, both BRET and FRET, has revolutionised the study of GPCR signalling over the last decade. Principally, the study of GPCR ligand pharmacology began through determination of physiological responses in isolated tissue preparations. The elucidation of GPCR signalling in such systems allowed for the development of higher throughput assays in recombinant systems, many based on known second messenger systems, such as

adenyl cyclase (cAMP accumulation) and phospholipase C ($Ca^{2+}$ accumulation) (Yasi et al., 2020). RET-based assays hold a number of advantages over their predecessors for the elucidation of GPCR pharmacology and the characterisation of novel GPCR ligands.

RET techniques can provide unique resolution to the dynamics and kinetics of GPCR activation (Bacart et al., 2008). Additionally they hold an advantage over some alternative approaches such as [$^{35}$S]GTP$\gamma$S assays of potency, radioligand binding assays of affinity and some assays of adenyl cyclase activity (for G$\alpha_s$ and G$\alpha_i$) such as ELISA-based methods of cAMP accumulation, as they are run in live, intact cells (Salahpour et al., 2012).

The primary advantage of RET-based approaches however is their adaptability. RET-assays can be utilised to study practically the entire range of GPCR signalling processes, with assays of ligand binding (Stoddart et al., 2016), G protein activation (Janetopoulos et al., 2001), arrestin recruitment (Hamdan et al., 2005), receptor-GRK interaction (Hasbi et al., 2004), receptor internalization (Foster et al., 2018) and receptor dimerization (Angers et al., 2000; Milligan, 2010) among other processes (Lohse et al., 2012). The overall scope of these assays is impressive, and with new RET-based tools for the study of GPCRs constantly being developed the potential of this approach is yet to be fully utilised. This is highlighted by the recent development of platforms such as TRUPATH (Olsen et al., 2020), a BRET-based biosensor platform which can provide detailed, novel information on the transducerome of well-studied GPCRs, or potentially unlock the study of orphan GPCRs, expanding our understanding of the therapeutic scope of GPCRs.

However, it is also clear that the application of RET techniques is limited by the need to transform cells to express genetically modified reporters and signalling counterparts. This brings a number of potential drawbacks. Firstly, the application of these methods is dependent on access to specific RET-based tools for the receptor or signalling pathway of interest. Additionally, the impact of large RET tags (such as GFP) on the dynamics of receptor interactions cannot simply be overlooked. One could argue that the ease of investigation in such assays has fostered an alarming move away from the study of GPCR function in systems which possess physiological expression of GPCRs and their signalling partners at endogenous expression levels, precipitating a translatability issue in the GPCR field. This highlights the necessity to validate and contextualise findings from convenient, high-throughput RET-based approaches in physiological systems expressing the receptor of interest (Chapter 3.2.3, Chapter 4).

### *3.3.5 Notes on inactivity of SR-17018*

The putative G protein-biased agonist SR-17018 was inactive in inhibiting DAMGO-induced arrestin-3 recruitment in our recombinant assay (Figure 3.5E) and similarly did not show any competition for the binding of DAMGO to MOPr in the RVD (Figure 3.12). Our inability to obtain evidence of MOPr binding or agonist activity (Ramos-Gonzales, unpublished data) resulted in us ending our use of SR-17018 as a tool compound in our studies.

While SR-17018 was described as G protein-biased in original reports, with a high efficacy for G protein activation (Schmid et al., 2017), studies from other groups have shown it be a very low efficacy agonist in other assays of G protein activity, lower than morphine, buprenorphine and TRV130 (Gillis et al., 2020a). This is likely due to the confounding effect of high amplification in assays presented in original reports (Schmid et al., 2017) (Chapter 3.3.3.). It could be that we do not see an effect of SR-17018 in recombinant systems due to its extremely low efficacy. This would support our findings in rat LC neurones (Chapter 4), in which we were unable to see a GIRK response elicited by SR-17018 (100μM; data not shown). However, low efficacy is not able to explain the lack of competitive binding observed with SR-17018 against DAMGO in the arrestin-3 BRET assay (Figure 3.5E; up to 30μM), in the RVD (Figure 3.12; up to 100μM) and in rat LC neurones (data not shown; up to 100μM).

A lack of competitive binding for SR-17018 could suggest that SR-17018 may act allosterically to exert its effects. However, it has been described to compete with the binding of radiolabelled DAMGO in receptor binding assays (Schmid et al., 2017).

Severe solubility issues and high protein binding have been suggested for SR-17018 in both *in vitro* assays and *in vivo* (Gillis et al., 2020a; Grim et al., 2020). While not described in the original report (Schmid et al., 2017), the same group reported that they required the inclusion of the surfactant Tween-80 in the vehicle in order to get SR-17018 into solution for both *in vitro* and *in vivo* testing (Grim et al., 2020). Even with the inclusion of Tween 80, this group reported that SR-17018 was still only soluble up to 2.5 mg/ml (~5mM) in their hands (Grim et al., 2020). This implies the concentrations used in our study were outside of the range of solubility and the lack of effect or competition binding for SR-17018 are potentially due to it coming out of solution. However, it should be noted that no notable precipitate was observed in the preparation of SR-17018 for work conducted in this chapter.

In light of accounts of solubility issues and, perhaps more importantly, subsequent reports of SR-17018 not being G protein biased as previously described (Gillis et al.,

2020a), we could not warrant its inclusion in our investigations as a tool compound for the study of biased agonists at MOPr.

### *3.3.6 Potential limitations of the RVD Schild experiment*

One potential problem with the experimental design in the RVD Schild experiments conducted in this chapter (Chapter 3.2.3) surrounds the logistics that increasing agonist concentrations were tested sequentially. This was undertaken to avoid potential contamination problems arising from agents residing after washing out the RVD preparation. As such, firstly the potency of DAMGO was assessed alone (control). Then in the presence of the lowest concentration of test partial agonist, before washing out and repeating in an increased test partial agonist concentration. The issue arising is that in the protocol for test agonist preincubation, the construction of these DAMGO concentration response curves and recovery of electrically-evokes responses takes around 1-2 hours. Should the potency of DAMGO fall due to a loss of responsiveness in the RVD over the collective 6-8 hour protocol, antagonists would be seen to be shifting the potency of DAMGO in a manner actually dependent on time. DAMGO responsiveness could not be assessed simply after test agonist effects on DAMGO potency were assessed as complete washout of inhibitory test agonists could not be assured. In the absence of a time-matched control experiment for DAMGO responsiveness over time, the results for SR17018 provide a control over a similar time-course with ligand demonstrated not to interact with MOPr (Figure 3.12). There was no significant reduction of DAMGO potency with time (or increasing SR17018 concentration, Figure 3.12) suggesting that observed effects with other ligands are not driven by time-dependent reductions in DAMGO potency.

### *3.3.7 Studying the long-term effects of G protein-biased agonists at MOPr*

The long-term physiological consequences of biased signalling at MOPr is currently understudied. Given that receptor desensitization induced by opioids, and resulting tolerance to opioids, is dependent on receptor modulation by arrestin and GRK pathways, it is hypothesised that G protein-biased agonists would induce less receptor desensitization than balanced MOPr agonists. If this hypothesis is true, G protein-biased agonists may have more clinical utility than traditional opioids as the development of tolerance to these agonists could be reduced compared to balanced agonists. The identification in this Chapter of Compound 1 as a G protein-biased agonist at MOPr provides a tool compound to study this hypothesis.

The following chapters will therefore be focussed on studying receptor desensitization potentially induced by Compound 1 and other opioids in rat locus coeruleus (LC)

neurons, using brain slice electrophysiology. Additionally, studying the agonist activity of Compound 1 and other opioids in a physiological system of receptor expression will support our findings in this Chapter around the importance of efficacy in considerations of biased agonism (Chapter 3.3.2). Furthermore, we will be investigating the analgesic effects of Compound 1 *in vivo*, in the hope of examining potential tolerance induce by G protein-biased agonists at the MOPr.

# Chapter 4: Investigating receptor desensitization induced by G protein-biased MOPr agonists

## 4.1 Introduction

The MOPr undergoes rapid desensitization upon exposure to various opioid agonists. The short-term regulation of MOPr through rapid agonist-induced receptor desensitization represents a key cellular mechanism that contributes to the development of tolerance to opioids (Bailey et al., 2009a). Given that canonical MOPr desensitization is driven by agonist-induced GRK phosphorylation and arrestin recruitment (Williams et al., 2013), it could be hypothesised that G protein-biased agonists, which would inherently have low coupling to GRK/arrestin pathways, would induce less desensitization than a balanced agonist. Under this hypothesis, G protein-biased agonists would be clinically beneficial as they produce less tolerance. In order to investigate the ability of G protein-biased MOPr agonists to induce receptor desensitization, we studied the real time function of opioids in rat locus coeruleus neurons using patch-clamp electrophysiology.

The locus coeruleus (LC) represents a dense cluster of largely homologous noradrenergic-neurons located near the wall of the fourth ventricle within the pons (Foote et al., 1983). Noradrenergic LC neurons express MOPr, but not DOPr or KOPr (Williams et al., 1984; North et al., 1987), giving them distinct utility as a model for the study of MOPr agonist function without the confounding effects of DOPr and KOPr agonism by these ligands. Activation of MOPrs in LC neurons produces hyperpolarising currents through inwardly rectifying potassium ion channels (Pepper et al., 1980; North et al., 1985), the function of which are dependent on MOPr coupling to G proteins (Aghajanian et al., 1986; North et al., 1987). Opioid-induced currents in LC neurons provide a real-time measure of receptor activation, making these currents ideal for the study of MOPr desensitization (Harris et al., 1991; Bailey et al., 2003).

In LC neurons, GIRK currents evoked by the full agonists DAMGO and met-enkephalin, as well as the arrestin-biased MOPr agonist endomorphin-2, have been shown to undergo rapid desensitization, resulting in around a 50% reduction in current amplitude over a short (~10 minute) application at approximately receptor saturating concentrations (Osborne et al., 1995; Bailey et al., 2003; Rivero et al., 2012; Lowe et al., 2015). The decline of these opioid-evoked GIRK currents is a result of a reduction in functional MOPrs due to receptor desensitization (Bailey et al., 2009a). Morphine-induced currents have been shown to undergo lower amounts of rapid desensitization in LC neurons when compared to full agonists (Bailey et al., 2003; Bailey et al., 2004), however a number of

investigations have nonetheless demonstrated a sizable (around 20%) loss of function in morphine-evoked currents over the same time frame (Rivero et al., 2012; Lowe et al., 2015).

The difference in rapid MOPr desensitization induced by full agonists such as DAMGO, and the partial agonist morphine is thought to be dependent on agonist efficacy and the related intrinsic efficacy of an agonist to recruitment of GRK and arrestin to MOPr (Kelly et al., 2008). Given that the G protein-biased agonist Compound 1 (characterised in the previous chapter) is a partial agonist at MOPr, with the same G protein efficacy as morphine, we hypothesised that it would similarly produce minimal desensitization in LC neurons. Additionally, given that Compound 1 was demonstrated to have lower efficacy for GRK/arrestin pathways than morphine, it would be hypothesised that it would induce lower levels of MOPr desensitization than morphine in LC neurones. In the timeframe of rapid desensitization of MOPr-evoked GIRK currents in LC neurones, this process is not driven by arrestin recruitment (Arttamangkul et al., 2008), but by interconnected and precursory receptor phosphorylation by GRK (Bailey et al., 2009b; Lowe et al., 2015). Regardless, this hypothesis is supported by the finding that endomorphin-2, an arrestin biased MOPr agonist with a similar efficacy to morphine for G protein pathways, but higher efficacy for arrestin recruitment (McPherson et al., 2010), induces substantially more rapid receptor desensitization than morphine in LC neurons (Rivero et al., 2012).

The work within this chapter aims to determine whether the G protein-biased agonist Compound 1 produces rapid MOPr desensitization in rat LC neurons. This was performed to inform us on the potential long-term functional consequences of G protein-biased agonists at MOPr. In order to achieve this, the ability of Compound 1 to evoke MOPr dependent GIRK currents was assessed through whole-cell voltage-clamped electrophysiological recordings from LC neurons within rat brain slices. The amplitude and desensitization of Compound 1-evoked currents were compared to currents evoked by the test agonists characterised in the previous chapter, DAMGO, morphine and PZM21. Following this, the antinociceptive properties of Compound 1 were assessed using a warm water tail withdrawal test in mice, in the hope that a reliable response could obtained in order to later study *in vivo* tolerance to Compound 1.

In this chapter, I demonstrate that the G protein biased MOPr agonist Compound 1 induces MOPr desensitization in LC neurons to a greater degree than morphine. This intriguing finding was the opposite to what we had hypothesised, given that Compound 1 displayed lower efficacy for arrestin-3 recruitment in the previous chapter. This finding implies that G protein-biased agonists at MOPr may not always induce less receptor desensitization than balanced agonists due to their low arrestin coupling, and highlights

concerns regarding their speculated ability to induce less tolerance than typical opioids. Additionally, considering the low arrestin recruitment efficacy of Compound 1, this finding potentially implies a non-arrestin/GRK mechanism of receptor desensitization may be involved in Compound 1-induced MOPr desensitization. Compound 1 induced MOPr-dependent antinociception in mice, however the amount of antinociception was substantially lower than that evoked by morphine. The reason for the low efficacy of Compound 1 *in vivo* is unclear but was speculated to be due to poor pharmacokinetics and blood-brain barrier permeability. The following chapter will aim to characterise the mechanism underlying Compound 1-induced MOPr desensitization in LC neurons.

## 4.2 Results

### *4.2.1 Assessing the function and desensitization of opioid-induced GIRK currents in rat locus coeruleus neurons*

Opioid-evoked currents were assessed in single rat LC neurons from brain slices prepared from 4-week-old rats using whole-cell patch clamp electrophysiology (Chapter 2.4). Approximately receptor saturating concentrations of DAMGO (Figure 4.1A, 10μM), morphine (Figure 4.1B, 30μM), PZM21 (Figure 4.1C, 30μM) and Compound 1 (Figure 4.1D, 30μM) all evoked outward potassium currents through GIRK channels. Assessed agonists were superfused for 10 minutes, in an attempt to track the rapid decay of agonist-induced currents for approximately double the fitted $t_{1/2}$ of an agonist's current decline, guided by previous findings (Bailey et al., 2003). All agonist-evoked currents were effectively reversed with superfusion of naloxone (Figure 4.1, 1μM or 10μM), demonstrating that they are driven by agonist-induced MOPr activation in the absence of DOPr and KOPr expression and functionality in the LC (Williams et al., 1984; North et al., 1987; Mansour et al., 1994). While a concentration of 1μM naloxone was initially used (Figure 4.1B-D), the slow reversal of Compound 1-evoked GIRK currents with this naloxone concentration (Figure 4.1D) prompted us to increase this working concentration to 10μM in subsequent experiments, which included examinations of DAMGO-induced desensitization (Figure 4.1A).

$\alpha_2$ adrenoceptors and MOPrs couple to the same population of GIRK channels in LC neurons upon receptor activation (North et al., 1985). The maximal $\alpha_2$-adrenoceptor-mediated current was assessed in each cell before and after the assessment of opioid-induced currents by application of 100μM noradrenaline (NA) in the presence of 1μM prazosin and 3μM cocaine (Figure 4.2). The inclusion of prazosin (an $\alpha_1$-adrenoceptor antagonist) and cocaine (monoamine reuptake inhibitor) was intended to maximise the $\alpha_2$-adrenoceptor dependent NA-evoked GIRK current (Williams et al., 1987b; Llorente et al., 2012). In order to reduce variation in evoked-current amplitude between cells, the magnitude of opioid-evoked current was normalised to maximal $\alpha_2$-adrenoceptor-mediated current evoked in the same cell prior to application of the opioid (Figure 4.2). The magnitudes of $\alpha_2$-adrenoceptor-mediated currents before and after opioid exposure were also assessed in order to investigate potential heterologous desensitization induced by opioids, as well as being indicative of current rundown over the duration of the experiment (Figure 4.2).

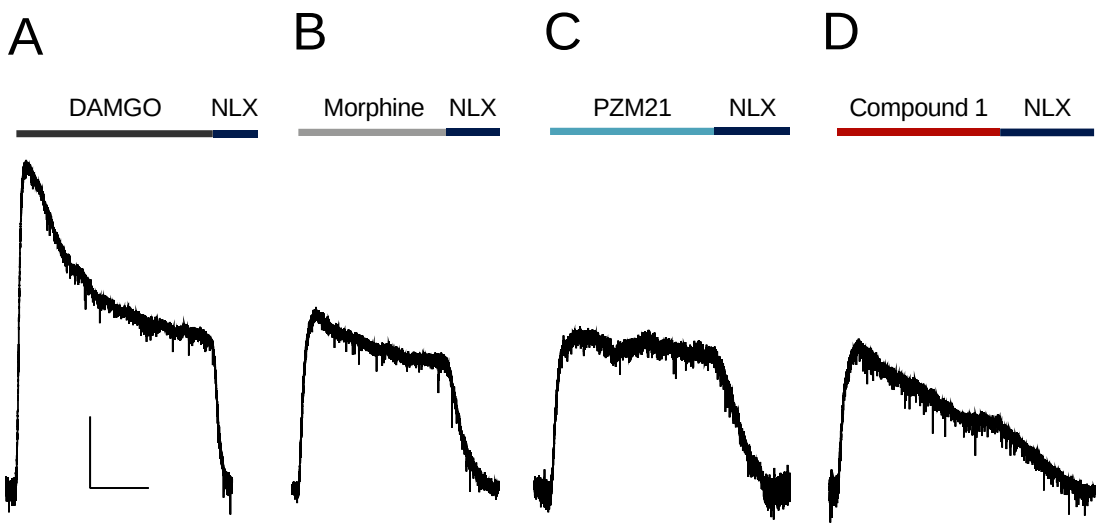


**Figure 4.1 – Example traces of opioid-evoked GIRK currents in rat LC neurones.**

*Representative traces showing outward potassium currents recorded from rat LC neurones in response to receptor saturating concentrations of DAMGO (10 μM, A), morphine (30 μM, B), PZM21 (30 μM, C) and Compound 1 (30 μM, D) over 10 mins of superfusion. Opioid-evoked currents were completely inhibited upon application of naloxone (NLX, 10 μM in A, 1 μM in B-D). Scale bars (shared across A-D) are representative of 50pA and 5 min.*

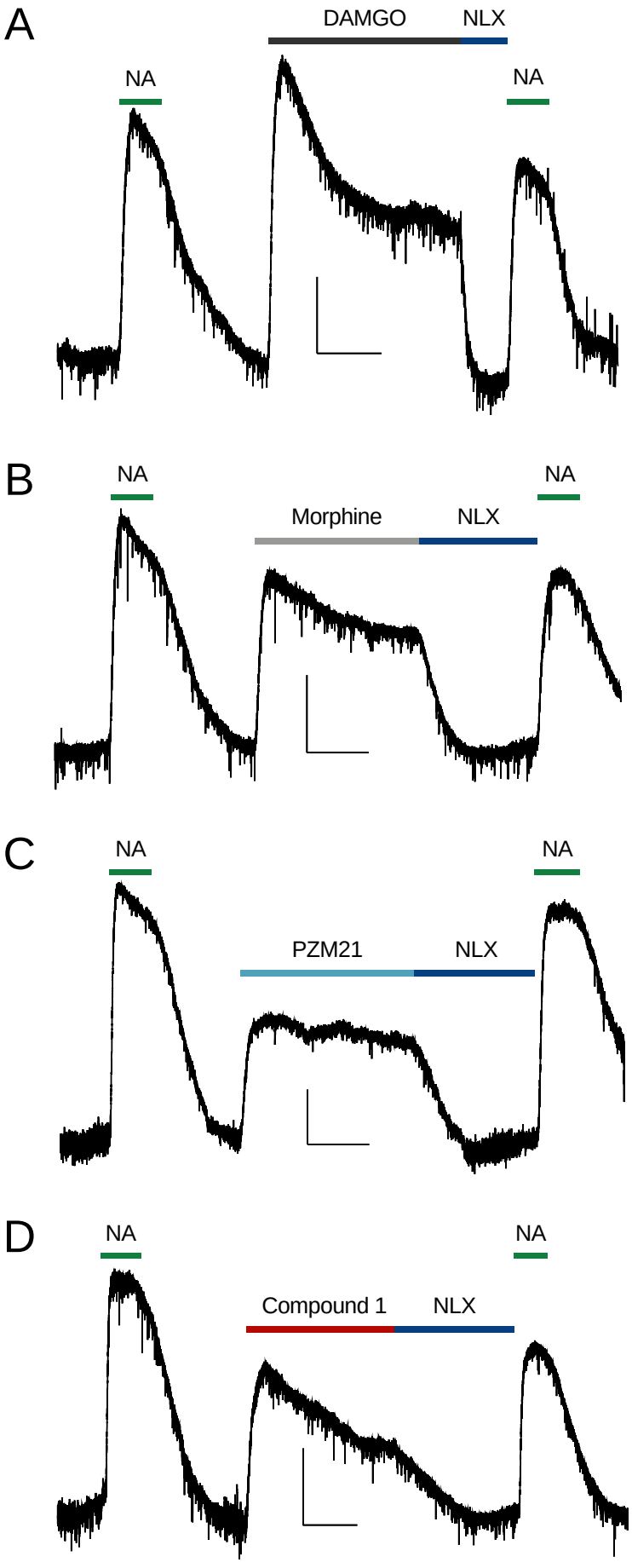
A
DAMGO
NLX
NA
NA
B
NA
NA
Morphine
NLX
C
NA
NA
PZM21
NLX
D
NA
NA
Compound 1
NLX

**Figure 4.2 – Example traces showing GIRK currents evoked through MOPr and $\alpha_2$ adrenoceptor activation in rat LC neurones**

*Representative traces demonstrating the full time-course for experiments investigating desensitization of opioid-evoked GIRK currents in rat LC neurons, of the type shown partially in Figure 4.1. At the beginning and end of each recording, the maximal $\alpha_2$-adrenoceptor-mediated current in each individual cell was assessed by superfusion of noradrenaline (NA, 100$\mu$M). In each case, prazosin (1$\mu$M) and cocaine (3$\mu$M) were perfused for 3 min prior to application of NA. The amplitude of NA-evoked currents before and after opioid application was compared to assess opioid-induced heterologous desensitization of GIRK currents as well as current rundown over time (see Figure 4.6). GIRK currents evoked by DAMGO (10$\mu$M, A), morphine (30$\mu$M, B), PZM21 (30$\mu$M, C) and Compound 1 (30$\mu$M, D) are also displayed, which were reversed by naloxone (NLX, 10 $\mu$M in A, 1 $\mu$M in B-D). Scale bars are representative of 50pA and 5 min.*

High, receptor saturating concentrations were used for the assessment of opioid-evoked desensitization, in an attempt to standardise the degree of agonist-receptor occupancy to its maximum when studying agonists of differing affinity. For DAMGO and morphine, concentrations used in this experiment were previously demonstrated to be receptor saturating (Bailey et al., 2003; Bailey et al., 2009a). In the case of PZM21 and Compound 1, 30$\mu$M was assumed to be a receptor saturating concentration given previous observations of agonist potency and affinity relative to morphine (Chapter 3). At the approximately receptor saturating concentrations at which the opioids investigated were applied, the peak magnitudes of GIRK currents evoked by partial agonists can be used as an approximation of their intrinsic efficacy. The peak GIRK currents evoked by morphine, PZM21 and Compound 1 were all significantly lower than that evoked by DAMGO (Figure 4.3), demonstrating that they are partial agonists in rat LC neurons. The magnitude of Compound 1-evoked GIRK currents was statistically similar to those evoked by morphine, whereas the magnitude of PZM21-evoked GIRK currents was significantly lower than morphine (Figure 4.3). These findings in a system of physiological receptor expression are in agreement with data presented in the previous chapter from heterologous expression systems (Figure 3.1 and Table 3.1), supporting the finding that Compound 1 and morphine have the same efficacy for G protein activation, while PZM21 is a lower efficacy agonist than morphine.

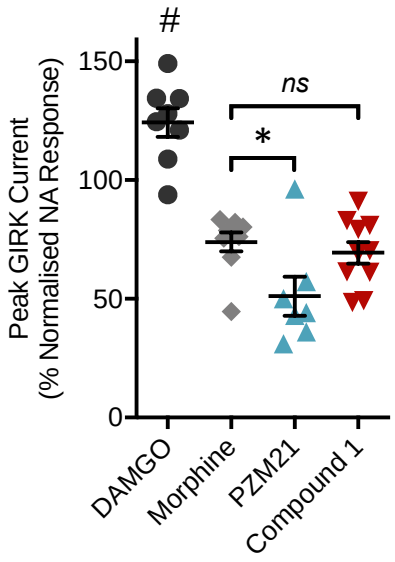


**Figure 4.3 – The amplitude of peak opioid-evoked GIRK currents in rat LC neurones**

*The average peak GIRK currents elicited by opioids at receptor saturating concentrations (DAMGO, 10$\mu$M; Morphine, PZM21 and Compound 1 , 30$\mu$M) in rat LC neurones. Data collected from experiments of the type presented in Figure 4.2. Responses are normalised to the maximal $\alpha_2$-adrenoceptor-mediated current evoked by noradrenaline (100$\mu$M) in the same cell. Data is presented as mean ± SEM, where n = 5 – 10. # P < 0.05, significantly different from all values for other agonists. * P < 0.05, significantly different from morphine value. ns P > 0.05, no significant difference from morphine value. One-way ANOVA with post-hoc Tukey test.*

The amplitude of DAMGO-, morphine-, PZM21- and Compound 1-evoked currents all decayed to different extents, in the continued presence of the drug (Figure 4.1). The time courses for the decay in currents evoked by all agonists could be fitted to a single-exponential decay (Figure 4.4). The R squared values for the fitting of a single exponential decay to the decline in evoked currents for each agonists were as follows: DAMGO = 0.9, morphine = 0.6, PZM21 = 0.6, Compound 1 = 0.8. The fitted half-life (min) for the decay of agonist-evoked currents were as follows: DAMGO = 4.1, morphine = 5.3, PZM21 = 8.6, Compound = 4.2. The 10 min drug incubation, which provided a window of around 8 min examination accounting for the time for the agonist effects to reach their peak, was therefore marginally insufficient to capture the decay of agonist-evoked currents for the duration of double the half-life of decay. The fitted plateau for the decay of agonist-evoked currents (expressed as % peak GIRK current ± SEM) were as follows: DAMGO = 36 ± 8, Morphine = 67 ± 11, PZM21 = 73 ± 22, Compound 1 56 ± 7.

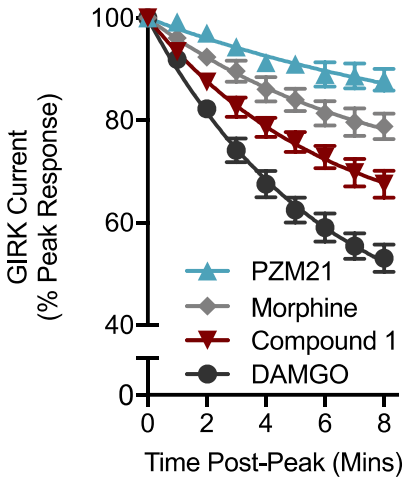


**Figure 4.4 – Rapid desensitization of opioid-evoked GIRK currents in rat LC neurones**

*Time-courses for the desensitization of GIRK currents evoked by receptor saturating concentrations (10μM DAMGO, 30μM morphine, PZM21 and Compound 1) in rat LC neurones post-peak responses. Data collected from experiments of the type presented in Figure 4.1. Responses are normalised to magnitude of the peak opioid-evoked GIRK current prior to desensitization. Data is presented as mean ± SEM, where n = 5 – 10.*

The observed rapid decline in the magnitude of agonist-evoked MOPr coupled-GIRK currents in LC neurons is indicative of rapid agonist-induced receptor desensitization (Bailey et al., 2009a). The rapid desensitization of agonist-evoked GIRK currents in rat LC neurons was quantified as the reduction in GIRK current magnitude at 8 min post-peak agonist response compared to the peak response.

The full agonist DAMGO (10μM) produced marked desensitization of the evoked current over the 10 min of exposure (Figure 4.5). The partial agonist morphine (30μM) produced significantly less MOPr desensitization than DAMGO (Figure 4.5). These findings are in line with previous studies of DAMGO-induced and morphine-induced desensitization in rat LC neurons (Alvarez et al., 2002; Bailey et al., 2003; Rivero et al., 2012; Lowe et al., 2015). Similarly, PZM21 (30μM) also produced relatively low levels of MOPr desensitization over the 10 min exposure (Figure 4.5), as would be expected for a partial agonist with a lower efficacy than morphine (Figure 4.3, Table 3.1). Unexpectedly, the G protein-biased agonist Compound 1 (30μM) induced significantly more MOPr desensitization than morphine (Figure 4.5). This surprising finding was counter to our initial hypothesis that G protein-biased agonists, such as Compound 1, would induce less receptor desensitization than balanced agonists, such as morphine, due to their low intrinsic efficacy for arrestin coupling (Figure 3.1, Table 3.1).

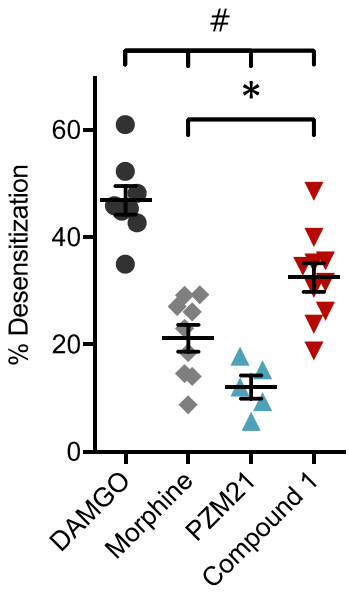


**Figure 4.5 – Opioid-induced desensitization in rat LC neurones**

*Average data for % desensitization in opioid-evoked GIRK currents after 8 min post-peak GIRK response. Data is presented as mean ± SEM, where n = 5 – 10. # P < 0.05, significantly different from DAMGO value. * P < 0.05, significantly different from morphine value. One-way ANOVA with post-hoc Tukey test.*

The magnitude of NA (100μM) evoked currents was assessed before and after the application of opioids in order to assess both potential opioid-induced heterologous desensitization and current rundown (Figure 4.2). The magnitude of NA-evoked currents after opioid application compared with those evoked before were similar for all agonists (Figure 4.6). This findings suggests that the desensitization observed in Compound 1-evoked currents is not due to heterologous desensitization.

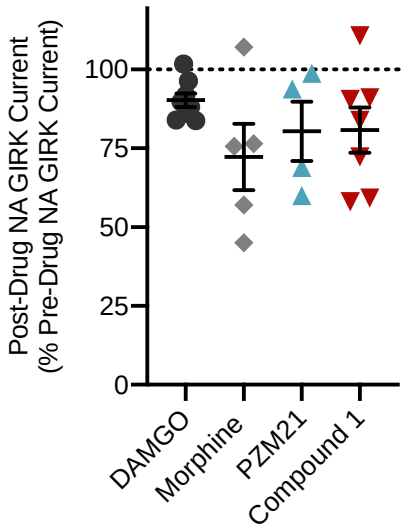


**Figure 4.6 – Noradrenaline-evoked GIRK currents in opioid-treated LC neurones**

*The magnitude of noradrenaline (NA, 100μM) evoked GIRK currents was assessed before and after application of described opioids, at receptor saturating concentrations, in the presence of prazosin (1μM) and cocaine (3μM). Data collected from experiments of the type presented in Figure 4.2. Data are presented as mean ± SEM, where n = 4 – 8. No significant difference was observed between the magnitudes of post-opioid NA-evoked GIRK currents in a one-way ANOVA (P = 0.33).*

### *4.2.2 Apparent Compound 1-induced MOPr desensitization is not due to peptide degradation or indirect GIRK inhibition*

One potential explanation for the decline in Compound 1-evoked currents could be that the peptide is readily degraded. A mechanism such as observed with Met-enkephalin, whereby the peptide is readily degraded by native peptidases when incubated with brain slices (Williams et al., 1987a; Konkoy et al., 1995), is unlikely in this case due to constant superfusion of Compound 1-containing aCSF. However, it is possible that Compound 1 undergoes a slow degradation within the aCSF solution before it is perfused on to the brain slice. Alternatively, the free concentration of Compound 1 within the solution could be gradually reduced through binding to the glass in which this solution is stored prior to perfusion, despite regular siliconization of glassware.

To test this hypothesis, Compound 1 (30μM) was applied for 10 min and the decline in evoked current was observed. Then, a freshly prepared solution of Compound 1 (30μM) was applied (Figure 4.7A). The application of freshly prepared Compound 1 did not increase the magnitude of the evoked-GIRK current (Figure 4.7B), demonstrating that the decline in Compound 1-evoked GIRK currents was not due to peptide degradation or loss within the system.

Another potential explanation of the rapid decline in Compound 1-evoked GIRK currents is that Compound 1 blocks GIRK channels with a slower kinetics of action to its activation of GIRK channels through MOPr. This hypothesis is informed by similar findings with methadone, which was identified as a GIRK blocker in LC neurons as well as being a MOPr agonist (Rodriguez-Martin et al., 2008).

To investigate this, the ability of Compound 1 (30μM) to inhibit GIRK currents evoked by a submaximal concentration of NA (3μM) was assessed in the presence of naloxone (10μM) to block MOPr-dependent actions of Compound 1 (Figure 4.8A). Compound 1 had no effect on NA-evoked GIRK currents (Figure 4.8B), demonstrating that it does not indirectly inhibit GIRK channels. This finding suggests that the decline in Compound 1-evoked GIRK currents was not due to GIRK channel inhibition.

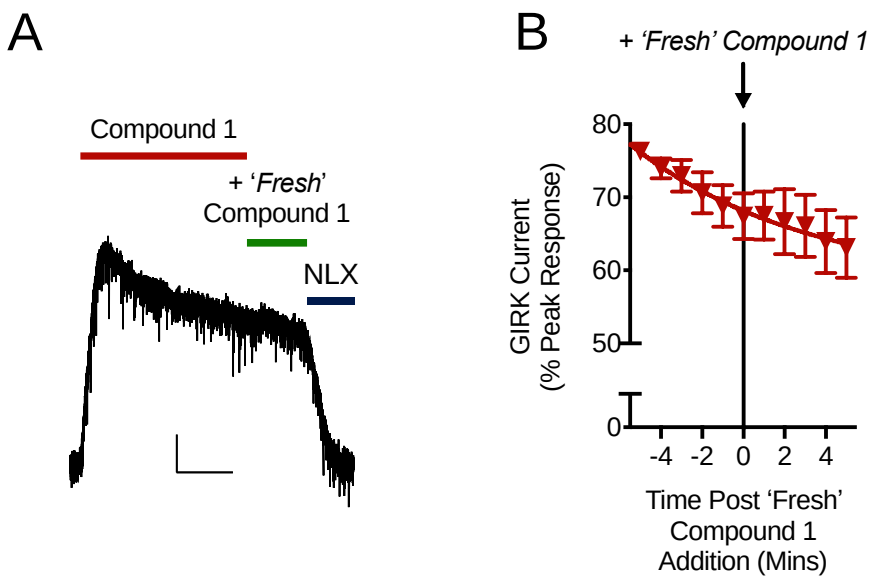


**Figure 4.7 – Decay in Compound 1 currents is not a product of peptide degradation**

*(A) A representative trace showing decline of Compound 1 (30 μM)-evoked GIRK current in a rat LC neuron. Decline of the evoked current was unaffected when the superfused Compound 1 which had been applied for 10 minutes was replaced with freshly prepared ('fresh') Compound 1 (30 μM). Compound 1-evoked currents were completely reversed with naloxone (NLX, 10 μM). Scale bars are representative of 20pA and 5 min. (B) Pooled average data from experiments of the type presented in A. The Compound 1-evoked current, expressed as a percentage of the peak response was unaffected by application of 'fresh' Compound 1 as described for A. Data are presented as mean ± SEM, where n = 5.*

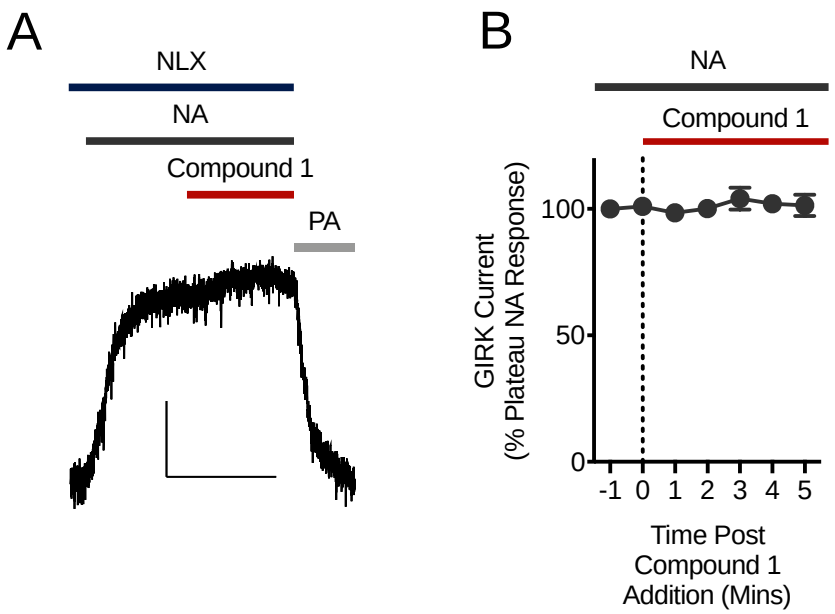


**Figure 4.8 – Decay in Compound 1 currents is not a product of indirect GIRK inhibition**

*(A) A representative trace of a GIRK currents evoked by a submaximal concentration (3μM) of noradrenaline (NA) in a rat LC neuron. The NA-evoked current was assessed in the presence of naloxone (NLX, 10μM), prazosin (1μM) and cocaine (3μM). With MOPr blocked by NLX, the application of Compound 1 (30μM) had no effect on the magnitude of NA-evoked GIRK currents. Phentolamine (PA, 10μM) completely reversed NA-evoked currents. Scale bars are representative of 20pA and 5 min. (B) Pooled average data from experiments of the type presented in A. Application of Compound 1 (30μM) had no effect on the amplitude of NA-evoked currents, normalised to amplitude of the plateau NA-evoked current. Data are presented as mean ± SEM, where n = 5.*

### *4.2.3 PZM21 is a low efficacy partial MOPr agonist in LC neurons*

The finding that the intrinsic efficacy of PZM21 for MOPr-GIRK activation was significantly lower than that of morphine in LC neurons was at odds with previous findings at the time of investigation. Initial characterisation of PZM21 by Manglik et al. (2016) described PZM21 as having an equivalent efficacy for G protein activation to morphine in heterologous cell-based assays. This is particularly important considering that efficacy is an important and potentially confounding factor in the assessment of relative bias (Kelly, 2013) (Chapter 3.3.2).

In order to illustrate whether the intrinsic efficacy of PZM21 for activation of MOPr-GIRK currents was notably different to that of morphine, we assessed the ability of a receptor saturating concentration of PZM21 (30μM) to inhibit the GIRK current evoked by morphine at a maximal concentration (10μM) (Figure 4.9). In this case, we would hypothesise that upon its application, PZM21 would displace morphine from MOPr and exert its own functional effect. If PZM21 were to have a lower intrinsic efficacy for MOPr-dependent GIRK activity than morphine, it would functionally act as an antagonist (Figure 3.5A). If PZM21 and morphine truly had equivalent intrinsic efficacies, it would have no effect on morphine-evoked GIRK currents.

The application of PZM21 markedly attenuated the magnitude of the morphine-evoked GIRK current, to around 65% of its original amplitude (Figure 4.9). The degree of inhibition observed here was proportionally similar to the relationship of the peak GIRK currents evoked by PZM21 (30μM) to that of morphine (30μM) (around 60%) (Figure 4.3). This finding further illustrates that PZM21 does in fact have a lower intrinsic efficacy than morphine for G protein activation downstream of MOPr, in agreement with data from cell-based assays presented in this thesis (Figure 3.1, Table 3.1).

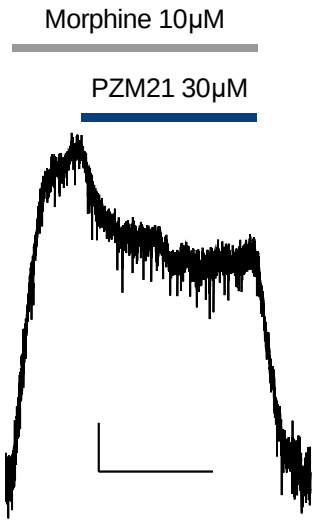


**Figure 4.9 – PZM21 partially antagonises morphine-evoked GIRK currents**

*A representative trace of a GIRK current evoked by an approximately maximal concentration of morphine (10μM) in a rat LC neuron. Application of a receptor saturating concentration of PZM21 (30μM) caused a robust reduction in the amplitude of morphine-evoked GIRK current. Scale bars are representative of 20pA and 5 min. Data presented are representative of an n of 1.*

### *4.2.4 Compound 1 induces small but measurable antinociception in mice*

The rapid and efficacious analgesic effects of opioids, such as morphine, have cemented them as mainstays of significant pain management. Opioids produce their analgesic effects through activation of MOPr (Matthes et al., 1996). The molecular mechanisms of MOPr-mediated analgesia are G protein-dependent, with opioid-induced analgesia dependent on the expression of GIRK channels (Marker et al., 2004) and enhanced in mice lacking arrestin-3 (Bohn et al., 1999) or expressing knock-in phosphorylation-deficient MOPr mutants (Kliewer et al., 2019).

The analgesic properties of pharmacological agents are often studied through assessment of their ability to increase an animals response threshold to an acute nociceptive stimulus (Le Bars et al., 2001). The warm water tail withdrawal assay (or 'Tail-Flick' test) is a simple, well-established animal model of nociception to thermal stimuli (Janssen et al., 1963). In this paradigm, the immersion of an animal's (often mouse or rat) tail into warm water (around 50°C) provokes a rapid movement of the tail away from the stimulus. The latency of an animal to evoke a response (tail flick) upon exposure to the stimuli is monitored as a measure of nociception.

It is well-defined that opioids increase the response latency in this paradigm (Janssen et al., 1963), acting as antinociceptive agents. Given the agonist activity of Compound 1 at MOPr, we sought to characterise its antinociceptive properties in mice using a warm water tail withdrawal assay.

Additionally, characterising the antinociceptive effects of Compound 1 would further enable us to study potential long-term tolerance induced by Compound 1 upon chronic administration. Repeated injection of opioids to naïve animals results in a rapid reduction in the function of these drugs (i.e., tolerance), which can be assessed through antinociceptive assays such as warm water tail-withdrawal (Bohn et al., 2000; Hull et al., 2010; Melief et al., 2010). The rapid development of tolerance to opioid drugs severely limits their clinical utility, especially for chronic pain states. Given that opioid-induced receptor desensitization is suggested to play an important role in the development of opioid tolerance (Bohn et al., 2000; Bailey et al., 2009a; Kliewer et al., 2019), we hoped to study Compound 1-induced tolerance to further our understanding of the long-term functional consequences of biased agonism at MOPr in whole-animals.

Nociceptive function in male CD1 mice (8 weeks) old was tested using a warm water tail-immersion test using a water bath maintained at 52.5°C. The control latency times of withdrawal were assessed 30 minutes and 15 minutes prior to injection in order to gain a baseline value for tail flick latency in each mouse (Figure 4.10A).

Upon injection, morphine (10 mg/kg, i.p.) produced a rapid and substantial increase in tail flick latency in the mice (Figure 4.10A). At 15 minutes post-injection, seven of the twelve mice administered morphine exhibited tail flick latency values which reached the set 15 second cut-off time. Both doses of Compound 1 (50 mg/kg and 100 mg/kg, i.p.) also appeared to increase the observed tail flick latency of the mice in the tail withdrawal assay (Figure 4.10A). In contrast to morphine, none of the six mice which received 50 mg/kg Compound 1 and only one of the six mice administered 100 mg/kg Compound 1 exhibited tail flick latency which reached the set 15 second cut-off time over the 60 minute-post injection observation time.

Raw tail latency time values (Figure 4.10A) were converted to % of maximum possible effect values (% MPE, Figure 4.10B), a metric of antinociception incorporating both the baseline response values and the set 15 second cut-off time (Harris et al., 1964). The % MPE data similarly demonstrates that both morphine (10mg/kg) and Compound 1 (50 mg/kg & 100 mg/kg) produce an increase in tail flick latency in mice (Figure 4.10B). While there was no significant difference (Two-way ANOVA with Bonferroni's comparison) between the peak antinociceptive effects induced by Compound 1 at both doses (50 mg/kg and 100 mg/kg) and those induced by morphine (10 mg/kg), it appears the peak responses induced by Compound 1 were substantially lower (Figure 4.10B).

The area under the curve (AUC) for the time-% MPE curves (Figure 4.10B) were taken in the case of each drug, in order to characterise their collective antinociceptive effect over the 60 minutes post-treatment (Meymandi et al., 2006). A Kruskal-Wallis test, used given the non-parametric nature of the AUC values due to the cut-off applied to response times, revealed a significant difference between the AUC values for time-effect curves for between treatment groups (Figure 4.10C). The AUC values for morphine (10 mg/kg) and both examined doses of Compound 1 (50 mg/kg and 100 mg/kg) were significantly higher than that of saline (following further Dunn's multiple comparisons test), demonstrating that the examined doses of morphine and Compound 1 all produced antinociception in mice (Figure 4.10C). While no significant differences were observed between the AUC values for morphine and Compound 1 induced antinociception, it is clear that Compound 1 was not as efficacious as morphine at 50 mg/kg, and its efficacy did not increase when the dose was doubled to 100 mg/kg (Figure 4.10B).

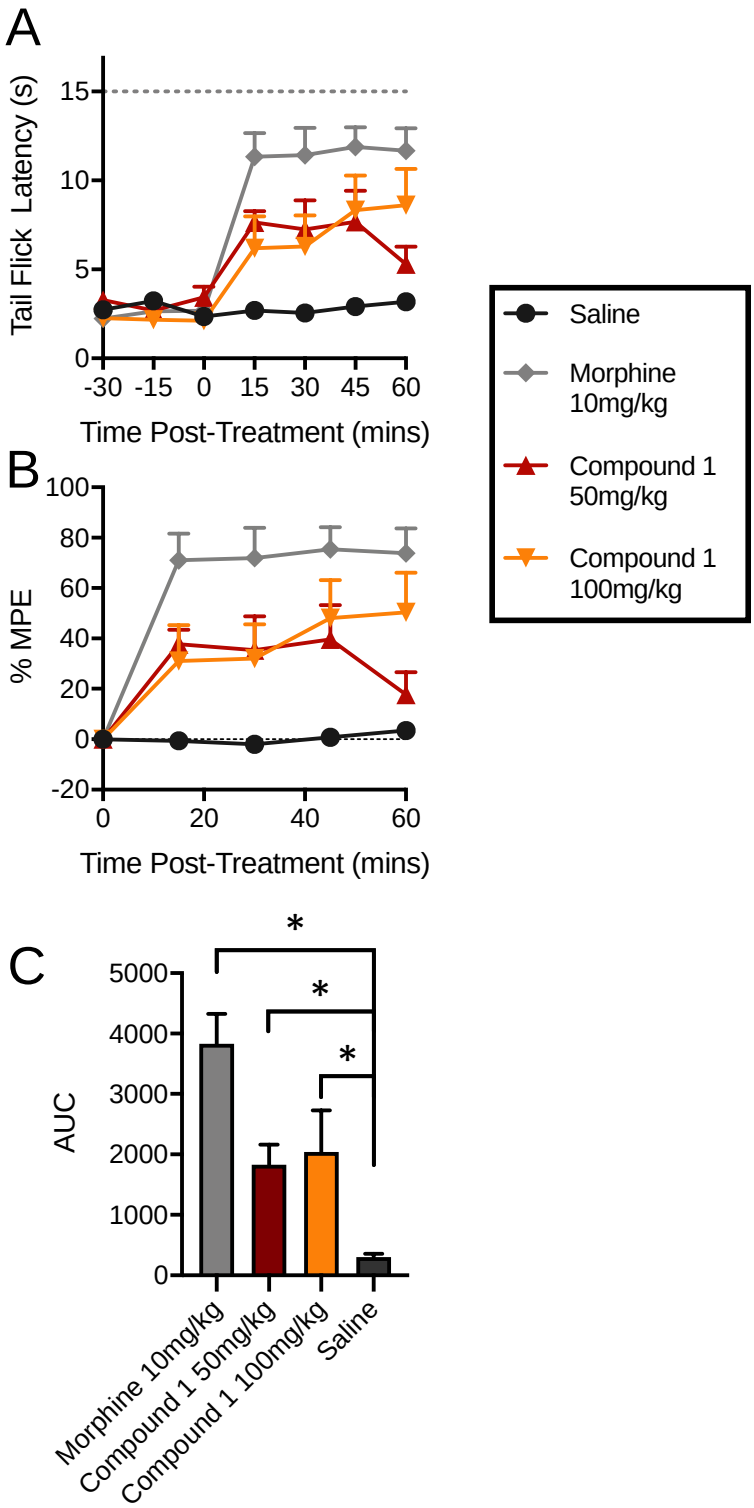


**Figure 4.10 – Antinociception induced by Compound 1 and morphine in CD1 mice**

*(A) Administration of morphine (10mg/kg, i.p.) and Compound 1 (50mg/kg and 100mg/kg, i.p.) increased the latency of tail flick responses (in seconds) of CD1 mice in a warm water tail withdrawal test of nociception. (B) Antinociceptive effects of Compound 1 and morphine displayed as a percentage of the maximum possible effect (% MPE), normalising to baseline nociceptive responses (0%) and the 15s cut off time (100%). (C)*

*Averaged area under the curve (AUC) data for Compound 1- and morphine-induced antinociception calculated from data presented in B. * P < 0.05, significantly different from saline AUC value. Kruskal-Wallis test with post-hoc Dunn's multiple comparisons test. n = 6 for Compound 1 50mg/kg and 100mg/kg groups, n = 12 for morphine 50mg/kg and saline groups. This work was performed with assistance from Dr Rob Hill (University of Bristol).*

Given the DOPr agonist properties previously demonstrated for Compound 1 (Figure 3.6), we sought to determine whether the observed antinociceptive properties of Compound 1 were MOPr-dependent through studying its effect in MOPr knockout (KO) mutant mice.

Similarly, to above, the nociception of both MOPr KO mice and wildtype C57/BLJ (background strain) (male and female, 25-30 g) was tested using a warm water tail-immersion test using a water bath maintained at 52.5°C. All animals received Compound 1 (50 mg/kg, i.p.). The lack of saline (negative) or morphine (positive) control groups arises from a limited number of MOPr KO animals available for this study.

Compound 1 did not produce an increase in tail flick latency in MOPr KO mice, when represented in raw values (Figure 4.11A) or as % MPE (Figure 4.11B). In contrast, Compound 1 produced a small increase in tail flick latency overall in C57/BLJ wildtype mice (Figure 4.11B). Compound 1-induced antinociception was significantly higher in C57/BLJ wild type mice than in MOPr KO mice at 45 mins and 60 mins post-treatment (Two-way ANOVA with Bonferroni's comparison). Two of the eight C57/BLJ wildtype mice examined exhibited the maximal possible effect for antinociception after administration with Compound 1 at one or more timepoints, where this was not observed in any of the MOPr KO mice. These findings demonstrate that the small antinociceptive effect induced by Compound 1 in mice is MOPr dependent. However, due to substantial error values in this study, there was no significant difference observed between the AUC values for MOPr KO and C57/BLJ wildtype mice (Figure 4.11C) calculated from the %MPE curves (Figure 4.11B) (Mann-Whitney Test, $p = 0.10$).

The lower magnitude of Compound 1 (50 mg/kg)-induced antinociception in the C57/BLJ mice (Figure 4.11B) compared to in the CD-1 mice (Figure 4.10B) likely results from the a lower opioid sensitivity of C57/BLJ mice in nociception assays, as previously reported (Pick et al., 1991). However, it is not possible to attribute this in the absence of a morphine control group in this small study.

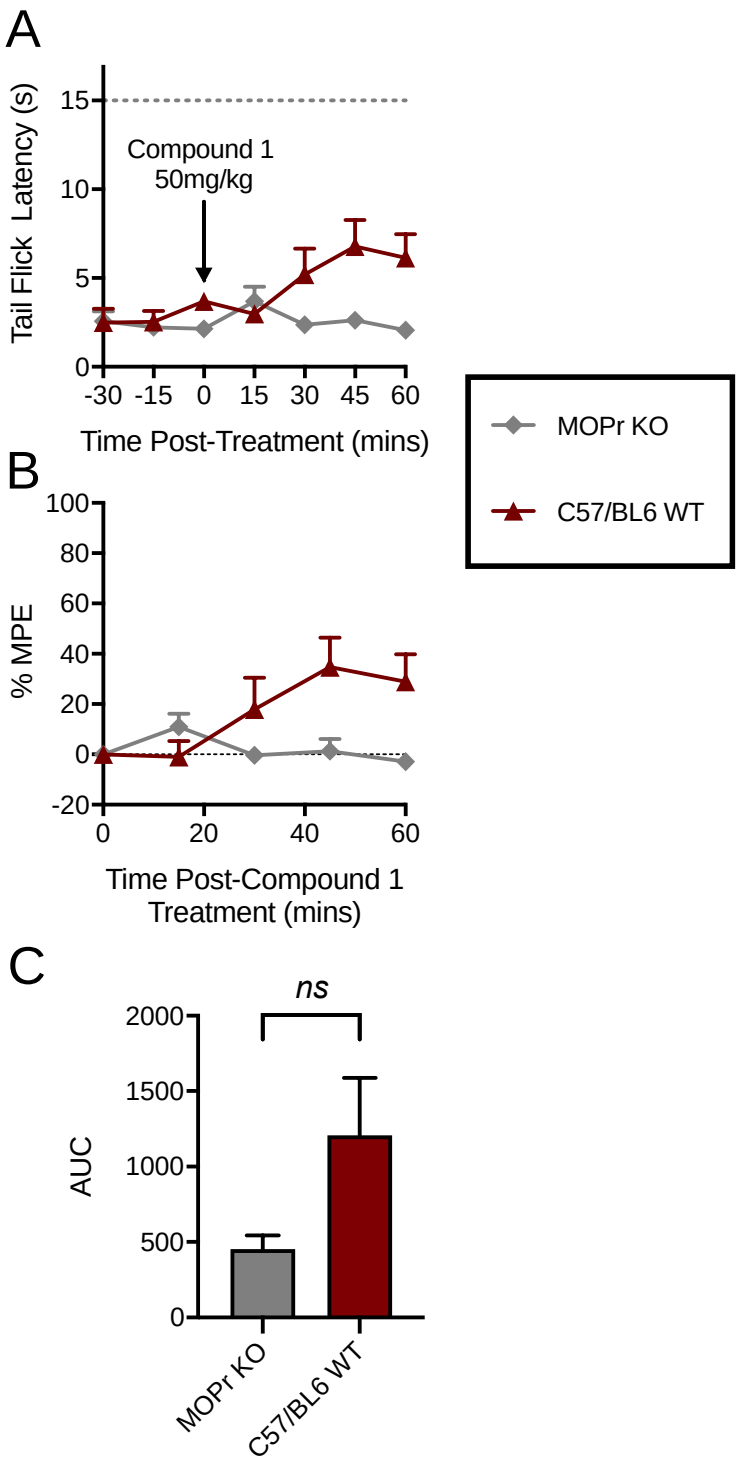


**Figure 4.11 – Compound 1-induced antinociception in C57/BL6 MOPr KO and WT mice**

*(A) Administration of Compound 1 (50mg/kg i.p.) caused a small increase in the latency of tail flick responses (in seconds) of C57/BL6 WT mice, but not MOPr KO mice (male and female 25-30g) in a warm water tail withdrawal test of nociception. (B) The effects of Compound 1 displayed as a percentage of the maximum possible effect (% MPE), normalising to baseline nociceptive responses (0%) and the 15s cut off time (100%). (C) Averaged area under the curve (AUC) data for Compound 1- induced antinociception*

*calculated from data presented in B. ns P > 0.05, no significant difference was observed between the AUC values observed in C57/BL6 WT and MOPr KO mice, assessed through a Mann-Whitney test (P = 0.10). n = 8 for both C57/BL6 WT and MOPr KO.*

## 4.3 Discussion

### *4.3.1 The intrinsic efficacy of Compound 1 and PZM21 in LC neurones*

Agonist intrinsic efficacy is an important and potentially confounding factor in the assessment of biased agonism at GPCRs (Kelly, 2013; Gillis et al., 2020c). The accurate assessment of agonist efficacy in heterologous systems is often distorted by receptor overexpression, ceiling for assay effects and high levels of amplification in particular G protein assays (Chapter 3.3.3). As such, G protein efficacy for partial agonists relative to full agonists is often exaggerated when assessed in heterologous systems. This becomes problematic considering the differential amplification between assays of G protein activity which often contain substantial signal amplification and the near linear process of arrestin recruitment. This can lead to partial agonists being classified as full agonists for G protein activity but weak partial agonists for arrestin recruitment due to simple system bias rather than actual biased agonism. For example, the prototypical partial agonist morphine has often been classified as a full agonist for G protein signalling in highly amplified cAMP-based assays (Zaki et al., 2000; Hothersall et al., 2017; Schmid et al., 2017; Pedersen et al., 2020), which has led to misleading conclusions about it being a G protein-biased agonist (Kelly, 2013). The characterization of agonist intrinsic efficacy in isolated tissue preparations can provide valuable, undistorted estimates of agonist efficacy. While this approach could be naïvely perceived as antiquated in the age of the recombinant system, the physiological levels of receptor expression in these preparations provide valuable, undistorted data which is less liable to misinterpretation.

The magnitude of peak GIRK currents induced by test opioids at receptor saturating concentrations in rat locus coeruleus neurons in this chapter provided an estimate of agonist intrinsic efficacy in the absence of full concentration response curves (Figure 4.3). The magnitude of GIRK currents evoked by Compound 1 were statistically similar to those evoked by morphine (Figure 4.3), supporting data from our G protein BRET assay (Figure 3.1, Table 3.1) which suggests that Compound 1 and morphine have equivalent G protein efficacy.

The lower magnitude of PZM21-evoked GIRK currents compared to those evoked by morphine was similarly in agreement with efficacy data from our G protein BRET assay (Figure 3.1, Table 3.1). Additionally, the fact that PZM21 partially antagonised morphine-evoked currents in LC neurons (Figure 4.9) clearly illustrates that it has a lower efficacy than morphine at MOPr. While this finding disagrees with some data within the original description of PZM21 (Manglik et al., 2016), it is in full agreement with more recent data from other groups (Hill et al., 2018b; Yudin et al., 2019; Gillis et al., 2020a). It is likely

that the reportedly improved adverse effect profiles of PZM21 (but see (Hill et al., 2018b)) are in fact attributed to its low intrinsic efficacy rather than any apparent bias (Gillis et al., 2020a).

### *4.3.2 PZM21 induced minimal rapid MOPr desensitization*

As a lower efficacy agonist than morphine, it is unsurprising that PZM21 visually appears to induce less rapid receptor desensitization in LC neurons (McPherson et al., 2010) (Figure 4.4). Although, statistically the extent of MOPr desensitization induced by PZM21 was not significantly different to that of morphine (Figure 4.5). Given that the fitted value of the half-life for the decline in PZM21-evoked currents was markedly slower than that of morphine (8.6 and 5.3 min respectively), it is possible that the time-scale used for investigations of PZM21-evoked currents was too short to observe the full extent of its desensitization. This is supported by the similarity of the plateau values (% peak response $\pm$ SEM) for fitted curves of PZM21 (73 $\pm$ 22) and morphine (67 $\pm$ 11) induced desensitization (Figure 4.4), which suggest the extent of desensitization evoked by PZM21 and morphine would be fairly similar if observed over a longer timeframe. Future experiments could examine this by tracking PZM21- and morphine-induced desensitization for longer time-periods post-peak opioid response (e.g. 30 min), however we believed this was outside of the focus of our current experiments.

Together, our data is in line with observations that tolerance to the antinociceptive effects of PZM21 develop in a similar rapid manner to that of morphine *in vivo* (Hill et al., 2018b). Our findings regarding PZM21-induced desensitization and other observations of PZM21 tolerance do question recent suggestions that low efficacy MOPr agonists are potentially being less liable to the development of tolerance (Gillis et al., 2020a).

### *4.3.3 Compound 1 induced substantial MOPr desensitization*

Compound 1-evoked currents underwent more rapid desensitization than those evoked by morphine. Previously the ability of agonists to induce GRK/arrestin mediated-phosphorylation and internalization has been strongly correlated with agonist G protein efficacy, with the important exception of the arrestin-biased agonist endomorphin-2 (McPherson et al., 2010). Under this association it would have been expected that Compound 1, when disregarding its biased agonism, would produce at most similar levels of MOPr desensitization to morphine considering they have equivalent G protein efficacy (Figure 3.1, Table 3.1, Figure 4.3).

Considering the propensity of arrestin-biased MOPr agonists to comparatively induce more receptor desensitization than the balanced agonist morphine, one would

hypothesise that the converse would be true for the G protein biased agonist Compound 1. For instance, the arrestin-biased agonist endomorphin-2 has an equivalent G protein efficacy to morphine but a relatively higher efficacy for Ser375 phosphorylation, arrestin recruitment and receptor internalization (McPherson et al., 2010; Rivero et al., 2012). Accordingly, endomorphin-2 induces substantially more rapid receptor desensitization in LC neurons (Rivero et al., 2012). Given Compound 1 had a lower efficacy for arrestin-3 recruitment than morphine (Figure 3.1, Table 3.1), we anticipated that it would produce less receptor desensitization in LC neurones. The fact that we found the opposite raises questions around the potential mechanisms of Compound 1-induced receptor desensitization.

I confirmed that apparent Compound 1-induced receptor desensitization was not due to the presence of potentially confounding effects, such as heterologous desensitization (Figure 4.6), peptide degradation (Figure 4.7) or indirect GIRK inhibition by Compound 1 (Figure 4.8). As such, the mechanism of Compound 1-induced MOPr desensitization could present a potentially novel mechanism responsible for the regulation of the long-term functional effects of G protein-biased agonists in the absence of GRK/arrestin modulation.

Aside from the canonical GRK/arrestin dependent mechanisms of MOPr desensitization, there have been a number of other kinase mediators e.g. PKC implicated in regulation of MOPr (Piñeyro et al., 2007; Kelly et al., 2008; Koch et al., 2008; Raehal et al., 2011b; Williams et al., 2013) (Chapter 1.2.5). In some cases, the involvement of these kinases is agonist-dependent (Kelly et al., 2008). It is possible that Compound 1 may induce MOPr desensitization through non-GRK/arrestin mechanisms previously implicated in MOPr regulation (further discussed in Chapter 5.1).

In the following chapter I will be investigating the potential mechanisms of Compound 1-induced MOPr desensitization in LC neurones, examining the role of kinases which have previously been implicated in MOPr regulation (GRK, PKC and JNK), through the use of known pharmacological inhibitors of these kinases.

### *4.3.4 Compound 1 induced antinociception*

Compound 1 was found to induce antinociception typical of opioids in a warm-water tail withdrawal assay in CD1 mice (Figure 4.10). The antinociceptive effects of Compound 1 were found to be mediated through MOPr, with an apparent absence of effect in MOPr KO mice (Figure 4.11). However, the antinociception induced by Compound 1 did not reach the levels achieved by morphine (10mg/kg) (Figure 4.11). Increasing the dose of

Compound 1 to 100mg/kg did not increase the antinociception elicited, suggesting a ceiling to its effect.

The finding that the peak antinociceptive effect induced by Compound 1 was substantially lower than morphine would not have been predicted based on results from our previous receptor pharmacology studies. Previous findings demonstrating that Compound 1 and morphine have equivalent intrinsic efficacy for G protein signalling in both our BRET assays (Table 3.1) and in rat LC neurons (Figure 4.3) suggest that the lower antinociceptive effect of Compound 1 is not due to its basic receptor pharmacology. Additionally, agonists of lower efficacy than morphine (such as pethidine, oxycodone and hydrocodone), often produce similar levels of analgesia to morphine in antinociceptive assays, in part due to a ceiling in reportable responses due to the time limits on nociceptive stimulus exposure applied for ethical reasons (Madia et al., 2009; Hull et al., 2010). Therefore, we suggest that the lower relative magnitude of antinociception produced by Compound 1 is not due to lower intrinsic efficacy.

The efficacy of drugs in whole-animal environments is influenced by factors beyond receptor pharmacology. For instance, the metabolic stability of Compound 1 is completely unknown. While this peptide has been cyclised in the hope of improving its metabolic stability (Li et al., 2016), degradation by peptidases upon systemic administration could feasibly explain limitations in its *in vivo* effects.

Additionally, the levels of Compound 1 reaching the site of action upon systemic administration is unknown. In order to exert its effects at spinal/CNS sites of action, this large cyclic peptide would have to cross the blood-brain barrier (BBB), which is dependent on the physiochemical properties of Compound 1, but also factors such as saturable bidirectional transport mechanisms across the BBB (Kastin et al., 1999). Although the extent of Compound 1 blood brain barrier (BBB) permeability and its pharmacokinetic properties are unknown, as a high molecular weight peptide, it is unlikely that it has high BBB permeability and as such the brain levels of Compound 1 could be limited One could entertain a possible mechanism whereby Compound 1 is transported across the BBB into the CNS through a saturable transport mechanism. If this was the case, it could explain the ceiling to the effect of Compound 1 (Figure 4.10).

Regardless, without real examination of the pharmacokinetic properties of Compound 1, including brain levels upon administration, it is not possible to conclude what the relatively low analgesic effect of this drug is due to. Potential issues surrounding BBB permeability of Compound 1 could be circumvented by examining its effects when administered intracerebroventricularly (i.c.v.) (Cook et al., 2009), however this is an intricate and potentially problematic procedure in mice. Without the necessary

experience, it was decided that this experiment was outside of the scope of this current study but could feasibly be addressed in future experiments.

In the absence of further pharmacokinetic data for Compound 1, we next focussed our research efforts on elucidating the mechanism of MOPr desensitization observed for Compound 1 in rat LC neurones rather than investigating potential in vivo tolerance to Compound 1.

# Chapter 5: Investigating the potential mechanisms of Compound 1-induced MOPr desensitization

## 5.1 Introduction

Work within the previous chapters of this thesis has characterised Compound 1 as a novel G protein-biased agonist. Compound 1 was demonstrated to induce substantial MOPr desensitization in rat LC neurones, opposing our original hypothesis that G protein-biased agonists would induce less receptor desensitization in this system.

The canonical mechanism of MOPr desensitization is initiated by GRK-dependent phosphorylation of MOPr C-terminal serine and threonine residues, with subsequent recruitment of arrestin-3 and related cellular machinery driving receptor internalization (Williams et al., 2013). Specifically, in LC neurones, expression of GRK2 has been demonstrated to be integral to MOPr desensitization induced by DAMGO (Bailey et al., 2009b). Additionally, the importance of C-terminal serine and threonine residue targets of GRK to Met-Enkephalin-induced MOPr desensitization has been demonstrated in both mouse and rat LC neurones, with loss of MOPr desensitization with the expression of phosphorylation-site deficient MOPrs (Arttamangkul et al., 2019a; Kliewer et al., 2019).

Given its low coupling to arrestin pathways (Figure 3.1D), we hypothesised that the MOPr desensitization induced by Compound 1 could be occurring through a non-GRK/arrestin based mechanism. Agonist-selective mechanisms of receptor desensitization and regulation have been widely discussed at MOPr, particularly in reference to that induced by morphine (Piñeyro et al., 2007; Kelly et al., 2008; Koch et al., 2008; Raehal et al., 2011b; Williams et al., 2013) (Chapter 1.2.5). It is possible that kinases previously implicated in agonist-selective mechanisms of MOPr desensitization could regulate Compound 1-induced desensitization.

One such mediator is PKC, which has been demonstrated to mediate the rapid receptor desensitization induced by morphine in LC neurones (Bailey et al., 2004; Bailey et al., 2009a; Bailey et al., 2009b) as well as the development of tolerance to morphine *in vivo* (Bohn et al., 2002; Hull et al., 2010). The relative contribution of PKC and/or GRK in opioid-induced MOPr desensitization has been associated with agonist intrinsic efficacy (Kelly et al., 2008). As such, high efficacy agonists at MOPr such as DAMGO and Met-Enkephalin would desensitize predominately through GRK pathways (Bailey et al., 2009b; Lowe et al., 2015) while lower efficacy agonists such as morphine would desensitize predominately through PKC (Bailey et al., 2004; Bailey et al., 2009a; Bailey et al., 2009b), with a smaller GRK component present (Lowe et al., 2015) (Chapter 1.2.5,

Figure 1.5). Given that Compound 1 is a partial MOPr agonist similar to morphine, it could be hypothesised that Compound 1-induced desensitization is mediated predominately by PKC rather than GRK.

In addition to PKC, there are a number of other kinases which have been implicated in MOPr regulation (Chapter 1.2.5) (Williams et al., 2013). One such kinase is c-Jun-N-terminal kinase 2 (JNK2). JNK2 has been implicated as a mediator of analgesic tolerance to morphine in mice (Melief et al., 2010). Additionally, JNK2 has been shown to regulate cellular tolerance to morphine in dorsal root ganglion neurons (Mittal et al., 2012). Recently, JNK has been demonstrated to play a role (alongside GRK and PKC) in MOPr downregulation in rat LC neurones, observed upon chronic morphine treatment (Leff et al., 2020). While it is possible that Compound 1-induced desensitization is JNK-mediated, the role of JNK appears to be linked to arrestin signalling (Mittal et al., 2012).

The work within this chapter sought to characterise the potential mechanisms involved in acute Compound 1-induced MOPr desensitization. By investigating potentially novel mechanisms of agonist-induced MOPr desensitization, we sought to further illustrate the long-term functional consequences of G protein-biased agonists at MOPr. In order to achieve this, we examined Compound 1-evoked GIRK currents in rat LC neurones in the presence of a number of pharmacological inhibitors of kinases previously implicated in the regulation of agonist-induced MOPr desensitization.

In this chapter, I demonstrate that Compound 1-induced desensitization in LC neurons is a GRK-dependent process, independent of PKC and JNK. This finding was somewhat unexpected given the low arrestin recruitment induced by Compound 1 in recombinant systems (Figure 3.1D). Following this, we again turned to recombinant systems to refine our understanding of the potentially GRK-dependent, arrestin-independent mechanism of Compound 1-induced MOPr desensitization through assays of arrestin recruitment (BRET), MOPr internalization (ELISA) and MOPr phosphorylation (phosphospecific immunoblotting). These assays provided data in line with Compound 1 being a G protein-biased agonist in recombinant systems, with Compound 1 inducing low recruitment of arrestins 2 and 3, minimal MOPr internalization, and nominal phosphorylation of serine and threonine residues known to be involved in GRK/arrestin-mediated MOPr desensitization and trafficking.

## 5.2 Results

### *5.2.1 Investigating the mechanisms of Compound 1-induced MOPr desensitization in rat LC neurones*

As described previously in Chapter 4, Compound 1 (30μM)-evoked GIRK currents were studied in single LC neurones from brain slices obtained from 4-week-old Wistar rats through whole-cell voltage-clamped electrophysiological recordings (Chapter 2.4). In order to study the potential role of select kinases in Compound 1-induced desensitization, we perfused brain slices with known inhibitors for 20 minutes prior to, and during, the application of Compound 1 and recording of evoked GIRK currents.

Kinase inhibitors were perfused for 20 min from the point of washing off the noradrenaline from the first control response (Figure 4.2). As such, the currents evoked in kinase inhibitor experiments would be observed at a later time point with respect to patching and application of noradrenaline, relative to the experiments done in Chapter 4 (Figure 4.2). Additionally, the potential effect of the vehicle for kinase inhibitors (0.1% v/v DMSO) on Compound 1-induced desensitization could confound any comparisons made between experiments presented in Chapter 4 (Figure 4.2) and these kinase inhibitor experiments.

As such, the extent of Compound 1-induced desensitization in the presence of select kinase inhibitors studied in this chapter was compared to that observed after 20 minutes perfusion of DMSO (0.1% v/v). As anticipated, the perfusion of DMSO had significant no effect on the magnitude of Compound-1 induced desensitization at 8 min post-peak opioid response ($P$ = 0.31, two-tailed unpaired t-test) (Figure 5.1). However, the rate of desensitization appeared to be slightly slowed in the DMSO conditions compared to in previous Compound 1-evoked currents (Figure 5.1). The half-life for the decay of Compound 1-evoked currents (min) was slightly increased from 4.2 to 5.1 in experiments with perfusion of DMSO for 20 min. Accordingly, the time for observation of Compound 1 currents post-peak response in all kinase inhibitor experiments was extended from 8 min to 10 min, in an attempt to capture double the half-life of evoked currents as previously discussed (Bailey et al., 2003). The specific reasoning behind this small slowing of Compound 1-induced desensitization is unclear, however it is likely related to the time at which Compound 1-evoked currents were examined relative to patching the cell, or to noradrenaline application.

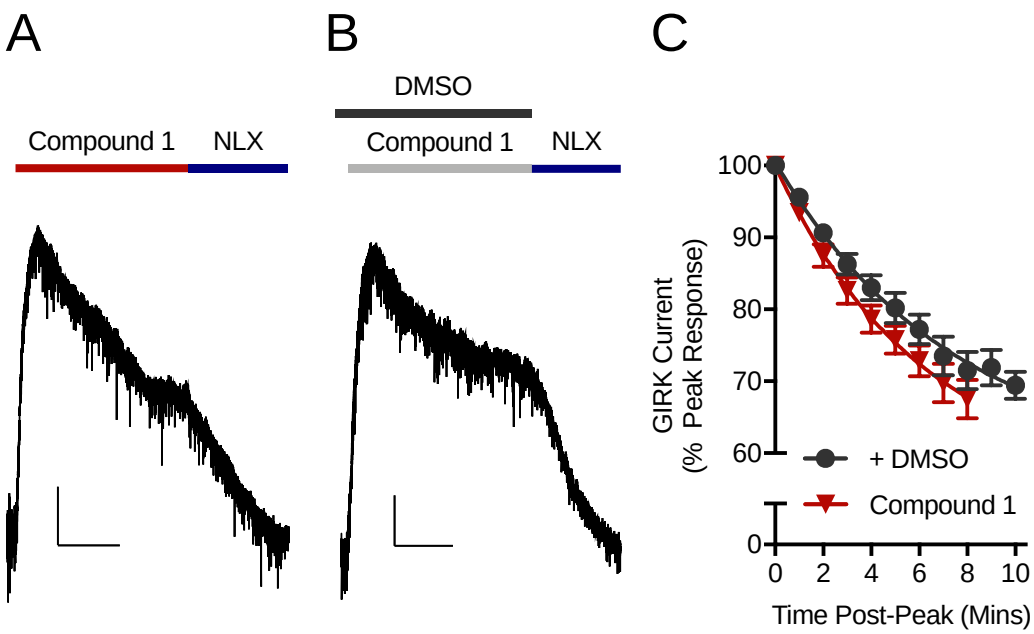


**Figure 5.1 – The effect of DMSO on desensitization of Compound 1-evoked GIRK currents**

*Representative traces of Compound 1 (30$\mu$M)-evoked potassium currents in rat LC neurones after no preincubation of additional agents (A) or after 20 min preincubation of DMSO (0.1% v/v; B). Compound 1-evoked GIRK currents were reversed by naloxone (NLX; A 1$\mu$M, B 10$\mu$M). Scale bars are representative of 20pA and 300s. (C) Pooled time courses from experiments of the type presented in A & B showing the desensitization of Compound 1-evoked currents post-peak response in the presence or absence of DMSO preincubation. Data for Compound 1-evoked currents presented here is reproduced from Chapter 4 (Figure 4.4). Data are presented as mean $\pm$ SEM, where n = 10 – 13.*

### *5.2.2 Compound 1-induced MOPr desensitization in rat LC neurones is not dependent on PKC*

PKC has been demonstrated to play a significant role in morphine-induced MOPr desensitization in both HEK 293 cells (Johnson et al., 2006) and in LC neurones (Bailey et al., 2004; Bailey et al., 2009b). The relative contribution of PKC to agonist-induced MOPr desensitization was postulated to be dependent on agonist efficacy (Kelly et al., 2008). This hypothesis was formed from observations of differential patterns of MOPr desensitization induced by DAMGO and morphine. In LC neurones, the full agonist DAMGO induces marked rapid receptor desensitization, through a GRK-dependent, but PKC-independent mechanism (Bailey et al., 2009b; Lowe et al., 2015). The partial agonist morphine induces minimal GRK-dependent receptor desensitization in LC neurones (Bailey et al., 2009b; Lowe et al., 2015), however morphine-induced desensitization is selectively enhanced when PKC activity was activated by phorbol-12-myristate-13-acetate (PMA) or through activation of $M_3$ muscarinic receptors in LC neurones (Bailey et al., 2004).

Oxycodone, which has a similar efficacy for G protein activation as morphine (McPherson et al., 2010), also produces minimal GRK-dependent desensitization in LC neurones (Arttamangkul et al., 2008). While the role of PKC in potential oxycodone-induced MOPr desensitization in LC neurones has not been examined, PKC does play a significant role in the development of tolerance to oxycodone (Hill et al., 2018a), as with the case of morphine, supporting efficacy as a determining factor in the relative contributions of GRK and PKC to agonist-induced MOPr desensitization.

Given that Compound 1 appears to have a similar efficacy to morphine (Figure 3.1, Table 3.1), we hypothesised that the observed Compound 1-induced desensitization in LC neurones could be regulated by PKC. I sought to test this hypothesis by first examining the effect of PKC inhibition on Compound 1-induced desensitization using GF109203X (Bailey et al., 2004), then investigating the effect of PKC activation on Compound 1-induced desensitization using PMA.

Brain slices were preincubated with GF109203X (1μM) for 20 min prior to, and during, the application of Compound 1 (Figure 5.2A). Inhibition of PKC through GF109203X had no effect on the desensitization of Compound 1-evoked GIRK currents compared to DMSO control (Figure 5.2). No visible differences were observed in the rate of Compound 1 desensitization (Figure 5.2B) and no significant differences were seen in the overall extent of desensitization (Figure 5.2C) between slices preincubated with GF109203X and DMSO control.

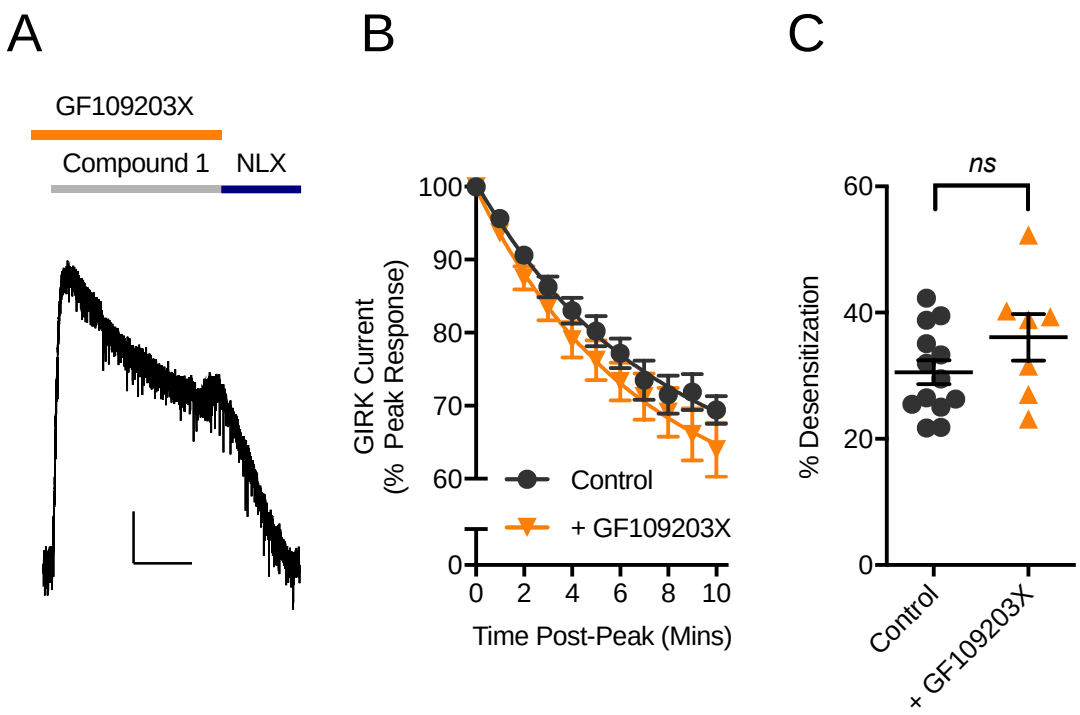


**Figure 5.2 – Inhibition of PKC has no effect on Compound 1-induced desensitization**

*(A) A representative trace of a Compound 1 (30 μM) evoked potassium currents in rat LC neurones after 20 min preincubation of GF109203X (1 μM). Compound 1-evoked GIRK currents were reversed by naloxone (NLX; 10 μM). Scale bars are representative of 20pA and 300s. (B) Pooled time-courses showing the desensitization of Compound 1-evoked currents post-peak response in the presence of GF109203X (1 μM) or control. (C) Pooled data for percentage of desensitization induced by Compound 1 10 min post-peak response following preincubation of GF109203X (1 μM) or control. Control represents 20 min preincubation with DMSO (0.1% v/v, Figure 5.1C). Data are presented as mean ± SEM, where n = 7 – 13. ns P > 0.05, two-tailed, unpaired t test.*

These findings with GF109203X suggest that PKC is not responsible for the acute rapid receptor desensitization observed in rat LC neurones in response to Compound 1. However, LC neurones in the slice preparation are considered to be relatively dormant, with basal PKC activity considerably lower than in the same neurones in an intact system (*in vivo*). This is probably due to activity of $G_q$-coupled GPCRs, as well as calcium permeable ionotropic receptors from ongoing synaptic activity (Bailey et al., 2009a). As such, exogenous activation of PKC in LC slices is used experimentally to attempt to mimic physiological levels of PKC activity in brain slices. As such, given that the endogenous PKC activity in brain slices must be raised in order to observe its role in MOPr desensitization, it is perhaps unsurprising that Compound 1-induced desensitization in basal conditions was unaffected by PKC inhibition. Similar findings have been demonstrated for GF109203X on MOPr desensitization in the case of morphine and Met-Enkephalin, where desensitization induced by these agonists do show PKC-dependence when PKC is exogenously stimulated (Bailey et al., 2004).

In order to study whether Compound 1-induced MOPr desensitization could be enhanced by activation of PKC, brain slices were preincubated with PMA (1μM) for 20 min prior to, and during, recording of Compound 1-evoked currents in rat LC neurones (Figure 5.3A). PMA had no significant effect on the overall desensitization of Compound 1-evoked GIRK currents (Figure 5.3B & 5.3C).

The increased apparent 'noise' levels in traces of the Compound 1-evoked GIRK current in Figure 5.3A was typical of all experiments with PMA. This 'noise' occurs through direct action of PMA to increase the frequency of spontaneous excitatory and inhibitory postsynaptic currents, which has been previously reported in rat LC neurones (Bailey et al., 2004) and other central nervous system synapses (Malenka et al., 1986). The occurrence of this induced 'noise' serves as a type of positive control confirming that PMA was active in these experiments.

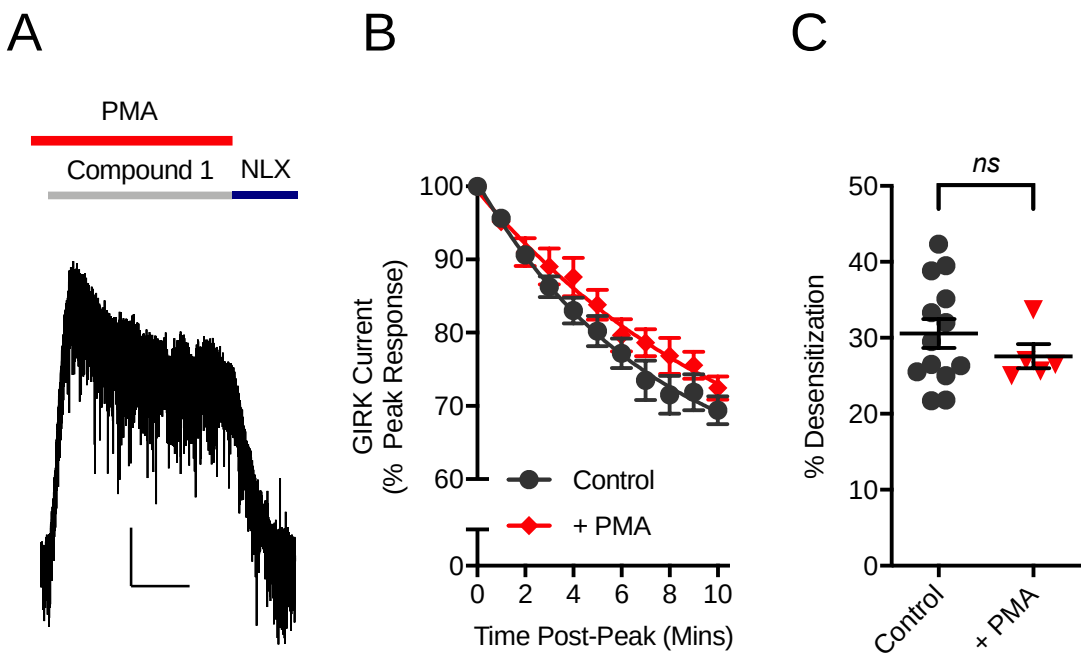


**Figure 5.3 – Activation of PKC has no impact on Compound 1-induced desensitization**

*(A) A representative trace of a Compound 1 (30 μM)-evoked potassium current in rat LC neurones after 20 min preincubation of PMA (1 μM). Compound 1-evoked GIRK currents were reversed by naloxone (NLX; 10 μM). Scale bars are representative of 20pA and 300s. (B) Pooled time-courses showing the desensitization of Compound 1-evoked currents post-peak response in the presence of PMA (1 μM) or control. (C) Pooled data for percentage of desensitization induced by Compound 1 ten min post-peak response following preincubation of PMA (1 μM) or control. Control represents 20 min preincubation with DMSO (0.1% v/v, Figure 5.1C). Data are presented as mean ± SEM, where n = 5 – 13. ns P > 0.05, two-tailed, unpaired t test.*

In order to exclude the possibility that inactivity of the GF109203X and PMA used in this study was responsible for the lack of PKC effect observed in Compound 1 induced desensitization, we sought to reproduce previous findings for PMA and GF109203X on morphine-induced MOPr desensitization. The ability of PMA (1 μM) to increase MOPr desensitization induced by morphine (30 μM) was assessed in rat LC neurones as previously described for Compound 1 (Figure 5.3). Preincubation of LC neurones with PMA significantly increased the magnitude of observed MOPr desensitization to morphine (Figure 5.4B, D & E). The impact of PMA on morphine desensitization was compared to control conditions where brain slices were preincubated with 0.1% DMSO for 20 minutes (Figure 5.4A), to mitigate the potential effect of the 20 min incubation period on the extent of opioid-induced desensitization (as outlined in Figure 5.1). This finding was in agreement with previous findings with morphine and PMA (Bailey et al., 2004), confirming the activity of PMA in our hands. In order to confirm the activity of GF109203X as a PKC inhibitor in our experiments, we investigated its effect on the PMA-mediated increase in morphine-induced MOPr desensitization by co-incubating GF109203X (1 μM) and PMA (1 μM) for 20 min prior to perfusion of morphine (30 μM) (Figure 5.4C). At concentrations used in previous experiments with Compound 1 (Figure 5.2), GF109203X effectively inhibited the PMA-mediated increase in morphine-induced MOPr desensitization, with desensitization in the combined presence of GF109203X and PMA being statistically similar to baseline levels (Figure 5.4D & E), confirming its activity as a PKC inhibitor in our experiments.

Together our findings for PMA and GF109203X intriguingly suggest that PKC is not involved in the mechanism of MOPr desensitization induced by Compound 1.

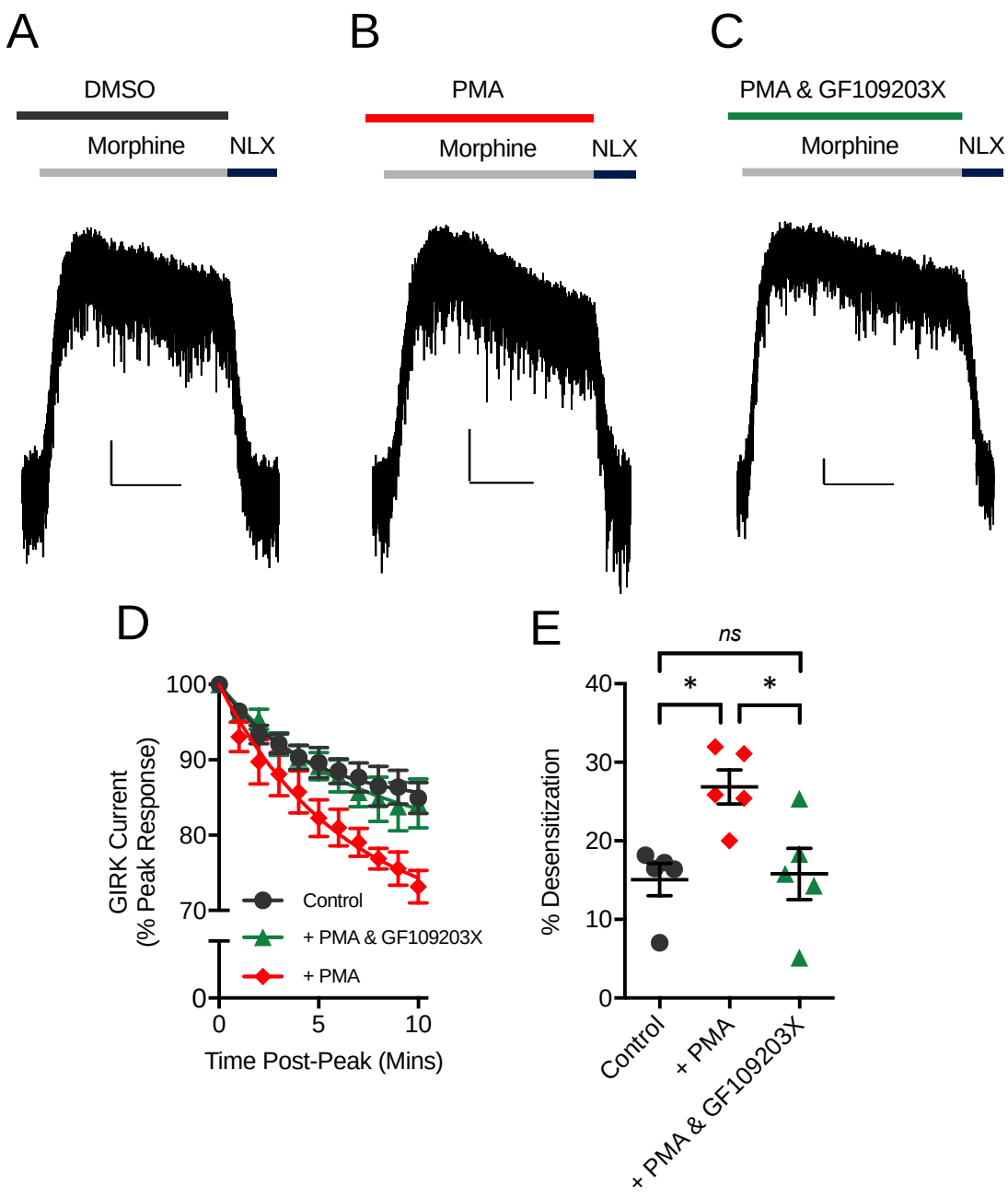


**Figure 5.4 –The role of PKC in morphine-induced MOPr desensitization in rat LC neurones**

*Representative traces of morphine (30 μM)-evoked GIRK currents in rat LC neurones after 20 min preincubation of DMSO (0.1% v/v) (A), PMA (1 μM) and (B) GF109203X (1μM) and PMA (1μM) (C). (A-C) Morphine-evoked currents were reversed by naloxone (NLX; 10 μM). Scale bars: 20pA and 300s. (D) Pooled time-courses from data shown in A-C showing the desensitization of morphine-evoked currents in the presence of DMSO control, PMA (1 μM) or GF109203X (1 μM) and PMA (1 μM). (E) Pooled data for percentage desensitization induced by morphine (30 μM) 10 min post-peak response*

*following preincubation of DMSO control, PMA (1 μM) or GF109203X (1 μM) and PMA (1 μM). n = 5. * P < 0.05, ns P > 0.05, one-way ANOVA with post-hoc Tukey tests.*

### *5.2.3 Compound 1-induced MOPr desensitization in rat LC neurones is GRK-dependent*

The canonical mechanism of receptor regulation at MOPr occurs through GRK- and arrestin-dependent mechanisms (Williams et al., 2013) (Chapter 1.2.5). Historically, the study of the role of GRK in MOPr desensitization in live neurones has been limited by the lack of selective tools. Additionally, genetic mouse models of GRK2 KO are embryonically lethal, limiting the utilisation of genetic approaches to study GRK function in MOPr desensitization.

The recent development of membrane permeable and selective small molecule inhibitors of GRK has greatly facilitated investigations into the role of GRKs in receptor desensitization (Thal et al., 2011). A comprehensive study in LC neurones showed that one such GRK inhibitor, Compound 101, significantly inhibited rapid MOPr desensitization induced by a range of MOPr agonists including the high efficacy agonists DAMGO and Met-Enkephalin, as well the partial agonist morphine and the arrestin-biased agonist endomorphin-2 (Lowe et al., 2015). The effect of Compound 101 on acute MOPr desensitization induced by Met-Enkephalin in rat LC neurones was indistinguishable from the effect of expressing a mutant MOPr deficient in sites of GRK-dependent phosphorylation (Leff et al., 2020), confirming that the effect of Compound 101 on MOPr desensitization in LC neurones is dependent on inhibition of GRK-mediated phosphorylation. In HEK 293 cells Compound 101 has been shown to inhibit DAMGO-induced MOPr internalization (Lowe et al., 2015), arrestin-3 recruitment (Miess et al., 2018) and phosphorylation of MOPr C-terminal serine and threonine residues (Gillis et al., 2020a). Compound 101 therefore provides a well-characterised tool to study the potential role of GRK in the MOPr desensitization induced by Compound 1 in rat LC neurones.

We first wanted to affirm the ability of Compound 101 to inhibit DAMGO-induced MOPr desensitization in rat LC neurones in our hands. As previously demonstrated (Lowe et al., 2015), preincubation of brain slices with Compound 101 (30μM) for 20 min prior to, and during, DAMGO application significantly attenuated DAMGO-induced MOPr desensitization in rat LC neurones (Figure 5.5). This confirms its ability to effectively inhibit GRK-mediated agonist-induced MOPr desensitization in rat LC neurones.

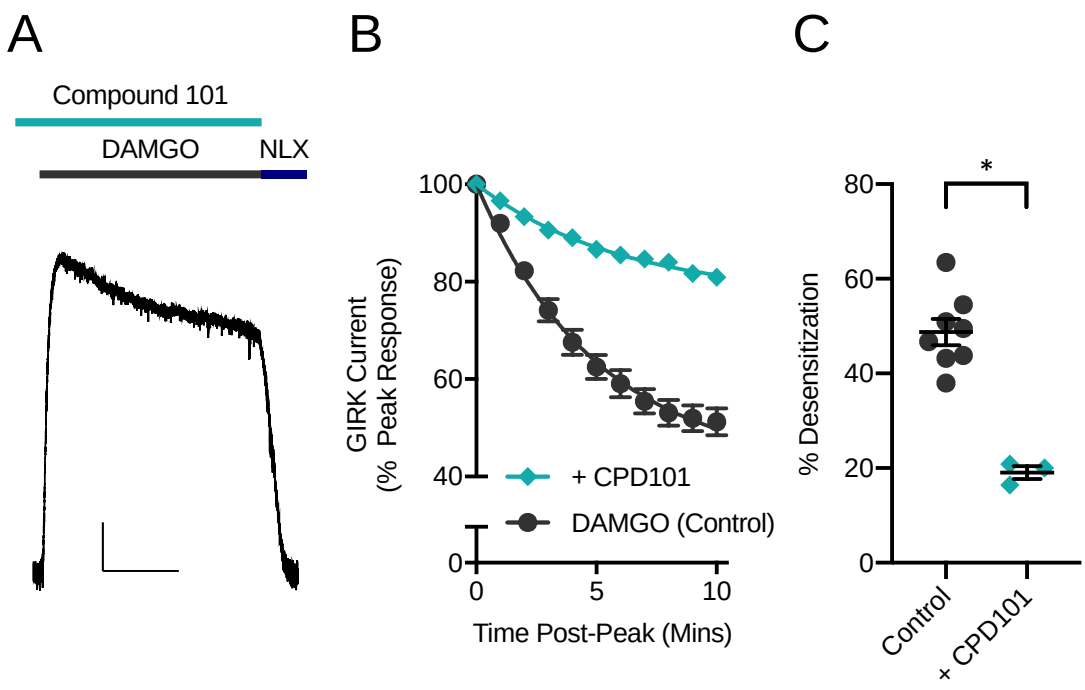


**Figure 5.5 – The GRK inhibitor Compound 101 inhibits DAMGO-induced desensitization**

*(A) A representative trace of a DAMGO (10μM)-evoked potassium current in rat LC neurones after 20 min preincubation of Compound 101 (30μM). DAMGO-evoked GIRK currents were reversed by naloxone (NLX; 10μM). Scale bars are representative of 50pA and 300s. (B) Pooled time-courses showing the desensitization of DAMGO-evoked currents post-peak response in the presence of Compound 101 (30μM) or control. (C) Pooled data for percentage of desensitization induced by DAMGO 10 min post-peak response following preincubation with Compound 101 (30μM) or control. Control represents DAMGO desensitization alone (Figure 4.4). Data are presented as mean ± SEM, where n = 3 – 8. * P < 0.05, two-tailed, unpaired t test.*

In order to assess the potential role of GRK in Compound 1-induced MOPr desensitization, we preincubated brain slices with Compound 101 (30μM) for 20 min prior to, and during, Compound 1 application (Figure 5.6A). Compound 101 preincubation significantly inhibited the desensitization of Compound 1-evoked GIRK currents in rat LC neurones (Figure 5.6B & Figure 5.6C). This finding was against our initial hypothesis that Compound 1-induced desensitization would occur through a GRK-independent mechanism, considering its low efficacy for arrestin-3 recruitment and G protein bias signalling profile (Figure 3.1, Figure 3.2 & Table 3.1).

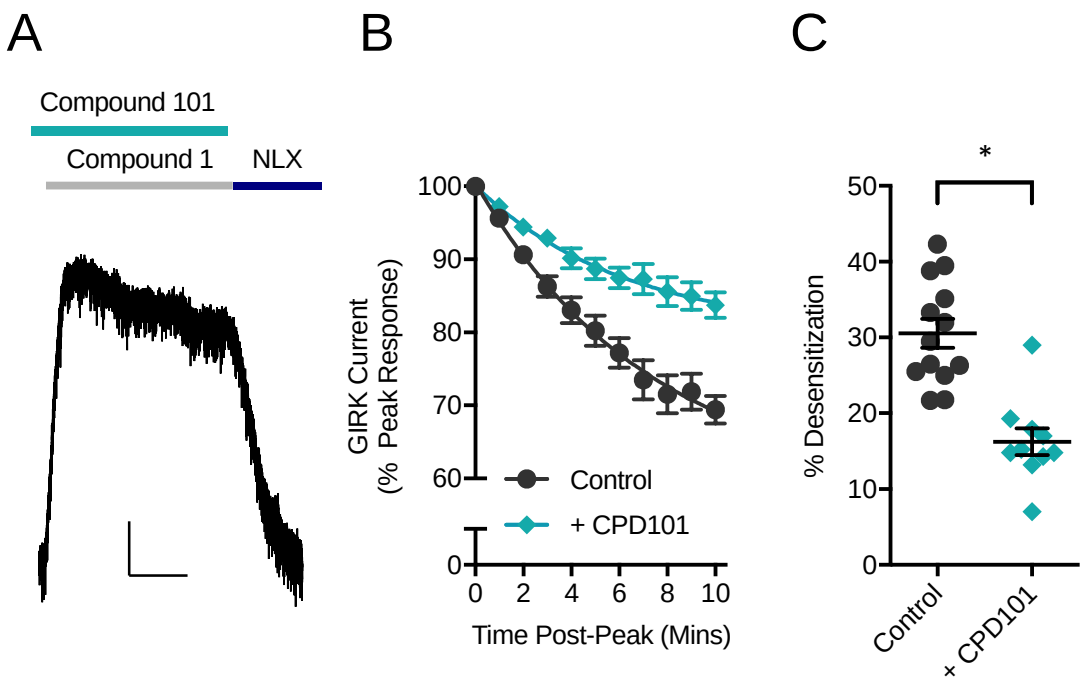


**Figure 5.6 – The GRK inhibitor Compound 101 attenuates Compound 1-induced desensitization**

*(A) A representative trace of a Compound 1 (30μM)-evoked potassium current in rat LC neurones after 20 min preincubation of Compound 101 (30μM). Compound 1-evoked GIRK currents were reversed by naloxone (NLX; 10μM). Scale bars are representative of 20pA and 300s. (B) Pooled time-courses showing the desensitization of Compound 1-evoked currents post-peak response in the presence of Compound 101 (30μM) or control. (C) Pooled data for percentage of desensitization induced by Compound 1 10 min post-peak response following preincubation of Compound 101 (30μM) or control. Control represents Compound 1 desensitization after 20 min preincubation with DMSO (0.1% v/v, Figure 5.1C). Data are presented as mean ± SEM, where n = 5 – 13. * P < 0.05, two-tailed, unpaired t test.*

Although Compound 101 is an effective GRK inhibitor, a previous screen has highlighted that this drug can to some extent inhibit a number of other ACG family kinases (Lowe et al., 2015). These off-target kinases include protein kinase C-related protein kinase (PRK2), serum and glucocorticoid-regulated kinase (SGK1) and Rho-associated protein kinase 2 (ROCK2). To test whether the effects of Compound 101 on Compound 1-induced desensitization were in fact mediated by off-target inhibition of these kinases rather than GRK, slices were preincubated with a combination of GSK650394 (10μM) and Y-27632 (50μM) (Figure 5.7A), collectively inhibiting PRK2, SGK1 and ROCK2.

GSK650394 and Y-27632 together had no effect on Compound 1-induced desensitization (Figure 5.7B & Figure 5.7C). This finding supports the hypothesis that the effects of Compound 101 on Compound 1-induced MOPr desensitization are GRK-dependent.

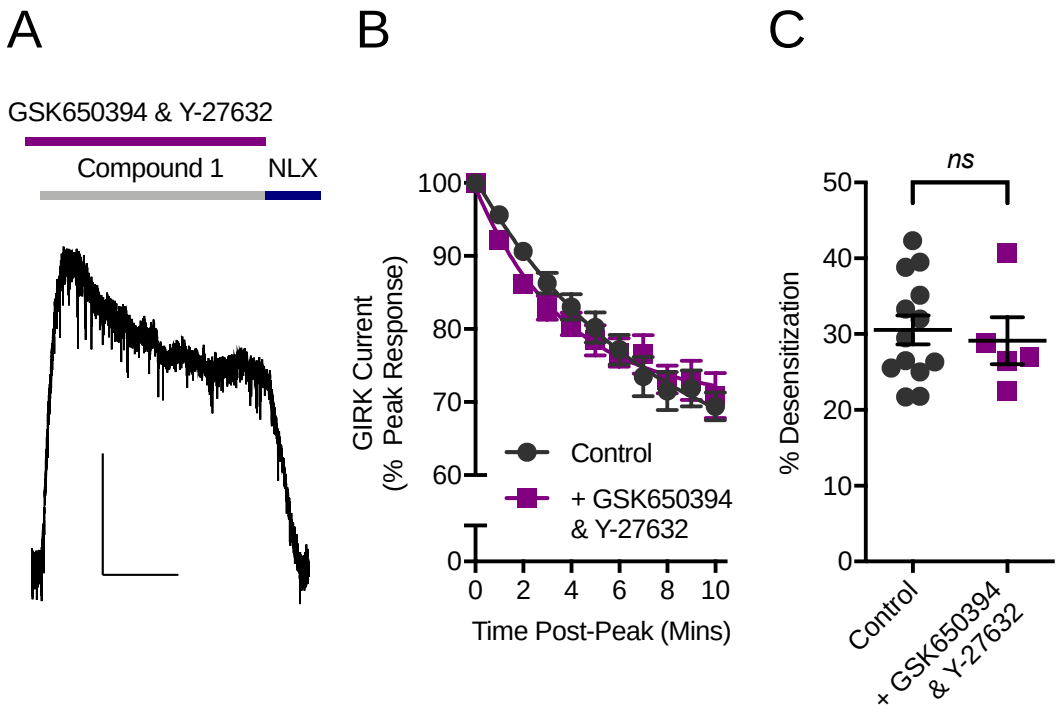


**Figure 5.7 – Inhibitors of off-target kinases inhibited by Compound 101 have no effect on Compound 1-induced desensitization**

*(A) A representative trace of a Compound 1 (30μM)-evoked potassium current in rat LC neurones after 20 min preincubation of GSK650394 (10μM) and Y-27632 (50μM). Compound 1-evoked GIRK currents were reversed by naloxone (NLX; 10μM). Scale bars are representative of 20pA and 300s. (B) Pooled time-courses showing the desensitization of Compound 1-evoked currents post-peak response in the combined presence of GSK650394 (10μM) and Y-27632 (50μM), or control. (C) Pooled data for percentage of desensitization induced by Compound 1 ten min post-peak response following preincubation of GSK650394 (10μM) and Y-27632 (50μM), or control. Control represents Compound 1 desensitization after 20 min preincubation with DMSO (0.1% v/v, Figure 5.1C). Data are presented as mean ± SEM, where n = 5 – 13. ns P > 0.05, two-tailed, unpaired t test.*

In order to confirm the role of GRK in Compound 1-induced MOPr desensitization, we sought to ulitise 14as; a novel, structurally distinct, paroxetine-derived GRK inhibitor (Waldschmidt et al., 2017).

With the effects of 14as on MOPr desensitization uncharacterised in neurones, we first characterised its ability to inhibit desensitization of DAMGO-evoked GIRK currents in rat LC neurones after 20 min preincubation (Figure 5.8A). 14as (30μM) inhibited DAMGO-induced desensitization in a preliminary experiment (n = 1), to a similar extent as Compound 101 (30μM) (Figure 5.8B & Figure 5.8C). Similarly, a preliminary experiment (n = 1) suggested that 14as (30μM) also inhibited desensitization of Compound 1-evoked GIRK currents in rat LC neurones to the same extent as Compound 101 after 20 min preincubation (Figure 5.9). The % desensitization values for Compound 1 (15.4) and DAMGO (23.9) induced desensitization in the presence of 14as, lie outside the 95% confidence intervals for control Compound 1 (26.4 – 34.7) and DAMGO (42.2 – 55.3) values. This suggests, in the absence of proper statistical analysis, that in these cases 14as inhibits agonist-induced desensitization in a similar manner to Compound 101.

These preliminary data with a structurally distinct GRK inhibitor supports findings with Compound 101, demonstrating a central role for GRK in MOPr desensitization induced by Compound 1. Unfortunately, due to limited amounts of compound available at the time of study, further experiments with 14as were not possible.

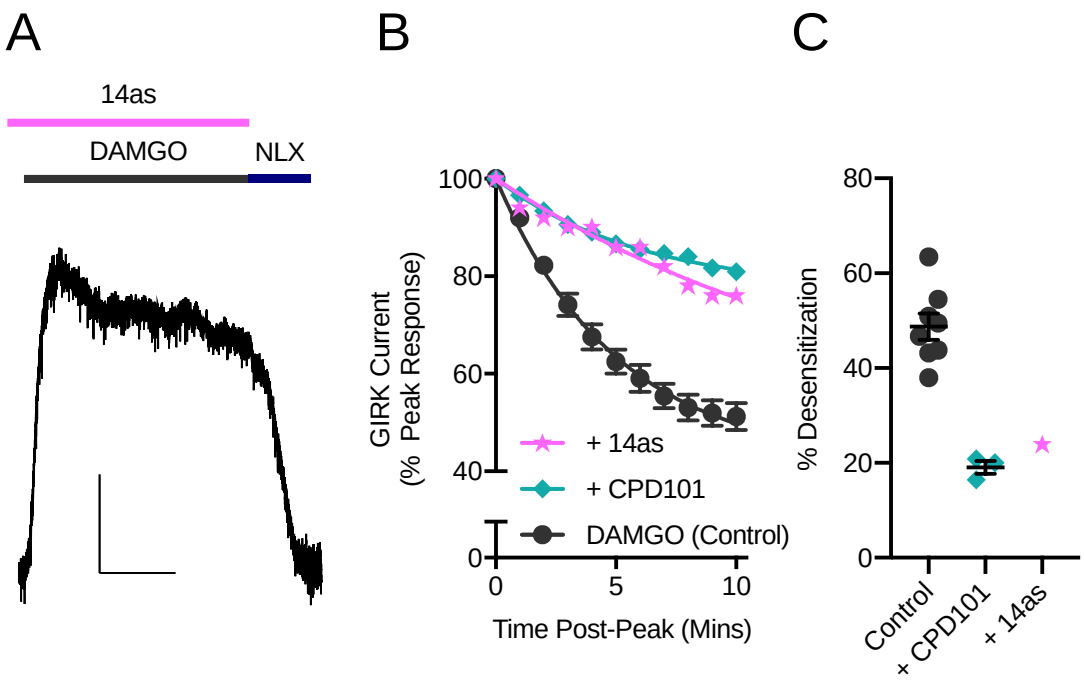


**Figure 5.8 – The GRK inhibitor 14as inhibits DAMGO-induced MOPr desensitization**

*(A) A representative trace of a DAMGO (10μM)-evoked potassium current in rat LC neurones after 20 min preincubation of 14as (30μM). DAMGO-evoked GIRK currents were reversed by naloxone (NLX; 10μM). Scale bars are representative of 50pA and 300s. (B) Pooled time-courses showing the desensitization of DAMGO-evoked currents post-peak response in the presence of 14as (30μM), Compound 101 (30μM, Figure 5.5) or control. (C) Pooled data for percentage of desensitization induced by DAMGO 10 min post-peak response following preincubation of 14as (30μM), Compound 101 (30μM, Figure 5.5) or control. Control represents DAMGO desensitization alone (Figure 4.4). Data are presented as mean ± SEM, where n = 1 – 8.*

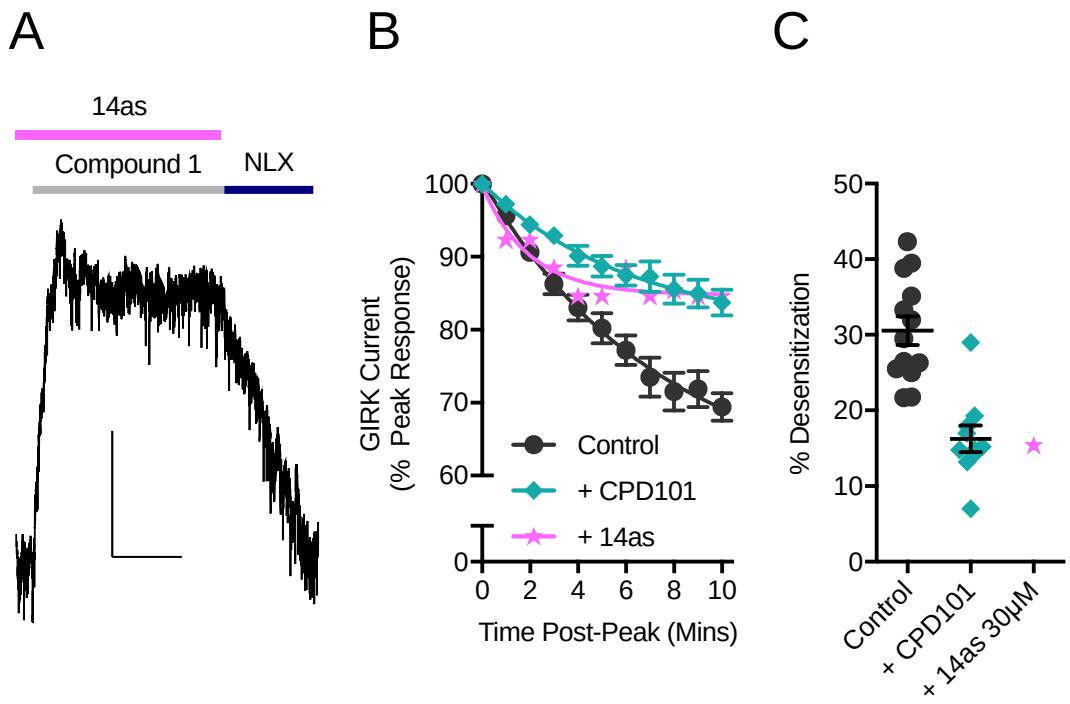


**Figure 5.9 – 14as inhibits Compound 1-induced MOPr desensitization**

*(A) A representative trace of a Compound 1 (30μM)-evoked potassium current in rat LC neurones after 20 min preincubation of 14as (30μM). Compound 1-evoked GIRK currents were reversed by naloxone (NLX; 10μM). Scale bars are representative of 20pA and 300s. (B) Pooled time-courses showing the desensitization of Compound 1-evoked current post-peak response in the presence of 14as (30μM), Compound 101 (30μM, Figure 5.6) or control. (C) Pooled data for percentage of desensitization induced by Compound 1 ten min post-peak response following preincubation of 14as (30μM), Compound 101 (30μM, Figure 5.6) or control. Control represents Compound 1 desensitization after 20 min preincubation with DMSO (0.1% v/v, Figure 5.1C). Data are presented as mean ± SEM, where n = 1 – 13.*

### *5.2.4 Compound 1-induced MOPr desensitization in rat LC neurones is independent of JNK*

Some reports have suggested that JNK regulates the development of tolerance to the effects of morphine *in vivo* (Melief et al., 2010; Kuhar et al., 2015; Marcus et al., 2015), suggesting a potential role for JNK in agonist-induced MOPr desensitization. Given the potentially novel mechanism involved in Compound 1-induced desensitization, we sought to investigate a possible role of JNK in MOPr desensitization in rat LC neurones using the inhibitor SP600125 (Han et al., 2001).

To investigate the potential role of JNK, brain slices were preincubated with SP600125 (30μM) for 20 min prior to, and during, application of either DAMGO or Compound 1 (Figure 5.10A & Figure 5.11A). SP600125 had no effect on the extent of rapid MOPr desensitization elicited by DAMGO (Figure 5.10) or Compound 1 (Figure 5.11) in rat LC neurones, therefore suggesting that JNK does not play a role in the acute rapid MOPr desensitization induced by these agonists.

Recent work in rat LC neurones, published after the period of our investigation, has demonstrated that JNK inhibitors are ineffective in inhibiting acute MOPr desensitization induced by Met-Enkephalin (Leff et al., 2020), in agreement with our findings for DAMGO and Compound 1. However, JNK was shown to play a partial role, alongside GRK and PKC, in MOPr desensitization observed in response to chronic morphine treatment (Leff et al., 2020). While we cannot exclude the possibility that JNK signalling is involved in cellular tolerance to Compound 1 and DAMGO over chronic exposure, our current findings suggest it is not involved in acute MOPr desensitization induced by either of these ligands.

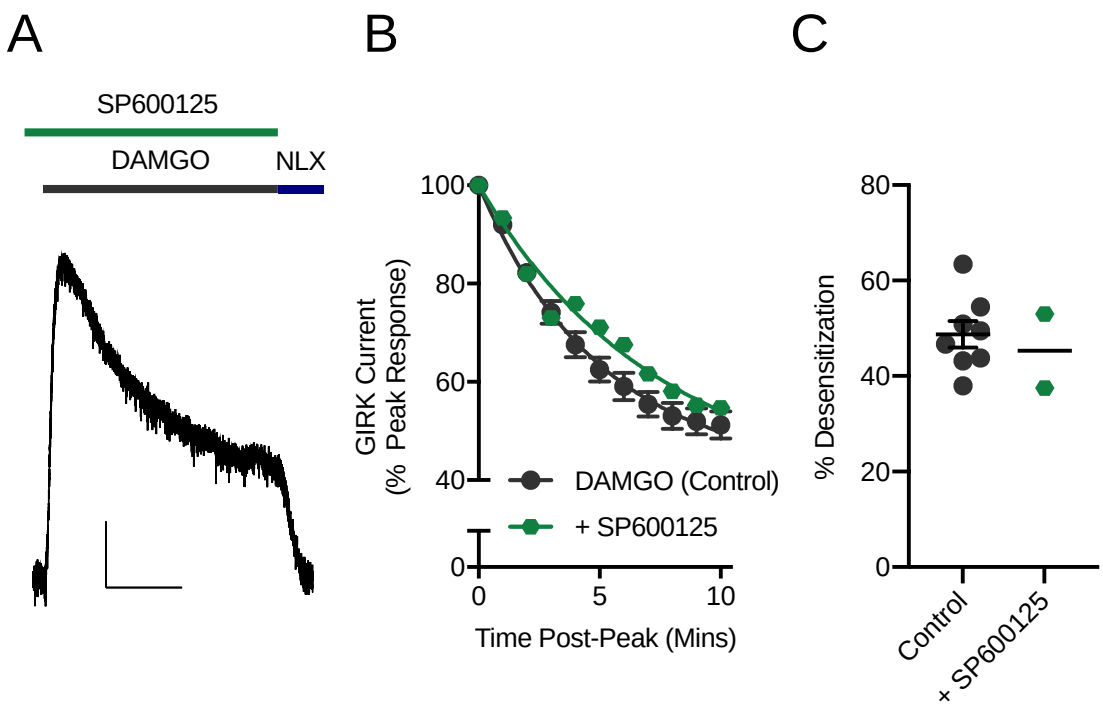


**Figure 5.10 – Inhibition of JNK has no impact on acute DAMGO-induced desensitization**

*(A) A representative trace of a DAMGO (10μM)-evoked potassium current in rat LC neurones after 20 min preincubation of SP600125 (30μM). DAMGO-evoked GIRK currents were reversed by naloxone (NLX; 10μM). Scale bars are representative of 50pA and 300s. (B) Pooled time-courses showing the desensitization of DAMGO-evoked currents post-peak response in the presence of SP600125 (30μM) or control. (C) Pooled data for percentage of desensitization induced by DAMGO 10 min post-peak response following preincubation of SP600125 (30μM) or control. Control represents DAMGO desensitization alone (Figure 4.4). Data are presented as mean ± SEM or mean alone, where n = 2 – 8.*

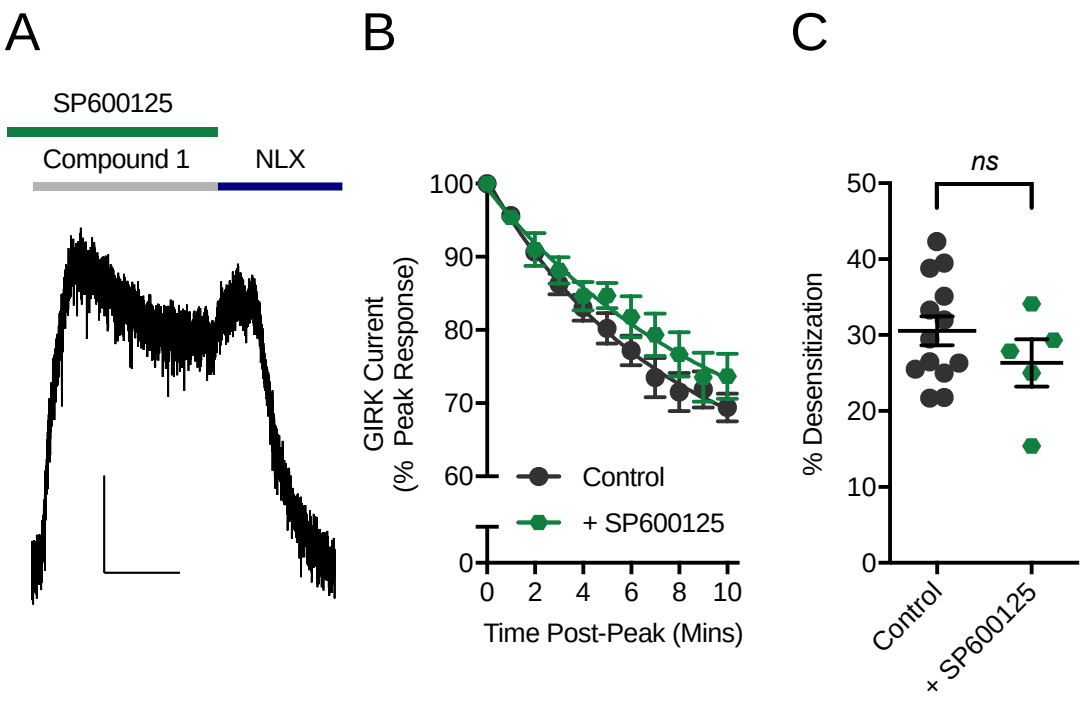


**Figure 5.11 – JNK inhibition has no effect on Compound 1-induced desensitization**

*(A) A representative trace of a Compound 1 (30 μM)-evoked potassium current in rat LC neurones after 20 min preincubation of SP600125 (30 μM). Compound 1-evoked GIRK currents were reversed by naloxone (NLX; 10 μM). Scale bars are representative of 20pA and 300s. (B) Pooled time-courses showing the desensitization of Compound 1-evoked currents post-peak response in the presence of SP600125 (30 μM) or control. (C) Pooled data for percentage of desensitization induced by Compound 1 ten min post-peak response following preincubation of SP600125 (30 μM) or control. Control represents Compound 1 desensitization after 20 min preincubation with DMSO (0.1% v/v, Figure 5.1C). Data are presented as mean ± SEM, where n = 5 – 13. ns P > 0.05, two-tailed, unpaired t test.*

### *5.2.5 Controls for kinase inhibition work in rat LC neurones and summary of current findings*

In order to assure that the observed effects of our kinase inhibitors of opioid-induced desensitization were not dependent on alterations in agonist intrinsic activity, we compared the relative intrinsic activities of our opioid agonists in these different conditions. This was achieved by comparing the peak GIRK currents elicited by these opioids in the presence or absence of kinase inhibitors, as an estimate of intrinsic activity at receptor saturating concentrations (Section 4.2.1). As described previously, opioid-evoked GIRK currents were normalised to the magnitude of noradrenaline-evoked GIRK currents within the same cell to reduce variability (Figure 4.2, Section 4.2.1).

No significant difference was observed between the peak GIRK currents elicited by DAMGO in the presence of Compound 101 or control (Unpaired, two-tailed *t*-test, $P = 0.94$; Figure 5.12). Similarly, no significant differences were observed in Compound 1 peak GIRK currents after incubation with examined kinase modulators versus control conditions (One-way ANOVA, $P = 0.85$; Figure 5.13). Statistical analysis was not conducted on the possible effect of 14as on Compound 1 peak GIRK currents or 14as and SP600125 on DAMGO peak GIRK currents as the number of repeats for these conditions was not sufficient to conduct such analysis (Compound 1 in 14as, n = 1, Figure 5.13; DAMGO in 14as, n = 1, DAMGO in SP600125, n = 2, Figure 5.12). However in these limited repeats, obtained values for peak opioid responses (% NA) for Compound 1 in 14as (41.9), DAMGO in 14as (73.5) and DAMGO in SP600125 (102.4) lie outside of the 95% confidence intervals for control Compound 1 (51.2 – 76.8) and DAMGO (110.1 – 138.4) values. This highlights the need for additional data for the above experimental conditions. More generally, these findings demonstrate that the observed effects of kinases modulators, in particular the effect of Compound 101 on Compound 1, are not due to a reduction in the intrinsic activity of Compound 1.

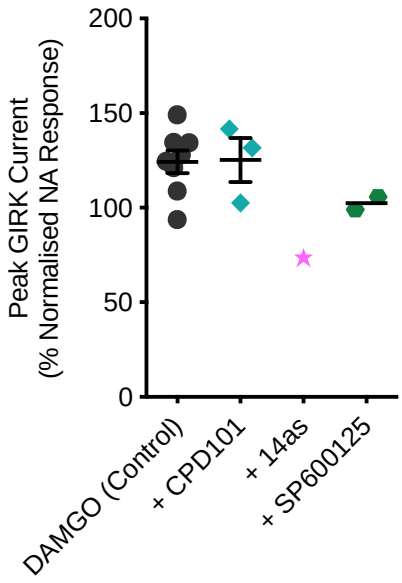


**Figure 5.12 – Examined kinase inhibitors had no effect on the magnitude of DAMGO-evoked GIRK currents**

*Pooled data from experiments of DAMGO-induced MOPr desensitization presented earlier in this chapter, examining the peak GIRK current evoked by DAMGO in control conditions (Figure 4.3) and after 20 min preincubation with Compound 101 (30 $\mu$M, Figure 5.5), 14as (30 $\mu$M, Figure 5.8) or SP600125 (30 $\mu$M, Figure 5.10). Responses were normalised to the maximal $\alpha_2$-adrenoceptor-mediated currents evoked by noradrenaline (100 $\mu$M) in the same cell. Data are presented as mean ± SEM, where n = 1 – 8.*

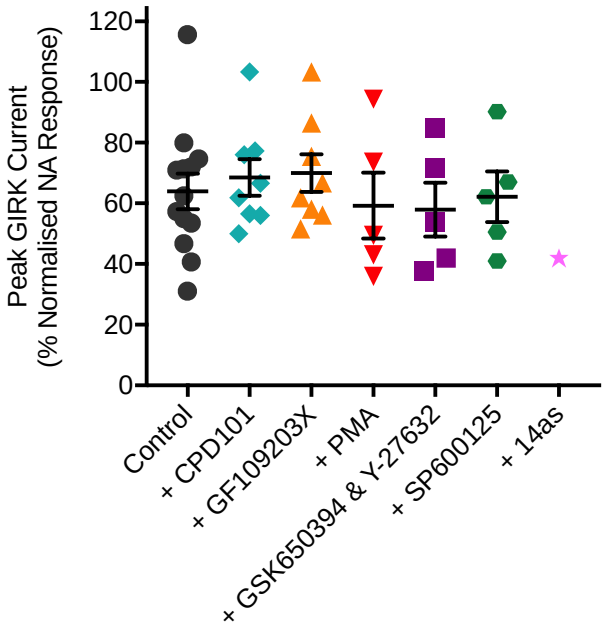


**Figure 5.13 – Examined kinase inhibitors had no effect on the magnitude of Compound 1-evoked GIRK currents**

*Pooled data from experiments of Compound 1-induced MOPr desensitization presented earlier in this chapter examining the peak GIRK current evoked by Compound 1 after 20 min preincubation with DMSO (0.1% v/v, Figure 5.1), Compound 101 (30 μM, Figure 5.6), GF109203X (1 μM, Figure 5.2), PMA (1 μM, Figure 5.3), GSK650394 & Y-27632 (10 μM and 50 μM respectively, Figure 5.7), SP600125 (30 μM, Figure 5.11) or 14as (30 μM, Figure 5.9). Responses were normalised to the maximal $\alpha_2$-adrenoceptor-mediated currents evoked by noradrenaline (100 μM) in the same cell. Data are presented as mean ± SEM, where n = 1 – 13.*

The magnitude of noradrenaline (100μM)-evoked currents was also assessed before and after application of Compound 1 and respective kinase modulators, as described previously (Figure 4.2, Figure 4.6). This was performed to examine potential heterologous desensitization induced by kinase modulators, as well as potential current rundown.

For experiments of DAMGO-evoked currents, there was no significant difference between the magnitude of noradrenaline-evoked currents pre- and post- incubation with Compound 101 and DAMGO, and control (Unpaired, two-tailed *t*-test *P* = 0.08; Figure 5.14). Similarly, in the case of experiments with Compound 1-evoked currents, no significant differences were observed between the magnitude of noradrenaline-evoked currents pre- and post- incubation when incubated with the described kinase inhibitors (One-way ANOVA, *P* = 0.09; Figure 5.15). Although the amplitude of NA-evoked currents post-Compound 1 appeared to be somewhat increased after incubation with Compound 101, no statistical difference was observed between these values and the values of our controls (*P* = 0.16). Overall, these data demonstrate that the observed action of our kinase inhibitors is not through indirect modulation of heterologous desensitization.

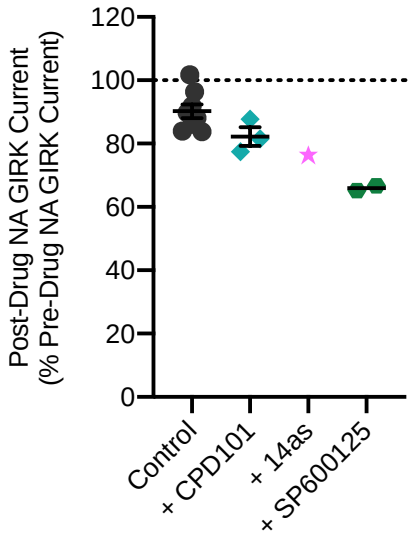


**Figure 5.14 – Kinase inhibitors and DAMGO have no heterologous effect on noradrenaline-evoked GIRK currents**

*Pooled data from experiments of DAMGO-induced MOPr desensitization presented earlier in this chapter examining the magnitude of noradrenaline (NA, 100μM) evoked currents before and after DAMGO application (Control, Figure 4.4) and / or 20 min preincubation with Compound 101 (30μM, Figure 5.5), 14as (30μM, Figure 5.8), or SP600125 (30μM, Figure 5.10). Data are presented as mean ± SEM, where n = 1 – 8.*

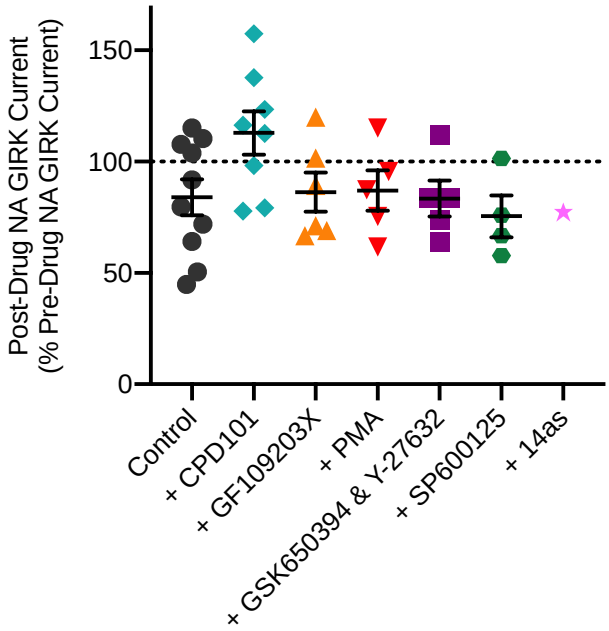


**Figure 5.15 – Kinase inhibitors and Compound 1 have no heterologous effect on noradrenaline-evoked GIRK currents**

*Pooled data from experiments of Compound 1-induced MOPr desensitization presented earlier in this chapter examining the magnitude of noradrenaline (NA, 100 μM) evoked currents before and after application of Compound 1 and 20 min preincubation with DMSO (0.1% v/v, Figure 5.1), Compound 101 (30 μM, Figure 5.6), GF109203X (1 μM, Figure 5.2), PMA (1 μM, Figure 5.3), GSK650394 & Y-27632 (10 μM and 50 μM respectively, Figure 5.7), SP600125 (30 μM, Figure 5.11) or 14as (30 μM, Figure 5.9). Data are presented as mean ± SEM, where n = 1 – 10.*

### *5.2.6 A summary of the mechanisms regulating Compound 1-induced MOPr desensitization in rat LC neurones*

A summary of our current work exploring the mechanism Compound 1-induced desensitization in rat LC neurones is presented in Figure 5.16. Our findings suggest that GRK appears to be the primary mediator of the observed MOPr desensitization induced by Compound 1, while PKC and JNK are not involved (Figure 5.16).

The GRK-dependent nature of Compound 1-induced MOPr desensitization in LC neurones is particularly intriguing given the relatively low arrestin-3 recruitment induced by Compound 1 in HEK 293 cells (Figure 3.1D, Table 3.1), and its G protein-biased signalling profile at MOPr (Figure 3.2). As such, we aimed to address a number of outstanding questions around the induction of GRK/arrestin pathways by Compound 1 in recombinant systems. Through addressing these outstanding questions, we hoped to build an understanding of the mechanistic basis of this potentially GRK-dependent, but arrestin-independent mechanism of MOPr desensitization induced by Compound 1.

The selected unresolved questions are as follows (Figure 5.16):

- Are differences in the levels of GRK expression causing a discrepancy in GRK/arrestin responses between assays in recombinant systems and in neurones?
- Does Compound 1 favour the induction of arrestin-2 recruitment over arrestin-3?
- Does Compound 1 induce MOPr internalization?
- Does Compound 1 induce MOPr phosphorylation at typical GRK-dependent sites?

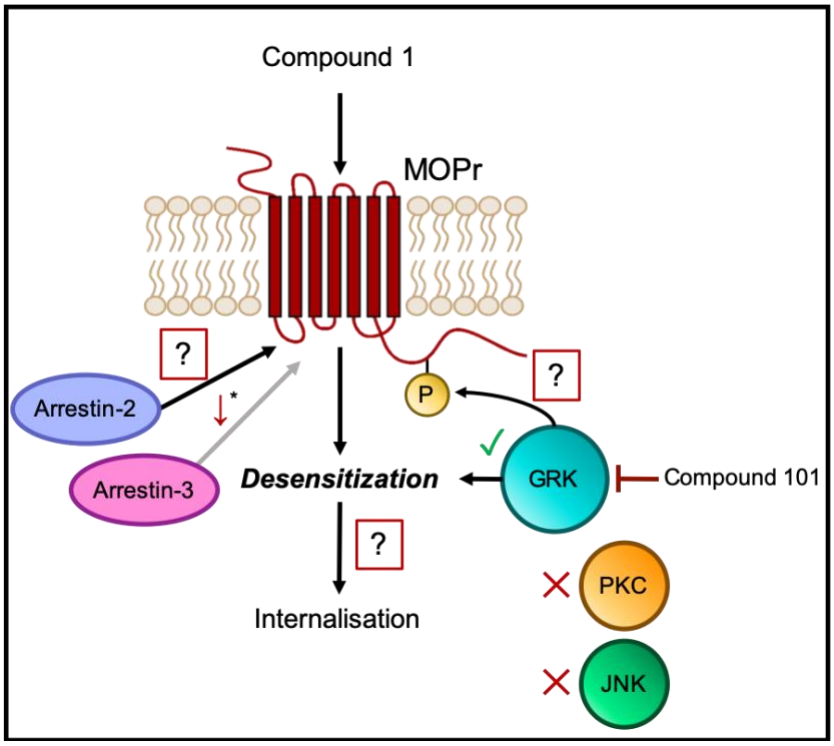


**Figure 5.16 – Summarising current findings around the mechanisms of Compound 1-induced MOPr regulation**

*A schematic summary of our current knowledge of the mechanism of Compound-1 induced MOPr regulation based on findings in this thesis so far. Compound 1 has been demonstrated to induce minimal arrestin-3 recruitment (denoted by '↓') in recombinant systems (denoted by '*' due to difference in system of investigation) (Figure 3.1B), however its ability to recruit arrestin-2 is unknown (denoted by '?'). It was demonstrated that Compound 1 induces substantial MOPr desensitization in rat LC neurones (Figure 4.5), which was dependent on GRK (Figure 5.6), but not PKC (Figure 5.2) or JNK (Figure 5.11). The ability of Compound 1 to induce GRK-dependent phosphorylation of C-terminal serine and threonine residues of MOPr is unknown. Additionally, while we have demonstrated that Compound 1 induces MOPr desensitization, the ability of Compound 1 to induce receptor internalization is unknown.*

### *5.2.7 Investigating the dependence of agonist-induced arrestin-3 recruitment on GRK2 expression in recombinant cells*

One possible explanation for the lack of translation between the low arrestin recruitment of Compound 1 observed in recombinant HEK 293 cells and the marked desensitization Compound 1 induced in LC neurones could be that there are different levels of GRK expression within each system. To examine this, we repeated our MOPr arrestin-3 recruitment BRET assay (Figure 3.1B and Figure 3.1D) in the presence of overexpressed GRK2, in an attempt to raise the endogenous GRK tone to levels which could be present in LC neurones.

Under these conditions, the overall level of signalling (BRET ratio) for opioid-induced arrestin-3 recruitment was substantially amplified to around 4-fold the levels observed in cells with endogenous expression levels (Figure 3.1D, reproduced in Figure 5.17A, & Figure 5.17C). The observed amplification of arrestin-3 recruitment in these conditions is in line with previous findings (Zhang et al., 1998).

While the overall level of agonist-induced arrestin-3 recruitment was amplified, there was no change in the rank order of intrinsic activity within our agonists for arrestin recruitment upon GRK2 overexpression (Figure 5.17). The rank order of intrinsic activity for arrestin-3 recruitment was conserved between the two assays as DAMGO > Morphine > PZM21 > Compound 1 (Figure 5.17D).

In addition to the amplification of overall signal, GRK2 overexpression also promoted a substantial (~10 fold) increase in the potency of agonist-induced arrestin-3 recruitment for all agonists observed (Figure 5.17B). The respective $pEC_{50}$ values were as follows: Arrestin 3, no GRK added: DAMGO, 6.0 $\pm$ 0.1; Morphine, 5.9 $\pm$ 0.2; PZM21, 6.5 $\pm$ 0.2; Compound 1 6.5 $\pm$ 0.4. Arrestin-3 + GRK2: DAMGO, 7.1 $\pm$ 0.1; Morphine, 6.8 $\pm$ 0.1; PZM21, 7.3 $\pm$ 0.2; Compound 1, 7.7$\pm$ 0.2.

The pattern of opioid-induced arrestin-3 recruitment was similar in cells additionally overexpressing a vector control (pcDNA3.1), in place of GRK2, compared with cells expressing only MOPr and arrestin-3 BRET reporters (Figure 5.17C & Figure 5.17A respectively). However, the lower R squared values for curves generated in the pcDNA3.1 cells compared with controls suggested that excessive expression of plasmid DNA had a detrimental effect on assay variability ($R^2$ values Control, Figure 5.17A: DAMGO = 0.86, morphine = 0.66, PZM21 = 0.48, Compound 1 = 0.34. $R^2$ values pcDNA3.1, Figure 5.17C: DAMGO = 0.79, morphine = 0.55, PZM21 = 0.24, Compound 1 = 0.23). As such, comparisons have been made between cells expressing MOPr and arrestin-3 BRET reporters, and cells additionally expressing GRK2.

The heightened signal-to-noise ratio observed for arrestin-3 recruitment in the presence of overexpressed GRK2 has led some groups to ulitise these conditions to characterise signalling bias at opioid receptors (Manglik et al., 2016; Dekan et al., 2019; Gillis et al., 2020a). As such, groups often compare agonist activity in G protein activation assays to arrestin recruitment assays in the presence of overexpressed GRK2. This act generally is deemed necessary to improve variable curve fitting for arrestin recruitment induced by weak partial agonists, however questions arise whether both systems utilised in these comparisons should be conducted in overexpressed GRK2.

We reconducted assessments of biased agonism previously used in this thesis, this time assessing biased agonism between arrestin-3 recruitment in the presence of overexpressed GRK2 (Figure 5.17B) and previous G protein activation data (Figure 3.1C) (Table 5.1). As suggested by the nature of $E_{max}$ values for arrestin-3 recruitment in different GRK2 conditions (Figure 5.17D), the normalised $\Delta$ $E_{max}$ values indicated Compound 1 displayed a similarly G protein-biased agonist compared to morphine for both arrestin-3 recruitment in an endogenous GRK environment and with the presence of overexpressed GRK2 (Table 5.1). The normalised $\Delta$ $E_{max}$ value for PZM21 in the presence of overexpressed GRK2 tended towards displaying G protein-biased agonism when compared to previous analysis in the regular arrestin-3 recruitment assay (Table 5.1). However, no significant difference was demonstrated between the normalised $\Delta$ $E_{max}$ value for PZM21 and that of morphine ($P$ = 0.12). Analysis of biased signalling through the $\Delta\Delta\log(\tau/K_A)$ method again suggested that neither Compound 1 or PZM21 display G protein biased signalling relative to morphine (Table 5.1). Interestingly, the $\Delta\Delta\log(\tau)$ method suggested that Compound 1 was significant bias for G protein activity when arrestin-3 activity was reassessed in overexpressed GRK2 (Table 5.1), in contrast to previous results (Figure 3.4B). This is likely due to the increased signal-to-noise ratio provided by the amplified arrestin-3 recruitment assay (Figure 5.17B).

Together these data suggest that the G protein-biased profile of Compound 1 is unaffected by system levels of GRK2 expression. As such, this finding weakens the potential for the biased profile of Compound 1 to vary between HEK 293 cells and rat LC neurones, which could explain the substantial MOPr desensitization observed in LC neurones, due to differential GRK2 expression levels. However, in the absence of further experiments we are unable to exclude the possibility that higher expression of other GRK subtypes in LC neurones could influence the signalling profile of Compound 1.

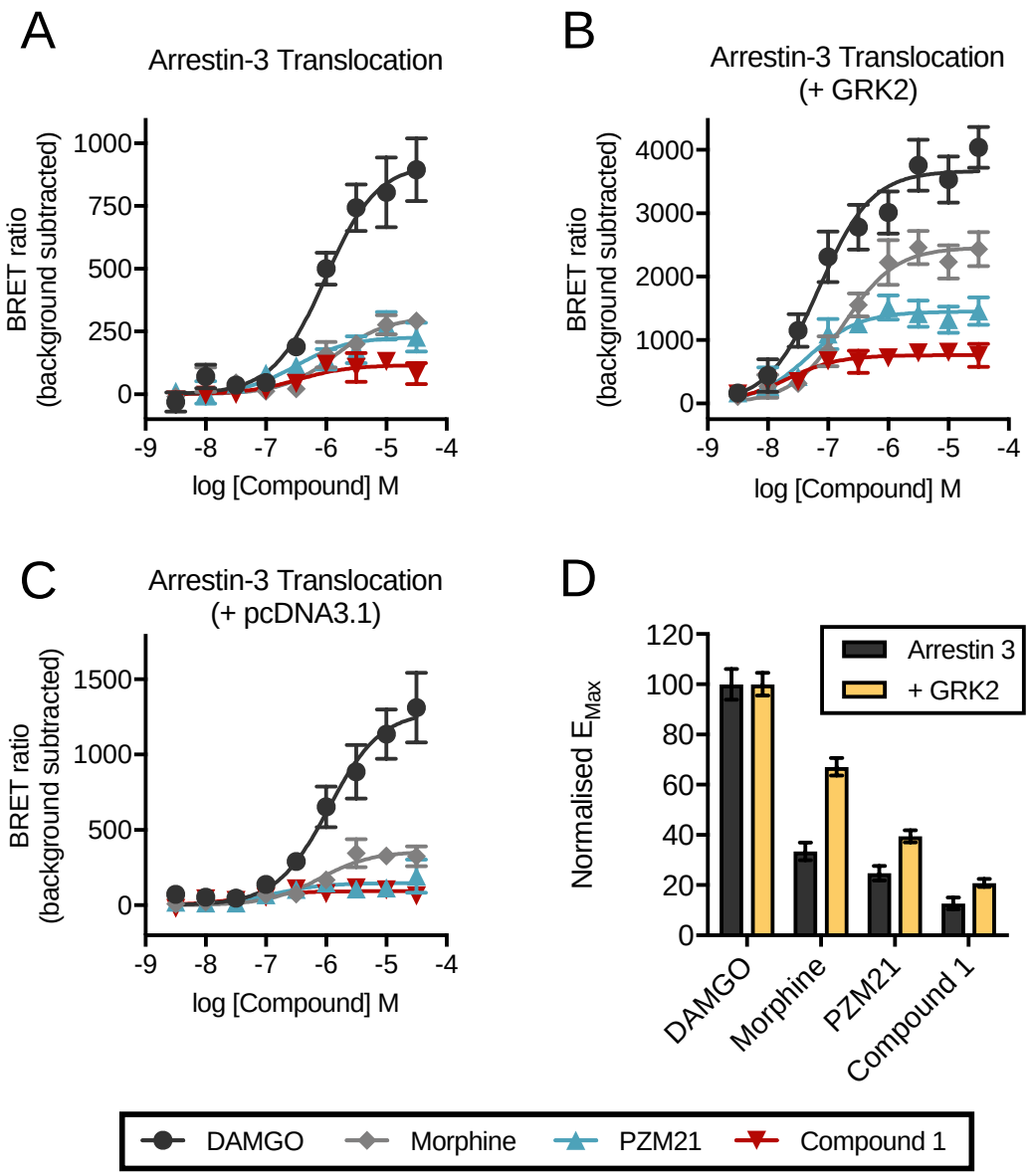


**Figure 5.17 – The impact of GRK2 expression on opioid-induced arrestin-3 recruitment in recombinant HEK 293 cells transiently expressing MOPr**

*Opioid-induced arrestin-3 recruitment in HEK 293 cells transiently expressing recombinant MOPrs in the absence (A, Figure 3.1D) or presence of GRK2 overexpression (B), or in the presence of additional pcDNA3.1 transfections (C). Arrestin-3 recruitment was assessed through BRET caused by agonist- and concentration-dependent association of arrestin-3-GFP$_{10}$ with MOPr-RlucII. (D) Fitted $E_{Max}$ values for concentration-responses for arrestin-3 recruitment to MOPr in HEK 293 cells in the absence (arrestin-3, A) or presence (+ GRK2, B) over overexpressed GRK2. Pooled $E_{Max}$ values were normalised to that of DAMGO. All data are presented as mean ± SEM, where n = 5.*

| | | Morphine | PZM21 | Compound 1 |
|---|---|---|---|---|
| Δ Normalised $E_{max}$ | *vs* Arrestin 3 | 0.00 ± 0.10 | 0.05 ± 0.06 | 0.53 ± 0.07 * |
| | + GRK2 | 0.00 ± 0.05 | 0.13 ± 0.04 | 0.60 ± 0.04 * |
| $10^{\Delta\Delta\log(\tau/KA)}$ | *vs* Arrestin 3 | 1.0 ± 1.6 | 0.8 ± 1.8 | 1.5 ± 2.4 |
| | + GRK2 | 1.0 ± 1.4 | 1.3 ± 1.7 | 0.5 ± 2.2 |
| $10^{\Delta\Delta\log(\tau)}$ | *vs* Arrestin 3 | 1.0 ± 1.3 | 0.4 ± 1.2 | 1.6 ± 1.3 |
| | + GRK2 | 1.0 ± 1.4 | 1.0 ± 1.2 | 6.7 ± 1.4 * |

**Table 5.1 – Revisiting quantification of biased agonism at MOPr in presence of overexpressed GRK2**

*Calculated biased signalling metrics for PZM21 and Compound 1 relative to morphine. Relative MOPr agonist activity in the $G_i$ G protein activation assay (Figure 3.1C) was compared to agonist activity in either the regular arrestin-3 recruitment assay (Figure 3.1D, Figure 5.17A) (vs Arrestin-3, white rows) or in the arrestin-3 recruitment assay in the presence of overexpressed GRK2 (Figure 5.17B) (+ GRK2, yellow rows). Values for the "vs Arrestin-3" rows are graphically represented in Figure 3.2B, Figure 3.3B and Figure 3.4B. Values are presented as mean ± SEM, where n=5. * $p < 0.05$, versus respective morphine value according to a one-way ANOVA with Tukey's post-hoc test.*

### *5.2.8 Investigating opioid-induced arrestin-2 recruitment in recombinant cells*

It is possible that in LC neurones Compound 1 induced-MOPr downregulation is mediated by arrestin-2, rather than arrestin-3, for which the coupling has been defined in HEK 293 cells (Figure 5.16). To explore this hypothesis, we examined arrestin-2 recruitment in HEK 293 cells using BRET techniques similar to those described previously (Figure 3.1B).

The levels of arrestin-2 recruitment to MOPr were considerably lower than that of arrestin-3 recruitment for all examined agonists (Figure 5.18A). The comparatively low coupling of arrestin-2 to MOPr demonstrated here is in line with previous findings at MOPr (Cheng et al., 1998; Thompson et al., 2015). This suggests that arrestin-2 has a lower coupling efficiency at MOPr than arrestin-3, however in this case we cannot exclude the potential that this effect is dependent on the relative efficiency of the interaction between specific arrestin BRET probes and the tagged MOPr (Thompson et al., 2015). While the full agonist DAMGO produced small but detectable levels of concentration-dependent arrestin-2 recruitment, no measurable responses could be obtained for the partial agonists morphine, PZM21 and Compound 1 (Figure 5.18B). This assay is subject to similar levels of noise as the arrestin-3 assay, for which the signal is substantially larger (Figure 5.18A), which results in the variability surrounding these small signals being particularly large (Figure 5.18B). Given these findings, it is therefore suggested that arrestin-2 recruitment is not responsible for Compound 1-induced desensitization in LC neurones.

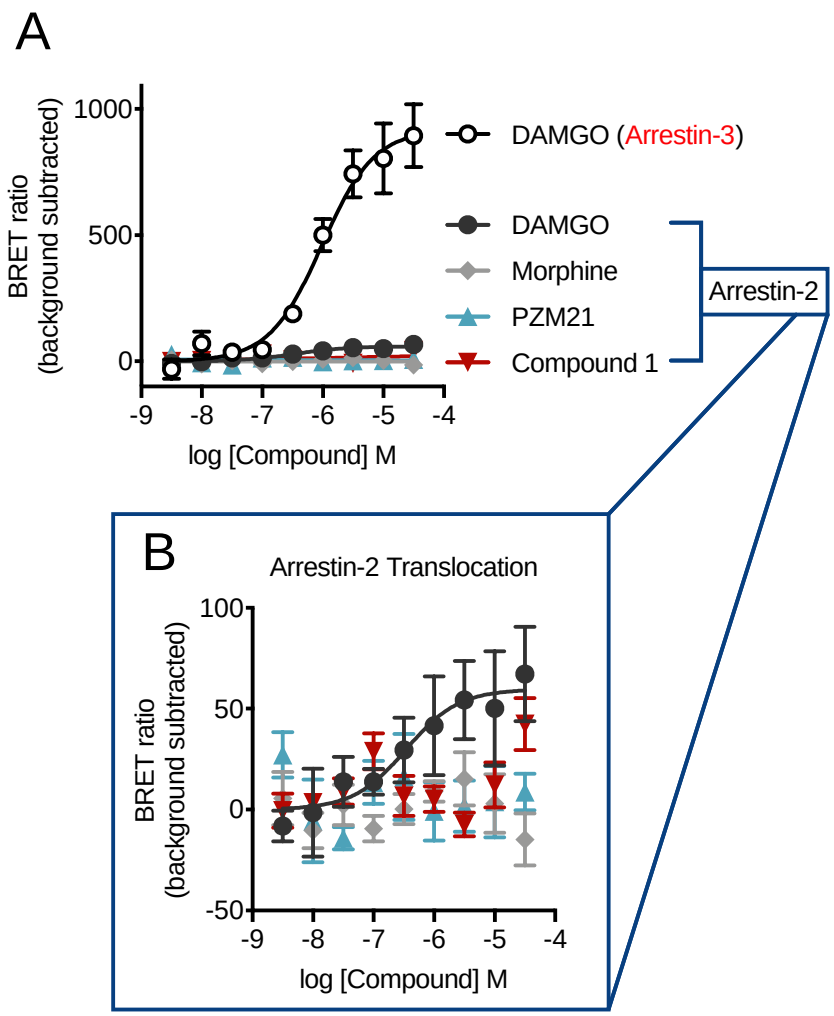


**Figure 5.18 – Assessing opioid-induced arrestin-2 recruitment in recombinant HEK 293 cells expressing MOPr**

*(A) Concentration-response curves for opioid-induced recruitment of arrestin 2-GFP$_{10}$ or arrestin 3-GFP$_{10}$ in HEK 293 cells expressing MOPr-RlucII as assessed by the BRET technique (Figure 3.1B). Presented arrestin-3 recruitment data is replotted from Figure 3.1D for comparison but was not run within the same experiment. (B) Data for opioid-induced arrestin-2 recruitment plotted alone on enlarged axis to accommodate for substantially smaller signal levels. Data are presented as mean ± SEM, where n = 5.*

### *5.2.9 Characterising opioid-induced MOPr internalization in recombinant cells*

While the low levels of arrestin recruitment induced by Compound 1 in HEK 293 cells (Figure 3.1D and Figure 5.18B) suggest that it would induce minimal internalization, the substantial MOPr desensitization produced by Compound 1 in rat LC neurones (Figure 4.5) could suggest differently. To further characterise MOPr regulation upon activation by Compound 1, we investigated agonist-induced MOPr internalization in HEK 293 cells expressing HA-MOPr using the ELISA technique (Chapter 2.1.4). The loss of surface MOPr induced by receptor saturating agonist concentrations was assessed after 15, 30 and 60 min of agonist incubation (Figure 5.19A). The area under the curve (AUC) values for agonist-induced loss of surface MOPr over time in the presence of different agonists were used for statistical analysis of agonist-induced effects (Figure 5.19B).

DAMGO (10μM) and, to a lesser degree, morphine (30μM) produced significant reductions in surface MOPr levels over the 60 min incubation, PZM21 (30μM) and Compound 1 (30μM) did not induce significant loss of surface MOPr expression (Figure 5.19). This indicates that Compound 1 does not induce MOPr internalization in HEK 293 cells, in line with its low efficacy for arrestin recruitment in these systems (Figure 3.1D and Figure 5.18B). Our findings are in line with previous reports demonstrating a strong positive correlation between the efficacy of an agonist for arrestin recruitment and its ability to induce receptor internalization (McPherson et al., 2010).

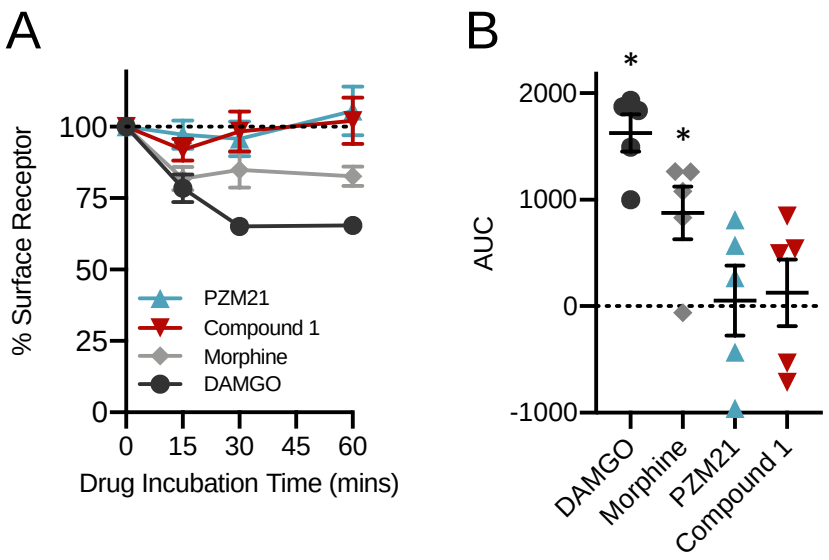


**Figure 5.19 – Characterising opioid-induced loss of surface MOPr in recombinant HEK 293 cells through ELISA.**

*(A) Surface expression of rat HA-MOPrs transiently expressed in HEK 293 cells was determined through ELISA using an anti-HA antibody, after preincubation with DAMGO (10$\mu$M), morphine, PZM21 or Compound 1 (30$\mu$M) at the described time points of drug incubation. Surface expression was normalised to signal levels in blank HEK 293 cells (0%) and expression levels observed in untreated HA-MOPr HEK 293 cells (100%). (B) The area under the curve (AUC) values for agonist-induced loss of surface HA-MOPr over time, as presented in A. Data are presented as mean ± SEM, where n = 5. * P < 0.05, values were significantly different from 0 in one-sample t test.*

### *5.2.10 Defining the patterns of agonist-induced MOPr phosphorylation*

Findings within the above experiments have reiterated the low coupling of Compound 1-activated MOPr to arrestin pathways, relative to the balanced agonist morphine. However, Compound 1 induced substantial MOPr desensitization in LC neurones (Figure 4.5), through an apparently GRK dependent mechanism (Figure 5.6). As such, we wished to explore the possibility of a GRK-dependent, but potentially arrestin-independent mechanism of MOPr desensitization induced by Compound 1.

The primary functional readout for GRK function at MOPr is the rapid agonist-induced phosphorylation of serine (Ser) and threonine (Thr) residues, primarily on the C-terminus of the receptor (Chapter 1.2.5). $Ser^{375}$ is typically considered the primary target of GRK-dependent, agonist-induced MOPr phosphorylation, with a number of additional C-terminal serine and threonine residues also implicated (including $Thr^{370}$, $Thr^{376}$ and $Thr^{379}$) (Doll et al., 2011; Mann et al., 2015; Miess et al., 2018). In order to gauge Compound 1-induced GRK activity, we studied the ability of Compound 1 to induce multisite C-terminal tail phosphorylation of MOPr compared to our reference agonists, through immunoblotting using phosphosite-specific antibodies. This work was kindly performed and analysed by Nina Kathleen Blum (University of Jena, Germany), who was supervised by Andrea Kliewer and Stefan Schulz (University of Jena, Germany).

The full agonist DAMGO (10μM) induced substantial phosphorylation at multiple C-terminal serine and threonine sites on MOPr (Figure 5.20A). The partial agonist morphine (30μM) induced significant phosphorylation at $Ser^{375}$, with lower but still evident phosphorylation at other investigated residues (Figure 5.20A). This observed pattern of phosphorylation with DAMGO and morphine is typical of previous observations (Doll et al., 2011; Just et al., 2013; Miess et al., 2018; Gillis et al., 2020a). A low efficacy agonist, PZM21 (30μM) induced minimal phosphorylation at the examined sites, with a low but noticeable levels of $Ser^{375}$ phosphorylation (Figure 5.20A), similar to previous findings (Gillis et al., 2020a). Similarly, Compound 1 (1nM - 30μM) induced minimal phosphorylation, with low levels of phosphorylation restricted to $Ser^{375}$ solely at the highest examined concentrations (Figure 5.20A and Figure 5.20C). At receptor saturating concentrations, DAMGO and morphine produce significant $Ser^{375}$ phosphorylation compared to controls, whereas the low levels of $Ser^{375}$ phosphorylation induced by PZM21 and Compound 1 were not significantly different from controls (Figure 5.20C).

Together, the pattern of Compound 1-induced MOPr phosphorylation is consistent with it being a G protein-biased agonist, showing minimal phosphorylation at key residues

implicated in GRK/arrestin mediated MOPr desensitization and trafficking. Based on findings from this experiment it is not evident that Compound 1 couples to GRKs in recombinant systems, however it is interesting to hypothesise that the GRK-dependent mechanism of Compound 1 evident in LC neurones could be mediated by factors other than phosphorylation of C-terminal serine and threonine residues (Chapter 6.5.2).

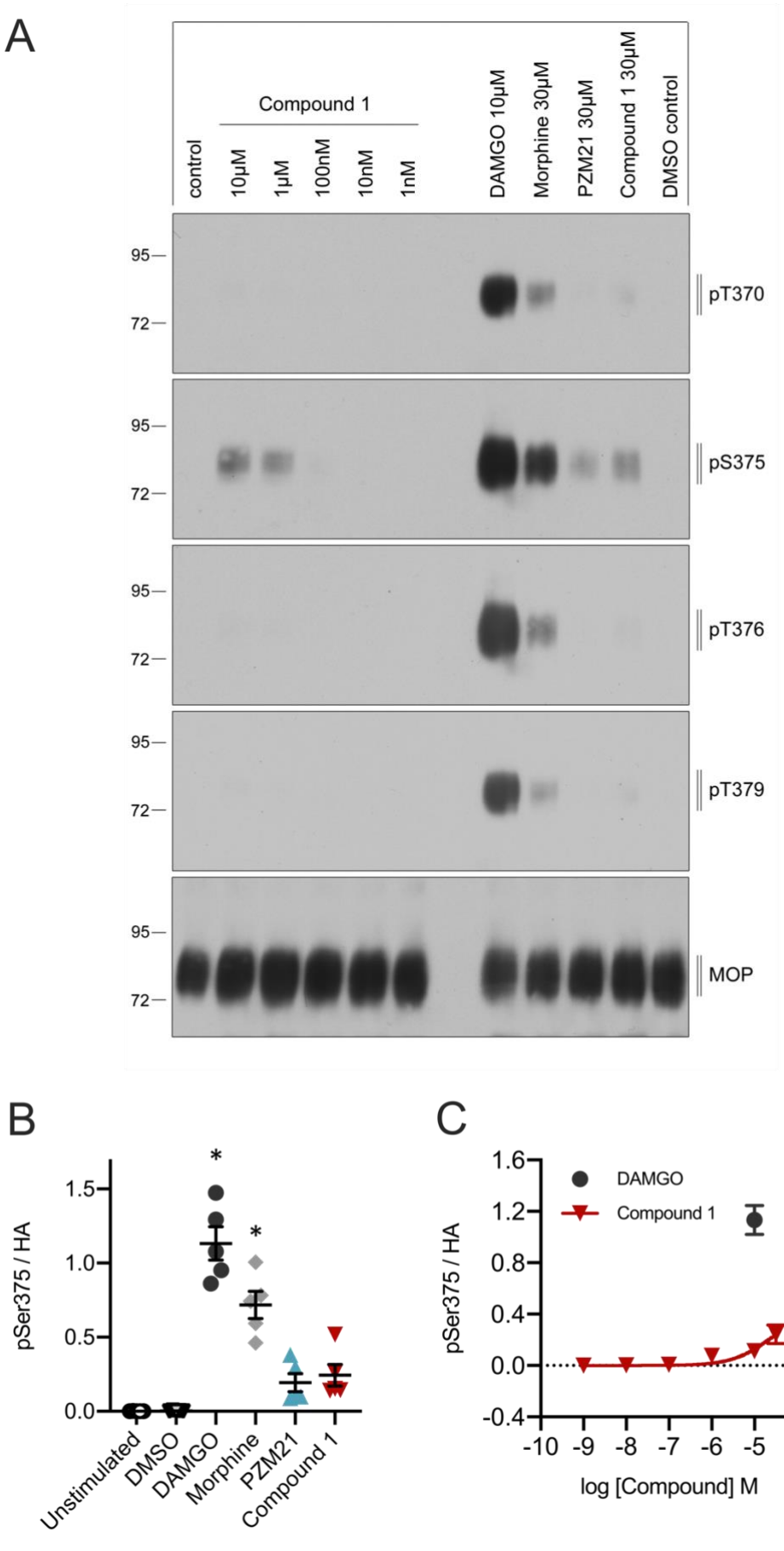
A
control
Compound 1
10μM
1μM
100nM
10nM
1nM
DAMGO 10μM
Morphine 30μM
PZM21 30μM
Compound 1 30μM
DMSO control
95
72
pT370
pS375
pT376
pT379
MOP
B
pSer375 / HA
1.5
1.0
0.5
0.0
Unstimulated
DMSO
DAMGO
Morphine
PZM21
Compound 1
C
pSer375 / HA
1.6
1.2
0.8
0.4
0.0
-0.4
DAMGO
Compound 1
-10 -9 -8 -7 -6 -5 -4
log [Compound] M

**Figure 5.20 – Determining the patterns of opioid-induced MOPr phosphorylation in recombinant HEK 293 cells through phosphospecific immunoblotting.**

*(A) HEK 293 cells stably expressing mouse HA-MOPr were preincubated with increasing concentrations of Compound 1 (1nM - 30$\mu$M) or supramaximal concentrations of DAMGO (10$\mu$M), morphine (30$\mu$M) or PZM21 (30$\mu$M) for 30 mins. Cells were lyzed and immunoblotted with phosphospecific antibodies labelling MOPr specifically phosphorylated at Thr$^{370}$ (pT370), Ser$^{375}$ (pS375), Thr$^{376}$ (pT376) or Thr$^{379}$ (pT379). To confirm equal loading of HA-MOPr, blots were subsequently stripped and immunoblotted with an anti-HA antibody (MOP). The blot presented here is representative of five individual experiments. The positions of molecular mass markers are indicated on the left in kDa. Pooled data from experiments as depicted in A is quantified in B and C. (B) Quantifying MOPr Ser$^{375}$ phosphorylation induced by supramaximal concentrations of opioids, expressed as a factor of total receptor loaded. * P < 0.05, significantly different from vehicle control values (DMSO), one-way ANOVA with post-hoc Dunnett's test. (C) Compound 1 (1nM - 30$\mu$M) induces minimal MOPr Ser$^{375}$ phosphorylation. DAMGO (10$\mu$M)-induced MOPr Ser$^{375}$ phosphorylation is also plotted for comparison of signal levels. For B & C, Data are expressed as mean $\pm$SEM where n = 5. This work was kindly performed and analysed by Nina Kathleen Blum (University of Jena, Germany), who was supervised by Andrea Kliewer and Stefan Schulz (University of Jena, Germany).*

## 5.3 Discussion

### *5.3.1 A summary of findings regarding the mechanisms of Compound 1-induced MOPr regulation in rat LC neurones and recombinant cells*

In this chapter, we aimed to characterise the regulatory mechanisms involved in the substantial MOPr desensitization induced by Compound 1 in rat LC neurones, outlined in Chapter 4. In light of previous work characterising Compound 1 as a G protein-biased agonist, we had hypothesised that Compound 1 would not couple strongly to GRK pathways in rat LC neurones. As such, it was postulated that observed Compound 1-induced MOPr desensitization could be regulated by other mechanisms; such as PKC, especially considering previously demonstrated links to PKC involvement in desensitization induced by lower efficacy MOPr agonists. Surprisingly, in this chapter I demonstrated that the substantial MOPr desensitization induced by Compound 1 in rat LC neurones is apparently mediated by GRK, not by PKC (Figure 5.21A).

Following these intriguing findings, we sought to address a number of unresolved questions around the involvement of GRK and arrestin pathways in Compound 1-induced MOPr desensitization using recombinant systems (Figure 5.16). These experiments yielded data for Compound 1 in line with its previously described G protein-biased profile; with it inducing significantly less arrestin-2 recruitment, MOPr internalization and $Ser^{375}$ phosphorylation than morphine (Figure 5.21B).

To summarise, in this chapter we characterised a GRK-dependent, potentially arrestin-independent mechanism for Compound 1-induced MOPr desensitization in LC neurones. However, a number of questions remain around the possible disconnect between our findings for Compound 1-induced MOPr desensitization in LC neurones and in recombinant systems (Figure 5.21).

The implications of findings from this chapter and previous will be more widely discussed as part of the final discussion of this thesis, alongside potential future experiments which could address outstanding questions (Chapter 6). In the following chapter-specific discussion, I will seek to address the more experimental-specific matters which have arisen in this chapter.

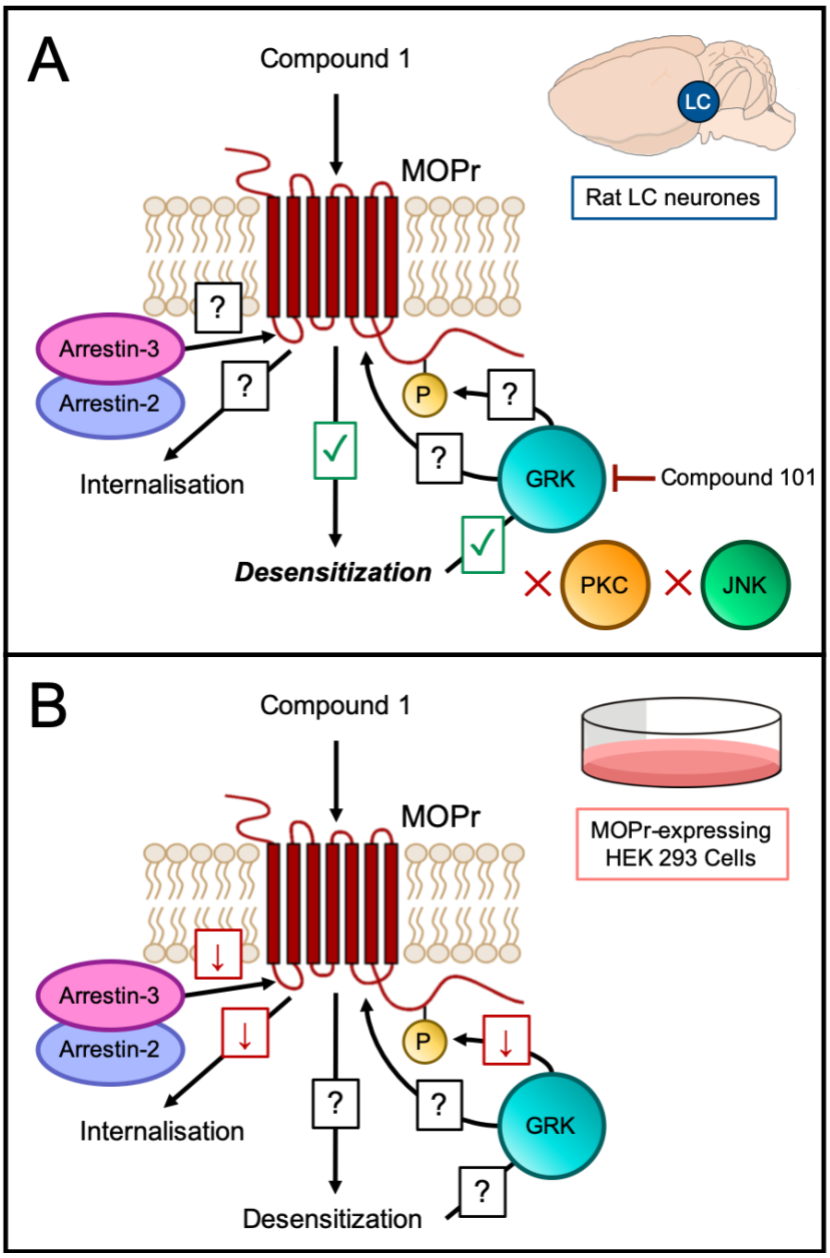


**Figure 5.21 – A schematic summary of our findings on the mechanisms of Compound 1-induced MOPr regulation in rat LC neurones and in recombinant HEK 293 cells**

*(A) A schematic summary of our current knowledge of the mechanism of Compound-1 induced MOPr regulation in rat LC neurones. Compound 1 induces substantial MOPr desensitization in rat LC neurones (Figure 4.5), which was dependent on GRK (Figure 5.6), but not PKC (Figure 5.2) or JNK (Figure 5.11). The coupling of arrestin-2 and arrestin-3 to Compound 1 activated-MOPr is unknown in rat LC neurones. Similarly, the ability of Compound 1 to induced MOPr internalization in rat LC neurones is unknown. While GRK was demonstrated to regulate Compound 1-induced MOPr desensitization in rat LC neurones (Figure 5.6), it is unknown whether Compound 1 induces typical GRK-dependent phosphorylation of serine and threonine residues in this system, or if*

*Compound 1 induces GRK recruitment to the receptor to regulate function in an alternate mechanism. (B) A schematic summary of our findings surrounding Compound-1 induced MOPr regulation in recombinant systems. We have demonstrated that Compound 1 induces relatively low levels of arrestin-2-GFP$_{10}$ and arrestin-3-GFP$_{10}$ recruitment to human MOPr-RlucII constructs in recombinant HEK 293 cells (Figure 5.18 and Figure 3.1B). Compound 1 induces relatively minimal internalization of rat HA-MOPr in recombinant HEK 293 cells (Figure 5.19). Additionally, we have shown that Compound 1 induces relatively minimal phosphorylation of C-terminal serine and threonine residues on mouse HA-MOPrs in HEK 293 cells (Figure 5.20). It is unknown whether GRK is alternatively activated by Compound 1 in recombinant systems to potentially phosphorylate non-C-terminal serine and threonine residues or whether it is recruited to receptor. Additionally, we have not determined whether Compound 1 induces MOPr desensitization in recombinant systems to comparable levels to that observed in rat LC neurones (Figure 4.5). '?' denotes the role of the outlined pathway is unknown. '↓' denotes that the coupling of Compound 1 to this pathway was relatively lower than that observed for morphine. Ticks and crosses denote that the coupling of Compound 1 to such pathways was confirmed or denied respectively.*

### *5.3.2 On positive controls for the study of the potential roles of JNK*

The power of our work characterising the role of JNK in opioid-induced MOPr desensitization in LC neurones is to an extent limited by lack of positive controls for the JNK inhibitor SP600125 (Figure 5.10 and Figure 5.11). In light of recent studies, published after these experiments were conducted, it is clear that JNK does not play a role in acute rapid MOPr desensitization in LC neurones (Leff et al., 2020). Therefore, no positive control of SP600125 activity could be performed in the paradigm of acute desensitization as we have assessed in this chapter. SP600125 activity could likely be confirmed through experiments examining cellular tolerance over chronic opioid exposure (Leff et al., 2020). While we are not able to provide a positive control for SP600125 activity in our experiments, our findings showing no effect of SP600125 on acute MOPr desensitization induced by DAMGO and Compound 1 are in line with those reported for acute MOPr desensitization induced by Met-Enkephalin (Leff et al., 2020).

### *5.3.3 The potential role of off-target kinases inhibited by Compound 101 in Compound 1-induced desensitization*

In this chapter, we attempted to address the possibility that off-target kinases inhibited by Compound 101 could mediate Compound 1-induced MOPr desensitization. This was investigated through inhibition of select off-target kinases targeted by Compound 101 using GSK650394 and Y-27632 (Figure 5.7). These well-characterised kinase inhibitors have been demonstrated to collectively inhibit PPK2, SGK1 and ROCK2, 3 non-GRK family kinases which were demonstrated to be inhibited by Compound 101 in a previous kinase screen (Lowe et al., 2015). The selection of these inhibitors and the concentrations at which they were used was guided by a previous experiment examining the potential role of these 'off-target' kinases in DAMGO-induced MOPr desensitization in rat LC neurones (Lowe et al., 2015). The power of this initial study, and therefore this study, is limited by the absence of a positive control for the activity of GSK650394 and Y-27632 in rat LC neurones at the examined concentrations. While the selection of these inhibitors and their concentrations was guided by previous effective concentrations of these inhibitors *in vitro*, we are unable to confirm their specific inhibitory activity in our experiments.

Data from the kinase screen itself also brings the design of this experiment into question, with the activity of other kinases to some extent being inhibited by Compound 101, but which are not inhibited by GSK650394 and Y-27632 (Lowe et al., 2015). Most notable of these kinases is mitogen- and stress-activated kinase 1 (MSK1). Additionally, with the relatively low concentration for which Compound 101 was screened (1μM) it is possible

that more kinases may be inhibited to a greater degree at the concentration examined in this and other studies (30μM). However, the presence of an intact cell membrane in our studies may provide a barrier to Compound 101 activity, where in the aforementioned kinase screen, which was not run in intact cells, activity would not be limited in such a way. It could be possible to add additional inhibitors to the cocktail used to examine the role of off-target kinases inhibited by Compound 101 in MOPr desensitization, such as the MSK1 inhibitor SB-747651A (Naqvi et al., 2012). However, the effect of increasing DMSO concentrations in the perfusing aCSF as well as wide-scale kinase inhibition, on the longevity and health of LC neurones provides a limiting factor to further addition of inhibitors.

A more practical means of confirming that the perceived effects of Compound 101 are not due to activity at non-GRK kinases could be through the study of structurally distinct GRK inhibitors. The availability of effective and selective GRK inhibitors has previously been limited. However, in recent years a number of selective GRK inhibitors have been described, with CCG224063 (Waldschmidt et al., 2016), 14as (Waldschmidt et al., 2017) and other indazole-paroxetine analogues (Bouley et al., 2017) all being based on a different chemical scaffold to Compound 101. It could be hypothesised that with different chemical scaffolds, these agents may differ from Compound 101 in their ability to interact with non-GRK targets. By demonstrating that 14as also inhibited DAMGO- and Compound 1-induced MOPr desensitization in rat LC neurones (Figure 5.8 and Figure 5.9), we believe we have strengthened our contention that the effects of Compound 101 are indeed dependent on inhibition of GRK. Unfortunately, our data for 14as is only preliminary (n = 1), with low availability of compound limiting the number of potential repeats.

### *5.3.4 On the partial inhibition of MOPr desensitization by GRK inhibitors in LC neurones*

Compound 101 was able to partially inhibit MOPr desensitization induced by both Compound 1 and DAMGO in rat LC neurones (Figure 5.5C and Figure 5.6C). Additionally, the structurally distinct GRK inhibitor 14as similarly produced partial inhibition of the effect of DAMGO and Compound 1 in preliminary experiments (Figure 5.8C and Figure 5.9C). The residual MOPr desensitization observed in the presence of Compound 101 is in line with previous observations in rat LC neurones (Lowe et al., 2015; Leff et al., 2020). The effects of Compound 101 were not limited by concentration, with no additional inhibition of DAMGO-induced MOPr desensitization being observed in rat LC neurones when the Compound 101 concentration was increased to 100μM (Lowe et al., 2015).

One possible reasoning behind this residual desensitization is that Compound 101 is only able to achieve partial inhibition of GRK action, given the amplification and strength of the response. Some data in HEK293 cells is in support of this hypothesis, with Compound 101 only partially inhibiting Ser375 phosphorylation (Gondin et al., 2019; Gillis et al., 2020a), arrestin-3 recruitment (Lowe et al., 2015; Miess et al., 2018), MOPr internalization (Lowe et al., 2015) and GRK2 recruitment to MOPr (Miess et al., 2018; Gondin et al., 2019) induced by DAMGO. However, the persistence of residual acute agonist-induced MOPr desensitization in both rat LC neurones overexpressing a GRK2 dominant negative mutant (Bailey et al., 2009b) and those expressing a mutant MOPr deficient in GRK-dependent phosphorylation sites (Leff et al., 2020) suggests that an additional mechanism, not incomplete inhibition of GRK, may drive this residual desensitization. In previous studies, residual acute MOPr desensitization in rat LC neurones treated with Compound 101 was unaffected by supplementary inhibition of PKC, JNK or ERK1/2 (Lowe et al., 2015). This suggests that while a secondary kinase-dependent mechanism is possible, kinases previously implicated in MOPr desensitization do not play a role.

Sequestration of G$\beta\gamma$ subunits by a non-catalytic component (PH-domain) of GRKs could also be responsible for the residual component of MOPr desensitization (Raveh et al., 2010). It is possible that this mechanism would not be attenuated by inhibition of GRK through pharmacological (Lowe et al., 2015) or genetic (Bailey et al., 2009b) approaches which target the active site of GRKs (Mundell et al., 1997; Thal et al., 2011). However, this mechanism has previously been shown to play little role in opioid receptor regulation in rat LC neurones (Llorente et al., 2012).

# Chapter 6: Discussion

## 6.1 Research Summary and Introduction to Discussion

The development of G protein-biased agonists at MOPr had been heralded by some as a holy grail, that is an opioid analgesic without associated adverse effects and in particular respiratory depression. A further advantage of G protein-biased agonists at MOPr might be that through low coupling to arrestin/GRK pathways, G protein-biased agonists may induce less receptor desensitization than balanced agonists, and therefore be less susceptible to the development of tolerance to their effects. If this hypothesis were true, then G protein-biased agonists at MOPr would be clinically beneficial, evading the common issue of tolerance development in the use of opioids for the treatment of chronic pain states. The research presented within this thesis broadly aimed to characterise the receptor desensitization and regulation induced by G protein-biased agonists at MOPr in order to further define their long-term functional effects and therapeutic potential.

We first sought to characterise the signalling properties of potentially biased agonists at MOPr using BRET assays in heterologous systems (Chapter 3). Through these experiments, we have identified the cyclic endomorphin analogue Compound 1 (Try-c[D-Lys-Phe-Try-Gly]) as a novel G protein-biased MOPr agonist, which possesses a greater degree of biased signalling than the previously described biased agonists at MOPr. The characterisation of Compound 1 as a G protein-biased MOPr agonist provides the field with a novel tool compound to further investigate the consequences of biased signalling at MOPr, as well as representing a potentially promising therapeutic lead.

Subsequently, having defined Compound 1 as a G protein-biased agonist at MOPr, we aimed to characterise its ability to induce rapid MOPr desensitization in rat LC neurones using electrophysiological techniques (Chapter 4). It had been hypothesised that G protein-biased agonists, such as Compound 1, would induce less receptor desensitization than balanced agonists given their relatively low coupling to arrestin and GRK pathways, which are well recognised pathways of receptor regulation. However, Compound 1 induced rapid receptor desensitization to a greater degree than morphine, opposing our initial hypothesis. This finding suggests that the low arrestin-coupling of G protein-biased agonists at GPCRs may not implicitly result in a lower propensity to undergo receptor desensitization and may have implications for their ability to induce tolerance *in vivo*, and as such, their overall clinical utility.

In an attempt to translate and progress our findings of Compound 1-induced MOPr desensitization in brain slice electrophysiology, we aimed to define the ability of Compound 1 to induce antinociceptive tolerance *in vivo* in a warm-water tail withdrawal test of nociception in mice (Chapter 4). In these tests of nociception, Compound 1 induced MOPr-dependent antinociception, however this effect was of a substantially lower magnitude than that of morphine. The reason for the low *in vivo* efficacy of Compound 1 was unclear but could feasibly be due to pharmacokinetic limitations given the unfavourable physicochemical properties of Compound 1 as a large cyclic peptide.

Aside from the potential tolerance induced by Compound 1 *in vivo*, the mechanism through which Compound 1 induced rapid receptor desensitization was of particular interest. Agonist-selective, non-GRK mediated, mechanisms of MOPr desensitization are well described, with PKC in particular demonstrated to regulate MOPr desensitization in the case of some agonists. We aimed to investigate the potential roles of GRK and PKC in Compound 1-induced MOPr desensitization in LC neurones using pharmacological tools that target these kinases (Chapter 5). In fact, this work clearly demonstrated that Compound 1-induced desensitization was GRK-dependent but PKC-independent. This was particularly surprising given the low arrestin coupling in recombinant cell systems. When considering findings in both of these systems, our findings highlight a potentially novel GRK-dependent, arrestin-independent mechanism of agonist-induced receptor desensitization at MOPr, providing new insight on the potential long-term functional effects of biased signalling at MOPr.

Following our work in LC neurones, we sought to refine our understanding of the GRK-dependent, potentially arrestin-independent nature of Compound 1-induced MOPr regulation through further experiments in recombinant cell systems. As such, we studied the ability of Compound 1 to induce arrestin-2 recruitment (as opposed to arrestin-3 which we have already studied), MOPr internalization and MOPr phosphorylation (Chapter 5). Data from these assays was in line with Compound 1 being a G protein-biased agonist, inducing no arrestin-2 recruitment, no MOPr internalization and minimal MOPr phosphorylation. These data confirm the G protein-biased profile of Compound 1 in recombinant systems and suggests a potentially non-canonical mechanism of GRK-dependent MOPr desensitization in the case of this novel drug.

The following general discussion chapter builds on the preceding chapter-specific discussions in this thesis (Chapters 3.3, 4.3 & 5.3). The purpose of these previous chapter-specific discussions was to elaborate on isolated, data-specific issues arising within in a single chapter. Whereas, the purpose of this discussion is to more generally contextualise and examine the impact of findings of this thesis as a whole. Throughout

this chapter, I will be outlining research questions resulting from such discussion and suggesting potential future experiments to address such research questions as and when they arise. In sections 6.8 and 6.9, I will conclude by taking a broader look at the field of biased agonism, both considering the clinical utility of current and future biased agonists at MOPr (Chapter 6.8) and briefly re-examining the overall potential of biased signalling as a tool for future drug development at GPCRs (Chapter 6.9).

## 6.2 PKC is not involved in Compound 1-induced desensitization in LC neurones

Given the well-demonstrated role of PKC in the regulation of MOPr desensitization induced by low efficacy agonists in LC neurones (Bailey et al., 2004; Bailey et al., 2009b) (Chapter 1.2.5 and Chapter 5.2.2), we had hypothesised that MOPr desensitization induced by Compound 1, a low efficacy agonist, would be regulated by PKC. However, in Chapter 5, it was demonstrated that the magnitude of Compound 1-induced MOPr desensitization in rat LC neurones was unaffected by pharmacological inhibition (Figure 5.2) or activation (Figure 5.3) of PKC but was instead dependent on GRK (Figure 5.6).

This finding in the case of Compound 1 refutes the well-accepted hypothesis that, for all MOPr agonists, the relative contribution of GRK and PKC to agonist-induced MOPr desensitization is dependent on the intrinsic efficacy of the agonist examined (Johnson et al., 2006; Kelly et al., 2008). As such, low efficacy agonists such as morphine couple more weakly to GRK and desensitize primarily through PKC, whereas high efficacy agonists such as DAMGO desensitize through GRK with little or no PKC component (Figure 6.1). This hypothesis is well characterised in the case of the aforementioned agonists in both LC neurones and in recombinant systems (Johnson et al., 2006; Bailey et al., 2009b). Despite this, the direct mechanisms underlying agonist-induced regulation of MOPr by PKC are poorly understood (Chapter 1.2.5). The PKC hypothesis is additionally supported by thorough subsequent work demonstrating that the coupling of GRK-mediated regulatory pathways ($Ser^{375}$ phosphorylation, internalization, arrestin recruitment, GRK2 recruitment) is closely correlated with agonist intrinsic efficacy, with all investigated low-efficacy agonists coupling weakly to these GRK-dependent pathways (McPherson et al., 2010; Gillis et al., 2020a). It is therefore speculated that in the relative absence of GRK coupling, PKC instead modulates MOPr regulation.

Our finding that the mechanism of Compound 1-induced MOPr does not involve PKC could suggest that the involvement of PKC is a phenomenon specific to morphine rather than all low efficacy agonists. The involvement of PKC in MOPr-induced desensitization by other low efficacy agonists is indeed understudied. However, the finding that the development of tolerance to the effects of oxycodone, which has similar G protein efficacy to morphine (McPherson et al., 2010), is PKC dependent suggests that MOPr desensitization induced by this ligand could be regulated in a similar manner to morphine (Hill et al., 2018a). Additionally, PKC has been demonstrated to partially regulate MOPr desensitization induced by Met-Enkephalin in rat LC neurones (Bailey et al., 2004). As an agonist of intermediate intrinsic efficacy compared to DAMGO and morphine, findings for Met-Enkephalin are in support of the ‘wedge’ model (Figure 6.1) representation of

PKC / GRK involvement in MOPr desensitization dependent on agonist efficacy (Kelly et al., 2008).

In light of our findings for Compound 1, it is the author's belief that further work is required to determine the validity of the previous hypothesis of the efficacy-dependent role of PKC in agonist-selective MOPr desensitization, for low efficacy agonists aside from morphine. One serendipitous outcome from the drive to develop potentially G protein-biased agonists at MOPr is that there is now a plethora of well-characterised, selective and potent partial agonists with lower intrinsic efficacy than morphine available for such study. These include, but are not limited to, TRV130, PZM21 and SR17018. These have advantages over previous tool low efficacy MOPr agonists buprenorphine and pethidine (meperidine), which could have other functional effects due to their promiscuous pharmacology (Latta et al., 2002; Falcon et al., 2016). We suggest that investigating the potential role of PKC in MOPr desensitization induced by PZM21 and TRV130 in rat LC neurones through pharmacological methods presented in this thesis (addition of PMA) would help determine whether morphine or Compound 1 is the outlier in the relationship of PKC to MOPr desensitization.

Alternatively, while Compound 1 has equivalent G protein efficacy to morphine, it is also G protein-biased. Therefore, it is possible that it may stabilise a distinct activated conformation of the MOPr compared to morphine (Schneider et al., 2016; Dekan et al., 2019). As such, this active state may have a lower coupling efficiency for PKC-mediated desensitization. Additionally, it could be speculated that in the absence of relatively ineffective regulation by PKC, even the low level of GRK activation induced by Compound 1 may be sufficient for the high level of MOPr desensitization it induces (Figure 4.5). Future work could study this hypothesis by examining the potential role of PKC in MOPr desensitization induced by bilorphin (Chapter 1.3.2) in LC neurones (Dekan et al., 2019), through pharmacological methods described in this thesis. Bilorphin has a similar pharmacological profile to Compound 1, being a G protein-biased MOPr agonist with equivalent efficacy for G protein signalling compared to morphine (Chapter 3.3.2) (Dekan et al., 2019). If bilorphin-induced MOPr desensitization is found to not be regulated by PKC, but that induced by TRV130 and PZM21 is found to be regulated by PKC, we could attribute the lack of PKC regulation in Compound 1-induced MOPr to its biased profile.

Together, the finding that Compound 1-induced desensitization is PKC-independent is in contention with our previous understanding of the PKC-dependence of MOPr regulation induced by lower efficacy agonists. Future work could investigate the role of PKC in desensitization induced by novel lower efficacy MOPr agonists (TRV130 and PZM21) to examine the validity of previous hypothesises beyond the case of morphine.

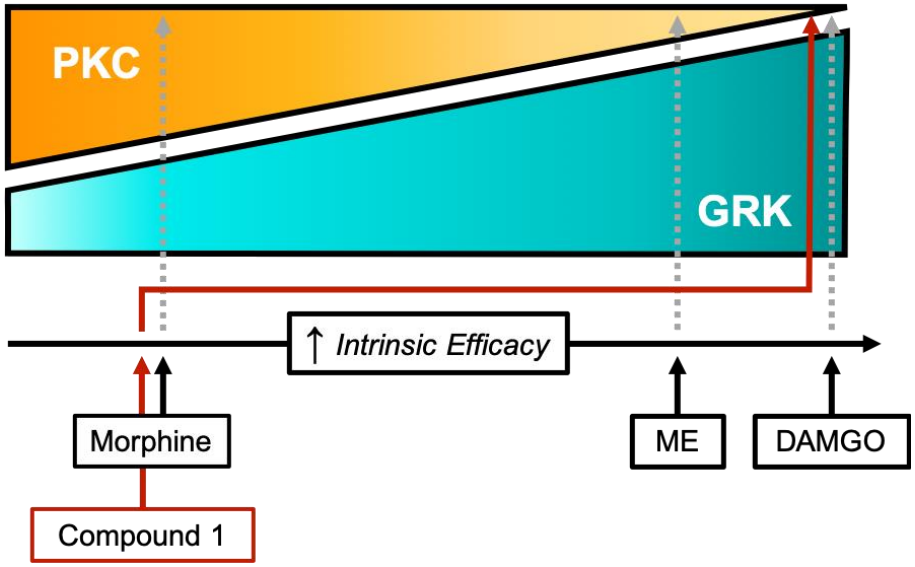


**Figure 6.1 – A schematic depicting the relative contribution of PKC and GRK to MOPr desensitization, dependent on agonist efficacy**

*An illustration of the current hypothesis around agonist-selective mechanisms of MOPr desensitization. MOPr desensitization induced by the partial agonist morphine is primarily mediated by PKC, with a smaller contribution by GRK. MOPr desensitization induced by the full agonist DAMGO is regulated solely by GRK with no contribution from PKC. Met-Enkephalin, an agonist of slightly lower efficacy than DAMGO, induces MOPr desensitization primarily through GRK, however PKC also has been demonstrated to play a partial role. Together this suggests the relative contribution of PKC to agonist-induced MOPr desensitization is dependent on agonist efficacy. However, in contrary to this hypothesis, in this thesis I have demonstrated that Compound 1, a partial agonist with equivalent G protein efficacy to morphine, induces MOPr desensitization through a GRK-dependent, PKC-independent mechanism. The presentation of this diagram was adapted from Kelly et al. (2008), with additional Compound 1 data from this thesis.*

## 6.3 Thoughts on our approach to characterise the mechanisms involved in Compound 1-induced desensitization in LC neurones

In Chapter 5, we used pharmacological means of kinase inhibition to characterise the mechanisms underlying Compound 1-induced MOPr desensitization in rat LC neurones. While in this case this approach has proved relatively fruitful, more widely its utility is restricted by its low throughput, as well as practical drawbacks associated with the use of brain slices. Below I will summarise and discuss some alternative methods or approaches we could have adopted to assess MOPr desensitization, highlighting their potential advantages and their shortcomings in our situation.

### *6.3.1 Non-selective kinase inhibition*

There has been a wide range of kinases which have been suggested to play a functional role in agonist-induced receptor desensitization at MOPr (Chapter 1.2.5) (Williams et al., 2013). As such, some groups have opted to use non-selective kinase inhibitors such as the microbial alkaloid staurosporine (Rüegg et al., 1989; Karaman et al., 2008) to define the potential involvement of kinases in receptor processes (Arttamangkul et al., 2012). In the MOPr field, staurosporine has been often been utilised as a non-selective PKC inhibitor, as an alternate to (or in the absence of) selective inhibitors such as GF109203X as used in this study (Johnson et al., 2006; Arttamangkul et al., 2015). Alternatively, the use of non-selective kinase inhibitors could serve as a primary, triaging step to confirm the involvement of kinases in such processes before moving in on to more selective approaches (Pan et al., 1994; Sanders et al., 2002; Ponimaskin et al., 2005). However, staurosporine is not a potent inhibitor of GRKs (Karaman et al., 2008) and as such does not impact acute MOPr desensitization induced by DAMGO in recombinant systems (Johnson et al., 2006). We could therefore postulate that staurosporine would have had no effect on Compound 1-induced desensitization, revealing no role for PKC or other kinases in this desensitization, but a role for GRK would yet to be eluded in this case.

### *6.3.2 Modulation of kinase activity through genetic approaches*

Genetic knockdown approaches could have been used to elucidate the role of kinases in MOPr regulation, as opposed to the pharmacological methods utilised in this study. One evident obstacle to this approach is the limited number of available knockout animal lines available for rats. In this study, opioid-evoked currents have been assessed in rat, rather than mouse, LC neurones, due to practical reasons surrounding the small magnitude of GIRK currents in mouse LC neurones (Bailey et al., 2009b). Additionally, GRK2 KO is embryonically lethal in mice, limiting the study of this principal kinase

through genetic means. *In vivo* viral-mediated gene-transfer has been utilised effectively as a method to overcome this problem in rat brain slices (Bailey et al., 2009b). In this case, viral transfection of rat LC neurones with dominant negative GRK mutants was used to demonstrate the role of GRK2, but not GRK6, in DAMGO-induced MOPr desensitization (Bailey et al., 2009b).

Similarly, with the availability of a MOPr knockout rat (Envigo, USA), one group has demonstrated the use of virally-mediated gene transfer to effectively replace wild type MOPr for transfected mutant MOPr, deficient in GRK-dependent phosphorylation sites (Arttamangkul et al., 2019a). This elegant approach was used to characterise the role of specific C-terminal MOPr serine and threonine residues in agonist-induced acute desensitization and longer-term tolerance in rat LC neurones (Arttamangkul et al., 2019a). The knock-in expression of phosphorylation-deficient MOPr has also been employed for studies of agonist-induced receptor desensitization in mouse LC neurones (Kliewer et al., 2019) and in AtT20 cells (Miess et al., 2018), as reviewed by Birdsong et al. (2020).

Such genetic approaches to ablate GRK activity could provide important supporting information as to the GRK-dependent mechanism of Compound 1-induced desensitization described in rat LC neurones (Chapter 6.4). However, the utilization of this methodology is dependent on the accessibility of such tools, which are far less accessible as a starting point of investigation than the use of pharmacological tools.

### *6.3.3 The viability of recombinant systems in the study of MOPr desensitization*

The use of cultured recombinant cells to study agonist-induced MOPr desensitization, in place of brain slices, could provide a substantial increase in throughput for such investigations. The relatively short lifespan and occasionally variable health of neurones in brain slice preparations often serves as a rate-limiting step in the generation of electrophysiological data. This is particularly evident in circumstances where experiments are relatively long in duration, as presented in Chapter 5 (~1 hr), and deteriorating cell health or seal quality can lead to lost recordings.

In AtT20 cells, recombinantly expressing MOPr, are often adopted for electrophysiological studies within the opioid field (Birdsong et al., 2020), as these cells endogenously express functional GIRK channel subunits (Kozasa et al., 1996). While the use of cultured cells for electrophysiological studies provide some advantages regarding convenience, as well as greater opportunity for utilisation of genetic manipulation, the throughput of such assays is still very limited given its dependence on single cell recordings.

Many common recombinant assays of MOPr report signals associated with receptor regulation; such as receptor internalization, phosphorylation and arrestin recruitment. However, there is no common assay which can match the ability of electrophysiology to directly monitor the real-time desensitization of receptor function through the signal of agonist-induced GIRK currents. One possible high throughput approach to monitor MOPr-coupled GIRK channel function is through changes in membrane potential using fluorescent membrane potential-sensitive dyes (Knapman et al., 2013). This has been well-characterised for studying function and desensitization of GPCRs, including MOPr, in AtT20 cells (Knapman et al., 2013; Udoh et al., 2019). The strength of this assay format comes from its ability to provide real-time, continuous measure of receptor activation, similar to electrophysiological techniques. Given this assay is based on fluorescence responses, plate reader technologies such as Flexstation or FLIPR (Molecular Devices) can be utilised, allowing for experiments to be run in 96-well or 384-well plates. As such, the sheer throughput of these assays compared to electrophysiological methods gives them an undeniable utility in the study of MOPr function and desensitization.

However, the scientific value of the electrophysiological studies in brain slices is very important, as a measure of receptor function in an endogenous environment. While alternative methods using recombinant systems provide useful information on receptor function, in a more convenient format, they are inevitably tied to translatability issues arising from the study of receptors in heterologous expression systems (Chapter 3.3.3 and Chapter 4.3.1).

## 6.4 Relating observations of Compound 1-induced MOPr desensitization between studies in recombinant systems and LC neurones

In Chapter 5, I demonstrated that the mechanism regulating Compound 1-induced MOPr desensitization in rat LC neurones was GRK-dependent. Subsequently, I aimed to follow up this surprising finding by further investigating MOPr regulation induced by Compound 1 in recombinant systems (Chapter 5.2.7 through 5.2.10). These investigations produced data in line with Compound 1 being a G protein-biased agonist, with it producing minimal arrestin recruitment, MOPr internalization and $Ser^{375}$ phosphorylation (Chapter 5.3.1). Accordingly, it appears as if our findings for the extent of, and potential mechanisms of, Compound 1-induced MOPr desensitization present disparate pictures between our two systems of investigation (Figure 5.21). As such, in assays performed in recombinant systems, Compound 1 reliably displays signalling in line with it being a G protein-biased agonist. However, in LC neurones, the extent and mechanism of MOPr desensitization it induces is more in line with expectations for an arrestin-biased agonist (Rivero et al., 2012), rather than the G protein-biased agonist it is.

### *6.4.1 Considering the influence of systems bias in the case of Compound 1*

It could be postulated that the contrasting profiles observed for Compound 1 in these two systems is simply an effect of systems bias (Smith et al., 2018), and potentially the bias profile of Compound 1 is altered in the environment in LC neurones. One factor which could drive systems bias was explored in Chapter 5, which was potentially differing levels of GRK2 expression (Chapter 5.2.7). Such system bias has been demonstrated to have functional relevance for the region-specific activity of $D_2$ agonists, with increased relative cortical versus striatal activity attributed to elevated GRK2 and arrestin-3 expression in the former region (Urs et al., 2016). However, in our studies, GRK2 overexpression in HEK 293 cells did not disproportionally increase Compound 1-induced arrestin-3 recruitment to MOPr (Figure 5.17). Based on this, we believe it is unlikely that potential differences in GRK tone between our systems effectively reverses the bias signalling profile of Compound 1.

Additionally, systems bias may occur in the case of Compound 1 due to differential signalling efficacy dependent on the species variants of MOPr in which its function was tested. Such a phenomenon has been reported at KOPr, where the biased signalling profile of the agonist nalfurafine is considered to be substantially higher at the human form of the receptor than the rodent form (Schattauer et al., 2017). Due to limited availability of suitable constructs, the species from which MOPr constructs were derived

varied in the collective work of this thesis (Chapter 2.1). BRET assays of G protein activation (Figure 3.1B) and ELISA for agonist-induced MOPr internalization (Figure 5.19) were performed using rat HA-MOPr, BRET assays of arrestin recruitment (Figure 3.1D, Figure 3.5, Figure 5.17, Figure 5.18) were conducted using a human MOPr-Rluc construct, and immunoblotting assays of agonist-induced MOPr phosphorylation (Figure 5.20) were conducted using mouse HA-MOPr. Evidently, when comparing the activity of Compound 1 in these assays to those conducted in LC neurones (rat MOPr), we must consider species of receptor as a factor. However, this seems unlikely given the high sequence homology of the human, rat and mouse MOPr (Pasternak et al., 2013). Regardless, theoretically if Compound 1 had equivalent efficacy to morphine at the rat MOPr (G protein BRET and LC), but had a lower efficacy than morphine at the human MOPr (arrestin-recruitment BRET), that could potentially be responsible for its reported G protein-biased profile as well as differences in the extent of its efficacy for receptor desensitization/regulation between recombinant systems and the LC. However, there are a number of lines of evidence against this hypothesis. Firstly, the ELISA which demonstrated Compound 1 did not induce MOPr internalization was run on a rat HA-MOPr construct (Figure 5.19). Similarly, preliminary studies of opioid induced MOPr phosphorylation performed in house (prior to outsourcing this work to the Schulz lab group at the Friedrich-Schiller University, Jena, Germany) using the rat HA-MOPr demonstrated that Compound 1 produced no detectable $Ser^{375}$ phosphorylation (Conibear & Kelly, unpublished findings), in line with findings in mouse (Figure 5.20).

Together these lines of evidence oppose the hypothesis that apparent disparity in our findings for Compound 1-induced coupling to MOPr regulatory pathways is driven by species differences in our assays of MOPr activity. However, this highlights species differences as a common problem in the characterisation of ligands at GPCRs, which is often overlooked for convenience or when availability of constructs is limited. Further work could assure the G protein-biased signalling profile of Compound 1 is not species dependent by rerunning our arrestin-recruitment BRET assays using a MOPr-Rluc construct derived from the rat MOPr sequence.

### *6.4.2 Potential methods to address remaining questions surrounding the mechanism of Compound 1-induced MOPr desensitization*

As illustrated in Figure 5.21, there are a number of additional questions which could be addressed in order to enhance our understanding of the mechanisms of Compound 1-induced MOPr desensitization and regulation between recombinant systems and LC neurones.

First, concerning experiments in LC neurones, it is unknown whether the mechanism of Compound 1-induced MOPr desensitization involves phosphorylation of MOPr C-terminal serine and threonine residues or recruitment of arrestin proteins (Figure 5.21). While the coupling of Compound 1 to these pathways has been demonstrated to be weak compared to morphine in recombinant systems, I will below explore potential experimental approaches to address this question in LC neurones.

Although appealing, the viability of potential studies of agonist-induced MOPr phosphorylation in LC neurones through immunoblotting experiments (Figure 5.20) is limited by a lack of suitable method for protein enrichment. This is due to the lack of a high quality MOPr antibody and the absence a tag (such as HA) at the natively expressed receptor. This could be overcome by virally overexpressing a tagged MOPr (HA or FLAG) in rat LC neurones or through genetic modification of the MOPr sequence to include such a tag. Therefore, under these circumstances one could feasibly assess Compound 1-induced MOPr phosphorylation through immunoblotting experiments similar to those presented here in recombinant systems (Figure 5.19).

An alternate, more functionally relevant, method of determining the potential role of phosphorylation of MOPr C-terminal serine and threonine residues in Compound 1-induced MOPr desensitization is to study Compound 1 function at mutant MOPrs deficient in GRK-dependent phosphorylation sites (11S/T-A) (Just et al., 2013). The recent development of these MOPr mutants has provided excellent tools to study the role of GRKs in MOPr desensitization in recombinant systems (Miess et al., 2018) as well as the contribution of GRK and arrestin pathways in physiological responses to opioids *in vivo* in mutant mice (Kliewer et al., 2019). Additionally, brain slices from knock-in phosphorylation-deficient MOPr mice have been utilised to demonstrate the importance of multisite-phosphorylation by GRKs in rapid desensitization of Met-Enkephalin-evoked GIRK currents in LC neurones (Kliewer et al., 2019). Rather elegantly, these phosphosite-deficient MOPr mutants have also been utilised in LC brain slice electrophysiology experiments in rat, through viral-mediated gene transfer of mutant MOPrs into a commercially available MOPr-KO rat (Arttamangkul et al., 2019a) (Chapter 6.3.2). These experiments demonstrated similarly that acute desensitization of Met-Enkephalin-evoked GIRK currents as well as the cellular opioid tolerance in rat LC neurones is dependent on the expression of these C-terminal serine and threonine residues (Arttamangkul et al., 2019a).

The investigation of Compound 1-induced MOPr desensitization in rat LC neurones expressing phosphosite-deficient MOPr mutants would represent a pivotal future experiment. If Compound 1-induced MOPr desensitization would be decreased upon

deletion of MOPr phosphorylation sites, it would inform us that GRK is acting in a typical manner to regulate the Compound 1-activated MOPr. Alternatively, if deletion of MOPr phosphorylation sites did not impact Compound 1-induced MOPr desensitization, it could inform us that GRK is acting in a non-canonical manner to mediate Compound 1-induced receptor desensitization (Chapter 6.5).

It would be of significant interest to be able to observe the agonist-induced recruitment of arrestins to MOPr in LC neurones (Figure 5.20). In the case of Compound 1, understanding the degree of its arrestin recruitment in LC neurones relative to morphine would likely reveal whether its G protein-bias profile is retained across different systems (Chapter 6.4.1). It may be possible in the near future to achieve this through BRET or FRET techniques in brain slices derived from genetically modified mice (Sun et al., 2016; Rathod et al., 2018), however the introduction of mutated receptor and arrestin constructs defeats the purpose of examining this process in a native environment. As such, a suitable methodology for the determination of unlabelled arrestin recruitment to MOPr in a native environment is currently unavailable.

Similarly, the study of native MOPr internalization in brain slices would be of particular interest in order to further characterise Compound 1-induced MOPr regulation in LC neurones. This may be possible through fluorescence microscopy with the expression of mutant GFP tagged-MOPr, either virally in MOPr-KO rats, or in a genetic knock-in mouse (Arttamangkul et al., 2006; Kieffer et al., 2009). However, this approach is again limited as it does not examine the endogenous receptor. Traceless affinity labelling of endogenous MOPr has recently been demonstrated in LC neurones in brain slices using a naltrexamine-acylimidazole fluorescent probe (Arttamangkul et al., 2019b). This probe is able to bind endogenous MOPr, covalently link a fluorescent dye to the receptor, and be liberated from the orthosteric site. There is great potential for use of this probe to explore internalization of endogenous MOPrs in native brain slices through two-photon fluorescence microscopy without the need for genetically encoded tags (Arttamangkul et al., 2019b). However, receptor internalization has been demonstrated not to be involved in rapid agonist-induced MOPr desensitization in LC neurones (Arttamangkul et al., 2006), suggesting that mechanism of Compound 1-induced MOPr desensitization in LC neurones does not involve MOPr internalization anyway.

Alternatively, the gap in our understanding regarding Compound 1-induced MOPr regulation could be approached using studies of recombinant systems. While Compound 1-induced arrestin recruitment, MOPr internalization and MOPr phosphorylation have been characterised in these systems, it is not known whether Compound 1 induces MOPr desensitization in such systems as observed in LC neurones (Figure 5.21). AtT20

cells are commonly used in recombinant study of MOPr desensitization, due to their endogenous expression of GIRK channels (Kozasa et al., 1996) (Chapter 6.3). Opioid-induced activation of GIRKs through MOPr can be effectively assessed in AtT20 cells (or HEK 293 cells recombinantly expressing GIRKs) through either electrophysiological techniques (Yousuf et al., 2015; Dekan et al., 2019; Birdsong et al., 2020) or through the use of membrane-potential sensitive fluorescent dyes (Knapman et al., 2013; Gillis et al., 2020a). Through these methods, acute agonist-induced MOPr desensitization can be assessed in a similar manner to that in LC neurones (Chapter 4). Indeed, these assays produce similar findings to those in LC neurones regarding opioid-induced MOPr desensitization (Yousuf et al., 2015). Future investigations of Compound 1-induced MOPr desensitization in recombinant cells through either electrophysiological or fluorescence-based methods could provide valuable information. Such experiments could outline whether the cellular context of LC neurones is responsible for the magnitude of Compound 1-induced MOPr desensitization observed, or whether this desensitization is conserved across systems (Chapter 6.4.1). Additionally, if Compound 1-induced MOPr desensitization was present in recombinant systems, its dependence of GRK could be similarly be assessed through pharmacological or genetic means. It would also be possible to conduct such experiments in HEK 293 cells expressing GIRKs, the same cellular background as assays of arrestin-recruitment, GRK phosphorylation and MOPr internalization used in this study (Gillis et al., 2020a).

## 6.5 Potential non-canonical roles of GRK in Compound 1-induced MOPr desensitization

In spite of demonstrating that Compound 1-induced MOPr desensitization in LC neurones is GRK-dependent (Figure 5.6), we did not observe significant phosphorylation of typical GRK-substrate residues on the C-terminal tail of MOPr by Compound 1 (Figure 5.20) (Just et al., 2013; Miess et al., 2018). It is possible therefore that GRK may be acting in a non-canonical manner to regulate MOPr desensitization induced by Compound 1 in LC neurones (Figure 5.21). Below I will discuss some potential non-canonical mechanisms through which GRK could be acting in the case of Compound 1.

### *6.5.1 GRK-dependent phosphorylation of non-C-terminal MOPr residues*

One possibility is that GRK regulates MOPr desensitization induced by Compound 1 through phosphorylation of serine and threonine residues outside of the well documented residues examined in this study. The involvement of such C-terminal MOPr residues in agonist-induced receptor desensitization is well characterised (Just et al., 2013; Miess et al., 2018), however the phosphorylation of other extra-C-terminal residues has been implicated in MOPr regulation (Williams et al., 2013). One such MOPr residue is $Thr^{180}$ in the second intracellular loop, which undergoes GRK3-dependent phosphorylation upon activation of MOPr by DAMGO in both oocytes and AtT20 cells (Celver et al., 2001; Celver et al., 2004). Phosphorylation of $Thr^{180}$ was demonstrated to play a functional role in DAMGO-induced MOPr desensitization, but not MOPr internalization, in oocytes and AtT20 cells (Celver et al., 2004), however the function of this residue has not been demonstrated in neurones. This residue could potentially be important in the Compound 101-sensitive mechanism of MOPr desensitization induced by Compound 1, and such agonist-induced phosphorylation will not have been recorded in our studies of MOPr phosphorylation (Figure 5.20). The phosphorylation of intracellular loop serine and threonine residues has similarly been demonstrated as a mechanism of receptor desensitization and internalization at other class A GPCRs (Pals-Rylaarsdam et al., 1997; Clayton et al., 2014).

The practicality of future investigations to determine the potential role of $Thr^{180}$ phosphorylation in Compound 1 induced-MOPr desensitization are limited by the lack of a phosphospecific antibody agonist this specific residue on MOPr. This means this interaction must be determined in a different way to the phosphospecific immunoblotting techniques used in Chapter 5 (Figure 5.20). Mutated MOPrs in recombinant systems could be used to characterise the function of $Thr^{180}$ in Compound 1-induced desensitization, examining the effect of a T180A mutant on desensitization of

Compound-1 evoked GIRK currents in recombinant AtT20 cells or oocytes (Celver et al., 2004). If Compound-1 induced desensitization is reduced at the T180A mutant MOPr, it would suggest that phosphorylation of this residue is important for Compound 1-induced MOPr regulation. However, difficulties could arise in translating this finding to neurones. Alternatively, phosphoproteomics of MOPr samples could give a wider, whole receptor view of the patterns of Compound 1-induced MOPr phosphorylation (Moulédous et al., 2015). This has been demonstrated as a viable technique to determine the phosphorylation status of mouse brain MOPr (Moulédous et al., 2015), suggesting the possibility of examining rat brain MOPr phosphorylation induced by Compound 1. This information could be valuable in linking current phosphorylation data in recombinant systems to MOPr desensitization observed for Compound 1 in rat LC neurones. Additionally, the wide scope of this technique would be highly beneficial, allowing us to observed potential Compound 1-induced phosphorylation beyond archetypal residues.

### *6.5.2 Exploring a potential non-phosphorylation-dependent mechanism of GRK in Compound 1-induced MOPr desensitization*

In light of observing no significant Compound 1-induced phosphorylation in recombinant systems, it could be speculated that the mechanism of GRK-mediated Compound 1-induced MOPr desensitization in rat LC neurones is regulated by a non-phosphorylation dependent regulation through GRK. Such a phosphorylation-independent regulatory mechanism has been characterised for GRK2 at the metabotropic glutamate receptors mGluR1 and mGluR5, which are Class C GPCRs. In these cases, GRK2 has been shown to functionally inhibit G protein signalling through recruitment and binding to the second intracellular loop of the receptor (Dhami et al., 2005; Ribeiro et al., 2009). Future experiments could investigate this by studying potential recruitment of GRK2 to MOPr through established BRET methods in recombinant systems (Miess et al., 2018; Gillis et al., 2020a). If a phosphorylation-independent, steric hinderance-based mechanism underpins the Compound 101-sensitive, GRK-dependent MOPr desensitization induced by Compound 1, one could hypothesise that such experiments would show Compound 1 inducing substantial GRK recruitment to MOPr. One could postulate based on the data from LC neurones that if this was the case, the standing of Compound 1 would be higher than morphine within the rank order for GRK-recruitment compared with its relative standing for arrestin recruitment and $Ser^{375}$ phosphorylation.

Another phosphorylation-independent mechanism of GRK action has also been demonstrated, with GRK able to induce heterologous desensitization of GPCR-linked GIRK currents through sequestration of $G\beta\gamma$ subunits in recombinant systems (Raveh et al., 2010). However, in rat LC neurones the extent of DAMGO-induced MOPr

desensitization that occurs through heterologous GRK-dependent Gβγ sequestration has been demonstrated to be minimal in mature cells (Llorente et al., 2012). Additionally, in the case of Compound 1, findings in Chapter 4 showing that Compound 1 did not induce marked heterologous desensitization of NA-evoked currents relative to other opioids (Figure 4.6). This finding suggests that this heterologous mechanism of GRK action is not responsible for observed Compound 1-induced desensitization in rat LC neurones.

## 6.6 The potential structural determinants underlying the biased signalling of Compound 1

In Chapter 3, I characterised the cyclic endomorphin analogue 'Compound 1' as a G protein-biased agonist at the MOPr (Figure 3.2). Compound 1 displayed a substantially higher degree of bias than previously purported biased agonists at MOPr (Conibear et al., 2019; Dekan et al., 2019). The factors underlying the distinctive pharmacology of Compound 1 warrant further study, in particular the structural determinants of its signalling profile. This question could be approached from two angles: Firstly, what factors around the structure of Compound 1 define its G protein-biased signalling profile? Secondly, what can the manner in which Compound 1 interacts with and stabilises MOPr tell us about the receptor conformations which give rise to biased receptor signalling at MOPr?

In the initial stages of this project, we speculated that the cyclic nature of Compound 1 may predispose it to being a G protein-biased agonist at MOPr (Li et al., 2016). Whether dependent on its cyclic nature or otherwise, we have conclusively characterised Compound 1 as a G protein-biased agonist at MOPr within this thesis (Figure 3.2, Chapter 3.3.2). This initial hypothesis was based on the similarity of the in vivo pharmacological profiles presented by previously reported cyclic endomorphin analogues, notably ZH853 and CYT-1010, to those of G protein-biased agonists (Zadina et al., 2016; Webster et al., 2020) (Chapter 1.3.2 and Chapter 3.1). While the signalling properties of these cyclic peptides has not been published, their pharmacological profiles are certainly akin to those previously associated with G protein-biased agonists at MOPr. With the cyclic Compound 1 outlined as a G protein-biased agonist in this thesis, and given that linear endomorpin-2 itself is an arrestin biased agonist at MOPr (Rivero et al., 2012), it could be hypothesised that the cyclisation of the endomorphin series provides the chemical 'switch' to provide signalling bias for G protein over arrestin signalling at MOPr.

It would be possible to test this hypothesis through the generation of linear analogues of Compound 1. In fact, both linear and head-to-tail cyclic analogues of Compound 1 have been generated by our collaborators (Li, unpublished data). Future experiments characterising the signalling profiles of these linear and head-to-tail cyclic Compound 1 analogues relative to Compound 1 through BRET based methods demonstrated in this thesis (Figure 3.1) could evaluate the impact of cyclisation on agonist signalling. If the linear analogue of Compound 1 was found to lack the G protein-biased signalling profile of its parent molecule at MOPr, it could indicate the value of cyclisation as an approach to develop G protein-biased peptide agonists at MOPr.

It is conventionally thought that biased signalling stems from the ability of certain agonists to stabilise distinct GPCR conformations which favour coupling to different intracellular signalling mechanisms (Kenakin, 2011). Through modelling approaches such as molecular dynamics, it could be possible to determine the possible MOPr conformations stabilised by Compound 1, as a mechanism for further elucidating the structural mechanisms of biased signalling at MOPr at a receptor level. Such modelling processes have been employed at MOPr in attempts to further understand biased signalling, however many of these studies suffer in that the test agonists examined have subsequently been demonstrated to be low efficacy agonists, rather than G protein-biased (Chapter 3.3.2). These include studies on TRV130 (Schneider et al., 2016; Cheng et al., 2018; Kapoor et al., 2020; Zhao et al., 2020) and PZM21 (Zhao et al., 2020). However, molecular dynamics studies contrasting the MOPr conformations stabilised by bilorphin and endomorphin-2 provide information on the distinct conformations underlying biased signalling in the case of a validated G protein-biased agonist (Dekan et al., 2019). This study interestingly highlighted that bilorphin, in contrast to the arrestin-biased agonist endomorphin-2, interacted with TM1 and evaded interactions with the extracellular loops of MOPr (Dekan et al., 2019). TM1 has similarly been implicated in TRV130-induced MOPr signalling and is part of the binding pocket for exendin-P5, a G protein-biased agonist at the GLP-1R (Liang et al., 2018).

It would be of significant interest to determine whether Compound 1 as a G protein-biased agonist also interacts with TM1 in a manner similar to bilorphin through future molecular dynamics experiments. If this interaction with TM1 is common to Compound 1 and bilorphin, it could be considered a distinct stabilization induced by G protein-biased agonists at MOPr and could provide valuable information for the further structure-based design of future G protein-biased agonists. However, given that Compound 1 is a large cyclic peptide, such molecular dynamics modelling would not be trivial. Additionally, the functional worth of identifying distinct conformations with such modelling methods could be questioned, particularly considering that in silico multiple distinct conformations have been illustrated for MOPr agonists such as TRV130, PZM21 and methadone (Schneider et al., 2016; Cheng et al., 2018; Kapoor et al., 2020; Zhao et al., 2020), a finding likely unrelated to potential biased signalling. As such, individual agonists may induce subtle individual differences in MOPr conformations with little to no functional consequence, highlighting the need for determining the significance of such distinct interactions in functional assays.

## 6.7 Investigating Compound 1-induced tolerance

In this thesis, I have demonstrated that Compound 1 induces substantial MOPr desensitization in rat LC neurones. Agonist-induced receptor desensitization is often studied as a cognate of agonist tolerance at GPCRs. Indeed, at MOPr, there is good experimental evidence that receptor desensitization is the inaugural process in the development of tolerance to opioids in vivo (Bohn et al., 2000; Bailey et al., 2009a; Kliewer et al., 2019). The direct study of the potential development of Compound 1-induced tolerance would further the translatability of our findings regarding the long-term functional consequences of biased signalling at MOPr. Normally, this could simply be assessed through repeated dosing and paired assessment of opioid function through standard assays of nociception (Chapter 4.2.4). However, in Chapter 4 I demonstrated that the MOPr-dependent antinociceptive effect of Compound 1 when administered i.p. was limited, potentially due to pharmacokinetic concerns or low BBB permeability (Figure 4.10 and Figure 4.11). Unfortunately, the limited effect of Compound 1 when administered i.p. hindered study of Compound 1-induced tolerance in such a system. Below I will discuss some other potential means to investigate Compound 1-induced tolerance and highlight issues which may be addressed through its study.

Firstly, issues surrounding the potentially problematic BBB permeability could be circumvented through administering the drug intracerebroventricularly (Cook et al., 2009) or intrathecally (Dekan et al., 2019). If the antinociceptive effect of Compound 1 was comparable to morphine through these administration routes, it could highlight that the limited effect of Compound 1 when administered i.p. is due to BBB permeability, rather than a result of its receptor pharmacology (Chapter 4.3.4). Additionally, of course, this would also open up opportunities to conduct repeated dose experiments with Compound 1 to study potential tolerance. However, it must be considered that the possible mechanisms and extent of agonist-induced tolerance may differ between administration routes. Furthermore, intracerebroventricular and intrathecal injection are intricate and potentially problematic procedures in mice which require adequate experience and training, which has prevented its immediate study.

Given the potentially therapeutically interesting G protein-biased profile of Compound 1, an immediate thought from a medicinal chemistry perspective would be to develop analogues of Compound 1 which possess more favourable pharmacokinetic and BBB penetration properties. Such agonists could provide valuable tool compounds for the study of the long-term functional consequences of biased agonism at MOPr, as well as potentially interesting therapeutic leads. Such chemical modifications could include glycosylation, previously show to improve the membrane permeability and

pharmacokinetics of enkephalins and endorphins (Li et al., 2012). Future development and functional study of Compound 1 analogues would be of particular interest for this project. However, a cautionary parallel can be drawn from such a study to the recent story of the G protein-biased MOPr agonist bilorphin (Dekan et al., 2019). Here, Dekan et al. (2019) demonstrated that bilorphin lacked activity in nociceptive assays upon systemic administration, however it did have antinociceptive activity when administered intrathecally, hereby attributing this systemic inactivity to poor BBB permeability. Bilactorphin was developed in attempts to develop bilorphin analogues with more favourable BBB penetration characteristics, indeed showing potent antinociceptive properties after system administration. However, through modifications made to bilorphin, bilactorphin lost the G protein-biased signalling profile of its parent molecule, making it a balanced MOPr agonist. As such, caution arises that developed analogues of Compound 1 may not possess the same signalling profile as Compound 1, and that therefore such pharmacological profiles must be thoroughly examined before the utility of such analogues is concluded.

An alternative approach to characterise the long-term functional effects of Compound 1 on MOPr would be to study cellular tolerance in rat LC neurones as opposed to whole animals. Such approaches have either revolved around assessing opioid function after long periods (4-6 hours) of low opioid exposure in vitro (Bailey et al., 2009a) or after repeated or continuous opioid administration in animals from which slices are derived (Dang et al., 2004; Bailey et al., 2009a; Leff et al., 2020). The latter approach is evidently limited in the circumstances of Compound 1, due to uncertainties around its BBB permeability upon systemic administration as outlined above. Future work characterising cellular tolerance to Compound 1 through chronic in vitro exposure however would be of particular interest. Such studies could provide scope on the long-term functional effect of Compound 1 beyond the short time-scale (10-15 mins) of rapid receptor desensitization examined thus far. Additionally, such studies could also provide insight into important regulatory processes which occur over a longer time-frame (Williams et al., 2013), which have been little discussed in this thesis up to this point; namely receptor resensitization and recycling. Of course, while such in vitro chronic exposure experiments could give further insight into Compound 1-induced MOPr regulation, they would not provide the translational information desired from experiments of chronic treatment in whole animals or assessment of analgesic tolerance.

Given the role of arrestin-3 in MOPr recycling, as well as internalization and desensitization (Chapter 1.1.4), one could hypothesise that Compound 1 activated MOPr, which couples weakly to arrestins (Figure 3.1), would likely undergo little recycling. This may imply that desensitization and tolerance to Compound 1 would be

protracted, as in the case of morphine, in the absence of receptor resensitization (Martini et al., 2007), under arguments set out under the “RAVE” (for “relative activation versus endocytosis”) hypothesis (Whistler et al., 1999). However, the recovery of MOPr function after receptor desensitization was unexpectedly accelerated in LC neurones of arrestin-3 KO mice compared to their wildtype counterparts (Dang et al., 2011). This suggests that arrestin pathways actually impair recovery of MOPr function, with resensitization in LC neurones likely dependent on dephosphorylation (Dang et al., 2011; Doll et al., 2011). It would be of interest to characterise the recovery from Compound 1-induced MOPr desensitization to gain a more complete picture of long-term MOPr regulation by Compound 1 in future experiments. Common protocols used to study recovery of MOPr function in brain slices rely on agonist wash out. As such, the readily degraded Met-Enkephalin (Williams et al., 1987a) is used as a test ligand, with repeated ‘pulses’ applied to track the recovery of MOPr function. (Arttamangkul et al., 2019a; Birdsong et al., 2020; Leff et al., 2020). As a consequence, unfortunately such experiments are not possible in the case of Compound 1, for which the time required for total washout is exceedingly long, similar to the majority of MOPr agonists which do not undergo assisted-degradation in brain slices.

## 6.8 Assessing the therapeutic potential of current and future biased agonists at MOPr

The development of G protein-biased agonists MOPr has dominated the field of opioid development over the last decade. Drug development campaigns from both industrial and academic groups have yielded a number of notable putatively G protein-biased agonists, including TRV130 (DeWire et al., 2013), PZM21 (Manglik et al., 2016) and SR17018 (Schmid et al., 2017). Similarly, opioids well established in our clinical arsenal, such as buprenorphine and morphine, have been retroactively categorised as G protein-biased by some groups (Raehal et al., 2011a; Ehrlich et al., 2019). To date, TRV130 (oliceridine, brand name Olinvyk) is the only new purportedly G protein-biased MOPr agonist to reach FDA approval for clinical use (Markham, 2020). It merits mention that the approval of TRV130 is quite remarkable given its previous refusal in 2018, with clinical trial data demonstrating little to no evidence of a favourable safety profile in comparison to morphine (Singla et al., 2019), and a widespread appreciation that it does not in fact possess a significant G protein-biased profile at all (Lambert et al., 2020).

As previously discussed in this thesis (Chapter 3.3.2 and 4.3.1), the putatively G protein-biased profiles of the current crop of novel agonists at MOPr have come under scrutiny (Conibear et al., 2019). Thorough work from Gillis et al. (2020a) has recently highlighted that the profiles of aforementioned 'G protein-biased' agonists may in fact be due to low intrinsic efficacy rather than any indication of biased signalling. This work echoes previous demonstrations of the importance of efficacy in the assessment of functional selectivity, which argued against the incorrect categorisation of the partial morphine as a biased agonist (Kelly, 2013). As such, the work of Gillis et al. (2020a) casts doubt on the proposed 'biased' profiles of TRV130, PZM21, SR17018 and buprenorphine, ascribing their pharmacological profiles instead to their low efficacy. The crisis of mis-accreditation within biased signalling, which is particularly evident in the case of MOPr, largely stems from limitations in the standard methods of bias calculations in the case of partial agonism, particularly in amplified systems (Chapter 3.3.3).

Despite contradictory findings around the pharmacological profiles of the current panel of purportedly G protein-biased agonist at MOPr, the same body of work suggested that in fact the low intrinsic efficacy of aforementioned agonists drives an increase in their therapeutic window (Gillis et al., 2020a). This inverse correlation between intrinsic efficacy and therapeutic window could provide good evidence that newly developed low efficacy agonists such as TRV130, PZM21 and SR17018 could possess a more favourable clinical safety profile over agonists such as morphine regardless of purported bias. Indeed, the intrinsic efficacy at receptor level required for an opioid to evoke reliable

analgesia is thought to be relatively low, with opioids such as buprenorphine, which have very low efficacy in cell systems, consistently considered ‘strong opioids’ in a clinical setting (Schmidt-Hansen et al., 2015). One could therefore argue that previous drug development, blinkered by the natural inclination that stronger equals better, has developed drugs that possess efficacy far beyond what is required for effective analgesia, potentially making them more liable to induce adverse effects. Therefore, the demonstration of this inverse correlation between intrinsic efficacy and improved therapeutic window by Gillis et al. (2020a) has prompted a drive within drug discovery to develop low efficacy partial MOPr agonists as potentially safer analgesics.

It could however be argued that the demonstration of this inverse correlation between intrinsic efficacy and therapeutic window by Gillis et al. (2020a) is heavily dependent on data from PZM21 and buprenorphine, which yields two contentious points: firstly, the favourable therapeutic window of PZM21 is heavily dependent on an apparent ceiling in the respiratory burden of PZM21 upon increasing doses. Furthermore, the extent of respiratory depression induced by PZM21 relative to morphine at 60 mg/kg and 100 mg/kg is substantially lower than that observed by Hill et al. (2018b) at 40 mg/kg. Additionally, the PZM21 ED50 data in the Gillis et al. (2020a) study from which its therapeutic window is derived was fitted from responses to only two doses, limiting confidence in curve fitting. Secondly, results for buprenorphine clearly drive the correlation, with buprenorphine producing minimal respiratory depression up to 10 mg/kg. However, low intrinsic efficacy at MOPr may not be the exclusive factor mediating this previously documented limited respiratory burden induced by buprenorphine (Dahan et al., 2006), with its pharmacokinetics and affinity at DOPr, KOPr and the nociceptin receptor all potentially confusing the interpretation of findings for this often perplexing drug (Gudin et al., 2020).

Regardless, the inadvertent development of highly specific MOPr weak partial agonists in TRV130, PZM21 and SR17018, among others, provides an excellent toolset to truly investigate whether MOPr agonists of lower intrinsic efficacy could provide safer analgesics as hypothesised (Gillis et al., 2020c). While weak partial agonists of MOPr currently exist and have been historically widely used in clinical practise, including buprenorphine, pethidine, tramadol and levorphanol, their utility as tool compounds and to some extent therapeutics is limited by their interaction with receptors other than MOPr.

One key question which influences the utility of lower efficacy MOPr in clinical practise is the potential development of tolerance to their analgesic effects. As hypothesised in the case of G protein-biased agonists, their lower relative coupling to arrestin and GRK regulatory pathways could make them less liable to induce receptor desensitization and

subsequent development of tolerance. Limited clinical evidence suggests, as expected for a weak partial agonist, that tolerance to the analgesic effects of buprenorphine develops more slowly than to the effects of fentanyl (Sittl et al., 2005). However, tolerance to the antinociceptive effects of buprenorphine is still evident in mouse models (Melief et al., 2010). Current knowledge around the ability of previously described G protein-biased agonists, or low efficacy agonists, is limited and variable. TRV130 was shown to induce less antinociceptive tolerance than morphine in mice after 3-4 days of repeated administration (Altarifi et al., 2017; Liang et al., 2019). Similarly, SR17018 has been reported to not produce analgesic tolerance after 6 days of oral dosing (Grim et al., 2020). On the other hand, PZM21 produces robust antinociceptive tolerance in mice over 4 days (Hill et al., 2018b). The variability of these findings may be in part due to differences in the efficacies of these specific agonists. Additionally, as outlined above, the varied experimental protocols and routes of administration could also account for the differences observed for these agonists. Nevertheless, further studies into the propensity of low efficacy opioids to induce MOPr desensitization and the subsequent development of tolerance to their effects will improve our understanding of their wider clinical utility.

As discussed above, the current crop of putatively 'G protein-biased agonists' at MOPr have not delivered on the pharmacological properties initially promised, an observation skewed by contradictory findings on the reality of the apparent bias of these ligands. This begs the question as to whether truly G protein-biased agonists would indeed induce less respiratory depression and tolerance while maintaining the analgesic properties of balanced MOPr agonists, as was originally hypothesised based on historical arrestin-3 knockout work by the Bohn group (Bohn et al., 1999; Raehal et al., 2005). Below I will be discussing recent findings which have caused a shift in the current thinking of biased signalling at MOPr. First, I will outline recent findings demonstrating the G protein signalling-dependent, arrestin-independent nature of opioid-induced respiratory depression. Subsequently I will be summarising recent work further examining the arrestin/GRK-dependent nature of tolerance to opioids, bringing in the findings around the G protein-biased agonist Compound 1.

The hypothesis that opioid-induced respiratory depression is mediated by MOPr/arrestin interactions is central to the proposed clinical benefit of G protein-biased MOPr agonists. In contradiction to the original findings of morphine-induced respiratory depression in arrestin 3 knockout mice (Bohn et al., 1999; Raehal et al., 2005), there is now good evidence that MOPr activation inhibits activity in nuclei involved in respiratory control (preBötzinger and Kölliker-Fuse neurones (Varga et al., 2019)) through G protein-dependent signalling (Gillis et al., 2020b). In the preBötzinger complex, morphine effects on respiratory rate have been shown to be mediated by GIRK channel activation

(Montandon et al., 2016). Additionally, a presynaptic mechanism of opioid-induced inhibition of preBötzinger neurons has been shown, through MOPr-dependent activation of voltage-gated calcium channels (Wei et al., 2019). Similarly, opioid-induced inhibition of Kölliker-Fuse neurones occurs through MOPr-dependent activation of GIRK, suppressing inspiratory drive (Levitt et al., 2015). These mechanistic studies refute the previous hypotheses of the arrestin-dependent nature of opioid induced respiratory depression based on previous arrestin-3 KO data. Additionally, reports demonstrating the worsening of morphine- and fentanyl-induced respiratory depression in mice expressing phosphorylation-site deficient MOPrs also refutes the previously held hypothesises of opioid-induced respiratory depression being arrestin-dependent (Kliewer et al., 2019). Finally, a report from a consortium of 3 independent laboratories showing that morphine- and fentanyl-induced respiratory depression persists in arrestin-3 knockout mice, directly refuting the findings of Raehal et al. (2005), raises concerns around the validity and reproducibility of the findings on which the arrestin hypothesis was built (Kliewer et al., 2020).

In light of this recent evidence, previous theories suggesting G protein-biased MOPr agonists will be safer analgesics with regard to their propensity to induce respiratory depression now appear to be mechanistically invalid. However, recent evidence has suggested that G protein-biased agonists could induce less receptor desensitization and tolerance than balanced agonists. In LC neurones from mice expressing phosphorylation-site deficient MOPrs, desensitization of Met-Enkephalin-evoked GIRK currents is significantly reduced (Kliewer et al., 2019). Additionally, tolerance to the antinociceptive effects of morphine and fentanyl is lost in mice expressing phosphorylation-site deficient MOPrs (Kliewer et al., 2019). While this evidence does suggest G protein-biased agonists may be clinically beneficial with regard to the induction of MOPr desensitization and subsequent tolerance, work within this thesis highlights that MOPr desensitization can occur in a agonist-specific manner, through multiple mechanisms (Kelly et al., 2008). The finding here that the G protein-biased MOPr agonist Compound 1 induces substantial receptor desensitization underscores that G protein-biased agonists at GPCRs could still induce receptor desensitization and tolerance through non-canonical, agonist-specific mechanisms. Further work is therefore required to fully understand the long-term functional consequences of G protein-biased agonism at MOPr and to interpret its clinical utility.

## 6.9 The potential of harnessing biased signalling to aid the development of effective therapeutics at other GPCR targets

The phenomenon of biased signalling has been applied to a multitude of GPCR targets in the anticipation that it will allow for the development of more refined, safer therapeutics. Biased agonism has been explored at GPCR targets including the M1 muscarinic acetylcholine receptor (Bradley et al., 2020), neurotensin receptor 1 (Slosky et al., 2020), the ghrelin receptor (Mende et al., 2018) and the ATIIR (Violin et al., 2010) for the development of novel therapeutics for conditions ranging from dementia and addiction to obesity and heart failure. More specifically, there is great interest in the development of biased agonists at other opioid receptors. In the case of DOPr, G protein-biased agonists are suggested to possess desired antihyperalgesic effects for the treatment of chronic pain states without producing the proconvulsant activity previously prohibiting the development of DOPr agonists (Dripps et al., 2018; Conibear et al., 2020). At KOPr, recently developed G protein-biased agonists have been reported to be effective antinociceptive and antipruritic agents, but do not induce dysphoria, psychosis and sedation which previously held back the development of KOPr agonists (Spetea et al., 2017; Mores et al., 2019).

However, despite the persistent efforts of drug discovery groups targeting GPCRs across the GPCR-ome, the MOPr agonist TRV130 is the only 'biased' GPCR therapeutic to reach licenced approval for clinical use (Lambert et al., 2020). One could argue that the currently unfulfilled promise of biased agonism as a viable drug discovery strategy is hindered by methodological limitations as well as our limited comprehension of the subtleties of GPCR signalling (Michel et al., 2018).

Methodologically, the development of biased agonists within drug discovery is limited by the non-trivial means of bias quantification. As previously discussed (Chapter 3.3.3) in relation to efficacy as a potentially confounding factor in calculations of bias signalling, great care must be taken when establishing GPCR signalling assays for calculation of bias. For example, the kinetic context of each assay must be given consideration which further complicates interpretation of such data (Lane et al., 2017). The unappreciated complexity of this process often leads to the misclassification of biased signalling in many settings. Practical considerations, such as the number of different GPCR signalling assays which must be run, also presents an obstacle for drug discovery to define or refine the biased signalling of their candidate ligands, where efficiency and high throughput are of paramount importance. Additionally, high profile clinical failures of bellwether biased agonists in clinical trials (Pang et al., 2017) along with the rising doubts about the supposed biased profile of developed agonists (Gillis et al., 2020a) has

currently increased concerns about the potential utilisation of biased signalling as a useful drug discovery tool.

Perhaps the biggest obstacle for drug discovery based on biased agonism is the current lack of understanding concerning pathway-specific GPCR signalling and its functional implications (Michel et al., 2018). Even for a target as established as the MOPr, long considered the front-running target for biased agonism drug discovery, new evidence highlighting our previous misconceptions regarding the consequences of arrestin-dependent signalling and its role in respiratory depression have shattered our hopes for this once promising approach (Gillis et al., 2020b; Kliewer et al., 2020). For biased agonism to be a viable approach in future drug development programmes, the specific physiological roles of GPCR signalling patterns (G proteins, arrestins, or other) which mediate the therapeutically beneficial and adverse effects of GPCR function must be conclusively defined. The recent development of more refined approaches and tools to study the functional roles of specific pathways in GPCR signalling could provide the proper target validation required for this process. These approaches include the development of knock-in mouse lines expressing phosphorylation-deficient 'G protein-biased' GPCRs, for example MOPr and M1 muscarinic acetylcholine receptor, to probe the role of arrestin-dependent signalling (Kliewer et al., 2019; Bradley et al., 2020). The main benefit of this approach is that observations are not dependent on or limited by the quality of available supposedly biased agonists at the GPCR of interest. However, caution should be exercised as perceived toxicity from stimulation of G protein-biased GPCRs in this approach could result from overstimulation stemming from a lack of regulatory arrestin control, rather than from G protein signalling specifically (Bradley et al., 2020).

Given the proposed requirement for such thorough signalling characterisation in the development of therapeutics harnessing biased signalling, one fears that its utilisation may be limited to cases where the GPCR of interest is an established therapeutic target. In turn this may limit the development of biased agonists to the second or third generation of therapeutics at a given target. The development of such refined agents at established therapeutic targets is important, and established targets bring a certain security from a drug discovery standpoint. However, one could argue that targeting lesser studied GPCR targets may yield more meaningful advances in the field of GPCR therapeutics and medicine generally, rather than attempting to teach an old dog new tricks.

Current FDA approved GPCR-targeting drugs mediate their effects through 108 GPCR targets, which accounts for 27% of the potential pool of human non-olfactory GPCRs currently targeted by therapeutics (Hauser et al., 2017). Each established GPCR target

is currently targeted by an average of 10.3 distinct approved agents (Hauser et al., 2017), highlighting a near saturation of drug discovery within the current target space. That said, the mass de-orphanisation of GPCRs which has occurred over the past 2 decades following the so-called cloning age (Hill, 2006) has advanced our knowledge of GPCR biology, leading to an expanded arsenal of druggable GPCRs. In turn, the field is beginning to bear the fruits of this labour with the recent approval of novel therapeutics targeting lesser known GPCR targets. Two recent examples of this are the orexin receptors (orexin receptor 1, OX1 and orexin receptor 2, OX2) and the CGRP receptor. Dual orexin receptor antagonists, including suvorexant (Yang, 2014) and lemborexant (Scott, 2020), have been approved as first-in-class hypnotic drugs, with OX1 receptor antagonists being clinical explored for the treatment of addiction (James et al., 2017). Similarly building on new biology at previously unstudied GPCR targets, the recent development and approval of several CGRP receptor antagonists for migraine has revolutionised treatment for this condition (Edvinsson et al., 2018; Markham, 2018). These advances among many others (Hauser et al., 2017), strengthens the case for expanding our search for novel therapeutics beyond currently established targets. This is particularly pertinent when considering that 30% of the non-olfactory human GPCRs are orphan receptors (not definitively paired with endogenous ligands), highlighting a wealth of unexplored biology which is likely to yield valuable therapeutic targets (Hauser et al., 2020).

Numerous lesser studied GPCRs are currently under investigation as novel therapeutic targets for the development of non-opioid analgesic drugs (Che, 2020). For instance, metabotropic glutamate receptors (mGluRs) are expressed throughout nociceptive pathways, regulating pain transmission (Latremoliere et al., 2009). Both the predominantly postsynaptic mGluR1 and 5 (Sevostianova et al., 2006) and presynaptic mGluR2 and 3 subtypes (Johnson et al., 2017) have been preclinically demonstrated as effective targets for the treatment of pain. Similarly to opioids, the use of cannabinoids for pain relief is deep-rooted into our history. The CB1 cannabinoid receptor is expressed in both ascending and descending pain pathways and is upregulated in chronic pain states (Lim et al., 2003). The development of G protein-biased agonists at CB1 such as PNR-4-20 could provide novel cannabinoid agonists with reduced propensity to produce typical cannabinoid psychoactive effects (Ford et al., 2017). The GPCR neurokinin 1 receptor (NK-1R), the primary target of the pronociceptive peptide Substance P, presents another potential GPCR target which has been explored for the development of novel analgesics (Sanger, 2004). Interestingly NK-1R and MOPr are co-expressed in sensory neurones, and bifunctional peptides with both MOPr agonist and NK-1R antagonist activity show analgesic efficacy with favourable adverse effect profiles (Starnowska et al., 2017). Current orphan GPCRs may also present future therapeutic

targets for the treatment of pain (Nourbakhsh et al., 2018). For instance, GPR40 (now identified as free fatty acid receptor 1 (FFA1 receptor)) has been implicated as a regulator of descending pain control, with activation of GPR40 decreasing formalin-induced pain behaviours in mice (Nakamoto et al., 2015).

## 6.10 Final Conclusion

The research presented within this thesis aimed to characterise the receptor desensitization and regulation induced by G protein-biased MOPr agonists, in order to further define their long-term functional effects and overall therapeutic potential. In this thesis I have characterised the cyclic endomorphin analogue Compound 1 as a novel G protein-biased agonist at MOPr. In spite of its G protein-biased signalling profile, Compound 1 induces substantial rapid receptor desensitization in LC neurons though a potentially novel GRK-dependent, arrestin-independent mechanism. More widely, our findings refute the assumption that G protein-biased agonists at MOPr, and at other GPCRs, will evade receptor desensitization and subsequent tolerance.

# Chapter 7: References

Abraham, A. D., Schattauer, S. S., Reichard, K. L., Cohen, J. H., Fontaine, H. M., Song, A. J., et al. (2018). Estrogen Regulation of GRK2 Inactivates Kappa Opioid Receptor Signaling Mediating Analgesia, But Not Aversion. *J Neurosci, 38*(37), 8031-8043. doi:10.1523/jneurosci.0653-18.2018

Aghajanian, G. K., & Wang, Y. Y. (1986). Pertussis toxin blocks the outward currents evoked by opiate and alpha 2-agonists in locus coeruleus neurons. *Brain Res, 371*(2), 390-394. doi:10.1016/0006-8993(86)90382-3

Aicher, S. A., Punnoose, A., & Goldberg, A. (2000). mu-Opioid receptors often colocalize with the substance P receptor (NK1) in the trigeminal dorsal horn. *J Neurosci, 20*(11), 4345-4354. doi:10.1523/jneurosci.20-11-04345.2000

Altarifi, A. A., David, B., Muchhala, K. H., Blough, B. E., Akbarali, H., & Negus, S. S. (2017). Effects of acute and repeated treatment with the biased mu opioid receptor agonist TRV130 (oliceridine) on measures of antinociception, gastrointestinal function, and abuse liability in rodents. *J Psychopharmacol, 31*(6), 730-739. doi:10.1177/0269881116689257

Alvarez, V. A., Arttamangkul, S., Dang, V., Salem, A., Whistler, J. L., Von Zastrow, M., et al. (2002). mu-Opioid receptors: Ligand-dependent activation of potassium conductance, desensitization, and internalization. *J Neurosci, 22*(13), 5769-5776. doi:20026560

Alvarez-Curto, E., Inoue, A., Jenkins, L., Raihan, S. Z., Prihandoko, R., Tobin, A. B., et al. (2016). Targeted Elimination of G Proteins and Arrestins Defines Their Specific Contributions to Both Intensity and Duration of G Protein-coupled Receptor Signaling. *J Biol Chem, 291*(53), 27147-27159. doi:10.1074/jbc.M116.754887

Angers, S., Salahpour, A., Joly, E., Hilairet, S., Chelsky, D., Dennis, M., et al. (2000). Detection of 2-adrenergic receptor dimerization in living cells using bioluminescence resonance energy transfer (BRET). *Proceedings of the National Academy of Sciences, 97*(7), 3684-3689. doi:10.1073/pnas.97.7.3684

Arttamangkul, S., Birdsong, W., & Williams, J. T. (2015). Does PKC activation increase the homologous desensitization of μ opioid receptors? *British Journal of Pharmacology, 172*(2), 583-592. doi:10.1111/bph.12712

Arttamangkul, S., Lau, E. K., Lu, H.-W., & Williams, J. T. (2012). Desensitization and Trafficking of μ-Opioid Receptors in Locus Ceruleus Neurons: Modulation by Kinases. *Molecular Pharmacology, 81*(3), 348-355. doi:10.1124/mol.111.076208

Arttamangkul, S., Leff, E. R., Koita, O., Birdsong, W. T., & Williams, J. T. (2019a). Separation of Acute Desensitization and Long-Term Tolerance of micro-Opioid Receptors Is Determined by the Degree of C-Terminal Phosphorylation. *Mol Pharmacol, 96*(4), 505-514. doi:10.1124/mol.119.117358

Arttamangkul, S., Plazek, A., Platt, E. J., Jin, H., Murray, T. F., Birdsong, W. T., et al. (2019b). Visualizing endogenous opioid receptors in living neurons using ligand-directed chemistry. *eLife, 8*. doi:10.7554/eLife.49319

Arttamangkul, S., Quillinan, N., Low, M. J., Von Zastrow, M., Pintar, J., & Williams, J. T. (2008). Differential Activation and Trafficking of μ-Opioid Receptors in Brain Slices. *Molecular Pharmacology, 74*(4), 972-979. doi:10.1124/mol.108.048512

Arttamangkul, S., Torrecilla, M., Kobayashi, K., Okano, H., & Williams, J. T. (2006). Separation of mu-opioid receptor desensitization and internalization: endogenous receptors in primary neuronal cultures. *J Neurosci, 26*(15), 4118-4125. doi:10.1523/JNEUROSCI.0303-06.2006

Arvidsson, U., Riedl, M., Chakrabarti, S., Lee, J., Nakano, A., Dado, R., et al. (1995). Distribution and targeting of a mu-opioid receptor (MOR1) in brain and spinal cord. *The Journal of Neuroscience, 15*(5), 3328-3341. doi:10.1523/jneurosci.15-05-03328.1995

Bacart, J., Corbel, C., Jockers, R., Bach, S., & Couturier, C. (2008). The BRET technology and its application to screening assays. *Biotechnology Journal, 3*(3), 311-324. doi:10.1002/biot.200700222

Bailey, C. P., Couch, D., Johnson, E., Griffiths, K., Kelly, E., & Henderson, G. (2003). Mu-opioid receptor desensitization in mature rat neurons: lack of interaction between DAMGO and morphine. *J Neurosci, 23*(33), 10515-10520. doi:10.1523/jneurosci.23-33-10515.2003

Bailey, C. P., Kelly, E., & Henderson, G. (2004). Protein kinase C activation enhances morphine-induced rapid desensitization of mu-opioid receptors in mature rat locus ceruleus neurons. *Mol Pharmacol, 66*(6), 1592-1598. doi:10.1124/mol.104.004747

Bailey, C. P., Llorente, J., Gabra, B. H., Smith, F. L., Dewey, W. L., Kelly, E., et al. (2009a). Role of protein kinase C and mu-opioid receptor (MOPr) desensitization in tolerance to morphine in rat locus coeruleus neurons. *Eur J Neurosci, 29*(2), 307-318. doi:10.1111/j.1460-9568.2008.06573.x

Bailey, C. P., Oldfield, S., Llorente, J., Caunt, C. J., Teschemacher, A. G., Roberts, L., et al. (2009b). Involvement of PKC alpha and G-protein-coupled receptor kinase 2 in agonist-selective desensitization of mu-opioid receptors in mature brain neurons. *Br J Pharmacol, 158*(1), 157-164. doi:10.1111/j.1476-5381.2009.00140.x

Beaulieu, J. M., Gainetdinov, R. R., & Caron, M. G. (2007). The Akt-GSK-3 signaling cascade in the actions of dopamine. *Trends Pharmacol Sci, 28*(4), 166-172. doi:10.1016/j.tips.2007.02.006

Bingel, U., Lorenz, J., Schoell, E., Weiller, C., & Büchel, C. (2006). Mechanisms of placebo analgesia: rACC recruitment of a subcortical antinociceptive network. *Pain, 120*(1-2), 8-15. doi:10.1016/j.pain.2005.08.027

Birdsong, W. T., & Williams, J. T. (2020). Recent progress in opioid research from an electrophysiological perspective. *Molecular Pharmacology*, mol.119.119040. doi:10.1124/mol.119.119040

Black, J. W., & Leff, P. (1983). Operational models of pharmacological agonism. *Proceedings of the Royal Society of London. Series B. Biological Sciences, 220*(1219), 141-162. doi:10.1098/rspb.1983.0093

Boerrigter, G., Lark, M. W., Whalen, E. J., Soergel, D. G., Violin, J. D., & Burnett, J. C., Jr. (2011). Cardiorenal actions of TRV120027, a novel ss-arrestin-biased ligand at the angiotensin II type I receptor, in healthy and heart failure canines: a novel therapeutic strategy for acute heart failure. *Circ Heart Fail, 4*(6), 770-778. doi:10.1161/CIRCHEARTFAILURE.111.962571

Bohn, L. M., Gainetdinov, R. R., Lin, F. T., Lefkowitz, R. J., & Caron, M. G. (2000). Mu-opioid receptor desensitization by beta-arrestin-2 determines morphine tolerance but not dependence. *Nature, 408*(6813), 720-723. doi:10.1038/35047086

Bohn, L. M., Lefkowitz, R. J., & Caron, M. G. (2002). Differential Mechanisms of Morphine Antinociceptive Tolerance Revealed in βArrestin-2 Knock-Out Mice. *The*

*Journal of Neuroscience, 22*(23), 10494-10500. doi:10.1523/jneurosci.22-23-10494.2002

Bohn, L. M., Lefkowitz, R. J., Gainetdinov, R. R., Peppel, K., Caron, M. G., & Lin, F. T. (1999). Enhanced morphine analgesia in mice lacking beta-arrestin 2. *Science, 286*(5449), 2495-2498. doi:10.1126/science.286.5449.2495

Borodovsky, A., Wang, Y., Ye, M., Shaw, J. C., Sachsenmeier, K., Deng, N., et al. (2018). Abstract 3751: Inhibition of A<sub>2A</sub>R by AZD4635 induces anti-tumor immunity alone and in combination with anti-PD-L1 in preclinical models. *Cancer Research, 78*(13 Supplement), 3751-3751. doi:10.1158/1538-7445.Am2018-3751

Bouley, R., Waldschmidt, H. V., Cato, M. C., Cannavo, A., Song, J., Cheung, J. Y., et al. (2017). Structural Determinants Influencing the Potency and Selectivity of Indazole-Paroxetine Hybrid G Protein-Coupled Receptor Kinase 2 Inhibitors. *Mol Pharmacol, 92*(6), 707-717. doi:10.1124/mol.117.110130

Bradley, S. J., Molloy, C., Valuskova, P., Dwomoh, L., Scarpa, M., Rossi, M., et al. (2020). Biased M1-muscarinic-receptor-mutant mice inform the design of next-generation drugs. *Nature Chemical Biology, 16*(3), 240-249. doi:10.1038/s41589-019-0453-9

Broom, D. C., Jutkiewicz, E. M., Folk, J. E., Traynor, J. R., Rice, K. C., & Woods, J. H. (2002). Convulsant activity of a non-peptidic delta-opioid receptor agonist is not required for its antidepressant-like effects in Sprague-Dawley rats. *Psychopharmacology (Berl), 164*(1), 42-48. doi:10.1007/s00213-002-1179-y

Brownstein, M. J. (1993). A brief history of opiates, opioid peptides, and opioid receptors. *Proceedings of the National Academy of Sciences, 90*(12), 5391-5393. doi:10.1073/pnas.90.12.5391

Burgueño, J., Pujol, M., Monroy, X., Roche, D., Varela, M. J., Merlos, M., et al. (2017). A Complementary Scale of Biased Agonism for Agonists with Differing Maximal Responses. *Scientific Reports, 7*(1). doi:10.1038/s41598-017-15258-z

Calo, G., Guerrini, R., Rizzi, A., Salvadori, S., & Regoli, D. (2000). Pharmacology of nociceptin and its receptor: a novel therapeutic target. *Br J Pharmacol, 129*(7), 1261-1283. doi:10.1038/sj.bjp.0703219

Campbell, A. P., & Smrcka, A. V. (2018). Targeting G protein-coupled receptor signalling by blocking G proteins. *Nature Reviews Drug Discovery, 17*(11), 789-803. doi:10.1038/nrd.2018.135

Celver, J., Xu, M., Jin, W., Lowe, J., & Chavkin, C. (2004). Distinct domains of the mu-opioid receptor control uncoupling and internalization. *Mol Pharmacol, 65*(3), 528-537. doi:10.1124/mol.65.3.528

Celver, J. P., Lowe, J., Kovoor, A., Gurevich, V. V., & Chavkin, C. (2001). Threonine 180 is required for G-protein-coupled receptor kinase 3- and beta-arrestin 2-mediated desensitization of the mu-opioid receptor in Xenopus oocytes. *J Biol Chem, 276*(7), 4894-4900. doi:10.1074/jbc.M007437200

Che, T. (2020). Advances in the Treatment of Chronic Pain by Targeting GPCRs. *Biochemistry*. doi:10.1021/acs.biochem.0c00644

Che, T., Majumdar, S., Zaidi, S. A., Ondachi, P., McCorvy, J. D., Wang, S., et al. (2018). Structure of the Nanobody-Stabilized Active State of the Kappa Opioid Receptor. *Cell, 172*(1-2), 55-67.e15. doi:10.1016/j.cell.2017.12.011

Cheng, J. X., Cheng, T., Li, W. H., Liu, G. X., Zhu, W. L., & Tang, Y. (2018). Computational insights into the G-protein-biased activation and inactivation mechanisms of the μ opioid receptor. *Acta Pharmacol Sin, 39*(1), 154-164. doi:10.1038/aps.2017.158

Cheng, Z. J., Yu, Q. M., Wu, Y. L., Ma, L., & Pei, G. (1998). Selective interference of beta-arrestin 1 with kappa and delta but not mu opioid receptor/G protein coupling. *J Biol Chem, 273*(38), 24328-24333. doi:10.1074/jbc.273.38.24328

Chun, E., Thompson, A. A., Liu, W., Roth, C. B., Griffith, M. T., Katritch, V., et al. (2012). Fusion partner toolchest for the stabilization and crystallization of G protein-coupled receptors. *Structure, 20*(6), 967-976. doi:10.1016/j.str.2012.04.010

Clayton, C. C., Donthamsetti, P., Lambert, N. A., Javitch, J. A., & Neve, K. A. (2014). Mutation of three residues in the third intracellular loop of the dopamine D2 receptor creates an internalization-defective receptor. *J Biol Chem, 289*(48), 33663-33675. doi:10.1074/jbc.M114.605378

Congreve, M., Andrews, S. P., Dore, A. S., Hollenstein, K., Hurrell, E., Langmead, C. J., et al. (2012). Discovery of 1,2,4-triazine derivatives as adenosine A(2A) antagonists

using structure based drug design. *J Med Chem, 55*(5), 1898-1903. doi:10.1021/jm201376w

Congreve, M., de Graaf, C., Swain, N. A., & Tate, C. G. (2020). Impact of GPCR Structures on Drug Discovery. *Cell, 181*(1), 81-91. doi:10.1016/j.cell.2020.03.003

Conibear, A. E., Asghar, J., Hill, R., Henderson, G., Borbely, E., Tekus, V., et al. (2020). A Novel G Protein–Biased Agonist at the δ Opioid Receptor with Analgesic Efficacy in Models of Chronic Pain. *Journal of Pharmacology and Experimental Therapeutics, 372*(2), 224-236. doi:10.1124/jpet.119.258640

Conibear, A. E., & Kelly, E. (2019). A Biased View of mu-Opioid Receptors? *Mol Pharmacol, 96*(5), 542-549. doi:10.1124/mol.119.115956

Conn, P. J., Christopoulos, A., & Lindsley, C. W. (2009). Allosteric modulators of GPCRs: a novel approach for the treatment of CNS disorders. *Nat Rev Drug Discov, 8*(1), 41-54. doi:10.1038/nrd2760

Cook, A. M., Mieure, K. D., Owen, R. D., Pesaturo, A. B., & Hatton, J. (2009). Intracerebroventricular Administration of Drugs. *Pharmacotherapy, 29*(7), 832-845. doi:10.1592/phco.29.7.832

Corbett, A. D., Henderson, G., McKnight, A. T., & Paterson, S. J. (2006). 75 years of opioid research: the exciting but vain quest for the Holy Grail. *British Journal of Pharmacology, 147*(S1), S153-S162. doi:10.1038/sj.bjp.0706435

Corder, G., Castro, D. C., Bruchas, M. R., & Scherrer, G. (2018). Endogenous and Exogenous Opioids in Pain. *Annu Rev Neurosci, 41*, 453-473. doi:10.1146/annurev-neuro-080317-061522

Corder, G., Tawfik, V. L., Wang, D., Sypek, E. I., Low, S. A., Dickinson, J. R., et al. (2017). Loss of μ opioid receptor signaling in nociceptors, but not microglia, abrogates morphine tolerance without disrupting analgesia. *Nat Med, 23*(2), 164-173. doi:10.1038/nm.4262

Crawford, K. W., Frey, E. A., & Cote, T. E. (1992). Angiotensin II receptor recognized by DuP753 regulates two distinct guanine nucleotide-binding protein signaling pathways. *Mol Pharmacol, 41*(1), 154-162.

Crowley, N. A., & Kash, T. L. (2015). Kappa opioid receptor signaling in the brain: Circuitry and implications for treatment. *Progress in Neuro-Psychopharmacology and Biological Psychiatry, 62*, 51-60. doi:10.1016/j.pnpbp.2015.01.001

Czapla, M. A., Gozal, D., Alea, O. A., Beckerman, R. C., & Zadina, J. E. (2000). Differential Cardiorespiratory Effects of Endomorphin 1, Endomorphin 2, DAMGO, and Morphine. *American Journal of Respiratory and Critical Care Medicine, 162*(3), 994-999. doi:10.1164/ajrccm.162.3.9911102

Dahan, A., Yassen, A., Romberg, R., Sarton, E., Teppema, L., Olofsen, E., et al. (2006). Buprenorphine induces ceiling in respiratory depression but not in analgesia. *Br J Anaesth, 96*(5), 627-632. doi:10.1093/bja/ael051

Dang, V. C., Chieng, B., Azriel, Y., & Christie, M. J. (2011). Cellular Morphine Tolerance Produced by Arrestin-2-Dependent Impairment of -Opioid Receptor Resensitization. *31*(19), 7122-7130. doi:10.1523/jneurosci.5999-10.2011

Dang, V. C., Napier, I. A., & Christie, M. J. (2009). Two Distinct Mechanisms Mediate Acute -Opioid Receptor Desensitization in Native Neurons. *Journal of Neuroscience, 29*(10), 3322-3327. doi:10.1523/jneurosci.4749-08.2009

Dang, V. C., & Williams, J. T. (2004). Chronic morphine treatment reduces recovery from opioid desensitization. *J Neurosci, 24*(35), 7699-7706. doi:10.1523/jneurosci.2499-04.2004

de Francisco, A. L. (2005). Cinacalcet HCl: a novel therapeutic for hyperparathyroidism. *Expert Opin Pharmacother, 6*(3), 441-452. doi:10.1517/14656566.6.3.441

Dekan, Z., Sianati, S., Yousuf, A., Sutcliffe, K. J., Gillis, A., Mallet, C., et al. (2019). A tetrapeptide class of biased analgesics from an Australian fungus targets the micro-opioid receptor. *Proc Natl Acad Sci U S A, 116*(44), 22353-22358. doi:10.1073/pnas.1908662116

Dershem, R., Metpally, R. P. R., Jeffreys, K., Krishnamurthy, S., Smelser, D. T., Hershfinkel, M., et al. (2019). Rare-variant pathogenicity triage and inclusion of synonymous variants improves analysis of disease associations of orphan G protein-coupled receptors. *J Biol Chem, 294*(48), 18109-18121. doi:10.1074/jbc.RA119.009253

DeWire, S. M., Yamashita, D. S., Rominger, D. H., Liu, G., Cowan, C. L., Graczyk, T. M., et al. (2013). A G protein-biased ligand at the mu-opioid receptor is potently analgesic with reduced gastrointestinal and respiratory dysfunction compared with morphine. *J Pharmacol Exp Ther, 344*(3), 708-717. doi:10.1124/jpet.112.201616

Dhami, G. K., Anborgh, P. H., Dale, L. B., Sterne-Marr, R., & Ferguson, S. S. (2002). Phosphorylation-independent regulation of metabotropic glutamate receptor signaling by G protein-coupled receptor kinase 2. *J Biol Chem, 277*(28), 25266-25272. doi:10.1074/jbc.M203593200

Dhami, G. K., Babwah, A. V., Sterne-Marr, R., & Ferguson, S. S. (2005). Phosphorylation-independent regulation of metabotropic glutamate receptor 1 signaling requires g protein-coupled receptor kinase 2 binding to the second intracellular loop. *J Biol Chem, 280*(26), 24420-24427. doi:10.1074/jbc.M501650200

Doll, C., Konietzko, J., Pöll, F., Koch, T., Höllt, V., & Schulz, S. (2011). Agonist-selective patterns of μ-opioid receptor phosphorylation revealed by phosphosite-specific antibodies. *British Journal of Pharmacology, 164*(2), 298-307. doi:10.1111/j.1476-5381.2011.01382.x

Doll, C., Pöll, F., Peuker, K., Loktev, A., Glück, L., & Schulz, S. (2012). Deciphering μ-opioid receptor phosphorylation and dephosphorylation in HEK293 cells. *Br J Pharmacol, 167*(6), 1259-1270. doi:10.1111/j.1476-5381.2012.02080.x

Dripps, I. J., Boyer, B. T., Neubig, R. R., Rice, K. C., Traynor, J. R., & Jutkiewicz, E. M. (2018). Role of signalling molecules in behaviours mediated by the δ opioid receptor agonist SNC80. *Br J Pharmacol, 175*(6), 891-901. doi:10.1111/bph.14131

Edvinsson, L., Haanes, K. A., Warfvinge, K., & Krause, D. N. (2018). CGRP as the target of new migraine therapies — successful translation from bench to clinic. *Nature Reviews Neurology, 14*(6), 338-350. doi:10.1038/s41582-018-0003-1

Ehrlich, A. T., Semache, M., Gross, F., Da Fonte, D. F., Runtz, L., Colley, C., et al. (2019). Biased Signaling of the Mu Opioid Receptor Revealed in Native Neurons. *iScience, 14*, 47-57. doi:10.1016/j.isci.2019.03.011

Falcon, E., Browne, C. A., Leon, R. M., Fleites, V. C., Sweeney, R., Kirby, L. G., et al. (2016). Antidepressant-like Effects of Buprenorphine are Mediated by Kappa Opioid Receptors. *Neuropsychopharmacology, 41*(9), 2344-2351. doi:10.1038/npp.2016.38

Fenalti, G., Zatsepin, N. A., Betti, C., Giguere, P., Han, G. W., Ishchenko, A., et al. (2015). Structural basis for bifunctional peptide recognition at human δ-opioid receptor. *Nat Struct Mol Biol, 22*(3), 265-268. doi:10.1038/nsmb.2965

Feng, B., Li, Z., & Wang, J. B. (2011). Protein kinase C-mediated phosphorylation of the μ-opioid receptor and its effects on receptor signaling. *Mol Pharmacol, 79*(4), 768-775. doi:10.1124/mol.110.069096

Foote, S. L., Bloom, F. E., & Aston-Jones, G. (1983). Nucleus locus ceruleus: new evidence of anatomical and physiological specificity. *Physiological Reviews, 63*(3), 844-914. doi:10.1152/physrev.1983.63.3.844

Ford, B. M., Franks, L. N., Tai, S., Fantegrossi, W. E., Stahl, E. L., Berquist, M. D., et al. (2017). Characterization of structurally novel G protein biased CB1 agonists: Implications for drug development. *Pharmacol Res, 125*(Pt B), 161-177. doi:10.1016/j.phrs.2017.08.008

Foster, D. J., & Conn, P. J. (2017). Allosteric Modulation of GPCRs: New Insights and Potential Utility for Treatment of Schizophrenia and Other CNS Disorders. *Neuron, 94*(3), 431-446. doi:10.1016/j.neuron.2017.03.016

Foster, S. R., & Bräuner-Osborne, H. (2018). Investigating Internalization and Intracellular Trafficking of GPCRs: New Techniques and Real-Time Experimental Approaches. *Handb Exp Pharmacol, 245*, 41-61. doi:10.1007/164_2017_57

Garcia-Nafria, J., & Tate, C. G. (2020). Cryo-Electron Microscopy: Moving Beyond X-Ray Crystal Structures for Drug Receptors and Drug Development. *Annu Rev Pharmacol Toxicol, 60*(1), 51-71. doi:10.1146/annurev-pharmtox-010919-023545

Gasiunaite, G. (2017). *Galanin receptor dimerisation.* (PhD). University of Bristol,

Gillis, A., Gondin, A. B., Kliewer, A., Sanchez, J., Lim, H. D., Alamein, C., et al. (2020a). Low intrinsic efficacy for G protein activation can explain the improved side effect profiles of new opioid agonists. *Sci Signal, 13*(625), eaaz3140. doi:10.1126/scisignal.aaz3140

Gillis, A., Kliewer, A., Kelly, E., Henderson, G., Christie, M. J., Schulz, S., et al. (2020b). Critical Assessment of G Protein-Biased Agonism at the mu-Opioid Receptor. *Trends Pharmacol Sci, 41*(12), 947-959. doi:10.1016/j.tips.2020.09.009

Gillis, A., Sreenivasan, V., & Christie, M. J. (2020c). Intrinsic efficacy of opioid ligands and its importance for apparent bias, operational analysis and therapeutic window. *Mol Pharmacol*, mol.119.119214. doi:10.1124/mol.119.119214

Gloriam, D. E., Fredriksson, R., & Schiöth, H. B. (2007). The G protein-coupled receptor subset of the rat genome. *BMC Genomics, 8*, 338. doi:10.1186/1471-2164-8-338

Gondin, A. B., Halls, M. L., Canals, M., & Briddon, S. J. (2019). GRK Mediates μ-Opioid Receptor Plasma Membrane Reorganization. *Frontiers in Molecular Neuroscience, 12*. doi:10.3389/fnmol.2019.00104

Goodman, O. B., Jr., Krupnick, J. G., Santini, F., Gurevich, V. V., Penn, R. B., Gagnon, A. W., et al. (1996). Beta-arrestin acts as a clathrin adaptor in endocytosis of the beta2-adrenergic receptor. *Nature, 383*(6599), 447-450. doi:10.1038/383447a0

Granier, S., Manglik, A., Kruse, A. C., Kobilka, T. S., Thian, F. S., Weis, W. I., et al. (2012). Structure of the δ-opioid receptor bound to naltrindole. *Nature, 485*(7398), 400-404. doi:10.1038/nature11111

Grecksch, G., Just, S., Pierstorff, C., Imhof, A. K., Glück, L., Doll, C., et al. (2011). Analgesic tolerance to high-efficacy agonists but not to morphine is diminished in phosphorylation-deficient S375A μ-opioid receptor knock-in mice. *J Neurosci, 31*(39), 13890-13896. doi:10.1523/jneurosci.2304-11.2011

Grim, T. W., Schmid, C. L., Stahl, E. L., Pantouli, F., Ho, J. H., Acevedo-Canabal, A., et al. (2020). A G protein signaling-biased agonist at the mu-opioid receptor reverses morphine tolerance while preventing morphine withdrawal. *Neuropsychopharmacology, 45*(2), 416-425. doi:10.1038/s41386-019-0491-8

Grundmann, M., Merten, N., Malfacini, D., Inoue, A., Preis, P., Simon, K., et al. (2018). Lack of beta-arrestin signaling in the absence of active G proteins. *Nature Communications, 9*(1), 341. doi:10.1038/s41467-017-02661-3

Gudin, J., & Fudin, J. (2020). A Narrative Pharmacological Review of Buprenorphine: A Unique Opioid for the Treatment of Chronic Pain. *Pain Ther, 9*(1), 41-54. doi:10.1007/s40122-019-00143-6

Gurevich, E. V., & Gurevich, V. V. (2006). Arrestins: ubiquitous regulators of cellular signaling pathways. *Genome Biol, 7*(9), 236. doi:10.1186/gb-2006-7-9-236

Gurevich, V. V., & Gurevich, E. V. (2019). GPCR Signaling Regulation: The Role of GRKs and Arrestins. *Frontiers in Pharmacology, 10*. doi:10.3389/fphar.2019.00125

Hamdan, F. F., Audet, M., Garneau, P., Pelletier, J., & Bouvier, M. (2005). High-throughput screening of G protein-coupled receptor antagonists using a bioluminescence resonance energy transfer 1-based beta-arrestin2 recruitment assay. *J Biomol Screen, 10*(5), 463-475. doi:10.1177/1087057105275344

Han, Z., Boyle, D. L., Chang, L., Bennett, B., Karin, M., Yang, L., et al. (2001). c-Jun N-terminal kinase is required for metalloproteinase expression and joint destruction in inflammatory arthritis. *Journal of Clinical Investigation, 108*(1), 73-81. doi:10.1172/jci12466

Hanyaloglu, A. C., & von Zastrow, M. (2008). Regulation of GPCRs by endocytic membrane trafficking and its potential implications. *Annu Rev Pharmacol Toxicol, 48*(1), 537-568. doi:10.1146/annurev.pharmtox.48.113006.094830

Harris, G. C., & Williams, J. T. (1991). Transient homologous mu-opioid receptor desensitization in rat locus coeruleus neurons. *J Neurosci, 11*(8), 2574-2581. doi:10.1523/jneurosci.11-08-02574.1991

Harris, L. S., & Pierson, A. K. (1964). Some Narcotic Antagonists in the Benzomorphan Series. *J Pharmacol Exp Ther, 143*, 141-148.

Hart, M. J., Jiang, X., Kozasa, T., Roscoe, W., Singer, W. D., Gilman, A. G., et al. (1998). Direct stimulation of the guanine nucleotide exchange activity of p115 RhoGEF by Galpha13. *Science, 280*(5372), 2112-2114. doi:10.1126/science.280.5372.2112

Hasbi, A., Devost, D., Laporte, S. p. A., & Zingg, H. H. (2004). Real-Time Detection of Interactions between the Human Oxytocin Receptor and G Protein-Coupled Receptor Kinase-2. *Molecular Endocrinology, 18*(5), 1277-1286. doi:10.1210/me.2003-0440

Hauser, A. S., Attwood, M. M., Rask-Andersen, M., Schioth, H. B., & Gloriam, D. E. (2017). Trends in GPCR drug discovery: new agents, targets and indications. *Nat Rev Drug Discov, 16*(12), 829-842. doi:10.1038/nrd.2017.178

Hauser, A. S., Gloriam, D. E., Brauner-Osborne, H., & Foster, S. R. (2020). Novel approaches leading towards peptide GPCR de-orphanisation. *Br J Pharmacol, 177*(5), 961-968. doi:10.1111/bph.14950

Henderson, G., & Hughes, J. (1976). THE EFFECTS OF MORPHINE ON THE RELEASE OF NORADRENALINE FROM THE MOUSE VAS DEFERENS. *British Journal of Pharmacology, 57*(4), 551-557. doi:10.1111/j.1476-5381.1976.tb10384.x

Henderson, G., & McKnight, A. T. (1997). The orphan opioid receptor and its endogenous ligand--nociceptin/orphanin FQ. *Trends Pharmacol Sci, 18*(8), 293-300.

Hepler, J. R., & Gilman, A. G. (1992). G proteins. *Trends Biochem Sci, 17*(10), 383-387. doi:10.1016/0968-0004(92)90005-t

Hill, R., Dewey, W. L., Kelly, E., & Henderson, G. (2018a). Oxycodone-induced tolerance to respiratory depression: reversal by ethanol, pregabalin and protein kinase C inhibition. *Br J Pharmacol, 175*(12), 2492-2503. doi:10.1111/bph.14219

Hill, R., Disney, A., Conibear, A., Sutcliffe, K., Dewey, W., Husbands, S., et al. (2018b). The novel mu-opioid receptor agonist PZM21 depresses respiration and induces tolerance to antinociception. *Br J Pharmacol, 175*(13), 2653-2661. doi:10.1111/bph.14224

Hill, R., Santhakumar, R., Dewey, W., Kelly, E., & Henderson, G. (2020). Fentanyl depression of respiration: Comparison with heroin and morphine. *British Journal of Pharmacology, 177*(2), 254-265. doi:10.1111/bph.14860

Hill, S. J. (2006). G-protein-coupled receptors: past, present and future. *Br J Pharmacol, 147 Suppl 1*(Suppl 1), S27-37. doi:10.1038/sj.bjp.0706455

Hothersall, J. D., Torella, R., Humphreys, S., Hooley, M., Brown, A., McMurray, G., et al. (2017). Residues W320 and Y328 within the binding site of the μ-opioid receptor influence opiate ligand bias. *Neuropharmacology, 118*, 46-58. doi:10.1016/j.neuropharm.2017.03.007

Huang, W., Manglik, A., Venkatakrishnan, A. J., Laeremans, T., Feinberg, E. N., Sanborn, A. L., et al. (2015). Structural insights into μ-opioid receptor activation. *Nature, 524*(7565), 315-321. doi:10.1038/nature14886

Hughes, J., Smith, T., Morgan, B., & Fothergill, L. (1975). Purification and properties of enkephalin — The possible endogenous ligand for the morphine receptor. *16*(12), 1753-1758. doi:10.1016/0024-3205(75)90268-4

Hull, L. C., Llorente, J., Gabra, B. H., Smith, F. L., Kelly, E., Bailey, C., et al. (2010). The effect of protein kinase C and G protein-coupled receptor kinase inhibition on tolerance induced by mu-opioid agonists of different efficacy. *J Pharmacol Exp Ther, 332*(3), 1127-1135. doi:10.1124/jpet.109.161455

Hutchinson, M. R., Shavit, Y., Grace, P. M., Rice, K. C., Maier, S. F., & Watkins, L. R. (2011). Exploring the neuroimmunopharmacology of opioids: an integrative review of mechanisms of central immune signaling and their implications for opioid analgesia. *Pharmacol Rev, 63*(3), 772-810. doi:10.1124/pr.110.004135

Irannejad, R., & von Zastrow, M. (2014). GPCR signaling along the endocytic pathway. *Curr Opin Cell Biol, 27*, 109-116. doi:10.1016/j.ceb.2013.10.003

Ishii, K., Yamamoto, S., Muraki, T., & Kato, R. (1981). Partial agonistic action of morphine in the rat vas deferens. *The Japanese Journal of Pharmacology, 31*(6), 905-909. doi:10.1254/jjp.31.905

James, M. H., Mahler, S. V., Moorman, D. E., & Aston-Jones, G. (2017). A Decade of Orexin/Hypocretin and Addiction: Where Are We Now? *Curr Top Behav Neurosci, 33*, 247-281. doi:10.1007/7854_2016_57

Janetopoulos, C., Jin, T., & Devreotes, P. (2001). Receptor-mediated activation of heterotrimeric G-proteins in living cells. *Science, 291*(5512), 2408-2411. doi:10.1126/science.1055835

Janssen, P. A., Niemegeers, C. J., & Dony, J. G. (1963). The inhibitory effect of fentanyl and other morphine-like analgesics on the warm water induced tail withdrawl reflex in rats. *Arzneimittelforschung, 13*, 502-507.

Jarpe, M. B., Knall, C., Mitchell, F. M., Buhl, A. M., Duzic, E., & Johnson, G. L. (1998). [D-Arg1,D-Phe5,D-Trp7,9,Leu11]Substance P acts as a biased agonist toward neuropeptide and chemokine receptors. *J Biol Chem, 273*(5), 3097-3104. doi:10.1074/jbc.273.5.3097

Johnson, E. A., Oldfield, S., Braksator, E., Gonzalez-Cuello, A., Couch, D., Hall, K. J., et al. (2006). Agonist-selective mechanisms of mu-opioid receptor desensitization in human embryonic kidney 293 cells. *Mol Pharmacol, 70*(2), 676-685. doi:10.1124/mol.106.022376

Johnson, M. P., Muhlhauser, M. A., Nisenbaum, E. S., Simmons, R. M., Forster, B. M., Knopp, K. L., et al. (2017). Broad spectrum efficacy with LY2969822, an oral prodrug of metabotropic glutamate 2/3 receptor agonist LY2934747, in rodent pain models. *Br J Pharmacol, 174*(9), 822-835. doi:10.1111/bph.13740

Just, S., Illing, S., Trester-Zedlitz, M., Lau, E. K., Kotowski, S. J., Miess, E., et al. (2013). Differentiation of opioid drug effects by hierarchical multi-site phosphorylation. *Mol Pharmacol, 83*(3), 633-639. doi:10.1124/mol.112.082875

Kapoor, A., Provasi, D., & Filizola, M. (2020). Atomic-Level Characterization of the Methadone-Stabilized Active Conformation of μ-Opioid Receptor. *Mol Pharmacol*. doi:10.1124/mol.119.119339

Karaman, M. W., Herrgard, S., Treiber, D. K., Gallant, P., Atteridge, C. E., Campbell, B. T., et al. (2008). A quantitative analysis of kinase inhibitor selectivity. *Nature Biotechnology, 26*(1), 127-132. doi:10.1038/nbt1358

Kastin, A. J., Pan, W., Maness, L. M., & Banks, W. A. (1999). Peptides crossing the blood-brain barrier: some unusual observations. *Brain Res, 848*(1-2), 96-100. doi:10.1016/s0006-8993(99)01961-7

Kelly, E. (2013). Efficacy and ligand bias at the mu-opioid receptor. *Br J Pharmacol, 169*(7), 1430-1446. doi:10.1111/bph.12222

Kelly, E., Bailey, C. P., & Henderson, G. (2008). Agonist-selective mechanisms of GPCR desensitization. *Br J Pharmacol, 153 Suppl 1*(S1), S379-388. doi:10.1038/sj.bjp.0707604

Kenakin, T. (2011). Functional selectivity and biased receptor signaling. *J Pharmacol Exp Ther, 336*(2), 296-302. doi:10.1124/jpet.110.173948

Kenakin, T. (2017). Signaling bias in drug discovery. *Expert Opinion on Drug Discovery, 12*(4), 321-333. doi:10.1080/17460441.2017.1297417

Kenakin, T. (2018). Is the Quest for Signaling Bias Worth the Effort? *Molecular Pharmacology, 93*(4), 266-269. doi:10.1124/mol.117.111187

Kenakin, T. (2020). Biased signaling as allosteric probe dependence. *Cell Signal*, 109844. doi:10.1016/j.cellsig.2020.109844

Kenakin, T. P. (2009). *A pharmacology primer : theory, applications, and methods*. Amsterdam; Boston: Academic Press/Elsevier.

Keov, P., Sexton, P. M., & Christopoulos, A. (2011). Allosteric modulation of G protein-coupled receptors: a pharmacological perspective. *Neuropharmacology, 60*(1), 24-35. doi:10.1016/j.neuropharm.2010.07.010

Khan, S. M., Sleno, R., Gora, S., Zylbergold, P., Laverdure, J. P., Labbé, J. C., et al. (2013). The expanding roles of Gβγ subunits in G protein-coupled receptor signaling and drug action. *Pharmacol Rev, 65*(2), 545-577. doi:10.1124/pr.111.005603

Kieffer, B. L., & Evans, C. J. (2009). Opioid receptors: from binding sites to visible molecules in vivo. *Neuropharmacology, 56 Suppl 1*(Suppl 1), 205-212. doi:10.1016/j.neuropharm.2008.07.033

Kilkenny, C., Browne, W. J., Cuthill, I. C., Emerson, M., & Altman, D. G. (2010). Improving bioscience research reporting: the ARRIVE guidelines for reporting animal research. *PLoS Biol, 8*(6), e1000412. doi:10.1371/journal.pbio.1000412

Kliewer, A., Gillis, A., Hill, R., Schmidel, F., Bailey, C., Kelly, E., et al. (2020). Morphine-induced respiratory depression is independent of beta-arrestin2 signalling. *Br J Pharmacol*. doi:10.1111/bph.15004

Kliewer, A., Schmiedel, F., Sianati, S., Bailey, A., Bateman, J. T., Levitt, E. S., et al. (2019). Phosphorylation-deficient G-protein-biased mu-opioid receptors improve analgesia and diminish tolerance but worsen opioid side effects. *Nat Commun, 10*(1), 367. doi:10.1038/s41467-018-08162-1

Knapman, A., Santiago, M., Du, Y. P., Bennallack, P. R., Christie, M. J., & Connor, M. (2013). A Continuous, Fluorescence-based Assay of μ-Opioid Receptor Activation in AtT-20 Cells. *Journal of Biomolecular Screening, 18*(3), 269-276. doi:10.1177/1087057112461376

Koch, T., Brandenburg, L. O., Liang, Y., Schulz, S., Beyer, A., Schroder, H., et al. (2004). Phospholipase D2 modulates agonist-induced mu-opioid receptor desensitization and resensitization. *J Neurochem, 88*(3), 680-688. doi:10.1046/j.1471-4159.2003.02189.x

Koch, T., & Höllt, V. (2008). Role of receptor internalization in opioid tolerance and dependence. *Pharmacol Ther, 117*(2), 199-206. doi:10.1016/j.pharmthera.2007.10.003

Koch, W. J., Inglese, J., Stone, W. C., & Lefkowitz, R. J. (1993). The binding site for the beta gamma subunits of heterotrimeric G proteins on the beta-adrenergic receptor kinase. *J Biol Chem, 268*(11), 8256-8260.

Koehl, A., Hu, H., Maeda, S., Zhang, Y., Qu, Q., Paggi, J. M., et al. (2018). Structure of the μ-opioid receptor-G(i) protein complex. *Nature, 558*(7711), 547-552. doi:10.1038/s41586-018-0219-7

Konkoy, C. S., & Davis, T. P. (1995). Regional metabolism of Met-enkephalin and cholecystokinin on intact ratbrain slices: characterization of specific peptidases. *J Neurochem, 65*(6), 2773-2782. doi:10.1046/j.1471-4159.1995.65062773.x

Kozasa, T., Kaziro, Y., Ohtsuka, T., Grigg, J. J., Nakajima, S., & Nakajima, Y. (1996). G protein specificity of the muscarine-induced increase in an inward rectifier potassium current in AtT-20 cells. *Neurosci Res, 26*(3), 289-297. doi:10.1016/s0168-0102(96)01111-x

Kuhar, J. R., Bedini, A., Melief, E. J., Chiu, Y.-C., Striegel, H. N., & Chavkin, C. (2015). Mu opioid receptor stimulation activates c-Jun N-terminal kinase 2 by distinct arrestin-dependent and independent mechanisms. *Cellular Signalling, 27*(9), 1799-1806. doi:10.1016/j.cellsig.2015.05.019

Lambert, D., & Calo, G. (2020). Approval of oliceridine (TRV130) for intravenous use in moderate to severe pain in adults. *British Journal of Anaesthesia, 125*(6), e473-e474. doi:10.1016/j.bja.2020.09.021

Lane, J. R., May, L. T., Parton, R. G., Sexton, P. M., & Christopoulos, A. (2017). A kinetic view of GPCR allostery and biased agonism. *Nat Chem Biol, 13*(9), 929-937. doi:10.1038/nchembio.2431

Laporte, S. A., Oakley, R. H., Zhang, J., Holt, J. A., Ferguson, S. S., Caron, M. G., et al. (1999). The beta2-adrenergic receptor/betaarrestin complex recruits the clathrin adaptor AP-2 during endocytosis. *Proc Natl Acad Sci U S A, 96*(7), 3712-3717. doi:10.1073/pnas.96.7.3712

Laschet, C., Dupuis, N., & Hanson, J. (2018). The G protein-coupled receptors deorphanization landscape. *Biochem Pharmacol, 153*, 62-74. doi:10.1016/j.bcp.2018.02.016

Latremoliere, A., & Woolf, C. J. (2009). Central sensitization: a generator of pain hypersensitivity by central neural plasticity. *J Pain, 10*(9), 895-926. doi:10.1016/j.jpain.2009.06.012

Latta, K. S., Ginsberg, B., & Barkin, R. L. (2002). Meperidine: a critical review. *Am J Ther, 9*(1), 53-68. doi:10.1097/00045391-200201000-00010

Le Bars, D., Gozariu, M., & Cadden, S. W. (2001). Animal models of nociception. *Pharmacol Rev, 53*(4), 597-652.

Leff, E. R., Arttamangkul, S., & Williams, J. T. (2020). Chronic treatment with morphine disrupts acute kinase-dependent desensitization of GPCRs. *Mol Pharmacol*. doi:10.1124/mol.119.119362

Lemaire, S., Magnan, J., & Regoli, D. (1978). RAT VAS DEFERENS: A SPECIFIC BIOASSAY FOR ENDOGENOUS OPIOID PEPTIDES. *British Journal of Pharmacology, 64*(3), 327-329. doi:10.1111/j.1476-5381.1978.tb08653.x

Lemel, L., Lane, J. R., & Canals, M. (2020). GRKs as Key Modulators of Opioid Receptor Function. *Cells, 9*(11), 2400. doi:10.3390/cells9112400

Levitt, E. S., Abdala, A. P., Paton, J. F. R., Bissonnette, J. M., & Williams, J. T. (2015). μ opioid receptor activation hyperpolarizes respiratory-controlling Kölliker-Fuse neurons and suppresses post-inspiratory drive. *The Journal of Physiology, 593*(19), 4453-4469. doi:10.1113/jp270822

Li, L., Homan, K. T., Vishnivetskiy, S. A., Manglik, A., Tesmer, J. J., Gurevich, V. V., et al. (2015). G Protein-coupled Receptor Kinases of the GRK4 Protein Subfamily Phosphorylate Inactive G Protein-coupled Receptors (GPCRs). *J Biol Chem, 290*(17), 10775-10790. doi:10.1074/jbc.M115.644773

Li, Y., Cazares, M., Wu, J., Houghten, R. A., Toll, L., & Dooley, C. (2016). Potent mu-Opioid Receptor Agonists from Cyclic Peptides Tyr-c[D-Lys-Xxx-Tyr-Gly]: Synthesis, Biological, and Structural Evaluation. *J Med Chem, 59*(3), 1239-1245. doi:10.1021/acs.jmedchem.5b01899

Li, Y., Lefever, M. R., Muthu, D., Bidlack, J. M., Bilsky, E. J., & Polt, R. (2012). Opioid glycopeptide analgesics derived from endogenous enkephalins and endorphins. *Future Med Chem, 4*(2), 205-226. doi:10.4155/fmc.11.195

Liang, D.-Y., Li, W.-W., Nwaneshiudu, C., Irvine, K.-A., & Clark, J. D. (2019). Pharmacological Characters of Oliceridine, a μ-Opioid Receptor G-Protein–Biased Ligand in Mice. *Anesthesia & Analgesia, 129*(5), 1414-1421. doi:10.1213/ane.0000000000003662

Liang, Y. L., Khoshouei, M., Glukhova, A., Furness, S. G. B., Zhao, P., Clydesdale, L., et al. (2018). Phase-plate cryo-EM structure of a biased agonist-bound human GLP-1 receptor-Gs complex. *Nature, 555*(7694), 121-125. doi:10.1038/nature25773

Lim, G., Sung, B., Ji, R. R., & Mao, J. (2003). Upregulation of spinal cannabinoid-1-receptors following nerve injury enhances the effects of Win 55,212-2 on neuropathic pain behaviors in rats. *Pain, 105*(1-2), 275-283. doi:10.1016/s0304-3959(03)00242-2

Liu, W., Chun, E., Thompson, A. A., Chubukov, P., Xu, F., Katritch, V., et al. (2012). Structural basis for allosteric regulation of GPCRs by sodium ions. *Science, 337*(6091), 232-236. doi:10.1126/science.1219218

Llorente, J., Lowe, J. D., Sanderson, H. S., Tsisanova, E., Kelly, E., Henderson, G., et al. (2012). mu-Opioid receptor desensitization: homologous or heterologous? *Eur J Neurosci, 36*(12), 3636-3642. doi:10.1111/ejn.12003

Lodowski, D. T., Pitcher, J. A., Capel, W. D., Lefkowitz, R. J., & Tesmer, J. J. (2003). Keeping G proteins at bay: a complex between G protein-coupled receptor kinase 2 and Gbetagamma. *Science, 300*(5623), 1256-1262. doi:10.1126/science.1082348

Lohse, M. J., Nuber, S., & Hoffmann, C. (2012). Fluorescence/Bioluminescence Resonance Energy Transfer Techniques to Study G-Protein-Coupled Receptor Activation and Signaling. *Pharmacological Reviews, 64*(2), 299-336. doi:10.1124/pr.110.004309

Lowe, J. D., Sanderson, H. S., Cooke, A. E., Ostovar, M., Tsisanova, E., Withey, S. L., et al. (2015). Role of G Protein-Coupled Receptor Kinases 2 and 3 in mu-Opioid Receptor Desensitization and Internalization. *Mol Pharmacol, 88*(2), 347-356. doi:10.1124/mol.115.098293

Luttrell, L. M., Ferguson, S. S., Daaka, Y., Miller, W. E., Maudsley, S., Della Rocca, G. J., et al. (1999). Beta-arrestin-dependent formation of beta2 adrenergic receptor-Src protein kinase complexes. *Science, 283*(5402), 655-661. doi:10.1126/science.283.5402.655

Luttrell, L. M., Roudabush, F. L., Choy, E. W., Miller, W. E., Field, M. E., Pierce, K. L., et al. (2001). Activation and targeting of extracellular signal-regulated kinases by beta-arrestin scaffolds. *Proc Natl Acad Sci U S A, 98*(5), 2449-2454. doi:10.1073/pnas.041604898

Macey, T. A., Lowe, J. D., & Chavkin, C. (2006). Mu opioid receptor activation of ERK1/2 is GRK3 and arrestin dependent in striatal neurons. *J Biol Chem, 281*(45), 34515-34524. doi:10.1074/jbc.M604278200

Madia, P. A., Dighe, S. V., Sirohi, S., Walker, E. A., & Yoburn, B. C. (2009). Dosing protocol and analgesic efficacy determine opioid tolerance in the mouse. *Psychopharmacology, 207*(3), 413-422. doi:10.1007/s00213-009-1673-6

Magalhaes, A. C., Dunn, H., & Ferguson, S. S. (2012). Regulation of GPCR activity, trafficking and localization by GPCR-interacting proteins. *Br J Pharmacol, 165*(6), 1717-1736. doi:10.1111/j.1476-5381.2011.01552.x

Magnani, F., Serrano-Vega, M. J., Shibata, Y., Abdul-Hussein, S., Lebon, G., Miller-Gallacher, J., et al. (2016). A mutagenesis and screening strategy to generate optimally thermostabilized membrane proteins for structural studies. *Nature Protocols, 11*(8), 1554-1571. doi:10.1038/nprot.2016.088

Malenka, R. C., Madison, D. V., & Nicoll, R. A. (1986). Potentiation of synaptic transmission in the hippocampus by phorbol esters. *Nature, 321*(6066), 175-177. doi:10.1038/321175a0

Manglik, A., Kruse, A. C., Kobilka, T. S., Thian, F. S., Mathiesen, J. M., Sunahara, R. K., et al. (2012). Crystal structure of the micro-opioid receptor bound to a morphinan antagonist. *Nature, 485*(7398), 321-326. doi:10.1038/nature10954

Manglik, A., Lin, H., Aryal, D. K., McCorvy, J. D., Dengler, D., Corder, G., et al. (2016). Structure-based discovery of opioid analgesics with reduced side effects. *Nature, 537*(7619), 185-190. doi:10.1038/nature19112

Manglik, A., Wingler, L. M., Rockman, H. A., & Lefkowitz, R. J. (2020). beta-Arrestin-Biased Angiotensin II Receptor Agonists for COVID-19. *Circulation, 142*(4), 318-320. doi:10.1161/CIRCULATIONAHA.120.048723

Mann, A., Illing, S., Miess, E., & Schulz, S. (2015). Different mechanisms of homologous and heterologous μ-opioid receptor phosphorylation. *British Journal of Pharmacology, 172*(2), 311-316. doi:10.1111/bph.12627

Mansour, A., Fox, C. A., Burke, S., Meng, F., Thompson, R. C., Akil, H., et al. (1994). Mu, delta, and kappa opioid receptor mRNA expression in the rat CNS: An in situ hybridization study. *The Journal of Comparative Neurology, 350*(3), 412-438. doi:10.1002/cne.903500307

Marcus, D. J., Zee, M., Hughes, A., Yuill, M. B., Hohmann, A. G., Mackie, K., et al. (2015). Tolerance to the Antinociceptive Effects of Chronic Morphine Requires C-Jun N-Terminal Kinase. *Molecular Pain, 11*(1), s12990-12015-10031. doi:10.1186/s12990-015-0031-4

Marker, C. L., Stoffel, M., & Wickman, K. (2004). Spinal G-protein-gated K+ channels formed by GIRK1 and GIRK2 subunits modulate thermal nociception and contribute to morphine analgesia. *J Neurosci, 24*(11), 2806-2812. doi:10.1523/jneurosci.5251-03.2004

Markham, A. (2018). Erenumab: First Global Approval. *Drugs, 78*(11), 1157-1161. doi:10.1007/s40265-018-0944-0

Markham, A. (2020). Oliceridine: First Approval. *Drugs, 80*(16), 1739-1744. doi:10.1007/s40265-020-01414-9

Martini, L., & Whistler, J. L. (2007). The role of mu opioid receptor desensitization and endocytosis in morphine tolerance and dependence. *Curr Opin Neurobiol, 17*(5), 556-564. doi:10.1016/j.conb.2007.10.004

Matthes, H. W., Maldonado, R., Simonin, F., Valverde, O., Slowe, S., Kitchen, I., et al. (1996). Loss of morphine-induced analgesia, reward effect and withdrawal symptoms in mice lacking the mu-opioid-receptor gene. *Nature, 383*(6603), 819-823. doi:10.1038/383819a0

McDonald, P. H., Chow, C. W., Miller, W. E., Laporte, S. A., Field, M. E., Lin, F. T., et al. (2000). Beta-arrestin 2: a receptor-regulated MAPK scaffold for the activation of JNK3. *Science, 290*(5496), 1574-1577. doi:10.1126/science.290.5496.1574

McPherson, J., Rivero, G., Baptist, M., Llorente, J., Al-Sabah, S., Krasel, C., et al. (2010). μ-Opioid Receptors: Correlation of Agonist Efficacy for Signalling with Ability to Activate Internalization. *Molecular Pharmacology, 78*(4), 756-766. doi:10.1124/mol.110.066613

McQuay, H. (1999). Opioids in pain management. *Lancet, 353*(9171), 2229-2232. doi:10.1016/s0140-6736(99)03528-x

Melief, E. J., Miyatake, M., Bruchas, M. R., & Chavkin, C. (2010). Ligand-directed c-Jun N-terminal kinase activation disrupts opioid receptor signaling. *Proc Natl Acad Sci U S A, 107*(25), 11608-11613. doi:10.1073/pnas.1000751107

Mende, F., Hundahl, C., Plouffe, B., Skov, L. J., Sivertsen, B., Madsen, A. N., et al. (2018). Translating biased signaling in the ghrelin receptor system into differential in vivo functions. *Proceedings of the National Academy of Sciences*, 201804003. doi:10.1073/pnas.1804003115

Meymandi, M. S., Sepehri, G., & Mobasher, M. (2006). Gabapentin enhances the analgesic response to morphine in acute model of pain in male rats. *Pharmacol Biochem Behav, 85*(1), 185-189. doi:10.1016/j.pbb.2006.07.037

Michel, M. C., & Charlton, S. J. (2018). Biased Agonism in Drug Discovery-Is It Too Soon to Choose a Path? *Mol Pharmacol, 93*(4), 259-265. doi:10.1124/mol.117.110890

Miess, E., Gondin, A. B., Yousuf, A., Steinborn, R., Mosslein, N., Yang, Y., et al. (2018). Multisite phosphorylation is required for sustained interaction with GRKs and arrestins during rapid mu-opioid receptor desensitization. *Sci Signal, 11*(539), eaas9609. doi:10.1126/scisignal.aas9609

Milligan, G. (2010). The role of dimerisation in the cellular trafficking of G-protein-coupled receptors. *Curr Opin Pharmacol, 10*(1), 23-29. doi:10.1016/j.coph.2009.09.010

Minneman, K. P., & Iversen, L. L. (1976). Enkephalin and opiate narcotics increase cyclic GMP accumulation in slices of rat neostriatum. *Nature, 262*(5566), 313-314. doi:10.1038/262313a0

Mittal, N., Tan, M., Egbuta, O., Desai, N., Crawford, C., Xie, C.-W., et al. (2012). Evidence that Behavioral Phenotypes of Morphine in β-arr2−/− Mice Are Due to the Unmasking of JNK Signaling. *Neuropsychopharmacology, 37*(8), 1953-1962. doi:10.1038/npp.2012.42

Møller, T. C., Pedersen, M. F., van Senten, J. R., Seiersen, S. D., Mathiesen, J. M., Bouvier, M., et al. (2020). Dissecting the roles of GRK2 and GRK3 in μ-opioid receptor internalization and β-arrestin2 recruitment using CRISPR/Cas9-edited HEK293 cells. *Sci Rep, 10*(1), 17395. doi:10.1038/s41598-020-73674-0

Mollereau, C., Parmentier, M., Mailleux, P., Butour, J. L., Moisand, C., Chalon, P., et al. (1994). ORL1, a novel member of the opioid receptor family. Cloning, functional expression and localization. *FEBS Lett, 341*(1), 33-38. doi:10.1016/0014-5793(94)80235-1

Montandon, G., Ren, J., Victoria, N. C., Liu, H., Wickman, K., Greer, J. J., et al. (2016). G-protein–gated Inwardly Rectifying Potassium Channels Modulate Respiratory Depression by Opioids. *Anesthesiology, 124*(3), 641-650. doi:10.1097/aln.0000000000000984

Mores, K. L., Cummins, B. R., Cassell, R. J., & Van Rijn, R. M. (2019). A Review of the Therapeutic Potential of Recently Developed G Protein-Biased Kappa Agonists. *Frontiers in Pharmacology, 10*. doi:10.3389/fphar.2019.00407

Morgan, M. M., & Christie, M. J. (2011). Analysis of opioid efficacy, tolerance, addiction and dependence from cell culture to human. *Br J Pharmacol, 164*(4), 1322-1334. doi:10.1111/j.1476-5381.2011.01335.x

Moulédous, L., Froment, C., Burlet-Schiltz, O., Schulz, S., & Mollereau, C. (2015). Phosphoproteomic analysis of the mouse brain mu-opioid (MOP) receptor. *FEBS Letters, 589*(18), 2401-2408. doi:10.1016/j.febslet.2015.07.025

Mundell, S. J., Benovic, J. L., & Kelly, E. (1997). A Dominant Negative Mutant of the G Protein-Coupled Receptor Kinase 2 Selectively Attenuates Adenosine A2 Receptor Desensitization. *Molecular Pharmacology, 51*(6), 991-998. doi:10.1124/mol.51.6.991

Nakamoto, K., Nishinaka, T., Sato, N., Aizawa, F., Yamashita, T., Mankura, M., et al. (2015). The activation of supraspinal GPR40/FFA1 receptor signalling regulates the descending pain control system. *Br J Pharmacol, 172*(5), 1250-1262. doi:10.1111/bph.13003

Naqvi, S., Macdonald, A., McCoy, C. E., Darragh, J., Reith, A. D., & Arthur, J. S. (2012). Characterization of the cellular action of the MSK inhibitor SB-747651A. *Biochem J, 441*(1), 347-357. doi:10.1042/bj20110970

North, R. A., & Williams, J. T. (1985). On the potassium conductance increased by opioids in rat locus coeruleus neurones. *J Physiol, 364*(1), 265-280. doi:10.1113/jphysiol.1985.sp015743

North, R. A., Williams, J. T., Surprenant, A., & Christie, M. J. (1987). Mu and delta receptors belong to a family of receptors that are coupled to potassium channels. *Proceedings of the National Academy of Sciences, 84*(15), 5487-5491. doi:10.1073/pnas.84.15.5487

Nourbakhsh, F., Atabaki, R., & Roohbakhsh, A. (2018). The role of orphan G protein-coupled receptors in the modulation of pain: A review. *Life Sciences, 212*, 59-69. doi:10.1016/j.lfs.2018.09.028

O'Hayre, M., Eichel, K., Avino, S., Zhao, X., Steffen, D. J., Feng, X., et al. (2017). Genetic evidence that β-arrestins are dispensable for the initiation of β(2)-adrenergic receptor signaling to ERK. *Sci Signal, 10*(484). doi:10.1126/scisignal.aal3395

Oldham, W. M., & Hamm, H. E. (2008). Heterotrimeric G protein activation by G-protein-coupled receptors. *Nat Rev Mol Cell Biol, 9*(1), 60-71. doi:10.1038/nrm2299

Olsen, R. H. J., Diberto, J. F., English, J. G., Glaudin, A. M., Krumm, B. E., Slocum, S. T., et al. (2020). TRUPATH, an open-source biosensor platform for interrogating the GPCR transducerome. *Nature Chemical Biology*. doi:10.1038/s41589-020-0535-8

Osborne, P. B., & Williams, J. T. (1995). Characterization of acute homologous desensitization of mu-opioid receptor-induced currents in locus coeruleus neurones. *Br J Pharmacol, 115*(6), 925-932. doi:10.1111/j.1476-5381.1995.tb15899.x

Pals-Rylaarsdam, R., & Hosey, M. M. (1997). Two homologous phosphorylation domains differentially contribute to desensitization and internalization of the m2 muscarinic acetylcholine receptor. *J Biol Chem, 272*(22), 14152-14158. doi:10.1074/jbc.272.22.14152

Pan, Z. Z., Grudt, T. J., & Williams, J. T. (1994). Alpha 1-adrenoceptors in rat dorsal raphe neurons: regulation of two potassium conductances. *The Journal of Physiology, 478*(3), 437-447. doi:10.1113/jphysiol.1994.sp020263

Pang, P. S., Butler, J., Collins, S. P., Cotter, G., Davison, B. A., Ezekowitz, J. A., et al. (2017). Biased ligand of the angiotensin II type 1 receptor in patients with acute heart

failure: a randomized, double-blind, placebo-controlled, phase IIB, dose ranging trial (BLAST-AHF). *European Heart Journal, 38*(30), 2364-2373. doi:10.1093/eurheartj/ehx196

Pasternak, G. W., & Pan, Y. X. (2013). Mu opioids and their receptors: evolution of a concept. *Pharmacol Rev, 65*(4), 1257-1317. doi:10.1124/pr.112.007138

Pavlos, N. J., & Friedman, P. A. (2017). GPCR Signaling and Trafficking: The Long and Short of It. *Trends Endocrinol Metab, 28*(3), 213-226. doi:10.1016/j.tem.2016.10.007

Pedersen, M. F., Wróbel, T. M., Märcher-Rørsted, E., Pedersen, D. S., Møller, T. C., Gabriele, F., et al. (2020). Biased agonism of clinically approved μ-opioid receptor agonists and TRV130 is not controlled by binding and signaling kinetics. *Neuropharmacology, 166*, 107718. doi:10.1016/j.neuropharm.2019.107718

Pepper, C., & Henderson, G. (1980). Opiates and opioid peptides hyperpolarize locus coeruleus neurons in vitro. *Science, 209*(4454), 394-395. doi:10.1126/science.7384811

Pick, C. G., Cheng, J., Paul, D., & Pasternak, G. W. (1991). Genetic influences in opioid analgesic sensitivity in mice. *Brain Res, 566*(1-2), 295-298. doi:10.1016/0006-8993(91)91712-a

Piñeyro, G., & Archer-Lahlou, E. (2007). Ligand-specific receptor states: implications for opiate receptor signalling and regulation. *Cell Signal, 19*(1), 8-19. doi:10.1016/j.cellsig.2006.05.026

Pitcher, J. A., Freedman, N. J., & Lefkowitz, R. J. (1998). G protein-coupled receptor kinases. *Annu Rev Biochem, 67*, 653-692. doi:10.1146/annurev.biochem.67.1.653

Ponimaskin, E., Dumuis, A., Gaven, F., Barthet, G., Heine, M., Glebov, K., et al. (2005). Palmitoylation of the 5-hydroxytryptamine4a receptor regulates receptor phosphorylation, desensitization, and beta-arrestin-mediated endocytosis. *Mol Pharmacol, 67*(5), 1434-1443. doi:10.1124/mol.104.008748

Pradhan, A. A., Befort, K., Nozaki, C., Gavériaux-Ruff, C., & Kieffer, B. L. (2011). The delta opioid receptor: an evolving target for the treatment of brain disorders. *Trends Pharmacol Sci, 32*(10), 581-590. doi:10.1016/j.tips.2011.06.008

Price, D. D., Von der Gruen, A., Miller, J., Rafii, A., & Price, C. (1985). A psychophysical analysis of morphine analgesia. *Pain, 22*(3), 261-269. doi:10.1016/0304-3959(85)90026-0

Raehal, K. M., Schmid, C. L., Groer, C. E., & Bohn, L. M. (2011a). Functional Selectivity at the μ-Opioid Receptor: Implications for Understanding Opioid Analgesia and Tolerance. *Pharmacological Reviews, 63*(4), 1001-1019. doi:10.1124/pr.111.004598

Raehal, K. M., Schmid, C. L., Groer, C. E., & Bohn, L. M. (2011b). Functional selectivity at the μ-opioid receptor: implications for understanding opioid analgesia and tolerance. *Pharmacol Rev, 63*(4), 1001-1019. doi:10.1124/pr.111.004598

Raehal, K. M., Walker, J. K., & Bohn, L. M. (2005). Morphine side effects in beta-arrestin 2 knockout mice. *J Pharmacol Exp Ther, 314*(3), 1195-1201. doi:10.1124/jpet.105.087254

Rathod, M., Mal, A., & De, A. (2018). Reporter-Based BRET Sensors for Measuring Biological Functions In Vivo. In (pp. 51-74): Springer New York.

Raveh, A., Cooper, A., Guy-David, L., & Reuveny, E. (2010). Nonenzymatic rapid control of GIRK channel function by a G protein-coupled receptor kinase. *Cell, 143*(5), 750-760. doi:10.1016/j.cell.2010.10.018

Ribeiro, F. M., Ferreira, L. T., Paquet, M., Cregan, T., Ding, Q., Gros, R., et al. (2009). Phosphorylation-independent regulation of metabotropic glutamate receptor 5 desensitization and internalization by G protein-coupled receptor kinase 2 in neurons. *J Biol Chem, 284*(35), 23444-23453. doi:10.1074/jbc.M109.000778

Rivero, G., Llorente, J., McPherson, J., Cooke, A., Mundell, S. J., McArdle, C. A., et al. (2012). Endomorphin-2: a biased agonist at the mu-opioid receptor. *Mol Pharmacol, 82*(2), 178-188. doi:10.1124/mol.112.078659

Rodriguez-Martin, I., Braksator, E., Bailey, C. P., Goodchild, S., Marrion, N. V., Kelly, E., et al. (2008). Methadone: does it really have low efficacy at micro-opioid receptors? *Neuroreport, 19*(5), 589-593. doi:10.1097/WNR.0b013e3282f97b64

Rossi, G. C., Pasternak, G. W., & Bodnar, R. J. (1994). Mu and delta opioid synergy between the periaqueductal gray and the rostro-ventral medulla. *Brain Res, 665*(1), 85-93. doi:10.1016/0006-8993(94)91155-x

Rüegg, U. T., & Gillian, B. (1989). Staurosporine, K-252 and UCN-01: potent but nonspecific inhibitors of protein kinases. *Trends in Pharmacological Sciences, 10*(6), 218-220. doi:10.1016/0165-6147(89)90263-0

Sakurai, T., Amemiya, A., Ishii, M., Matsuzaki, I., Chemelli, R. M., Tanaka, H., et al. (1998). Orexins and orexin receptors: a family of hypothalamic neuropeptides and G protein-coupled receptors that regulate feeding behavior. *Cell, 92*(4), 573-585. doi:10.1016/s0092-8674(00)80949-6

Salahpour, A., Espinoza, S., Masri, B., Lam, V., Barak, L. S., & Gainetdinov, R. R. (2012). BRET biosensors to study GPCR biology, pharmacology, and signal transduction. *Front Endocrinol (Lausanne), 3*, 105. doi:10.3389/fendo.2012.00105

Sanders, M. A., & Levine, H. (2002). Desensitization of the Neurokinin 1 Receptor Is Mediated by the Receptor Carboxy-Terminal Region, but Is Not Caused by Receptor Internalization. *Journal of Neurochemistry, 67*(6), 2362-2372. doi:10.1046/j.1471-4159.1996.67062362.x

Sanger, G. J. (2004). Neurokinin NK1 and NK3 receptors as targets for drugs to treat gastrointestinal motility disorders and pain. *Br J Pharmacol, 141*(8), 1303-1312. doi:10.1038/sj.bjp.0705742

Schattauer, S. S., Kuhar, J. R., Song, A., & Chavkin, C. (2017). Nalfurafine is a G-protein biased agonist having significantly greater bias at the human than rodent form of the kappa opioid receptor. *Cellular Signalling, 32*, 59-65. doi:10.1016/j.cellsig.2017.01.016

Schild, H. O. (1947). pA, A NEW SCALE FOR THE MEASUREMENT OF DRUG ANTAGONISM. *British Journal of Pharmacology and Chemotherapy, 2*(3), 189-206. doi:10.1111/j.1476-5381.1947.tb00336.x

Schiöth, H. B., & Fredriksson, R. (2005). The GRAFS classification system of G-protein coupled receptors in comparative perspective. *Gen Comp Endocrinol, 142*(1-2), 94-101. doi:10.1016/j.ygcen.2004.12.018

Schmid, C. L., Kennedy, N. M., Ross, N. C., Lovell, K. M., Yue, Z., Morgenweck, J., et al. (2017). Bias Factor and Therapeutic Window Correlate to Predict Safer Opioid Analgesics. *Cell, 171*(5), 1165-1175 e1113. doi:10.1016/j.cell.2017.10.035

Schmidt, M., Bienek, C., van Koppen, C. J., Michel, M. C., & Jakobs, K. H. (1995). Differential calcium signalling by m2 and m3 muscarinic acetylcholine receptors in a single cell type. *Naunyn-Schmiedeberg's Archives of Pharmacology, 352*(5), 469-476. doi:10.1007/BF00169379

Schmidt-Hansen, M., Bromham, N., Taubert, M., Arnold, S., & Hilgart, J. S. (2015). Buprenorphine for treating cancer pain. *Cochrane Database of Systematic Reviews*. doi:10.1002/14651858.cd009596.pub4

Schneider, S., Provasi, D., & Filizola, M. (2016). How Oliceridine (TRV-130) Binds and Stabilizes a mu-Opioid Receptor Conformational State That Selectively Triggers G Protein Signaling Pathways. *Biochemistry, 55*(46), 6456-6466. doi:10.1021/acs.biochem.6b00948

Schroeder, J. E., Fischbach, P. S., Zheng, D., & McCleskey, E. W. (1991). Activation of mu opioid receptors inhibits transient high- and low-threshold Ca2+ currents, but spares a sustained current. *Neuron, 6*(1), 13-20. doi:10.1016/0896-6273(91)90117-i

Scott, L. J. (2020). Lemborexant: First Approval. *Drugs, 80*(4), 425-432. doi:10.1007/s40265-020-01276-1

Sevostianova, N., & Danysz, W. (2006). Analgesic effects of mGlu1 and mGlu5 receptor antagonists in the rat formalin test. *Neuropharmacology, 51*(3), 623-630. doi:10.1016/j.neuropharm.2006.05.004

Seward, E., Hammond, C., & Henderson, G. (1991). Mu-opioid-receptor-mediated inhibition of the N-type calcium-channel current. *Proc Biol Sci, 244*(1310), 129-135. doi:10.1098/rspb.1991.0061

Shirey, J. K., Brady, A. E., Jones, P. J., Davis, A. A., Bridges, T. M., Kennedy, J. P., et al. (2009). A selective allosteric potentiator of the M1 muscarinic acetylcholine receptor increases activity of medial prefrontal cortical neurons and restores impairments in reversal learning. *J Neurosci, 29*(45), 14271-14286. doi:10.1523/jneurosci.3930-09.2009

Shoichet, B. K., & Kobilka, B. K. (2012). Structure-based drug screening for G-protein-coupled receptors. *Trends Pharmacol Sci, 33*(5), 268-272. doi:10.1016/j.tips.2012.03.007

Singla, N. K., Skobieranda, F., Soergel, D. G., Salamea, M., Burt, D. A., Demitrack, M. A., et al. (2019). APOLLO-2: A Randomized, Placebo and Active-Controlled Phase III Study Investigating Oliceridine (TRV130), a G Protein-Biased Ligand at the mu-Opioid Receptor, for Management of Moderate to Severe Acute Pain Following Abdominoplasty. *Pain Pract, 19*(7), 715-731. doi:10.1111/papr.12801

Singleton, S., Baptista-Hon, D. T., Edelsten, E., McCaughey, K. S., Camplisson, E., & Hales, T. G. (2021). TRV130 partial agonism and capacity to induce anti-nociceptive tolerance revealed through reducing available mu-opioid receptor number. *Br J Pharmacol, 178*(8), 1855-1868. doi:10.1111/bph.15409

Sittl, R., Nuijten, M., & Nautrup, B. P. (2005). Changes in the prescribed daily doses of transdermal fentanyl and transdermal buprenorphine during treatment of patients with cancer and noncancer pain in Germany: results of a retrospective cohort study. *Clin Ther, 27*(7), 1022-1031. doi:10.1016/j.clinthera.2005.06.024

Slosky, L. M., Bai, Y., Toth, K., Ray, C., Rochelle, L. K., Badea, A., et al. (2020). β-Arrestin-Biased Allosteric Modulator of NTSR1 Selectively Attenuates Addictive Behaviors. *Cell, 181*(6), 1364-1379.e1314. doi:10.1016/j.cell.2020.04.053

Smith, J. S., Lefkowitz, R. J., & Rajagopal, S. (2018). Biased signalling: from simple switches to allosteric microprocessors. *Nat Rev Drug Discov, 17*(4), 243-260. doi:10.1038/nrd.2017.229

Sonoda, N., Imamura, T., Yoshizaki, T., Babendure, J. L., Lu, J.-C., & Olefsky, J. M. (2008). β-Arrestin-1 mediates glucagon-like peptide-1 signaling to insulin secretion in cultured pancreatic β cells. *Proceedings of the National Academy of Sciences, 105*(18), 6614-6619. doi:10.1073/pnas.0710402105

Spetea, M., Eans, S. O., Ganno, M. L., Lantero, A., Mairegger, M., Toll, L., et al. (2017). Selective κ receptor partial agonist HS666 produces potent antinociception without inducing aversion after i.c.v. administration in mice. *British Journal of Pharmacology, 174*(15), 2444-2456. doi:10.1111/bph.13854

Stahl, E. L., Zhou, L., Ehlert, F. J., & Bohn, L. M. (2015). A Novel Method for Analyzing Extremely Biased Agonism at G Protein–Coupled Receptors. *Molecular Pharmacology, 87*(5), 866-877. doi:10.1124/mol.114.096503

Starnowska, J., Costante, R., Guillemyn, K., Popiolek-Barczyk, K., Chung, N. N., Lemieux, C., et al. (2017). Analgesic Properties of Opioid/NK1 Multitarget Ligands with Distinct in Vitro Profiles in Naive and Chronic Constriction Injury Mice. *ACS Chem Neurosci, 8*(10), 2315-2324. doi:10.1021/acschemneuro.7b00226

Stephenson, R. P. (1956). A modification of receptor theory. *Br J Pharmacol Chemother, 11*(4), 379-393. doi:10.1111/j.1476-5381.1956.tb00006.x

Steyaert, J., & Kobilka, B. K. (2011). Nanobody stabilization of G protein-coupled receptor conformational states. *Curr Opin Struct Biol, 21*(4), 567-572. doi:10.1016/j.sbi.2011.06.011

Stoddart, L. A., White, C. W., Nguyen, K., Hill, S. J., & Pfleger, K. D. (2016). Fluorescence- and bioluminescence-based approaches to study GPCR ligand binding. *Br J Pharmacol, 173*(20), 3028-3037. doi:10.1111/bph.13316

Stoffel, R. H., Randall, R. R., Premont, R. T., Lefkowitz, R. J., & Inglese, J. (1994). Palmitoylation of G protein-coupled receptor kinase, GRK6. Lipid modification diversity in the GRK family. *J Biol Chem, 269*(45), 27791-27794.

Sun, S., Yang, X., Wang, Y., & Shen, X. (2016). In Vivo Analysis of Protein–Protein Interactions with Bioluminescence Resonance Energy Transfer (BRET): Progress and Prospects. *International Journal of Molecular Sciences, 17*(10), 1704. doi:10.3390/ijms17101704

Sutcliffe, K. (2019). *Molecular dynamics simulations and mutagenesis to identify the mechinams of ligand efficacy and bias at the mu opioid receptor.* (PhD). University of Bristol,

Terskiy, A., Wannemacher, K. M., Yadav, P. N., Tsai, M., Tian, B., & Howells, R. D. (2007). Search of the human proteome for endomorphin-1 and endomorphin-2 precursor proteins. *Life Sci, 81*(23-24), 1593-1601. doi:10.1016/j.lfs.2007.09.025

Thal, D. M., Sun, B., Feng, D., Nawaratne, V., Leach, K., Felder, C. C., et al. (2016). Crystal structures of the M1 and M4 muscarinic acetylcholine receptors. *Nature, 531*(7594), 335-340. doi:10.1038/nature17188

Thal, D. M., Yeow, R. Y., Schoenau, C., Huber, J., & Tesmer, J. J. (2011). Molecular mechanism of selectivity among G protein-coupled receptor kinase 2 inhibitors. *Mol Pharmacol, 80*(2), 294-303. doi:10.1124/mol.111.071522

Thompson, A. A., Liu, W., Chun, E., Katritch, V., Wu, H., Vardy, E., et al. (2012). Structure of the nociceptin/orphanin FQ receptor in complex with a peptide mimetic. *Nature, 485*(7398), 395-399. doi:10.1038/nature11085

Thompson, G. L., Lane, J. R., Coudrat, T., Sexton, P. M., Christopoulos, A., & Canals, M. (2015). Biased Agonism of Endogenous Opioid Peptides at the μ-Opioid Receptor. *Molecular Pharmacology, 88*(2), 335-346. doi:10.1124/mol.115.098848

Udoh, M., Santiago, M., Devenish, S., McGregor, I. S., & Connor, M. (2019). Cannabichromene is a cannabinoid CB 2 receptor agonist. *British Journal of Pharmacology, 176*(23), 4537-4547. doi:10.1111/bph.14815

Urs, N. M., Gee, S. M., Pack, T. F., McCorvy, J. D., Evron, T., Snyder, J. C., et al. (2016). Distinct cortical and striatal actions of a β-arrestin–biased dopamine D2 receptor ligand reveal unique antipsychotic-like properties. *Proceedings of the National Academy of Sciences, 113*(50), E8178-E8186. doi:10.1073/pnas.1614347113

Vadivelu, N., Mitra, S., & Hines, R. L. (2011). Peripheral opioid receptor agonists for analgesia: a comprehensive review. *J Opioid Manag, 7*(1), 55-68. doi:10.5055/jom.2011.0049

Varga, A. G., Reid, B. T., Kieffer, B. L., & Levitt, E. S. (2019). Differential impact of two critical respiratory centres in opioid-induced respiratory depression in awake mice. *The Journal of Physiology*. doi:10.1113/jp278612

Vasudevan, L., Vandeputte, M., Deventer, M., Wouters, E., Cannaert, A., & Stove, C. P. (2020). Assessment of structure-activity relationships and biased agonism at the Mu opioid receptor of novel synthetic opioids using a novel, stable bio-assay platform. *Biochem Pharmacol, 177*, 113910. doi:10.1016/j.bcp.2020.113910

Violin, J. D., DeWire, S. M., Yamashita, D., Rominger, D. H., Nguyen, L., Schiller, K., et al. (2010). Selectively Engaging β-Arrestins at the Angiotensin II Type 1 Receptor Reduces Blood Pressure and Increases Cardiac Performance. *Journal of Pharmacology and Experimental Therapeutics, 335*(3), 572-579. doi:10.1124/jpet.110.173005

Waldschmidt, H. V., Homan, K. T., Cato, M. C., Cruz-Rodríguez, O., Cannavo, A., Wilson, M. W., et al. (2017). Structure-Based Design of Highly Selective and Potent G Protein-Coupled Receptor Kinase 2 Inhibitors Based on Paroxetine. *Journal of Medicinal Chemistry, 60*(7), 3052-3069. doi:10.1021/acs.jmedchem.7b00112

Waldschmidt, H. V., Homan, K. T., Cruz-Rodríguez, O., Cato, M. C., Waninger-Saroni, J., Larimore, K. M., et al. (2016). Structure-Based Design, Synthesis, and Biological Evaluation of Highly Selective and Potent G Protein-Coupled Receptor Kinase 2 Inhibitors. *Journal of Medicinal Chemistry, 59*(8), 3793-3807. doi:10.1021/acs.jmedchem.5b02000

Walwyn, W., Evans, C. J., & Hales, T. G. (2007). Beta-arrestin2 and c-Src regulate the constitutive activity and recycling of mu opioid receptors in dorsal root ganglion neurons. *J Neurosci, 27*(19), 5092-5104. doi:10.1523/JNEUROSCI.1157-07.2007

Wang, J., Hua, T., & Liu, Z.-J. (2020). Structural features of activated GPCR signaling complexes. *Current Opinion in Structural Biology, 63*, 82-89. doi:10.1016/j.sbi.2020.04.008

Wang, P., & DeFea, K. A. (2006). Protease-activated receptor-2 simultaneously directs beta-arrestin-1-dependent inhibition and Galphaq-dependent activation of phosphatidylinositol 3-kinase. *Biochemistry, 45*(31), 9374-9385. doi:10.1021/bi0602617

Webster, L., & Schmidt, W. K. (2020). Dilemma of Addiction and Respiratory Depression in the Treatment of Pain: A Prototypical Endomorphin as a New Approach. *Pain Medicine, 21*(5), 992-1004. doi:10.1093/pm/pnz122

Wei, A. D., & Ramirez, J.-M. (2019). Presynaptic Mechanisms and KCNQ Potassium Channels Modulate Opioid Depression of Respiratory Drive. *Frontiers in Physiology, 10*. doi:10.3389/fphys.2019.01407

Weis, W. I., & Kobilka, B. K. (2018). The Molecular Basis of G Protein-Coupled Receptor Activation. *Annu Rev Biochem, 87*(1), 897-919. doi:10.1146/annurev-biochem-060614-033910

Wettschureck, N., & Offermanns, S. (2005). Mammalian G proteins and their cell type specific functions. *Physiol Rev, 85*(4), 1159-1204. doi:10.1152/physrev.00003.2005

Whistler, J. L., Chuang, H. H., Chu, P., Jan, L. Y., & von Zastrow, M. (1999). Functional dissociation of mu opioid receptor signaling and endocytosis: implications for the biology of opiate tolerance and addiction. *Neuron, 23*(4), 737-746. doi:10.1016/s0896-6273(01)80032-5

Williams, J. T., Christie, M. J., North, R. A., & Roques, B. P. (1987a). Potentiation of enkephalin action by peptidase inhibitors in rat locus ceruleus in vitro. *J Pharmacol Exp Ther, 243*(1), 397-401.

Williams, J. T., Egan, T. M., & North, R. A. (1982). Enkephalin opens potassium channels on mammalian central neurones. *Nature, 299*(5878), 74-77. doi:10.1038/299074a0

Williams, J. T., Ingram, S. L., Henderson, G., Chavkin, C., von Zastrow, M., Schulz, S., et al. (2013). Regulation of mu-opioid receptors: desensitization, phosphorylation, internalization, and tolerance. *Pharmacol Rev, 65*(1), 223-254. doi:10.1124/pr.112.005942

Williams, J. T., & Marshall, K. C. (1987b). Membrane properties and adrenergic responses in locus coeruleus neurons of young rats. *J Neurosci, 7*(11), 3687-3694. doi:10.1523/jneurosci.07-11-03687.1987

Williams, J. T., & North, R. A. (1984). Opiate-receptor interactions on single locus coeruleus neurones. *Mol Pharmacol, 26*(3), 489-497.

Wilson, A. M., Soignier, R. D., Zadina, J. E., Kastin, A. J., Nores, W. L., Olson, R. D., et al. (2000). Dissociation of analgesic and rewarding effects of endomorphin-1 in rats. *Peptides, 21*(12), 1871-1874. doi:10.1016/s0196-9781(00)00340-5

Wingler, L. M., & Lefkowitz, R. J. (2020). Conformational Basis of G Protein-Coupled Receptor Signaling Versatility. *Trends in Cell Biology, 30*(9), 736-747. doi:10.1016/j.tcb.2020.06.002

Wisler, J. W., DeWire, S. M., Whalen, E. J., Violin, J. D., Drake, M. T., Ahn, S., et al. (2007). A unique mechanism of beta-blocker action: carvedilol stimulates beta-arrestin signaling. *Proc Natl Acad Sci U S A, 104*(42), 16657-16662. doi:10.1073/pnas.0707936104

Xiao, K., McClatchy, D. B., Shukla, A. K., Zhao, Y., Chen, M., Shenoy, S. K., et al. (2007). Functional specialization of beta-arrestin interactions revealed by proteomic analysis. *Proc Natl Acad Sci U S A, 104*(29), 12011-12016. doi:10.1073/pnas.0704849104

Yang, L. P. (2014). Suvorexant: first global approval. *Drugs, 74*(15), 1817-1822. doi:10.1007/s40265-014-0294-5

Yasi, E. A., Kruyer, N. S., & Peralta-Yahya, P. (2020). Advances in G protein-coupled receptor high-throughput screening. *Curr Opin Biotechnol, 64*, 210-217. doi:10.1016/j.copbio.2020.06.004

Yousuf, A., Miess, E., Sianati, S., Du, Y. P., Schulz, S., & Christie, M. J. (2015). Role of Phosphorylation Sites in Desensitization of μ-Opioid Receptor. *Mol Pharmacol, 88*(4), 825-835. doi:10.1124/mol.115.098244

Yudin, Y., & Rohacs, T. (2019). The G-protein-biased agents PZM21 and TRV130 are partial agonists of mu-opioid receptor-mediated signalling to ion channels. *Br J Pharmacol, 176*(17), 3110-3125. doi:10.1111/bph.14702

Zadina, J. E., Hackler, L., Ge, L. J., & Kastin, A. J. (1997). A potent and selective endogenous agonist for the mu-opiate receptor. *Nature, 386*(6624), 499-502. doi:10.1038/386499a0

Zadina, J. E., Nilges, M. R., Morgenweck, J., Zhang, X., Hackler, L., & Fasold, M. B. (2016). Endomorphin analog analgesics with reduced abuse liability, respiratory depression, motor impairment, tolerance, and glial activation relative to morphine. *Neuropharmacology, 105*, 215-227. doi:10.1016/j.neuropharm.2015.12.024

Zaki, P. A., Keith, D. E., Jr., Brine, G. A., Carroll, F. I., & Evans, C. J. (2000). Ligand-induced changes in surface mu-opioid receptor number: relationship to G protein activation? *J Pharmacol Exp Ther, 292*(3), 1127-1134.

Zhang, J., Ferguson, S. S., Barak, L. S., Bodduluri, S. R., Laporte, S. A., Law, P. Y., et al. (1998). Role for G protein-coupled receptor kinase in agonist-specific regulation of mu-opioid receptor responsiveness. *Proc Natl Acad Sci U S A, 95*(12), 7157-7162. doi:10.1073/pnas.95.12.7157

Zhang, X., Stevens, R. C., & Xu, F. (2015). The importance of ligands for G protein-coupled receptor stability. *Trends in Biochemical Sciences, 40*(2), 79-87. doi:10.1016/j.tibs.2014.12.005

Zhao, Z., Huang, T., & Li, J. (2020). Molecular Dynamics Simulations to Investigate How PZM21 Affects the Conformational State of the μ-Opioid Receptor Upon Activation. *Int J Mol Sci, 21*(13). doi:10.3390/ijms21134699